CEREBROVASCULATURE IN HEALTH AND DISEASES

EDITED BY: Anne-Clémence Vion, Yacine Boulaftali and Emma Gordon
PUBLISHED IN: Frontiers in Cardiovascular Medicine

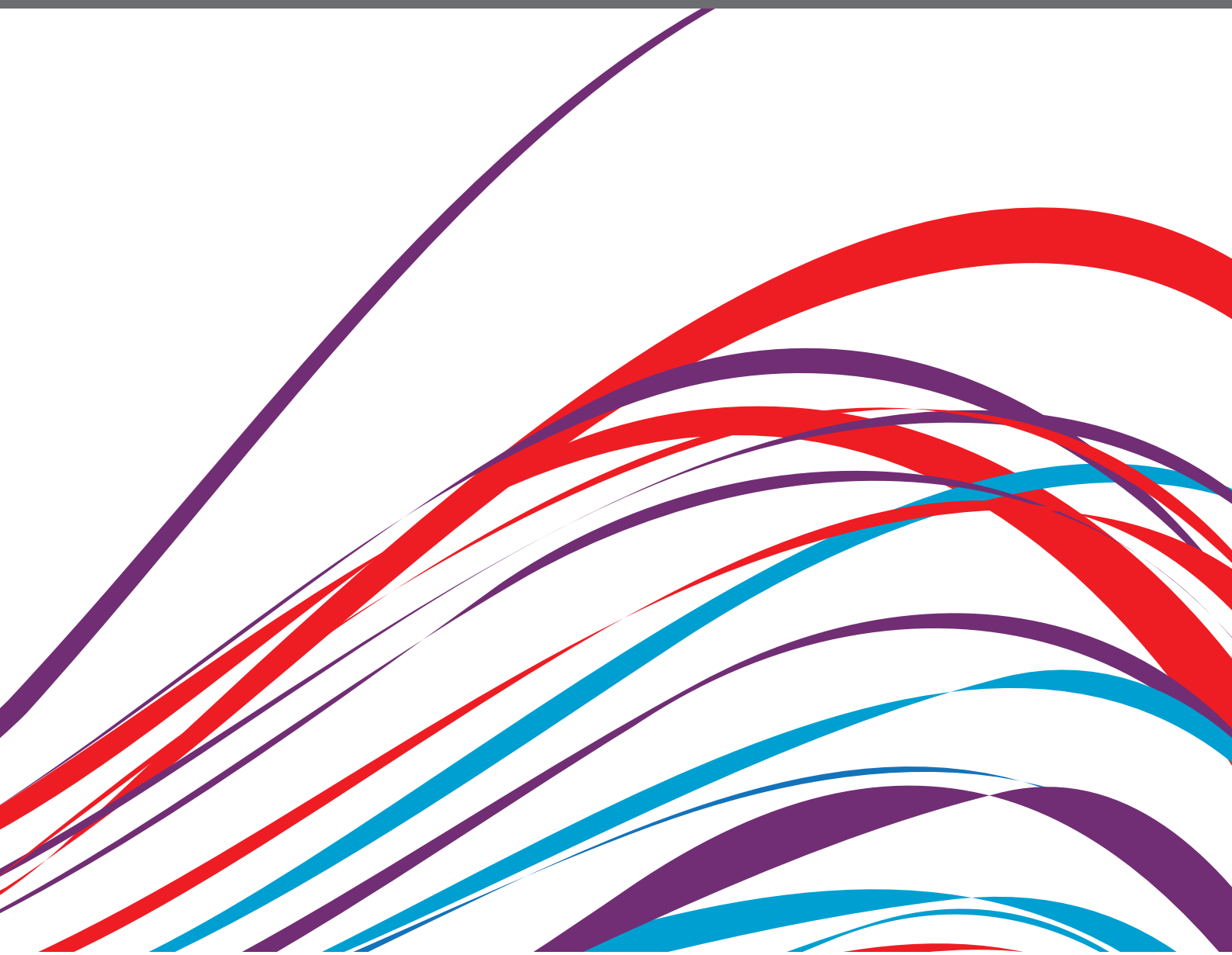

frontiers Research Topics

Frontiers eBook Copyright Statement

The copyright in the text of individual articles in this eBook is the property of their respective authors or their respective institutions or funders. The copyright in graphics and images within each article may be subject to copyright of other parties. In both cases this is subject to a license granted to Frontiers.

The compilation of articles constituting this eBook is the property of Frontiers.

Each article within this eBook, and the eBook itself, are published under the most recent version of the Creative Commons CC-BY licence. The version current at the date of publication of this eBook is CC-BY 4.0. If the CC-BY licence is updated, the licence granted by Frontiers is automatically updated to the new version.

When exercising any right under the CC-BY licence, Frontiers must be attributed as the original publisher of the article or eBook, as applicable.

Authors have the responsibility of ensuring that any graphics or other materials which are the property of others may be included in the CC-BY licence, but this should be checked before relying on the CC-BY licence to reproduce those materials. Any copyright notices relating to those materials must be complied with.

Copyright and source acknowledgement notices may not be removed and must be displayed in any copy, derivative work or partial copy which includes the elements in question.

All copyright, and all rights therein, are protected by national and international copyright laws. The above represents a summary only. For further information please read Frontiers' Conditions for Website Use and Copyright Statement, and the applicable CC-BY licence.

ISSN 1664-8714
ISBN 978-2-83250-161-0
DOI 10.3389/978-2-83250-161-0

About Frontiers

Frontiers is more than just an open-access publisher of scholarly articles: it is a pioneering approach to the world of academia, radically improving the way scholarly research is managed. The grand vision of Frontiers is a world where all people have an equal opportunity to seek, share and generate knowledge. Frontiers provides immediate and permanent online open access to all its publications, but this alone is not enough to realize our grand goals.

Frontiers Journal Series

The Frontiers Journal Series is a multi-tier and interdisciplinary set of open-access, online journals, promising a paradigm shift from the current review, selection and dissemination processes in academic publishing. All Frontiers journals are driven by researchers for researchers; therefore, they constitute a service to the scholarly community. At the same time, the Frontiers Journal Series operates on a revolutionary invention, the tiered publishing system, initially addressing specific communities of scholars, and gradually climbing up to broader public understanding, thus serving the interests of the lay society, too.

Dedication to Quality

Each Frontiers article is a landmark of the highest quality, thanks to genuinely collaborative interactions between authors and review editors, who include some of the world's best academicians. Research must be certified by peers before entering a stream of knowledge that may eventually reach the public - and shape society; therefore, Frontiers only applies the most rigorous and unbiased reviews.
Frontiers revolutionizes research publishing by freely delivering the most outstanding research, evaluated with no bias from both the academic and social point of view. By applying the most advanced information technologies, Frontiers is catapulting scholarly publishing into a new generation.

What are Frontiers Research Topics?

Frontiers Research Topics are very popular trademarks of the Frontiers Journals Series: they are collections of at least ten articles, all centered on a particular subject. With their unique mix of varied contributions from Original Research to Review Articles, Frontiers Research Topics unify the most influential researchers, the latest key findings and historical advances in a hot research area! Find out more on how to host your own Frontiers Research Topic or contribute to one as an author by contacting the Frontiers Editorial Office: frontiersin.org/about/contact

CEREBROVASCULATURE IN HEALTH AND DISEASES

Topic Editors:
Anne-Clémence Vion, INSERM U1087 Institut du Thorax, France
Yacine Boulaftali, Institut National de la Santé et de la Recherche Médicale (INSERM), France
Emma Gordon, The University of Queensland, Australia

Citation: Vion, A.-C., Boulaftali, Y., Gordon, E., eds. (2022). Cerebrovasculature in Health and Diseases. Lausanne: Frontiers Media SA. doi: 10.3389/978-2-83250-161-0

Table of Contents

frontiers in Cardiovascular Medicine

SYSTEMATIC REVIEW
published: 15 November 2021
doi: 10.3389/fcvm.2021.752769

Delayed Cerebral Ischemia After Subarachnoid Hemorrhage: Is There a Relevant Experimental Model? A Systematic Review of Preclinical Literature

Suzanne Goursaud[1,2]*, *Sara Martinez de Lizarrondo*[2], *François Grolleau*[3], *Audrey Chagnot*[2], *Véronique Agin*[2], *Eric Maubert*[2], *Maxime Gauberti*[2], *Denis Vivien*[2,4], *Carine Ali*[2] *and Clément Gakuba*[2,5]

[1] CHU de Caen Normandie, Service de Réanimation Médicale, Caen, France, [2] Normandie University, UNICAEN, INSERM, U1237, PhIND ≪ Physiopathology and Imaging of Neurological Disorders ≫, Institut Blood and Brain @ Caen-Normandie, Cyceron, Caen, France, [3] Centre d'Epidémiologie Clinique, AP-HP (Assistance Publique des Hôpitaux de Paris), Hôpital Hôtel Dieu, Paris, France, [4] CHU Caen, Department of Clinical Research, CHU Caen Côte de Nacre, Caen, France, [5] CHU de Caen Normandie, Service d'Anesthésie-Réanimation Chirurgicale, Caen, France

OPEN ACCESS

Edited by:
Yacine Boulaftali,
Institut National de la Santé et de la Recherche Médicale (INSERM), France

Reviewed by:
Christoph Eugen Hagemeyer,
Monash University, Australia
Subhi Marwari,
University of Pennsylvania, United States

***Correspondence:**
Suzanne Goursaud
goursaud-s@chu-caen.fr

Specialty section:
This article was submitted to Atherosclerosis and Vascular Medicine, a section of the journal Frontiers in Cardiovascular Medicine

Received: 03 August 2021
Accepted: 21 October 2021
Published: 15 November 2021

Citation:
Goursaud S, Martinez de Lizarrondo S, Grolleau F, Chagnot A, Agin V, Maubert E, Gauberti M, Vivien D, Ali C and Gakuba C (2021) Delayed Cerebral Ischemia After Subarachnoid Hemorrhage: Is There a Relevant Experimental Model? A Systematic Review of Preclinical Literature. Front. Cardiovasc. Med. 8:752769. doi: 10.3389/fcvm.2021.752769

Delayed cerebral ischemia (DCI) is one of the main prognosis factors for disability after aneurysmal subarachnoid hemorrhage (SAH). The lack of a consensual definition for DCI had limited investigation and care in human until 2010, when a multidisciplinary research expert group proposed to define DCI as the occurrence of cerebral infarction (identified on imaging or histology) associated with clinical deterioration. We performed a systematic review to assess whether preclinical models of SAH meet this definition, focusing on the combination of noninvasive imaging and neurological deficits. To this aim, we searched in PUBMED database and included all rodent SAH models that considered cerebral ischemia and/or neurological outcome and/or vasospasm. Seventy-eight publications were included. Eight different methods were performed to induce SAH, with blood injection in the *cisterna magna* being the most widely used ($n = 39$, 50%). Vasospasm was the most investigated SAH-related complication ($n = 52$, 67%) compared to cerebral ischemia ($n = 30$, 38%), which was never investigated with imaging. Neurological deficits were also explored ($n = 19$, 24%). This systematic review shows that no preclinical SAH model meets the 2010 clinical definition of DCI, highlighting the inconsistencies between preclinical and clinical standards. In order to enhance research and favor translation to humans, pertinent SAH animal models reproducing DCI are urgently needed.

Keywords: delayed cerebral ischemia, experimental models, subarachnoid hemorrhage, vasospasm, systematic review

INTRODUCTION

Subarachnoid hemorrhage (SAH) is a neurological emergency characterized by the extravasation of blood into subarachnoid spaces. Around 80% of non-traumatic subarachnoid hemorrhage result from the rupture of an intracranial aneurysm, and have a high rate of death and complications. Aneurysmal SAH is therefore one of the most frequent causes of admission in neurocritical

care. Delayed cerebral ischemia (DCI) occurs in ∼30% of cases after aneurysmal SAH (1) and is the leading cause of morbidity for surviving SAH patients. To date, no treatment of DCI improves neurological outcome. Unfortunately, the exact mechanisms of DCI pathophysiology remain poorly understood. The current consensus suggests that the origin of DCI is a multifactorial and complex process. It not only includes the narrowing of cerebral arteries (i.e., vasospasm) but also the activation of others pathways, including a neuroinflammatory reaction that promotes perfusion mismatch with neurovascular uncoupling, as well as other pathological phenomena such as microthrombosis, cortical spreading depolarization and breakdown of the blood-brain barrier (**Figure 1**) (2, 3). All these local and systemic inflammatory responses are involved in the genesis and development of DCI.

These different mechanisms start at ictus, during early brain injury, and result in neuronal injury and sometimes in parenchymal infarction. Large vessel vasospasm was commonly recognized as the main factor leading to DCI after SAH. In fact, recent studies support that large vessel narrowing is a delayed contributor to a cascade of events that starts earlier during the acute phase after SAH. This critical earlier phase with multifactorial pathophysiological pathways is probably the most promising therapeutic target to improve patient outcomes. To better understand SAH and its complications and to facilitate the development of an effective treatment, many animal models have been developed. The lack of a consensual definition of DCI led to a large diversity of terms used and parameters studied. As a result, findings from preclinical research were controversial (4). But in 2010, an international expert panel involved in SAH research developed a definition of DCI in humans. The consortium decided that a uniform definition of DCI should capture both cerebral infarction (imaging) and clinical deterioration (functional) elements in terms of morphological and clinical characteristics. They stated that in clinical trials aiming to develop therapeutics against DCI after SAH, the two main outcome measures should be: (1) infarction identified on computed tomography (CT) or magnetic resonance imaging (MRI) or proven at autopsy, after exclusion of procedure-related infarctions and (2) functional outcome (3).

The definition of DCI-related cerebral infarction was as follows: diagnosis of cerebral infarction performed by either a brain CT or MR scan within 6 weeks after SAH, or on the latest CT or MRI scan made before death within 6 weeks, or proven at autopsy, not present on the CT or MRI scan between 24 and 48 h after early aneurysm occlusion, and not attributable to other causes, such as surgical clipping or endovascular treatment.

Regarding the functional outcome, experts specified that the definition of clinical deterioration caused by DCI is the occurrence of focal neurological impairment (such as hemiparesis, aphasia, apraxia, hemianopia, or neglect), or a decrease of at least 2 points on the Glasgow Coma Scale, which is not apparent immediately after aneurysm occlusion, and cannot be attributed to other causes.

Based on clinical assessment in humans and considering the occurrence of DCI as the main determinant for the functional

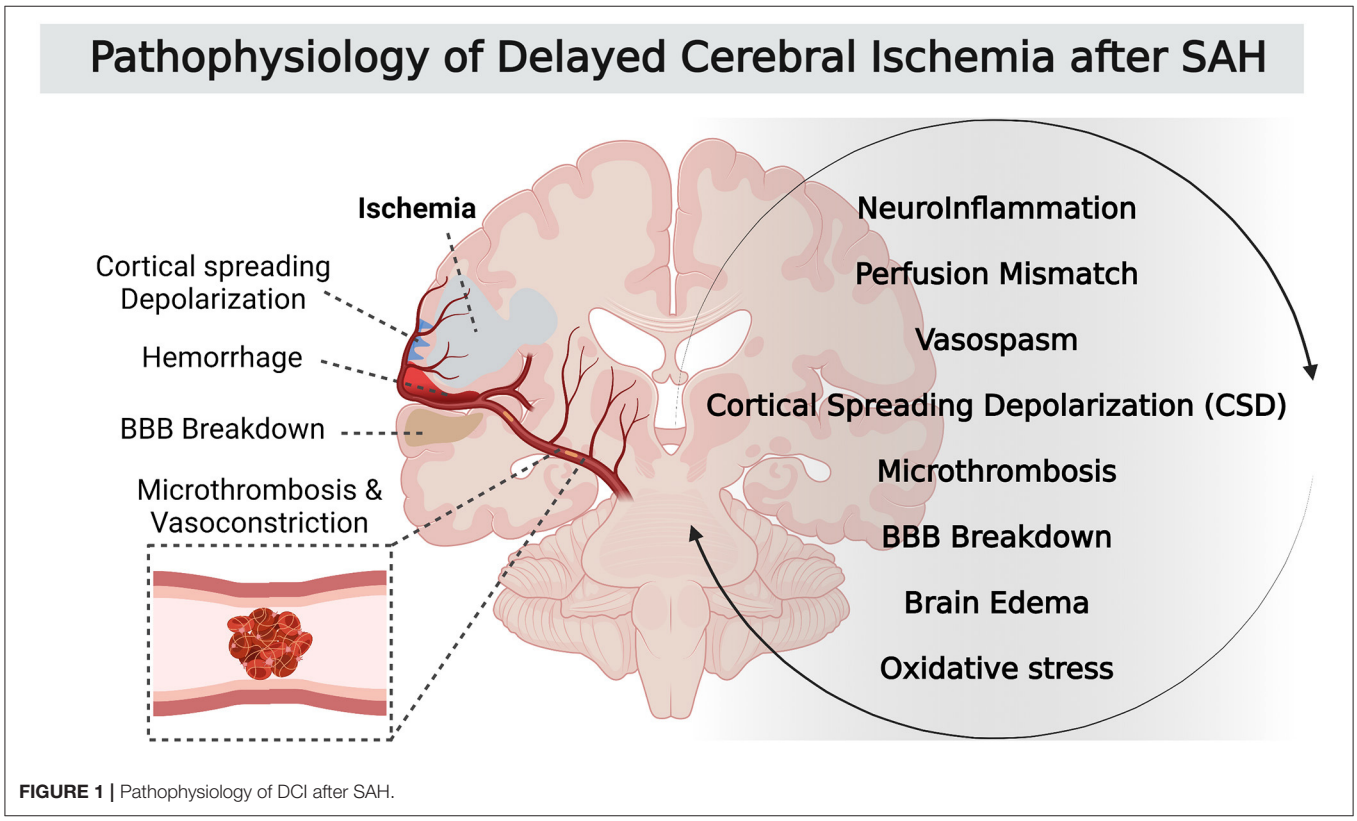

FIGURE 1 | Pathophysiology of DCI after SAH.

outcome, this consensus-building approach allowed to determine that the ideal SAH model should associate both the occurrence of cerebral infarction evidenced on brain imaging or histology and some altered functional outcome. In a translational perspective, noninvasive imaging is preferable to histology for several reasons. Brain imaging is the most common way to investigate cerebral ischemia in clinical trials, and ischemia proved on brain imaging is up to date the only paraclinical outcome that was improved with use of therapeutics that enhance SAH-patients functional outcome (5). Moreover, infarction is well defined by imaging in contrast to histology, which is difficult to define with a consensual diagnostic method.

This systematic review aimed at identifying and analyze the different murine models of SAH, and to describe the extent to which they meet the human definition of DCI, i.e., more specifically according to the associating of the two most relevant evaluation criteria that are the proof of brain ischemia with imaging and the occurrence of neurological deficits.

MATERIALS AND METHODS

Systematic Search

This systematic review was reported following the Preferred Reporting Items for Systematic Reviews and Meta-analysis (PRISMA) statement (6, 7). We searched the PUBMED database on July 1, 2020 with the search terms "subarachnoid hemorrhage," "models, animal," "mice," "rats," "vasospasm, intracranial," and "delayed cerebral ischemia." Abstracts from relevant congresses were also considered. Two authors independently screened the titles and abstracts and reviewed the full text of any potentially eligible publication. Divergences were resolved by consensus.

Eligibility Criteria for Included Animal Studies

Studies were included if they involved (1) description and/or modification of a subarachnoid hemorrhage model in rats or mice (2) study of arterial cerebral vasospasm and/or ischemia and/or neurological outcome. Systematic reviews and meta-analyses as well as *in vitro* studies were excluded. Among the experimental studies developing a method and/or assessing therapeutic strategies, only those, which described a new SAH model, were included The included studies were limited to articles written in English, Spanish, German, Russian, Italian, Portuguese, and French. There was no restriction for year of publication.

Data Collection

For each study, we extracted the journal and authors names, the year of publication, number of citations for each article and the impact factor corresponding to that year. Two publications were classified as coming from the same team if they had one or more author in common considering only authors in first, second, last or penultimate position. Animal characteristics were extracted as follows: species, strain, sex, and weight; model of SAH as follows: method of induction, vascular territory, rupture of an aneurysmal vessel, location of blood injection, using of a pharmaceutical adjuvant to induce ischemia, characteristics of blood used (nature, volume, and number of injections); anesthesia and monitoring as follows: general anesthesia, mechanical ventilation, temperature, blood glucose levels, cerebral blood flow, intracranial pressure, and blood pressure monitoring; study of vasospasm as follows: method (imaging, histology, times studies of vasospasm, study of cerebral blood flow); study of cerebral ischemia as follows: method (imaging, histology, times studies of ischemia, topography, and related searches like neuroinflammation, microthrombosis or microglial activation); mortality and behavioral study as follows: general condition, weight, sensory-motor, and cognitive tests.

Statistical Analysis

We represented the median and extreme values (median [minimum—maximum]) of continuous variables, and the number of occurrences with proportions represented as percentages for categorical variables.

RESULTS

Included Rodent Studies

Of 3,561 articles, only 78 reports proved eligible (8–85) (**Figure 2**).

Characteristics of the Rodent Studies

The 78 articles were published in 26 different journals. The median impact factor of the year of publication was 2.45 [0.82-6.12]. The year of publication ranged from 1979 to 2020. Fifty-nine studies (76%) were published between 2,000 and 2020, 27 of which were published following the 2010 article that defined DCI (3). Fifty-three different teams were identified. Half of publications (n = 39; 50%) resulted from 14 teams. Five (6%) publications were extracted from team A (Bederson, Mount Sinai School of Medecine, New York), 5 (6%) publications were extracted from team B (Prunell, Department of Clinical Neuroscience, Section for neurosurgery, Karolinska Institute, Stockholm, Sweden), and 3 (4%) publications were extracted from team C (Solomon, the Department of Neurological Surgery, Columbia University College of Physicians and Surgeons, New York). Almost two thirds (64%) of citations were issued from 26 studies published by 7 teams (**Figure 3**).

Characteristics of SAH Models in Rats and Mice

The characteristics of SAH models are summarized in **Table 1**. The most commonly used species was rats (66 publications, **Figure 4**). The two main strains of rats were Sprague-Dawley (n = 49; 74%) and Wistar (n = 17; 26%). Two publications used a model with comorbidity that was diabetes (64) or hypertension (12). No model used female animals. With respect to the surgical procedure, 58% of the models (n = 45) corresponded to SAH involving posterior cerebral circulation. The two most frequently used models were blood injection in the *cisterna magna* (n = 39; 50%) and endovascular perforation (n = 23; 29%) (**Figure 5**). Among vascular perforation models, four variants were described: endovascular perforation, endoscopic

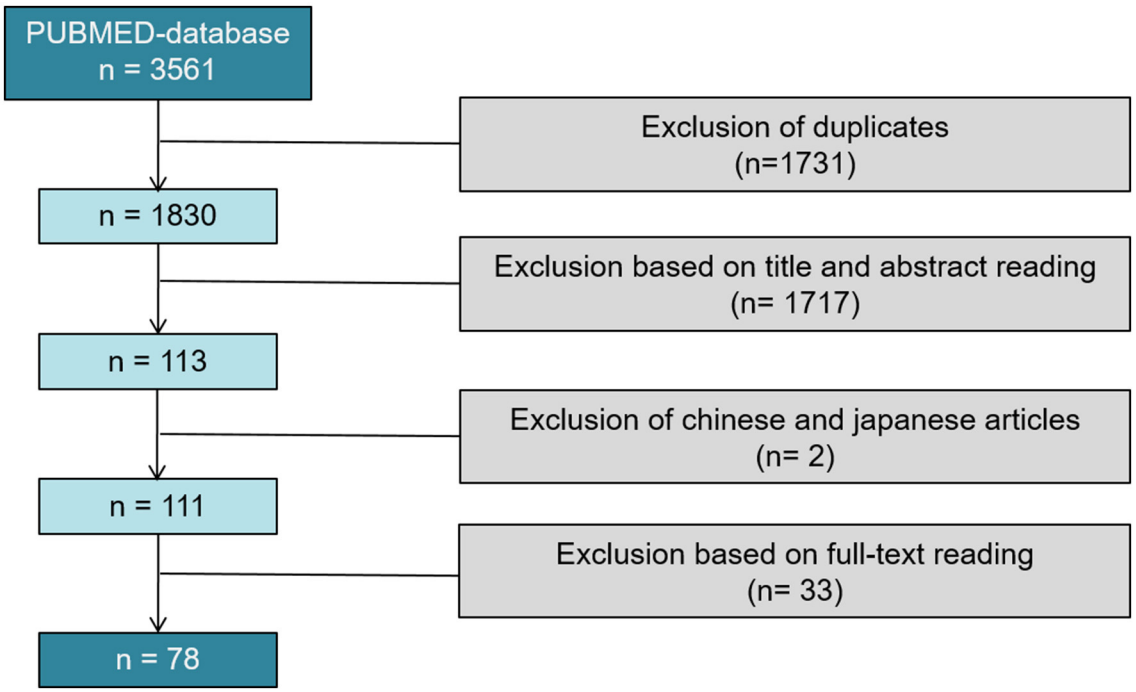

FIGURE 2 | PRISMA flow diagram of the systematic review; 78 studies were included in our systematical review.

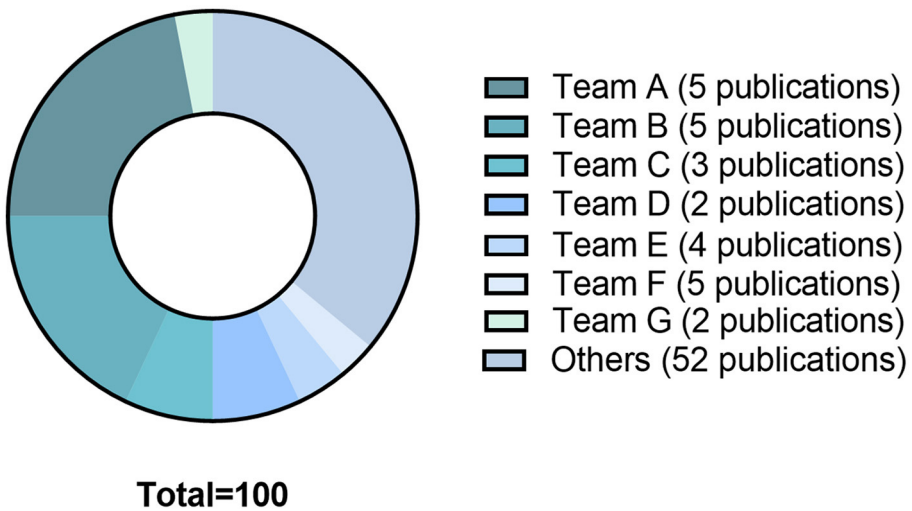

FIGURE 3 | The 78 studies included in the systematical review generated since their publication 3681 citations. The graph shows the distribution of citations by teams: Team A: Bederson, Mount Sinai School of Medicine, New York; Team B: Prunell, Department of Clinical Neuroscience, Section for Neurosurgery, Karolinska Institute, Stockholm, Sweden; Team C: Solomon, Department of Neurological Surgery, Columbia University College of Physicians and Surgeons, New York; Team D: Yamamoto, Department of Neurosurgery, Hamamatsu University School of Medicine, Hamamatsu, Japan; Team E: Macdonald RL, Division of Neurosurgery, University of Alberta, Edmonton, Canada. Team F: Thal Institute for Surgical Research, University of Munich Medical Center—Grosshadern, Munich, Germany; Team G: Warner DS, Department of Anesthesiology, Duke University Medical Center, Durham, North Carolina 27710, USA.

technique, perforation of the basilar artery and perforation of subarachnoid veins. Among the direct injection models, blood was injected into the *cisterna magna*, the pre-chiasmatic cistern, the cerebral cortex or directly into the circle of Willis. Blood was from autologous origin in 97% of publications ($n = 76$). Blood could be arterial ($n = 67$; 92%) or venous ($n = 7$; 10%). The nature of the blood was not specified in 3 studies. The injected blood volume varied across studies: the median

TABLE 1 | Characteristics of SAH models.

Characteristics of subarachnoid hemorrhage models	Number (%)
Species	
Rats	66 (85)
Mice	13 (17)
Method of induction of SAH	
Vascular perforation	
Circle of Willis	23 (29)
Basilar artery	4 (5)
Subarachnoid vein	1 (1)
Direct injection	
Cisterna magna	39 (50)
Prechiasmatic cistern	12 (15)
Cerebral cortex	1 (1)
Circle of Willis	1 (1)
Induced hypertension and elastase	1 (1)
Models with factors promoting cerebral ischemia	4 (5)
Number of direct blood injection in the subarachnoid space	
0	28 (37)
1	36 (47)
2	15 (20)
Vascular territory of SAH	
Anterior	38 (49)
Posterior	45 (58)
Blood	
Arterial	67 (92)
Venous	7 (10)
No specified	4 (5)
Management of anesthesia	
General anesthesia	77 (99)
No specified	1 (1)
Mechanical ventilation	38 (49)
Monitoring	
Invasive blood pressure	45 (58)
Intracranial pressure	30 (38)
Global cerebral blood flow	23 (29)
Local cerebral blood flow	21 (27)
Temperature	58 (75)
Glucose level	9 (12)
Study of cerebral ischemia	30 (38)
Positive diagnostic of ischemia	24 (26)
Ischemia at distance of subarachnoid hemorrhage	21 (27)
Cerebral cortex	16 (21)
Hippocampus	16 (21)
Cerebellum	1 (1)
Basal ganglia	4 (5)
Diagnostic of cerebral ischemia	
Imaging	3 (4)
Histology	24 (31)
Fluorojade B	5 (6)
Apoptosis	7 (9)
Quantitative assessment	8 (10)
Qualitative assessment	7 (9)
Parameters associated with ischemia	
Microthrombosis	6 (8)
Microglial activation	2 (3)
Inflammation (neutrophil polynuclear labeling)	1 (1)
Study of vasospasm	51 (67)
Imaging	25 (32)
Histology	34 (44)
Hematoxylin and eosin	20 (26)
Positive diagnostic of vasospasm	48 (62)
Study of cerebral blood flow	39 (50)
Doppler	25 (32)
Magnetic resonance imaging	11 (14)
Angiography	9 (10)
Others	7 (9)
Physical and behavioral examination	
Neurological assessment	19 (24)
Sensory-motor tests	18 (23)
Cognitive tests	7 (9)
General condition	32 (41)
Weight	12 (15)
Death	45 (58)

blood volume injected was 300 μL [100–700 μL] and 80 μL [50–100 μL] in rats and mice, respectively. Thirty-six studies (47%) described a model with a single injection. Two injections separated by a free period of 24 to 48 h were performed in 15 studies (20%). The aim of these double injection models was to increase the severity of the SAH, while maintaining an acceptable mortality rate. These double injection models were only performed in rats. One model used the induction of hypertension associated with elastase injection into the cerebrospinal fluid in order to promote the aneurysmal rupture (70). Some studies reported the use of adjuvants to promote the occurrence of ischemia. The first study published in 2011 described a direct injection model in insulin-resistant rats (64). Other studies combined induction of SAH by simple or double direct blood injections with the occlusion of the common carotid artery as an ischemia promoting factor (71). One of these models promoted occurrence of DCI, which was associated to the injection of blood, the occlusion of common carotid and the induction of spreading depolarization. Then, authors investigated the effect of an administration of a pro-inflammatory agent, before SAH induction (73).

In all studies, the procedure took place under general anesthesia. In 40 studies, the animals were kept in spontaneous ventilation during general anesthesia. An invasive blood pressure monitoring was used in 58% of the studies. Three studies performed an invasive monitoring of blood pressure in mice. Intracranial pressure was monitored during the procedure in 38% of the studies. One study performed an intracranial pressure monitoring in mice with the help of a sensor placed in the *cisterna magna* (42). Blood glucose monitoring was performed in 12% of studies ($n = 9$) and temperature monitoring was carried out in 75% of the studies ($n = 58$).

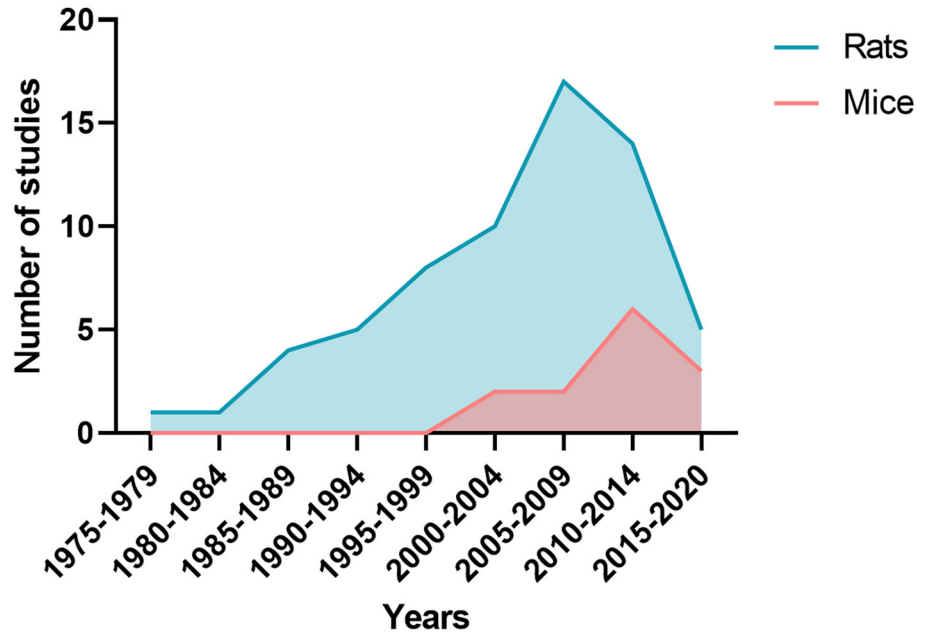

FIGURE 4 | Number of publications by five-year periods depending whether studies were performed on rats or mice.

Study of Vasospasm

From the 39 studies evaluating cerebral hemodynamics, 37 observed a decreased cerebral blood flow following SAH. The study window of cerebral blood flow varied according to the publications (**Figure 6**). Twenty-five studies searched the occurrence of arterial vasoconstriction with MRI, Doppler, angiography, videomicroscopy, positron emission tomography (PET) or photomicrography. All of them observed vasospasm. Thirty-four studies assessed vasospasm with histology (**Table 1**). The main staining was Hematoxylin and Eosin (20 studies). Histological study were performed at different times. The authors diagnosed vasospasm in 30 studies with histology. Vasospasm was studied in a total of 588 animals in 34 publications. The diagnosis was made in 513 animals (87%) but some authors did not specify the number of animals studied.

Study of Ischemia

Overall, 532 animals were screened for cerebral ischemia in 30 publications. A positive diagnosis was made in 196 animals (37%) but some of these publications ($n = 9$) did not specify the exact number of animals for which the positive diagnosis of ischemia was made. Out of 29 publications searching for ischemia with histological study, 24 reported evidence of ischemia. All these authors described occurrence of ischemia remotely from the origin of SAH. The existence of ischemia was mainly studied in two brain regions: the cortex and the hippocampus. The other brain regions explored were the cerebellum and basal ganglia. Different methods for studying ischemia were used in histology. Neuronal quantification was the main method (in 8 studies). The detection of apoptosis appeared to be the second way to explore ischemia (7 publications). Apoptosis was assessed by TUNEL staining or caspase activity assays. A specific labeling of neuronal death was also used by fluorojade B in 5 studies. Qualitative assessment of neurons was performed in 7 studies. Histological studies of ischemia were achieved at early and/or late times, as summarized on **Figure 6**. Some publications focused on the pathophysiological mechanisms underlying ischemia. Indeed, several studies have attempted to highlight phenomena of microthrombosis and neuroinflammation. Microthrombosis was evaluated by the presence of fibrin [anti-fibrin(ogen)] and platelet (anti-platelet GpIIbIIIa) aggregates by immunofluorescences studies. Neuroinflammation was evidenced at the local level by histological studies (neutrophils labeling), but also at the systemic level using markers, such as TNF and IL-1β. Two publications studied microglial activation *via* specific immuno-staining of microglia such as Iba-1 (73, 78). Only 4 studies investigated ischemia with MRI.

Behavioral Evaluation and Body Weight Monitoring

Behavioral assessment was performed in 32 studies. The general status of animals was described using the spontaneous locomotor activity, circling behavior, whisker movements, and coat state. Eighteen studies used sensorimotor tests for the quantitative behavioral assessment. These studies were performed with delays ranging from <24-h to 4 weeks after SAH induction. Three studies used the rotarod test. Tests assessing the cognitive abilities of animals were conducted in 7 studies. Among these studies, 4 used the Morris water maze to assess working memory. Body weight monitoring was carried out in 12 studies.

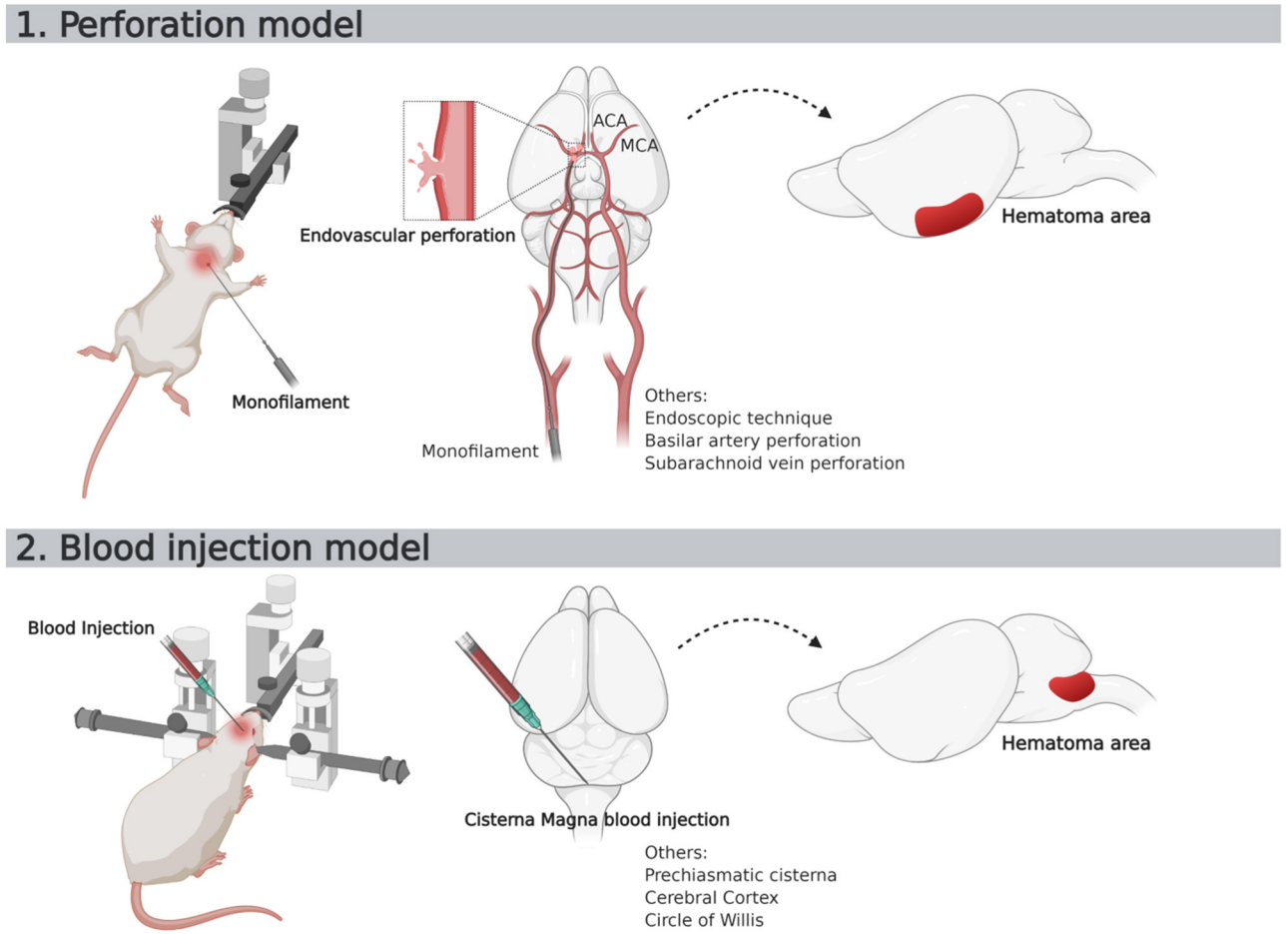

FIGURE 5 | Schematic representation of two most used SAH murine models. ACA, Anterior Cerebral Artery; MCA, Middle Cerebral Artery.

Mortality Rate

The mortality rate was reported in 58% of the studies ($n = 45$). However, the mortality study period and the death rate varied between studies. The direct-injection model into the *cisterna magna* was responsible for a mortality rate between 0 and 52%. The prechiasmatic cistern injection pattern induced a mortality rate ranging from 0 to 100%. The endovascular perforation model was responsible for a mortality rate between 6 to 65%.

Included Non-primates Studies

Finally, we also reviewed non-human primate models keeping the same eligibility criteria. Of 175 articles, citations from 22 reports were proved eligible (86–107). Then, we compared their principal characteristic to the rodent models, as shown on **Table 2**.

DISCUSSION

In this systematic review, we evaluated 78 publications and found that 8 different methods were used to induce hemorrhage in the subarachnoid spaces. These methods can be classified into three groups. In the first group, SAH is due to perforation of an arterial or venular vessel. In the second, a blood injection is performed in cerebrospinal fluid or directly in the brain parenchyma. In the third, SAH is induced by the combination of hypertension (angiotensin infusion) and elastase injection. The diversity of protocols notwithstanding, we found that no model was consistent with the clinical definition of DCI in humans; meaning that no model confirmed the evidence of cerebral infarction with imaging plus neurological deficits.

Many publications came from a small number of teams. In fact, over half of publications came from only 14 teams. Different modalities were used for SAH induction with various origin of the blood, vascular territory involved, severity of SAH, method for the monitoring, and management of anesthesia. The inconsistency of SAH models may threaten the reproducibility of preclinical research. For instance, in models involving injection of blood in rodent brains, stereotactic coordinates guide the injection, but the diagnostic of SAH through imaging or necropsy was rarely performed. Similarly, endovascular perforation models did not control the quantity of blood released in cerebrospinal fluid and thus variability occurs at this level.

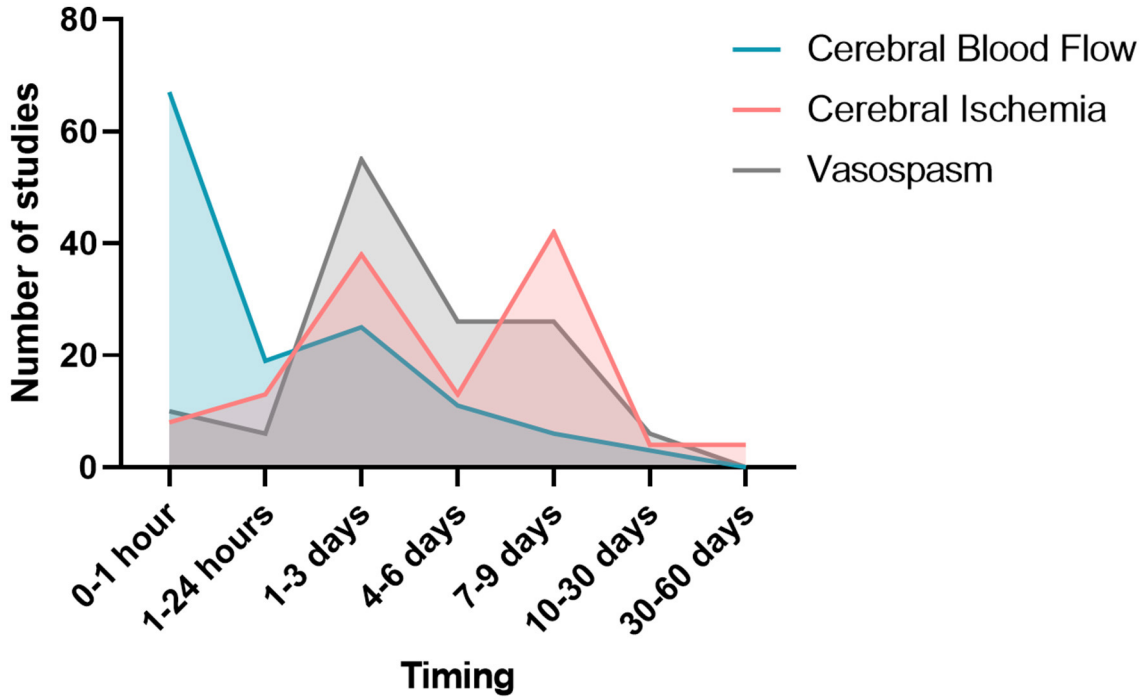

FIGURE 6 | Study window of vasospasm, cerebral blood flow, and cerebral ischemia.

TABLE 2 | Comparison between primates and rodents SAH models focusing on main characteristics.

Characteristics of experimental SAH models	**Number of publications (%)**	
Species	Primates ($n = 22$)	Rodents ($n = 78$)
SAH induction method		
Direct blood injection	22 (100)	53 (68)
Vascular perforation	0 (0)	28 (36)
Study of cerebral ischemia	3 (14)	30 (38)
Imaging	0 (0)	3 (4)
Histology	3 (14)	24 (31)
Study of cerebral vasospasm	21 (95)	51 (67)
Angiography	20	9 (10)
Histology	5 (23)	34 (44)
Positive diagnosis of vasospasm	22 (100)	48 (62)
Study of cerebral blood flow	6 (27)	39 (50)
Neurological examination	15 (68)	19 (24)
Delayed neurological deficits	3 (14)	ND

ND, not documented.

Besides, different methods may result in different hemodynamic and homeostasis conditions thereby affecting cerebral perfusion differently. Another concern is the possible irrelevance of described models to humans. More than half (58%) of the here-described SAH models involve the posterior cerebral circulation. In contrast, in humans, SAH occurs in most cases (90%) in the anterior cerebral circulation. We found that arterial vasospasm was the most frequently assessed outcome (67%; $n = 51$). On the other hand, cerebral ischemia, and neurological status, which lie at the root of DCI definition, were the outcomes assessed in only 38 and 24% of publications respectively (**Table 1**). Although it is difficult to estimate accurately the rate of vasospasm in these preclinical studies given the lack of precise data on the incidence rate, vasospasm is probably overestimated. Indeed, vasospasm was evidenced in 87% of animals as compared to a two third proportion of vasospasm observed in humans, only half of whom are symptomatic (108). With respect to ischemia outcomes, only 4 publications assessed ischemia through imaging (43). For the first of them, the result is questionable given that the surgical procedure contributes to early ischemia. This result was not consistent with the experts' definition of DCI in humans since ischemia was assessed 1 h after SAH induction while the definition excludes early lesions (occurring in the first 48 h) and procedure-related infarctions. In most publications, ischemia was assessed through histology as illustrated on the 10 most cited studies included in our systematic review (**Supplementary Table**). Different histological techniques were used for ischemia assessment such as neuronal counting or detection of apoptosis. These modalities could be challenged because, as in vasospasm, the incidence of ischemia may be overestimated in comparison with epidemiological human data. In humans, however, DCI is routinely diagnosed through MRI or computed tomography scan. We trust it would be valuable to use imaging more often in preclinical settings since ischemia is well defined by imaging. We found that behavioral studies of animals were rarely performed, and no standardized protocol was used to diagnose neurological deficits after brain injury.

Regarding the literature on the same topic, a previous systematic review focused on *in vivo* models of vasospasm (4). Authors concluded that despite a great number of experimental SAH methods, no consistent models could be identified and recommended. In this review, 66 inductions method of SAH were identified. But there results were not only restricted to rodents. In contrast, in our systematic review we purposely restricted our search to only rodents given that this species are far the most used in biomedical research. Rodents have a well-characterized genome, with a high quantity, and quality of resources available for preclinical studies. Another review by Kamp et al. (109) focused on the mortality in mouse models analyzing DCI after SAH. They found that the mortality rate following aneurysmal SAH and DCI was significantly lower in mice than in humans. As in our review, the timing to assess mortality was not standardized in mouse models, potentially influencing the mortality rate. The authors concluded that further analyses would be required to establish a link between mortality and DCI models. This conclusion challenge DCI models themselves as well as their outcomes. In a last systematic review, Oka et al. screened SAH animal models and focused on DCI and neurological deficit. The authors equally found that preclinical models do not consistently lead to DCI (110). These conclusions further challenge DCI models as well as their outcomes.

In we look in the literature, several pharmacological treatments have been tested in the last few years to prevent or treat DCI. Unfortunately, most were either negative or led to only mild improvement in clinical outcome.

The only treatment which has shown an improvement in the functional outcome and which is currently recommended with a Level of Evidence grade A, by the American Heart Association/American Stroke Association for prophylactic treatment after SAH is Nimodipine (111). Nimodipine is a calcium channel blocker, which has largely been tested. A meta-analysis conducted in 2011 found a reduction of death or severe disability in patients treated with a prophylactic administration as compared to controls (112). Interestingly, cerebral infarctions were reduced in the treated group, but vasospasm was not significantly impacted.

Dorhout Mees et al. made a review about antiplatelet agents that have failed to show any beneficial effect on outcome (measure by death or handicap) and DCI (113). An antagonist of Endothelin-1, Clazosentan has shown some improvement in both vasospasm and DCI, demonstrated in the large meta-analysis over 1900 patients (114). However, the phase III clinical trial CONSCIOUS 2 reported that Clazosentan has no significant effect on mortality and vasospasm-related morbidity or functional outcome (115). Besides these two targets, several anti-oxidants agents have been tested at large scale, with no positive result on the outcome (116). Statins have also been studied in large phase III randomized and controlled trials, as a therapeutic strategy blocking different pathophysiological targets at the same time, but they failed to show any beneficial effect on outcome (117).

These results of clinical trials are interesting both to understand the pathophysiology of DCI and to design better experimental models. For instance, since it showed benefit on DCI in clinical trials, nimodipine could be used to demonstrate the clinical relevance of experimental models of SAH. In a clinically relevant model, nimodipine should have beneficial effects, whereas the other treatments presented above should not.

We hope these results will influence future SAH preclinical research. Our findings emphasize the need to standardize the method for DCI diagnosis through short and long-term behavioral motor, emotional and cognitive evaluations, histology, and/or imaging. Most of preclinical studies assessed solely intracranial vasospasm while it may not be a relevant outcome. Indeed, it has been shown in therapeutic clinical trials that pharmacological treatments can reduce the angiographic vasospasm without any effect on functional outcome or mortality (118). We believe that a comprehensive neurobehavioral assessment, mortality and imaging proof of ischemia should be the preferred outcomes in animal studies. This approach is consistent with recommendations for animal studies of ischemic stroke (119) or intracerebral hemorrhage (120). The methodological heterogeneity we observed in experimental SAH studies could also be found in pathologies such as stroke (121), intracerebral hemorrhage (120) or brain tumor (122). We trust that the assessment of ischemia through the association of neurological evaluation and imaging in experimental studies will enhance the quality of translational research.

Our review has some limitations. First, we excluded publications evaluating therapeutic agents. This may exclude a number of articles with SAH models, but we considered that the aim of these studies was not to describe new SAH models but to assess drugs' efficacy. Therefore, these studies were not considered. Moreover, most of these studies used SAH models previously described. Second, we selected only *in vivo* studies. This point can be questionable because one could consider *in vitro* studies more relevant to understand pathophysiological mechanisms and to test therapeutics. But such *in vitro* models cannot recapitulate all features of the DCI definition, in particular neurological outcome, so that preclinical animal models remain the only option.

Finally, in our meta-analysis we decided to focus on rodents and not include other animals. Our choice was justified a priori considering the prevalence of these species in biomedical research. These species offer several possibilities with genetically modified strains to focus on a therapeutic approach. Nevertheless, aware of this limit of our review, we also reviewed non-human primate models (but this was not a pre-planned analysis) (**Table 2**).

This review demonstrates first the high proportion of non-human primate models with blood injection either directly with perivascular clot placement or by injection into a cerebrospinal fluid cisterna (prechiasmatic or *cisterna magna*). These models have the disadvantage to shifting away from pathophysiological mechanisms involving aneurysm rupture and acute autologous arterial blood extravasation. However, non-human primate models have an unquestionable benefit for neurological examination to detect delayed neurological deficit. This is a crucial advantage over rodent models to

make longitudinal examinations in the same animal and to relate more closely to the human disease, since the occurrence of neurological deficit is a diagnostic criterion of DCI.

Furthermore, as noted with rodent models, the study of vasospasm is largely overrepresented in non-human primate models (21 studies) compared to the study of DCI (3 studies) (**Table 2**). Thus, despite the possibility of more efficient clinical longitudinal follow-up in non-human primates, most of the studies did not take full advantage of the possibilities offered by these experimental models. Additionally, it is difficult to consider non-human primate models for exploratory research because of reproducibility, ethical issues, and cost. Non-human primates models could be envisaged for preclinical SAH research especially to monitor neurological status, in order to test therapeutic efficacy before clinical trial.

At the end of this review, we were able to highlight that no SAH model consistently lead to DCI rodents. In order to improve translational research, efforts should focus on developing clinical relevant models rather than continuing experimental studies with irrelevant models.

Moreover, we insist on future studies with an urgent need to develop SAH models focusing on the clinically relevant outcomes. Future studies should choose the appropriate experimental design study, in accordance with the existing data in DCI, while reflecting on the choice of species, SAH induction method and experimental study to answer the question from therapeutics and/or pathophysiological mechanistic.

Furthermore, researchers should respect principles of good laboratory practice with rigor and reproducibility as it is currently recommended (123), in order to standardize preclinical studies and results.

CONCLUSION

We described 8 published preclinical SAH models for rats and mice. Some of them allow for the assessment of vasospasm and/or ischemia; however, none allows the assessment of DCI as the scientific community in humans defined it with association between neurological evaluation and brain imaging. We believe developing a consensual preclinical model matching the human description of DCI will help enhance translational research.

DATA AVAILABILITY STATEMENT

The original contributions presented in the study are included in the article/**Supplementary Material**, further inquiries can be directed to the corresponding author/s.

AUTHOR CONTRIBUTIONS

All authors listed have made a substantial, direct and intellectual contribution to the work, and approved it for publication.

FUNDING

This work was supported by the French National Research Agency program PREDICT. SG was funded of Fondation pour la Recherche Medicale (FRM). **Figures 1**, **5** was created with BioRender.com.

SUPPLEMENTARY MATERIAL

The Supplementary Material for this article can be found online at: https://www.frontiersin.org/articles/10.3389/fcvm.2021.752769/full#supplementary-material

REFERENCES

1. Kassell NF, Torner JC, Haley EC, Jane JA, Adams HP, Kongable GL. The international cooperative study on the timing of aneurysm surgery. part 1: Overall management results. *J Neurosurg.* (1990) 73:18–36. doi: 10.3171/jns.1990.73.1.0037
2. Foreman B. The pathophysiology of delayed cerebral ischemia. *J Clin Neurophysiol.* (2016) 33:174–182. doi: 10.1097/WNP.0000000000000273
3. Dodd WS, Laurent D, Dumont AS, Hasan DM, Jabbour PM, Starke RM, et al. Pathophysiology of delayed cerebral ischemia after subarachnoid hemorrhage: a review. *J Am Heart Assoc.* (2021) 10:2145. doi: 10.1161/JAHA.121.021845
4. Marbacher S, Fandino J, Kitchen ND. Standard intracranial in vivo animal models of delayed cerebral vasospasm. *Br J Neurosurg.* (2010) 24:415–34. doi: 10.3109/02688691003746274
5. Pickard JD, Murray GD, Illingworth R, Shaw MDM, Teasdale GM, Foy PM, et al. Effect of oral nimodipine on cerebral infarction and outcome after subarachnoid haemorrhage : British aneurysm nimodipine trial. *Bmj.* (1989) 298:636–42. doi: 10.1136/bmj.298.6674.636
6. Moher D, Liberati A, Tetzlaff J. Altman DG. Preferred reporting items for systematic reviews and meta-analyses. *Ann Intern Med.* (2014) 151:264–9. doi: 10.7326/0003-4819-151-4-200908180-00135
7. Liberati A, Altman DG, Tetzlaff J, Mulrow C, Ioannidis JP, Clarke M, et al. Annals of internal medicine academia and clinic the PRISMA statement for reporting systematic reviews and meta-analyses of studies that evaluate health care interventions. *Ann Intern Med.* (2009) 151:W65–94. doi: 10.1371/journal.pmed.1000100
8. Barry KJ, Gogjian MA, Stein BM. Small animal model for investigation of subarachnoid hemorrhage and cerebral. *Vasospasm.* (1979) 5:538–542. doi: 10.1161/01.STR.10.5.538
9. Lacy PS, Earle M. A small animal model for electrocardiographic abnormalities observed after an experimental subarachnoid hemorrhage. *Stroke.* 14:371–7. doi: 10.1161/01.STR.14.3.371
10. Solomon R, Antunes JL, Chen RY, Bland L, Chien S. Decrease in cerebral blood flow in rats after experimental subarachnoid hemorrhage: a new animal model. *Stroke.* (1985) 16:58–64. doi: 10.1161/01.STR.16.1.58
11. Delgado TJ, Brismar J, Svendgaard NA. Subarachnoid haemorrhage in the rat: angiography and fluorescence microscopy of the major cerebral arteries. *Stroke.* 16:595–602. doi: 10.1161/01.STR.16.4.595
12. Dóczi T, Joó F, Sonkodi S, Adám G. Increased vulnerability of the blood-brain barrier to experimental subarachnoid hemorrhage in spontaneously hypertensive rats. *Stroke.* (1986) 17:498–501. doi: 10.1161/01.STR.17.3.498

13. Swift DM, Solomon R. Subarachnoid hemorrhage fails to produce vasculopathy or chronic blood flow changes in rats. *Stroke.* (1988) 19:878–82. doi: 10.1161/01.STR.19.7.878
14. Rickels E. Corrugation of cerebral vessels following subarachnoid hemorrhage : comparison of two experimental models of chronic. *Cerebr Vasospasm.* (1990) 186:178–186. doi: 10.1016/0014-4886(90)90156-M
15. Kader A, Krauss WE, Onesti ST, Elliott JP, Solomon RA. Chronic cerebral blood flow changes following experimental subarachnoid hemorrhage in rats. *Stroke.* (1990) 21(4):577-81.
16. Jackowski, Crockard, Burnstock G, Russell RR, Kristek F. The time course of intracranial pathophysiological changes following experimental subarachnoid haemorrhage in the rat. *J Cereb Blood Flow Metab.* (1990) 10:835–849. doi: 10.1038/jcbfm.1990.140
17. Ram Z, Sahar A, Hadani M. Ntdurochlrurgica vasospasm due to massive subarachnoid haemorrhage-a. *Rat Model.* (1991) 7:181–184. doi: 10.1007/BF01400688
18. Verlooy J, Van Reempts J, Haseldonckx M, Borgers M, Selosse P. The course of vasospasm following subarachnoid haemorrhage in rats. a vertebrobasilar angiographic study. *Acta Neurochir.* (1992) 117:48–52. doi: 10.1007/BF01400635
19. Bederson JB, Germano IM, Guarino L. Cortical blood flow and cerebral perfusion pressure in a new noncraniotomy model of subarachnoid hemorrhage in the Rat. *Stroke.* (1995) 26:1086–92. doi: 10.1161/01.STR.26.6.1086
20. Piepgras A, Thomé C, Schmiedek P. Characterization of an anterior circulation rat subarachnoid hemorrhage model. *Stroke.* (1995) 26:2347–52. doi: 10.1161/01.STR.26.12.2347
21. Veelken JA, Laing RJ, Jakubowski J. The Sheffield model of subarachnoid hemorrhage in rats. *Stroke.* (1995) 26:1279–1283. doi: 10.1161/01.STR.26.7.1279
22. Yamamoto S, Nishizawa S, Tsukada H, Kakiuchi T, Yokoyama T, Ryu H, et al. Cerebral blood flow autoregulation following subarachnoid hemorrhage in rats: Chronic vasospasm shifts the upper and lower limits of the autoregulatory range toward higher blood pressures. *Brain Res.* (1998) 782:194–201. doi: 10.1016/S0006-8993(97)01278-X
23. Bederson JB, Levy AL, Ding WH, Kahn R, DiPerna C, Jenkins AL, Vallabhajosyula P. Acute vasoconstriction after subarachnoid hemorrhage. *Neurosurgery.* (1998) 42:352–62. doi: 10.1097/00006123-199802000-00091
24. Busch E, Beaulieu C, de Crespigny A, Moseley ME. Diffusion MR imaging during acute subarachnoid hemorrhage in rats. *Stroke.* (1998) 29:2155–61. doi: 10.1161/01.STR.29.10.2155
25. Yamamoto S, Teng W, Kakiuchi T, Tsukada H. Disturbance of cerebral blood flow autoregulation in hypertension is attributable to ischaemia following subarachnoid haemorrhage in rats: a PET study. *Acta Neurochir.* (1999) 141:1213–9. doi: 10.1007/s007010050421
26. Zhao W, Ujiie H, Tamano Y, Akimoto K, Hori T, Takakura K. Sudden death in a rat subarachnoid hemorrhage model. *Neurol Med Chir.* (1999) 39:735–741. doi: 10.2176/nmc.39.735
27. Schwartz AY, Masago A, Sehba F, Bederson JB. Experimental models of subarachnoid hemorrhage in the rat: a refinement of the endovascular filament model. *J Neurosci Methods.* (2000) 96:161–7. doi: 10.1016/S0165-0270(00)00156-4
28. Alkan T, Tureyen K, Ulutas M, Kahveci N, Goren B, Korfali E, et al. Acute and delayed vasoconstriction after subarachnoid hemorrhage: local cerebral blood flow, histopathology, and morphology in the rat basilar artery. *Arch Physiol Biochem.* (2001) 109:145–53. doi: 10.1076/apab.109.2.145.4267
29. Alkan T, Kahveci N, Goren B, Korfali E, Ozluk K. Effects of interrupted and uninterrupted occlusion of the basilar artery on cerebral blood flow, and on neurological and histological outcome in rats with subarachnoid hemorrhage. *Arch Physiol Biochem.* (2001) 109:154–60. doi: 10.1076/apab.109.2.154.4275
30. Ergün R, Fernandez J, Misra M, Dujovny M. Endoscopic technique: a new model of subarachnoid hemorrhage in rats. *Neurol Res.* (2001) 2:627–30. doi: 10.1179/016164101101198910
31. Prunell GF, Mathiesen T, Svendgaard N. A new experimental model in rats for study of the pathophysiology of subarachnoid hemorrhage. *Neuroreport.* (2002) 13:2553–6. doi: 10.1097/00001756-200212200-00034
32. Longo M. Blandino a., Ascenti G, Ricciardi GK, Granata F, Vinci S. Cerebral angiography in the rat with mammographic equipment: a simple, cost-effective method for assessing vasospasm in experimental subarachnoid haemorrhage. *Neuroradiology.* (2002) 44:689–94. doi: 10.1007/s00234-002-0781-3
33. Gules I, Satoh M, Clower BENR, Nanda A. Zhang JH. Comparison of three rat models of cerebral vasospasm. *Physiology.* (2002) 3932:2551–9. doi: 10.1152/ajpheart.00616.2002
34. Glenn TC, Patel AB, Martin NA, Samii A, Jesus CDE, Hovda DA. Al GET. subarachnoid hemorrhage induces dynamic changes in regional cerebral metabolism in rats. *Physiology.* (2002) 19:2406. doi: 10.1089/089771502529324406
35. Parra A, Mcgirt MJ, Sheng H, Laskowitz DT, Pearlstein RD. Warner DS. Mouse model of subarachnoid hemorrhage associated cerebral vasospasm. *Methodol Anal.* (2002) 24:510–6. doi: 10.1179/016164102101200276
36. Lin C, Calisaneller T, Ukita N, Dumont AS, Kassell NF. Lee S. A murine model of subarachnoid hemorrhage-induced. *Cerebral v Asospasm.* (2003) 123:89–97. doi: 10.1016/S0165-0270(02)00344-8
37. Prunell GF. Experimental subarachnoid hemorrhage: subarachnoid blood volume,mortality rate, neuronal death,cerebral blood flow, and perfusion pressure in three different rat models. *Neurosurgery.* (2003) 52:165–76. doi: 10.1227/00006123-200301000-00022
38. Ono S, Date I, Onoda K, Ohmoto T. Time course of the diameter of the major cerebral arteries after subarachnoid. *Neurologic Res.* (2003) 25:535. doi: 10.1179/016164103101201535
39. Prunell GF, Mathiesen T, Svendgaard NA. Experimental subarachnoid hemorrhage: cerebral blood flow and brain metabolism during the acute phase in three different models in the rat. *Neurosurgery.* (2004) 54:426–36. doi: 10.1227/01.NEU.0000103670.09687.7A
40. Sehba F a, Mostafa G, Friedrich V, Bederson JB. Acute microvascular platelet aggregation after subarachnoid hemorrhage. *J Neurosurg.* (2005) 102:1094–100. doi: 10.3171/jns.2005.102.6.1094
41. Prunell GF, Svendgaard N-A, Alkass K, Mathiesen T. Delayed cell death related to acute cerebral blood flow changes following subarachnoid hemorrhage in the rat brain. *J Neurosurg.* (2005) 102:1046–54. doi: 10.3171/jns.2005.102.6.1046
42. Türeyen K, Nazlioglu HÖ, Alkan T, Kahveci N, Korfali E. Single or multiple small subarachnoid hemorrhages by puncturing a small branch of the rat basilar artery causes chronic cerebral vasospasm. *Neurosurgery.* (2005) 56:382–9. doi: 10.1227/01.NEU.0000148004.61621.D2
43. Van Den Bergh WM, Schepers J, Veldhuis WB, Nicolay K, Tulleken CF, Rinkel GJE. Magnetic resonance imaging in experimental subarachnoid haemorrhage. *Acta Neurochir.* (2005) 147:977–83. doi: 10.1007/s00701-005-0539-x
44. Weidauer S, Dettmann E. Assessment of vasospasm in experimental subarachnoid hemorrhage in rats by selective biplane digital subtraction angiography. *Neuroradiology.* (2006) 176–181. doi: 10.1007/s00234-005-0021-8
45. Vatter H, Weidauer S, Konczalla J, Dettmann E, Zimmermann M, Raabe A, et al. Time course in the development of cerebral vasospasm after experimental subarachnoid hemorrhage: clinical and neuroradiological assessment of the rat double hemorrhage model. *Neurosurgery.* (2006) 58:1190–6. doi: 10.1227/01.NEU.0000199346.74649.66

46. Turowski B, Hänggi D, Beck A, Aurich V. New angiographic measurement tool for analysis of small cerebral vessels : application to a subarachnoid haemorrhage model in the rat. *Neuroradiology.* (2007) 129–137. doi: 10.1007/s00234-006-0168-y
47. Britz GW, Meno JR, Park IS, Abel TJ, Chowdhary A, Nguyen TSK, et al. Time-dependent alterations in functional and pharmacological arteriolar reactivity after subarachnoid hemorrhage. *Stroke.* (2007) 38:1329–35. doi: 10.1161/01.STR.0000259853.43084.03
48. Sugawara T, Ayer R, Jadhav V, Zhang JH. A new grading system evaluating bleeding scale in filament perforation subarachnoid hemorrhage rat model. *J Neurosci Methods.* (2008) 167:327–34. doi: 10.1016/j.jneumeth.2007.08.004
49. Lee JY, Huang DL, Keep R, Sagher O. Characterization of an improved double hemorrhage rat model for the study of delayed cerebral vasospasm. *J Neurosci Methods.* (2008) 168:358–66. doi: 10.1016/j.jneumeth.2007.10.029
50. Takata K, Sheng H, Borel CO, Laskowitz DT, Warner DS. Lombard FW. Long-term cognitive dysfunction following experimental subarachnoid hemorrhage. . *New Perspect.* (2008) 213:336–44. doi: 10.1016/j.expneurol.2008.06.009
51. Thal SC, Meßmer K. Schmid-elsaesser R, Zausinger S. Neurological impairment in rats after subarachnoid hemorrhage—a comparison of functional tests. *J Neueologic Sci.* (2008) 268:150–9. doi: 10.1016/j.jns.2007.12.002
52. Park I, Meno JR, Witt CE, Suttle TK, Chowdhary A, Nguyen T, et al. Subarachnoid hemorrhage model in the rat : modification of the endovascular filament model. *J Neuro Sci Method.* (2008) 172:195–200. doi: 10.1016/j.jneumeth.2008.04.027
53. Altay T, Smithason S, Volokh N, Rasmussen PA, Ransohoff RM, Provencio JJ, et al. novel method for subarachnoid hemorrhage to induce vasospasm in mice. *J Neurosci Methods.* (2009) 183:136–40. doi: 10.1016/j.jneumeth.2009.06.027
54. Sabri M, Jeon H, Ai J, Tariq A, Shang X, Chen G, et al. Anterior circulation mouse model of subarachnoid hemorrhage. *Brain Res.* (2009) 1295:179–85. doi: 10.1016/j.brainres.2009.08.021
55. Sun BL, Zheng CB, Yang MF, Yuan H, Zhang SM, Wang LX. Dynamic alterations of cerebral pial microcirculation during experimental subarachnoid hemorrhage. *Cell Mol Neurobiol.* (2009) 29:235–41. doi: 10.1007/s10571-008-9316-8
56. Cansever T, Canbolat A, Talat K, Sencer A, Civelek E. Karasu A. Effects of arterial and venous wall homogenates, arterial and venous blood, and different combinations to the cerebral vasospasm in an experimental model. *Surgic Neurol.* (2009) 71:573–9. doi: 10.1016/j.surneu.2008.02.048
57. Silasi G. Colbourne F. Long-term assessment of motor and cognitive behaviours in the intraluminal perforation model of subarachnoid hemorrhage in rats. *Surgic Neurol.* (2009) 198:380–7. doi: 10.1016/j.bbr.2008.11.019
58. Westermaier T, Jauss A, Kunze E, Roosen K. Time-course of cerebral perfusion and tissue oxygenation in the first 6 h after experimental subarachnoid hemorrhage in rats. *Surgic Neurol.* (2009) 771–779. doi: 10.1038/jcbfm.2008.169
59. Güresir E, Raabe A, Jaiimsin A, Dias S, Raab P, Seifert V. Journal of the neurological sciences histological evidence of delayed ischemic brain tissue damage in the rat double-hemorrhage model. *J Neurol Sci.* (2010) 293:18–22. doi: 10.1016/j.jns.2010.03.023
60. Jeon H, Ai J, Sabri M, Tariq A, Macdonald RL. Learning deficits after experimental subarachnoid hemorrhage in rats. *NSC.* (2010) 169:1805–14. doi: 10.1016/j.neuroscience.2010.06.039
61. Tariq A, Ai J, Chen G, Sabri M, Jeon H, Shang X, et al. Loss of long-term potentiation in the hippocampus after experimental subarachnoid hemorrhage in rats. *NSC.* (2010) 165:418–26. doi: 10.1016/j.neuroscience.2009.10.040
62. Ramdurg SR, Suri A, Gupta D, Mewar S, Sharma U, Jagannathan NR, et al. Magnetic resonance imaging evaluation of subarachnoid hemorrhage in rats and the effects of intracisternal injection of papaverine and nitroglycerine in the management of cerebral vasospasm. *Neurol India.* (2010) 58:377–83. doi: 10.4103/0028-3886.65686
63. Feiler S, Friedrich B, Schöller K, Thal SC, Plesnila N. Standardized induction of subarachnoid hemorrhage in mice by intracranial pressure monitoring. *J Neurosci Methods.* (2010) 190:164–70. doi: 10.1016/j.jneumeth.2010.05.005
64. Institoris A, Snipes JA, Katakam P V, Domoki F, Boda K, Bari F, Busija DW. Impaired vascular responses of insulin-resistant rats after mild subarachnoid hemorrhage. *J Neurosci Methods.* (2011) 11:2080–2087. doi: 10.1152/ajpheart.01169.2010
65. Muñoz-Sánchez M, Egea-Guerrero JJ, Revuelto-Rey J, Moreno-Valladares M, Murillo-Cabezas F. A new percutaneous model of Subarachnoid Haemorrhage in rats. *J Neurosci Methods.* (2012) 211:88–93. doi: 10.1016/j.jneumeth.2012.08.010
66. Cai J, Sun Y, Yuan F, Chen L, He C, Bao Y, et al. A novel intravital method to evaluate cerebral vasospasm in rat models of subarachnoid hemorrhage : a study with synchrotron radiation. *Angiography.* (2012) 7:1–9. doi: 10.1371/journal.pone.0033366
67. Friedrich V, Flores R, Sehba FA. Cell death starts early after subarachnoid hemorrhage. *Neurosci Lett.* (2012) 512:6–11. doi: 10.1016/j.neulet.2012.01.036
68. Friedrich B, Müller F, Feiler S, Schöller K, Plesnila N. Experimental subarachnoid hemorrhage causes early and long-lasting microarterial constriction and microthrombosis: an in-vivo microscopy study. *J Cereb Blood Flow Metab.* (2012) 32:447–55. doi: 10.1038/jcbfm.2011.154
69. Sabri M, Ai J, Lakovic K, Ilodigwe D. Macdonald RL. Mechanisms of microthrombi formation after experimental subarachnoid hemorrhage. *J Neurosci Methods.* (2012) 224:26–37. doi: 10.1016/j.neuroscience.2012.08.002
70. Makino H, Tada Y, Wada K, Liang EI, Chang M, Mobashery S, et al. Pharmacological stabilization of intracranial aneurysms in mice: a feasibility study. *Stroke.* (2012) 43:2450–6. doi: 10.1161/STROKEAHA.112.659821
71. Güresir E, Vasiliadis N, Dias S, Raab P, Seifert V, Vatter H. The effect of common carotid artery occlusion on delayed brain tissue damage in the rat double subarachnoid hemorrhage model. *Acta Neurochir.* (2012) 154:11–9. doi: 10.1007/s00701-011-1191-2
72. Dudhani R V, Kyle M, Dedeo C, Riordan M, Deshaies EM. A low mortality rat model to assess delayed cerebral vasospasm after experimental subarachnoid hemorrhage. *J Vis Exp*. (2013) 71:e4157. doi: 10.3791/4157
73. Smithason S, Moore SK, Provencio JJ. Low-dose lipopolysaccharide injection prior to subarachnoid hemorrhage modulates delayed deterioration associated with vasospasm in subarachnoid hemorrhage. in Acta Neurochirurgica. *Supplementum*. (2013) 13:253–258. doi: 10.1007/978-3-7091-1192-5_45
74. Tiebosch CW, Van Den Bergh WM, Bouts MJRJ, Zwartbol R, Van Der Toorn A, Dijkhuizen RM. Progression of brain lesions in relation to hyperperfusion from subacute to chronic stages after experimental subarachnoid hemorrhage: a multiparametric MRI study. *Cerebrovasc Dis*. (2013) 36:167–72. doi: 10.1159/000352048
75. Koide M, Bonev AD, Nelson MT, Wellman GC. "Subarachnoid blood converts neurally evoked vasodilation to vasoconstriction in rat brain cortex," in *Acta Neurochirurgica, Supplementum*, p. 167–171. (2013).
76. Boyko M, Azab AN, Kuts R, Fredrick B, Evan S, Melamed I, et al. The neurobehavioral profile in rats after subarachnoid hemorrhage. *Brain Res.* (2013) 1491:109–16. doi: 10.1016/j.brainres.2012.10.061
77. Milner E, Holtzman JC, Friess S, Hartman RE, Brody DL, Han BH, et al. Endovascular perforation subarachnoid hemorrhage fails to cause Morris water maze deficits in the mouse. *J Cereb Blood Flow Metab.* (2014) 14:1–9. doi: 10.1038/jcbfm.2014.108
78. Kooijman E, Nijboer CH, Van Velthoven CTJ, Mol W, Dijkhuizen RM, Kesecioglu J, et al. Long-term functional consequences and ongoing cerebral inflammation after subarachnoid hemorrhage in the rat. *PLoS ONE*. (2014) 9:90584. doi: 10.1371/journal.pone.0090584
79. Hamming AM, Wermer MJH, Umesh Rudrapatna S, Lanier C, van Os HJA, van den Bergh WM, et al. Spreading depolarizations increase delayed brain injury in a rat model of subarachnoid hemorrhage. *J Cereb Blood Flow Metab*. (2016) 36:1224–31. doi: 10.1177/0271678X15619189

80. Sun Y, Shen Q, Watts LT, Muir ER, Huang S, Yang GY, et al. Multimodal MRI characterization of experimental subarachnoid hemorrhage. *Neuroscience*. (2016) 316:53–62. doi: 10.1016/j.neuroscience.2015.12.027
81. Oka F, Hoffmann U, Lee JH, Shin HK, Chung DY, Yuzawa I, et al. Requisite ischemia for spreading depolarization occurrence after subarachnoid hemorrhage in rodents. *J Cereb Blood Flow Metab*. (2017) 37:1829–40. doi: 10.1177/0271678X16659303
82. El Amki M, Dubois M, Lefevre-Scelles A, Magne N, Roussel M, Clavier T, et al. Long-lasting cerebral vasospasm, microthrombosis, apoptosis and paravascular alterations associated with neurological deficits in a mouse model of subarachnoid hemorrhage. *Mol Neurobiol*. (2018) 55:2763–79. doi: 10.1007/s12035-017-0514-6
83. Malinova V, Psychogios MN, Tsogkas I, Koennecke B, Bleuel K, Iliev B, et al. MR-angiography allows defining severity grades of cerebral vasospasm in an experimental double blood injection subarachnoid hemorrhage model in rats. *PLoS ONE*. (2017) 12:e0171121. doi: 10.1371/journal.pone.0171121
84. Yang L, Lai WT, Wu YS, Zhang JA, Zhou XH, Yan J, et al. Simple and efficient rat model for studying delayed cerebral ischemia after subarachnoid hemorrhage. *J Neurosci Methods*. (2018) 304:146–53. doi: 10.1016/j.jneumeth.2018.04.011
85. Dienel A, Ammassam Veettil R, Hong SH, Matsumura K, Kumar TP, Yan Y, et al. Microthrombi correlates with infarction and delayed neurological deficits after subarachnoid hemorrhage in mice. *Stroke*. (2020) 51:2249–54. doi: 10.1161/STROKEAHA.120.029753
86. Goulay R, Flament J, Gauberti M, Naveau M, Pasquet N, Gakuba C, et al. Subarachnoid hemorrhage severely impairs brain parenchymal cerebrospinal fluid circulation in nonhuman primate. *Stroke*. (2017) 48:2301–5. doi: 10.1161/STROKEAHA.117.017014
87. Fathi AR, Pluta RM, Bakhtian KD Qi M, Lonser RR. Reversal of cerebral vasospasm *via* intravenous sodium nitrite after subarachnoid hemorrhage in primates: laboratory investigation. *J Neurosurg*. (2011) 115:1213–20. doi: 10.3171/2011.7.JNS11390
88. Schatlo B, Dreier JP, Gläsker S, Fathi AR, Moncrief T, Oldfield EH, et al. Report of selective cortical infarcts in the primate clot model of vasospasm after subarachnoid hemorrhage. *Neurosurgery*. (2010) 67:721–8. doi: 10.1227/01.NEU.0000378024.70848.8F
89. Schatlo B, Gläsker S, Zauner A, Thompson BG, Oldfield EH, Pluta RM. Continuous neuromonitoring using transcranial Doppler reflects blood flow during carbon dioxide challenge in primates with global cerebral ischemia. *Neurosurgery*. (2009) 64:1148–54. doi: 10.1227/01.NEU.0000343542.61238.DF
90. Clatterbuck RE, Gailloud P, Tierney T, Clatterbuck VM, Murphy KJ, Tamargo RJ. Controlled release of a nitric oxide donor for the prevention of delayed cerebral vasospasm following experimental subarachnoid hemorrhage in nonhuman primates. *J Neurosurg*. (2005) 103:745–51. doi: 10.3171/jns.2005.103.4.0745
91. Clatterbuck RE, Gailloud P, Ogata L, Gebremariam A, Dietsch GN, Murphy KJ, et al. Prevention of cerebral vasospasm by a humanized anti-CD11/CD18 monoclonal antibody administered after experimental subarachnoid hemorrhage in nonhuman primates. *J Neurosurg*. (2003) 99:376–82. doi: 10.3171/jns.2003.99.2.0376
92. Macdonald RL, Zhang ZD, Curry D, Elas M, Aihara Y, Halern H, Jahromi BS, Johns L. Intracisternal sodium nitroprusside fails to prevent vasospasm in nonhuman primates. *Neurosurgery*. (2002) 51:761–770. doi: 10.1097/00006123-200209000-00027
93. Handa Y, Kaneko M, Takeuchi H, Tsuchida A, Kobayashi H, Kubota T. Effect of an antioxidant, ebselen, on development of chronic cerebral vasospasm after subarachnoid hemorrhage in primates. *Surg Neurol*. (2000) 53:323–9. doi: 10.1016/S0090-3019(00)00168-3
94. Handa Y, Kaneko M, Matuda T, Kobayashi H, Kubota T. In vivo proton magnetic resonance spectroscopy for metabolic changes in brain during chronic cerebral vasospasm in primates. *Neurosurgery*. (1997) 40:773–81. doi: 10.1097/00006123-199704000-00023
95. Pluta RM, Thompson BG, Dawson TM, Snyder SH, Boock RJ, Oldfield EH. Loss of nitric oxide synthase immunoreactivity in cerebral vasospasm. *J Neurosurg*. (1996) 84:648–54. doi: 10.3171/jns.1996.84.4.0648
96. Hariton GB, Findlay JM, Weir BKA, Kasuya H, Grace MGA, Mielke BW. Comparison of intrathecal administration of urokinase and tissue plasminogen activator on subarachnoid clot and chronic vasospasm in a primate model. *Neurosurgery*. (1993) 33:691–7. doi: 10.1227/00006123-199310000-00020
97. Kobayashi H, Ide H, Aradachi H, Arai Y, Handa Y, Kubota T. Histological studies of intracranial vessels in primates following transluminal angioplasty for vasospasm. *J Neurosurg*. (1993) 78:481–6. doi: 10.3171/jns.1993.78.3.0481
98. Handa Y, Kubota T, Tsuchida A, Kaneko M, Caner H, Kobayashi H, et al. Effect of systemic hypotension on cerebral energy metabolism during chronic cerebral vasospasm in primates. *J Neurosurg*. (1993) 78:112–9. doi: 10.3171/jns.1993.78.1.0112
99. Handa Y, Hayashi M, Takeuchi H, Kubota T, Kobayashi H, Kawano H. Time course of the impairment of cerebral autoregulation during chronic cerebral vasospasm after subarachnoid hemorrhage in primates. *J Neurosurg*. (1992) 76:493–501. doi: 10.3171/jns.1992.76.3.0493
100. Macdonald RL, Weir BKA, Runzer TD, Grace MGA, Findlay JM, Saito K, et al. Etiology of cerebral vasospasm in primates. *J Neurosurg*. (1991) 75:415–24. doi: 10.3171/jns.1991.75.3.0415
101. Handa Y, Kabuto M, Kobayashi H, Kawano H, Takeuchi H, Hayashi M. The correlation between immunological reaction in the arterial wall and the time course of the development of cerebral vasospasm in a primate model. *Neurosurgery*. (1991) 10:542. doi: 10.1097/00006123-199104000-00010
102. Takeuchi H, Handa Y, Kobayashi H, Kawano H, Hayashi M. Impairment of cerebral autoregulation during the development of chronic cerebral vasospasm after subarachnoid hemorrhage in primates. *Neurosurgery*. (1991) 19:41. doi: 10.1097/00006123-199101000-00007
103. Kanamaru K, Weir BK, Findlay JM, Grace M, Macdonald RL. A dosage study of the effect of the 21-aminosteroid U74006F on chronic cerebral vasospasm in a primate model. *Neurosurgery*. (1990) 27:28–29. doi: 10.1097/00006123-199007000-00004
104. Findlay JM, Weir BK, Kanamaru K, Grace M, Baughman R. The effect of timing of intrathecal fibrinolytic therapy on cerebral vasospasm in a primate model of subarachnoid hemorrhage. *Neurosurgery*. (1990) 26:201–16. doi: 10.1097/00006123-199002000-00003
105. Noseworthy TW, Weir B, Boisvert D, Espinosa F, Overton T, Marshal ML. Effect of reserpine-kanamycin treatment on chronic vasospasm after platelet-enriched subarachnoid hemorrhage in primates. *Neurosurgery*. (1984) 14:193–7. doi: 10.1227/00006123-198402000-00013
106. Svendgaard NA, Brismar J, Delgado T, Egund N, Owman C, Rodacki MA, et al. Late cerebral arterial spasm: the cerebrovascular response to hypercapnia, induced hypertension and the effect of Nimodipine on blood flow autoregulation in experimental subarachnoid hemorrhage in primates. *Gen Pharmacol*. (1983) 14:167–72. doi: 10.1016/0306-3623(83)90093-9
107. Rothberg CS, Weir B, Overton TR. Treatment of subarachnoid hemorrhage with sodium nitroprusside and phenylephrine: An experimental study. *Neurosurgery*. (1979) 5:588–95. doi: 10.1227/00006123-197911000-00008
108. Vergouwen MDI, Ilodigwe D, Macdonald RL. Contributes to poor outcome by vasospasm-dependent and -independent effects. *Stroke*. (2011) 42924–929. doi: 10.1161/STROKEAHA.110.597914
109. Kamp MA, Lieshout JH. Van, Dibué-adjei M, Weber JK, Schneider T, Restin T, Fischer I. A systematic and meta-analysis of mortality in experimental mouse models analyzing delayed cerebral ischemia after subarachnoid hemorrhage. *Transl Stroke Res*. (2017) 8:206–19. doi: 10.1007/s12975-016-0513-3
110. Care N, Oka F, Chung DY, Suzuki M, Ayata C. Delayed cerebral ischemia after subarachnoid hemorrhage : experimental—clinical disconnect and the unmet need. *Neurocrit Care*. (2019) 32:238–51. doi: 10.1007/s12028-018-0650-5
111. Connolly ES, Rabinstein AA, Carhuapoma JR, Derdeyn CP, Dion J, Higashida RT, et al. Guidelines for the management of aneurysmal subarachnoid hemorrhage: a guideline for healthcare professionals from the American Heart Association/american Stroke Association. *Stroke*. (2012) 43:1711–37. doi: 10.1161/STR.0b013e3182587839
112. Liu GJ, Luo J, Zhang LP, et al. Meta-analysis of the effectiveness and safety of prophylactic use of nimodipine in patients with an aneurysmal subarachnoid haemorrhage. *CNS Neurol Disord Drug Targets*. (2011) 10:834–44. doi: 10.2174/187152711798072383
113. Dorhout Mees SM, Kinkel GJ, Feigin VL, Alga A, van der Bergh WM, Vermeulen M, van Gijn J. Calcium antagonists for aneurysmal

subarachnoid haemorrhage. *Cochrane database Syst Rev.* (2007) 2007:pub3. doi: 10.1002/14651858.CD000277.pub3
114. Guo J, Shi Z, Yang K, Jiang L. Endothelin receptor antagonists for subarachnoid hemorrhage. *Cochrane database Syst Rev.* (2012) 9:pb2. doi: 10.1002/14651858.CD008354.pub2
115. Macdonald RL, Higashida RT, Keller E, Mayer SA, Molyneux A, Raabe A, Vajkoczy P, Wanke I, Bach D, Frey A, et al. Clazosentan, an endothelin receptor antagonist, in patients with aneurysmal subarachnoid haemorrhage undergoing surgical clipping: a randomised, double-blind, placebo-controlled phase 3 trial (CONSCIOUS-2). *Lancet Neurol.* (2011) 10:618–25. doi: 10.1016/S1474-4422(11)70108-9
116. Zhang S, Wang L, Liu M, Wu B. Tirilazad for aneurysmal subarachnoid haemorrhage. *Cochrane Database Syst Rev.* (2010) 12:688362. doi: 10.1002/14651858.CD006778.pub2
117. Kirkpatrick PJ, Turner CL, Smith C, Hutchinson PJ, Murray GD. STASH collaborators. Simvastatin in aneurysmal subarachnoid haemorrhage (STASH): a multicentre randomised phase 3 trial. *Lancet Neurol.* (2014) 13:666–75. doi: 10.1016/S1474-4422(14)70084-5
118. Trial PPD, Macdonald RL, Kassell NF, Mayer S, Ruefenacht D, Schmiedek P, et al. Clazosentan to overcome neurological ischemia and hemorrhage (CONSCIOUS-1). *Stroke.* (2008) 8:3015–21. doi: 10.1161/STROKEAHA.108.519942
119. Bart van der Worp H, Howells DW, Sena ES, Porritt MJ, Rewell S, O'Collins V, Macleod MR. Can animal models of disease reliably inform human studies? *PLoS Med.* (2010) 7:1–8. doi: 10.1371/journal.pmed.1000245
120. Frantzias J, Sena ES, MacLeod MR, Salman RAS. Treatment of intracerebral hemorrhage in animal models: Meta-analysis. *Ann Neurol.* (2011) 69:389–99. doi: 10.1002/ana.22243
121. Van Der Worp HB, De Haan P, Morrema E, Kalkman CJ. Methodological quality of animal studies on neuroprotection in focal cerebral ischaemia. *J Neurol.* (2005) 252:1108–14. doi: 10.1007/s00415-005-0802-3
122. Hirst TC, Vesterinen HM, Sena ES, Egan KJ, MacLeod MR, Whittle IR. Systematic review and meta-analysis of temozolomide in animal models of glioma: Was clinical efficacy predicted. *Br J Cancer.* (2013) 108:64–71. doi: 10.1038/bjc.2012.504
123. Percie du Stert N, Hurst V, Ahluwalia A, et al. The ARRIVE guidelines 2.0: Updated guidelines for reporting animal research. *PLoS Biol.* (2020) 18:3000140. doi: 10.1371/journal.pbio.3000410

Conflict of Interest: The authors declare that the research was conducted in the absence of any commercial or financial relationships that could be construed as a potential conflict of interest.

Publisher's Note: All claims expressed in this article are solely those of the authors and do not necessarily represent those of their affiliated organizations, or those of the publisher, the editors and the reviewers. Any product that may be evaluated in this article, or claim that may be made by its manufacturer, is not guaranteed or endorsed by the publisher.

Copyright © 2021 Goursaud, Martinez de Lizarrondo, Grolleau, Chagnot, Agin, Maubert, Gauberti, Vivien, Ali and Gakuba. This is an open-access article distributed under the terms of the Creative Commons Attribution License (CC BY). The use, distribution or reproduction in other forums is permitted, provided the original author(s) and the copyright owner(s) are credited and that the original publication in this journal is cited, in accordance with accepted academic practice. No use, distribution or reproduction is permitted which does not comply with these terms.

frontiers in Cardiovascular Medicine

ORIGINAL RESEARCH
published: 18 November 2021
doi: 10.3389/fcvm.2021.734392

Pre-operative Cerebral Small Vessel Disease on MR Imaging Is Associated With Cerebral Hyperperfusion After Carotid Endarterectomy

Xiaoyuan Fan[1†], Zhichao Lai[2†], Tianye Lin[1], Hui You[1], Juan Wei[3], Mingli Li[1], Changwei Liu[2] and Feng Feng[1,4]*

[1] Department of Radiology, Peking Union Medical College Hospital, Chinese Academy of Medical Sciences and Peking Union Medical College, Beijing, China, [2] Department of Vascular Surgery, Peking Union Medical College Hospital, Chinese Academy of Medical Sciences and Peking Union Medical College, Beijing, China, [3] General Electric Healthcare, MR Research China, Beijing, China, [4] State Key Laboratory of Difficult, Severe and Rare Diseases, Peking Union Medical College Hospital, Chinese Academy of Medical Sciences and Peking Union Medical College, Beijing, China

OPEN ACCESS

Edited by:
Yacine Boulaftali,
Institut National de la Santé et de la Recherche Médicale (INSERM), France

Reviewed by:
Jose Paulo Andrade,
Universidade do Porto, Portugal
George Galyfos,
National and Kapodistrian University of Athens, Greece

***Correspondence:**
Feng Feng
cjr.fengfeng@vip.163.com

[†] These authors have contributed equally to this work and share first authorship

Specialty section:
This article was submitted to Atherosclerosis and Vascular Medicine, a section of the journal Frontiers in Cardiovascular Medicine

Received: 01 July 2021
Accepted: 21 October 2021
Published: 18 November 2021

Citation:
Fan X, Lai Z, Lin T, You H, Wei J, Li M, Liu C and Feng F (2021) Pre-operative Cerebral Small Vessel Disease on MR Imaging Is Associated With Cerebral Hyperperfusion After Carotid Endarterectomy. Front. Cardiovasc. Med. 8:734392. doi: 10.3389/fcvm.2021.734392

Objectives: To determine whether pre-operative cerebral small vessel disease is associated with cerebral hyperperfusion (CH) after carotid endarterectomy (CEA).

Methods: Seventy-seven patients (mean age of 66 years and 58% male) undergoing CEA for carotid stenosis were investigated using brain MRI before and after surgery. CH was defined as an increase in cerebral blood flow > 100% compared with pre-operative values on arterial spin labeling MR images. The grade or the number of four cerebral small vessel disease markers (white matter hyperintensities, lacunes, perivascular spaces, and cerebral microbleeds) were evaluated based on pre-operative MRI. Cerebral small vessel disease markers were correlated with CH by using multivariate logistic regression analysis. The cutoff values of cerebral small vessel disease markers for predicting CH were assessed by receiver-operating characteristic curve analysis.

Results: CH after CEA was observed in 16 patients (20.78%). Logistic regression analysis revealed that white matter hyperintensities (OR 3.09, 95% CI 1.72–5.54; $p < 0.001$) and lacunes (OR 1.37, 95% CI 1.06–1.76; $p = 0.014$) were independently associated with post-operative CH. Receiver-operating characteristic curve analysis showed that Fazekas score of white matter hyperintensities ≥3 points [area under the curve (AUC) = 0.84, sensitivity = 81.3%, specificity = 73.8%, positive predictive value (PPV) = 44.8% and negative predictive value (NPV) = 93.8%] and number of lacunes ≥ 2 (AUC = 0.73, sensitivity = 68.8%, specificity = 78.7%, PPV = 45.8% and NPV = 90.6%) were the optimal cutoff values for predicting CH.

Conclusion: In patients with carotid stenosis, white matter hyperintensities and lacunes adversely affect CH after CEA. Based on the NPVs, pre-operative MR imaging can help identify patients who are not at risk of CH.

Keywords: cerebral small vessel disease, carotid stenosis, carotid endarterectomy, hyperperfusion syndrome, magnetic resonance imaging

INTRODUCTION

Carotid endarterectomy (CEA) is an established procedure for the prevention of further ischemic events caused by carotid stenosis. However, post-operative complications may reduce the benefits of surgery. Cerebral hyperperfusion syndrome (CHS), characterized by severe throbbing headache, confusion, seizures, focal neurological deficits and occasional intracranial hemorrhage, is associated with a mortality rate of 38.2% and permanent disability of 28% (1). CHS often occurs in patients with cerebral hyperperfusion (CH), which is defined as an increase in perfusion by >100% after surgery compared with baseline (2). If not recognized and treated early, a subset of CH-patients may further develop CHS. Impaired cerebral autoregulation is the most accepted mechanism for CH (3). After carotid revascularization, impaired cerebral autoregulation cannot maintain a stable cerebral blood flow (CBF) *via* constriction of cerebral arterioles and capillaries in response to a sudden increase in cerebral perfusion pressure, which leads to CH.

From the perspective of the pathogenesis of CH, pre-operative cerebral small vessel disease (SVD) may adversely affect CH after CEA (2). Cerebral SVD is a disorder of the cerebral arterioles and capillaries with cerebral small vessel endothelial dysfunction being the major pathological mechanism. Endothelial damage leads to the limitation of vasomotor function of cerebral small vessels, and then impaired cerebrovascular autoregulation ability (4). Common cerebral SVD lesions on magnetic resonance imaging (MRI) include white matter hyperintensity (WMHs), lacunes, perivascular spaces (PVSs), and cerebral microbleeds (CMBs) (5). A previous study (6) found in patients with carotid occlusion, ipsilateral WMHs were specific and sensitive for the presence and severity of decreased cerebrovascular reserve, which is an important manifestation of cerebral autoregulation (7) and recommended as the gold standard for predicting CH (8). This study also gave a hint that pre-operative cerebral SVD may be associated with CH after CEA. However, the relationship between cerebral SVD and CH has not been confirmed until now.

The common cerebral SVD lesions on MRI are reliable and easy to collect as long as the standardized definitions are adopted (5); thus, pre-operative cerebral SVD may be useful imaging markers for the prediction of CH that can be applied in clinical practice. This study aimed to investigate whether pre-operative cerebral SVD was associated with CH after CEA, and to exhibit practical cutoff values of cerebral SVD markers for predicting CH. In a group of patients undergoing CEA for carotid stenosis, we evaluated the relationship between cerebral SVD and CH using a combination of MRI methods including conventional structural imaging and perfusion weighted imaging.

MATERIALS AND METHODS

Study Design and Patients

This prospective, single-center observational study was approved by the Medical Ethics Committee of the Peking Union Medical College Hospital, in line with the Declaration of Helsinki. All participants provided written informed consent for this study.

We consecutively enrolled patients who underwent CEA for unilateral or bilateral carotid stenosis [≥50% for symptomatic stenosis or ≥70% for asymptomatic stenosis, according to the North American Symptomatic Carotid Endarterectomy Trial (NASCET) grading (9)] diagnosed with computed tomography angiography. The exclusion criteria included: (1) patients with intracranial artery stenosis ≥50% or occlusion shown by pre-operative computed tomography angiography, (2) history of ipsilateral CEA and re-admission due to carotid re-stenosis, (3) contraindications of MRI scanning or refuse MRI scanning, or (4) artifacts on MR images that interfere with evaluation. Pre-operative MRI was obtained within 2 weeks before CEA and post-operative MRI was obtained within 7 days after CEA. From May 2015 to March 2021, 97 patients were initially included in this study. Three patients had ipsilateral middle cerebral artery occlusion, 2 patients had a history of ipsilateral CEA, 12 patients had contraindications of MRI scanning and 3 patients had artifacts on MRI. A final 77 patients were enrolled in our study. A flow chart of the patient enrollment is shown in **Figure 1**.

MRI

All MRI examinations were performed on a 3.0 T scanner (Discovery 750, GE Healthcare) with an eight-channel phased-array head coil. Standard pseudo-continuous arterial spin labeling (ASL) was performed with a 3D stack-of-spirals fast-spin-echo readout: labeling duration/post labeling delay = 1,450/2,025 ms, TR/TE = 4,886/10.5 ms, in-plane spiral number 8, points per spiral 512, field of view (FOV) = 240 mm × 240 mm, in-plane resolution 3.75 mm × 3.75 mm, 40 slices and slice thickness = 4 mm. CBF maps of standard ASL were generated on GE AW 4.5 workstation by a commercial software 3D ASL Functool kit. Conventional MRI sequences including diffusion-weighted imaging, T1-weighted, T2-weighted, fluid-attenuated inversion recovery, and T2*-weighted gradient-recalled echo imaging were also performed (**Supplementary Table 1**).

Evaluation of Cerebral SVD

Four imaging markers of cerebral SVD on MRI including WMHs, lacunes, PVSs, and CMBs were recorded according to the previously reported neuroimaging standards (5). **Table 1** shows the detailed evaluation criteria of four MRI markers and the total cerebral SVD burden score. Briefly, WMHs were graded using the Fazekas score ranged from 0 to 6 by summing the deep and periventricular WMH scores (10). The number of lacunes located in the territory of a perforating arteriole was conservatively counted. The number of CMBs not strictly located in lobes was also recorded. We graded the number of PVSs in the basal ganglia with a three-category ordinal scale as follows: 0–10 (category 1), 11–25 (category 2), and >25 (category 3) (10). For each patient, an overall cerebral SVD burden score was calculated according to the presence of each cerebral SVD marker (11). The overall cerebral SVD score ranged from 0 to 4.

Two neuroradiologists (H. You and T. Lin, with 19 and 7 years of neuroradiology experience, respectively) were trained before evaluation and assessed the MRI data blindly for clinical information. Disagreements were resolved by consensus.

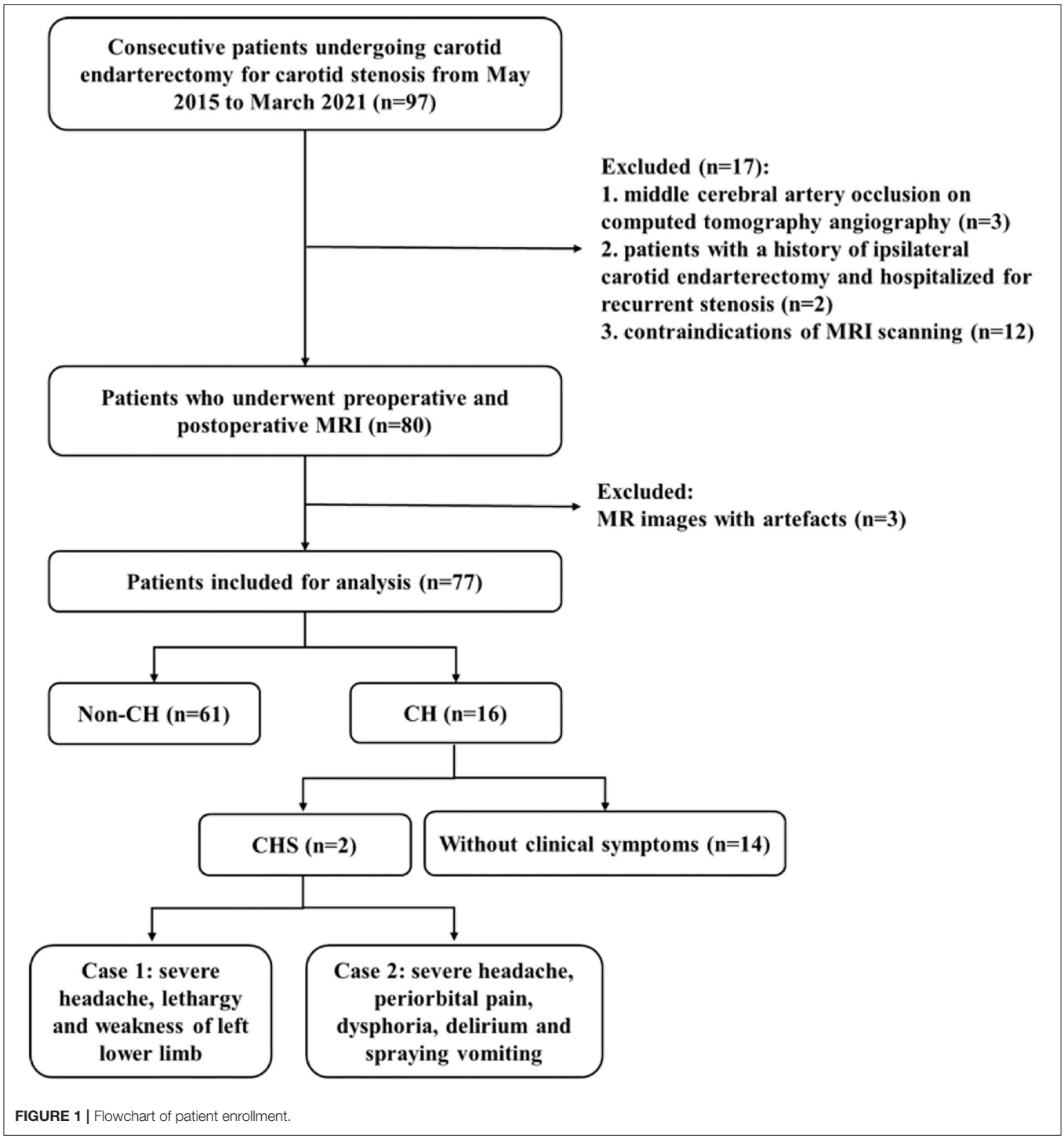

FIGURE 1 | Flowchart of patient enrollment.

Diagnosis of CH and CHS

Regions of interest were set at the cerebral cortex perfused by ipsilateral carotid artery in watershed areas and 8 perfusion territories (2 anterior and 6 middle cerebral artery territories), corresponding with the Alberta Stroke Programme Early Computed Tomography Score locations (12). The region of interest placement was consistent between pre-operative and post-operative CBF images. CH was defined as an increase in CBF >100% compared with pre-operative values in ≥1 regions of interest with or without clinical symptoms or signs (2).

CHS was defined as: (1) existence of CH, (2) occurrence of a throbbing frontotemporal or periorbital headache on the ipsilateral side of the CEA, seizure, confusion, deterioration of consciousness level, development of focal neurological signs, or

TABLE 1 | Evaluation criteria of the four cerebral SVD markers and the total cerebral SVD burden score.

MRI markers	Definition and grades	Number or degree	Score
WMHs	WMHs were defined as hyperintensity on T2-weighted images and fluid-attenuated inversion recovery without cavitation. Periventricular WMHs were graded as: 0 = absent, 1 = caps or pencil-thin lining, 2 = smooth halo, or 3 = irregular periventricular WMHs extending into the deep white matter. Deep WMHs were graded as: 0 = absent, 1 = punctate foci, 2 = beginning confluent foci, or 3 = large confluent areas.	Fazekas score <2 in the deep white matter and <3 in the periventricular white matter	0
		Fazekas score ≥2 in the deep white matter or ≥3 in the periventricular white matter	1
Lacune	Lacune was defined as a round or ovoid, subcortical, fluid-filled cavity of between 3 mm and about 15 mm in diameter located in the territory of a perforating arteriole. Number of lacunes was conservatively counted.	0	0
		≥1 lesion	1
CMBs	CMBs were defined as a small (generally 2–5 mm in diameter) area of signal void with associated blooming seen on T2*-weighted MRI. Number of CMBs were counted. CMBs strictly located in lobes were not recorded.	0	0
		≥1 lesion	1
PVSs	PVSs were round or ovoid, with a diameter generally smaller than 3 mm and had signal intensity similar to cerebrospinal fluid on all sequences. The number of PVSs in the basal ganglia was graded with a three-category ordinal scale as follows: 0–10 (category 1), 11–25 (category 2), and >25 (category 3).	Category-1 PVSs	0
		Category-2 or−3 PVSs	1

SVD, small vessel disease; MRI, magnetic resonance imaging; WMHs, white matter hyperintensity; CMBs cerebral microbleeds; PVSs, perivascular spaces.

intracranial hemorrhage, and (3) absence of new ischemic lesions on post-operative MRI (2).

Other Clinical and Imaging Characteristics

The presence of symptoms and time elapsed since the last cerebrovascular event were recorded by an experienced vascular surgeon. Age, sex, and vascular risk factors including hypertension, diabetes mellitus, dyslipidemia, coronary heart disease, history of smoking and alcohol were collected, according to self-reported history, medication history or referring to the results of laboratory examination. The use of intraluminal shunt during surgery, baseline systolic blood pressure (BP) on admission, the highest systolic BP within 24 h after CEA and the highest systolic BP from the second day after CEA to discharge were also recorded. The degree of stenosis was determined according to the NASCET criteria (9) by computed tomography angiography. We carefully performed the diagnosis of carotid near-occlusion by using an interpretive approach based on previous studies (13, 14).

Perioperative and Post-operative Management

CEA was performed under general anesthesia. A bolus of heparin (100 U/kg) was administered intravenously for systemic anticoagulation. All CEAs were carefully performed by vascular surgeons with more than 10 years of experience. Carotid atherosclerotic plaques were removed by classic longitudinal arteriotomy with patching or eversion surgery. If patients were observed with poor collateral circulation before surgery (15) or with asymmetry or diffuse slowing of the electroencephalogram during clamping (16), an intraluminal shunt was used. Following surgery, patients were transferred to the post-anesthesia care unit for about 1 h until the blood pressure (BP) was stable, before transfer back to the vascular ward.

Patients received electrocardiogram monitoring for 1–2 days after surgery. BP was closely monitored to control systolic BP between 120 and 140 mmHg. BP was measured three times daily using a sphygmomanometer after removal of electrocardiogram monitoring. Patients with a systolic BP > 140 mmHg received oral antihypertensive drugs as the first-line treatment. If systolic BP remains elevated, intravenous antihypertensive drugs were given. For patients who complained of CHS symptoms, intravenous mannitol or glycerol fructose was added to lower intracranial pressure.

Statistical Analysis

All data was analyzed using statistical software (IBM SPSS v25.0). The κ value was calculated for the inter-observer agreement of each cerebral SVD marker. The κ values ≤ 0.40 represented poor agreement, values > 0.40 and ≤ 0.65 represented general agreement, values > 0.65 and ≤ 0.75 represented good agreement, and values > 0.75 represented excellent agreement. The relationship between each variable and CH was analyzed by univariate analysis. To determine the association of cerebral SVD with CH adjusted for other risk factors, we performed multivariate logistic regression analysis by using a forward stepwise method. Age, sex and variables with $p < 0.2$ in univariate analysis were entered into the logistic regression models as covariables. Since SVD markers share the common pathogenesis and often coexist, to avoid the risk of multicollinearity, each cerebral SVD marker and the total cerebral SVD score entered different regression models, respectively, rather than including them in the one model. The remaining covariates entered all models consistently. The optimal cutoff values of cerebral SVD markers for predicting CH were assessed using receiver-operating characteristic (ROC) curve analysis. The sensitivity, specificity, and negative and positive predictive values of cerebral SVD markers for differentiating patients with and without CH were calculated. All *p*-values were calculated

TABLE 2 | Clinical characteristics and cerebral small vessel disease markers of patients.

	All ($n = 77$)	CH ($n = 16$)	Non-CH ($n = 61$)	p
Age, years	66.0 ± 7.3	66.4 ± 8.5	65.8 ± 7.0	0.765
Male	58 (75.3)	15 (93.8)	43 (70.5)	0.099
Presence of symptoms				0.324
Asymptomatic stenosis	47 (61)	7 (43.8)	40 (65.6)	
TIA	14 (18.2)	4 (25)	10 (16.4)	
Stroke	16 (20.8)	5 (31.3)	11 (18)	
Days since the last cerebrovascular event	42.5 [27, 75]	45 [20, 120]	40 [33, 60]	0.304
Large infarcts on MRI[a]	15 (19.5)	6 (37.5)	9 (14.8)	0.071
Hypertension	53 (68.8)	13 (81.3)	40 (65.6)	0.364
Diabetes	28 (36.4)	7 (43.8)	21 (34.4)	0.490
Dyslipidemia	37 (48.1)	7 (43.8)	30 (49.2)	0.783
Coronary artery disease	17 (22.1)	6 (37.5)	11 (18.0)	0.172
Smoking	41 (53.2)	10 (62.5)	31 (50.8)	0.405
alcohol	22 (28.6)	3 (18.8)	19 (31.1)	0.375
Ipsilateral stenosis				*0.002**
50–70%	10 (13)	0 (0)	10 (16.4)	
70–99%	52 (67.5)	8 (50)	44 (72.1)	
Near-occlusion	15 (19.5)	8 (50)	7 (11.5)	
Contralateral stenosis				0.608
0	26 (33.8)	5 (31.3)	21 (34.4)	
<50%	34 (44.2)	7 (43.8)	27 (44.3)	
50–70%	8 (10.4)	1 (6.3)	7 (11.5)	
70–99%	7 (9.1)	3 (18.8)	4 (6.6)	
Occlusion	2 (2.6)	0 (0)	2 (3.3)	
Shunt use	49 (63.6)	11 (68.8)	38 (62.3)	0.633
BP_baseline, mmHg	136.7 ± 15.7	140.7 ± 17.9	135.7 ± 15	0.258
BP_post_1st day, mmHg	126.0 ± 14.9	130.5 ± 20.7	124.8 ± 12.9	0.308
BP_before discharge, mmHg	139.4 ± 14.2	139.9 ± 21.1	139.3 ± 12.0	0.933
Cerebral SVD markers				
Total SVD score	1 [0–2]	2 [1.25–3]	1 [0–2]	*0.001*†
0	23 (29.9)	1 (6.3)	22 (36.1)	
1	25 (32.5)	3 (18.8)	22 (36.1)	
2	15 (19.5)	7 (43.8)	8 (13.1)	
3	10 (13)	3 (18.8)	7 (11.5)	
4	4 (5.2)	2 (12.5)	2 (3.3)	
Fazekas score of WMHs	2 [1–3]	4 [3–5]	1 [1–3]	*<0.001*†
Any lacunes	38 (49.4)	12 (75)	26 (42.6)	*0.021**
Number of lacunes	0 [0–2]	2.5 [0.25–4.75]	0 [0–1]	*0.003*†
Category of PVSs	1 [1–2]	1 [1–2]	1 [1–1.5]	0.198
Any CMBs	20 (25.3)	5 (31.3)	15 (24.6)	0.749
Number of CMBs	0 [0–1]	0 [0–1]	0 [0–0.5]	0.492

CH, cerebral hyperperfusion; TIA, transient ischemic attack; BP_baseline, baseline systolic blood pressure on admission; BP_post_1st day, the highest systolic blood pressure within 24 h after surgery; BP_before discharge, the highest systolic blood pressure from the second day after surgery to discharge; SVD, small vessel disease; WMHs, white matter hyperintensities; PVSs, perivascular spaces; CMBs, cerebral microbleeds.

Normally distributed continuous variables were expressed as means ± standard deviation. Categorical variables were expressed as percentages of patients who satisfied the criteria. Discrete variables were expressed as median [interquartile range].

[a]*Cortical infarcts or subcortical hemispheric infarcts >1.5 cm in diameter within the territory of ipsilateral carotid artery on MRI.*

**Chi-square test or Fisher's exact test.*

†*Mann-Whitney U test.*

Italic values mean $p < 0.05$ between CH and non-CH groups.

using two-tailed tests. A value of $p < 0.05$ was considered statistically significant.

RESULTS

Characteristics of the Study Population

CEA was successfully performed in all patients. Of the 77 patients, 16 (20.78%) met CBF criteria for CH. The clinical and radiological characteristics of the study population are shown in **Table 2**. The mean age was 66 ± 7 years and 75.3% were males. Of the 77 patients, 14 (18.2%) patients had transient ischemic attack and 16 (20.8%) patients had ischemic stroke. No emergency surgery was performed. The median Fazekas score was 2 points and median PVSs category was 1 grade. Thirty-eight (49.4%) patients had lacunes and 20 (25.3%) patients had CMBs.

Inter-observer Agreement

Inter-observer agreement for each cerebral SVD marker was good or excellent (Fazekas score, $\kappa = 0.78$; number of lacunes, $\kappa = 0.72$; PVSs category: $\kappa = 0.77$; number of CMBs, $\kappa = 0.86$).

Relationship Between Cerebral SVD and CH

The results of univariate analysis between CH and non-CH group are shown in **Table 1**. The total cerebral SVD score was significantly higher in patients with CH compared with patients without CH ($p = 0.001$). As for the four cerebral SVD markers, the Fazekas score ($p < 0.001$), presence of lacunes ($p = 0.021$) and number of lacunes ($p = 0.003$) were associated with CH after CEA. There were no significant differences in PVSs or CMBs between the two groups ($p = 0.198$ and $p = 0.749$, respectively). In terms of clinical characteristics, patients with CH had a significantly higher degree of ipsilateral carotid stenosis than those without CH ($p = 0.002$). Patients with carotid near-occlusion had the highest risk of CH after CEA (**Supplementary Figure 1**). No statistical difference was found in other clinical variables.

Age, gender, large infarcts on MRI, coronary artery disease and degree of ipsilateral carotid stenosis were included as covariates according to the result of univariate analysis. In the logistic regression models, Fazekas score of WMHs [OR 3.09, 95% CI (1.72–5.54); $p < 0.001$], number of lacunes [OR 1.37, 95% CI (1.06–1.76); $p = 0.014$] and total cerebral SVD score [OR 2.68, 95% CI (1.42–5.07); $p = 0.002$] were still significantly associated with post-operative CH (**Table 3**). No association was found between PVSs and CH ($p = 0.184$). Ipsilateral degree of stenosis was associated with CH in all regression models ($p < 0.05$). No statistical difference was observed between CH and other variables.

ROC Curves Analysis

Fazekas score ≥ 3 points [area under the curve (AUC) = 0.84, sensitivity = 81.3%, specificity = 73.8%, positive predictive value (PPV) = 44.8% and negative predictive value (NPV) = 93.8%] and number of lacunes ≥ 2 (AUC = 0.73, sensitivity = 68.8%, specificity = 78.7%, PPV = 45.8% and NPV = 90.6%) were the optimal cutoff values for the prediction of post-operative CH (**Figures 2A,B**). The relationships between the Fazekas score, the number of lacunes and CH are shown in **Figure 2C**. Of the 41 patients with a Fazekas score < 3 and the number of lacunes < 2, only 2 (4.88%) patients had CH after CEA. And importantly, both the 2 patients had ipsilateral carotid near-occlusion. A representative case of CH is shown in **Figure 3**.

TABLE 3 | Logistic regression analysis of relationships between cerebral SVD markers and post-operative cerebral hyperperfusion.

Cerebral SVD markers	*p*	OR	95% CI
WMHs	<0.001	3.09	1.72–5.54
Number of lacunes	0.014	1.37	1.06–1.76
PVSs	0.184	NA	NA
Total cerebral SVD score	0.002	2.68	1.42–5.07

SVD, small vessel disease; WMHs, the Fazekas score of white matter hyperintensities; PVSs, category of perivascular spaces.

Patients Diagnosed With CHS

Of the 16 patients with post-CEA CH, 2 developed CHS. One patient diagnosed with CHS complained of an ipsilateral severe throbbing headache, lethargy, and weakness of the left lower limb. Another CHS patient had an ipsilateral severe throbbing headache, periorbital pain, dysphoria, delirium and spraying vomiting. After strict control of BP and reduction of intracranial pressure, further intracranial hemorrhage did not occur.

The basic data of the 16 patients are listed in **Supplementary Table 2**. Both of the 2 CHS patients were male, had coronary artery disease, and showed clinical symptoms before surgery. Moreover, the two CHS patients showed a trend toward a higher maximum systolic BP within 24 h after surgery (160 and 170 mmHg) compared with the other 14 patients (mean value = 126 mmHg). A representative case of CHS is shown in **Figure 4**.

DISCUSSION

As a large artery atherosclerotic disease, the role of cerebral SVD was less mentioned in patients with carotid stenosis. Actually, carotid stenosis often coexists with cerebral SVD because they share common systematic vascular risk factors such as aging and hypertension (17). In this preliminary study, we explored the relationship between cerebral SVD MRI markers and CH after CEA in patients with carotid stenosis and we found that pre-operative WMHs and lacunes adversely affected CH after CEA. This is, to the best of our knowledge, the first study to examine the association between cerebral SVD and CH after CEA in patients with carotid stenosis.

CHS is a serious perioperative complication after CEA and a major cause of intracerebral hemorrhage during hospitalization (18). The North American Symptomatic Endarterectomy Trial (19) demonstrated that WMHs were associated with a higher risk of any stroke (non-fatal or fatal ischemic stroke and hemorrhagic stroke confirmed by brain imaging) within 30

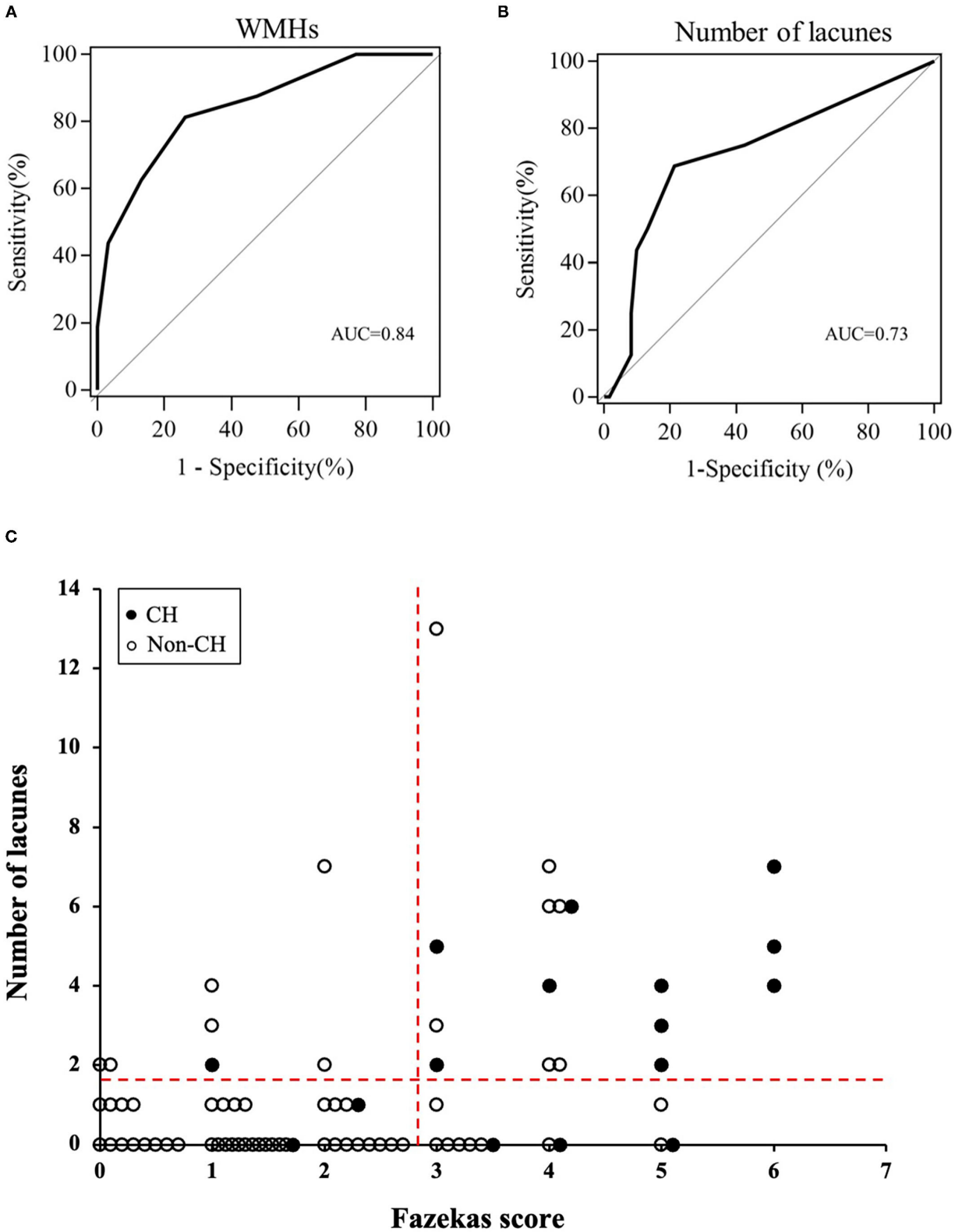

FIGURE 2 | The receiver operating characteristic (ROC) curves of pre-operative Fazekas score **(A)** and number of lacunes **(B)** for the prediction of cerebral hyperperfusion (CH) after surgery. **(C)** Relationships between the Fazekas score, number of lacunes, and post-operative CH. The dotted horizontal line denotes the cutoff value of lacunes (≥2) obtained from the ROC curve for prediction of CH. The dotted vertical line denotes the cutoff value of Fazekas score (≥3) obtained from the ROC curve for prediction of CH.

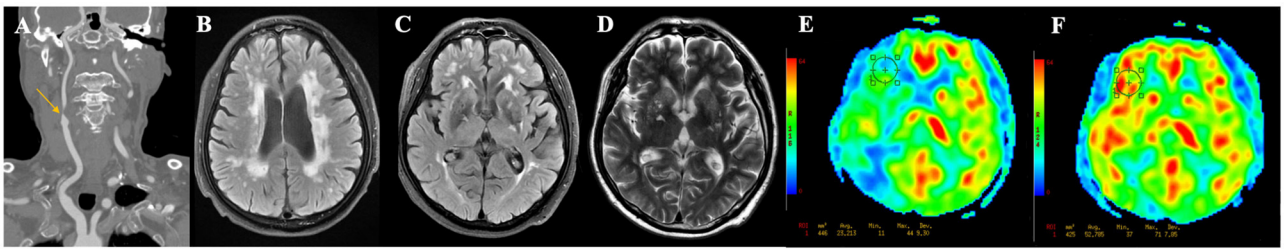

FIGURE 3 | A representative case of cerebral hyperperfusion. **(A)** Pre-operative computed tomography angiography shows severe stenosis of the right carotid artery. **(B–D)** Pre-operative T2WI and FLAIR show severe white matter hyperintensities (Fazekas score = 6), multiple lacunes in bilateral basal ganglia, and category-3 perivascular spaces. **(E)** Pre-operative arterial spin labeling image shows a significantly decreased cerebral blood flow (23.21 ml/100 g/min) in the watershed area. **(F)** Post-operative arterial spin labeling image shows the cerebral blood flow (52.79 ml/100 g/min) increase >100% compared with pre-operative values.

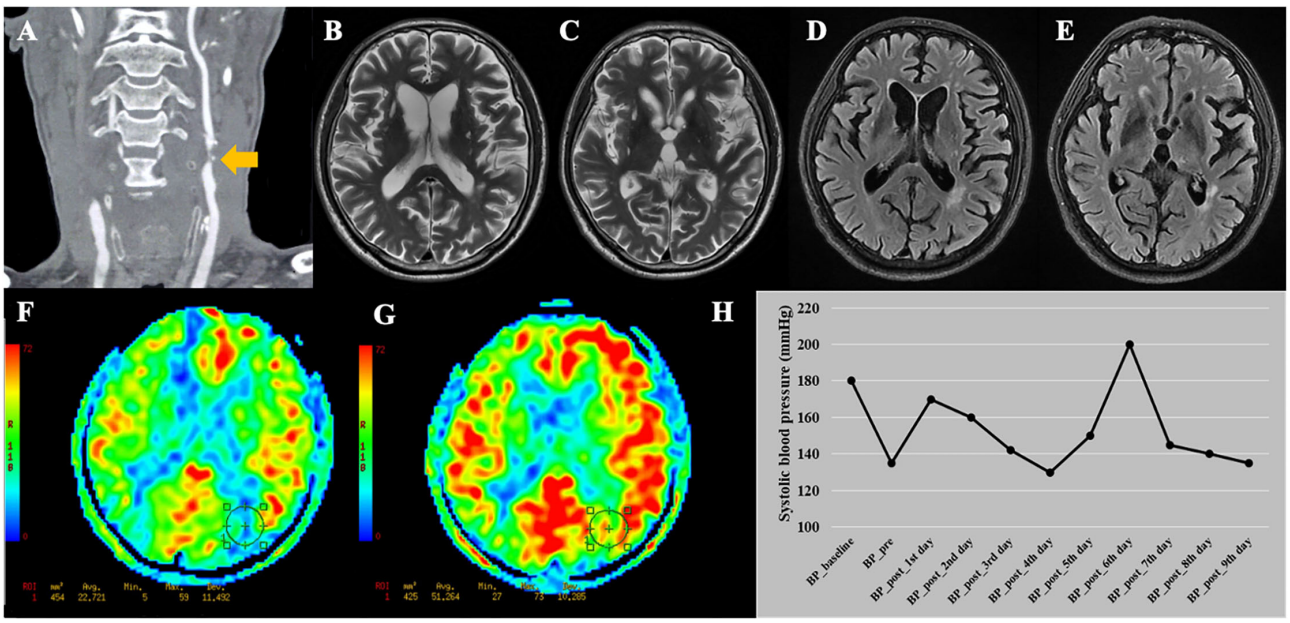

FIGURE 4 | A representative case of cerebral hyperperfusion syndrome. **(A)** This patient was diagnosed with bilateral severe carotid stenosis. During this hospitalization, this patient received carotid endarterectomy (CEA) on the left side. **(B–E)** Pre-operative T2WI and FLAIR show Fazekas score of 4 points and multiple lacunes in bilateral basal ganglia and left thalamus. **(F)** Pre-operative arterial spin labeling image shows a significantly decreased cerebral blood flow (22.72 ml/100 g/min) in the watershed area. **(G)** Post-operative arterial spin labeling image shows the cerebral blood flow (51.26 ml/100 g/min) increase >100% compared with pre-operative values. **(H)** This patient developed cerebral hyperperfusion syndrome during the first day after CEA with systolic blood pressure of 170 mmHg. The patient experienced dysphoria, delirium under fluctuating blood pressure. After adjusting the medication, the patient discharged with stable blood pressure. BP_baseline, baseline systolic blood pressure on admission; BP_pre, systolic blood pressure measured the day before surgery; BP_post, systolic blood pressure measured everyday after CEA before discharge.

days after CEA. However, that study did not report the rate of ischemic and hemorrhagic stroke separately or the presence of CH or CHS. Our findings showed that pre-operative WMHs and lacunes were independently associated with post-operative CH. A possible mechanism for this association involves impaired cerebrovascular autoregulation, which is known as the main mechanism of CH (2, 3). WMHs and lacunes are common MRI markers for cerebral SVD caused by cerebral microvascular endothelial dysfunction (4). Patankar et al. reported that even in the presence of severe stenotic/occlusive large vessel disease, microvascular abnormalities are the predominant pathogenetic factor in WMHs (20). With increasing WMH burden and lacunes, permeability of the small vessel wall increases, followed by inflammatory reaction, thickening and stiffness of the vessel wall, and impaired cerebral autoregulation ability (15). Another possible mechanism may be the free oxygen radicals. Patients with cerebral SVD would suffer from cerebrovascular oxidative stress and extensive reactive

oxygen species production (21), which can cause vasodilation and increased permeability of cerebral vessels during ischemia reperfusion (2).

The NPVs of Fazekas score ≥ 3 points and number of lacunes ≥ 2 were >90%. In our study, none of patients with both Fazekas score < 3 points and number of lacunes < 2 ($n = 41$) experience CH, except for 2 patients with carotid near-occlusion. These findings indicate that combining the information of WMHs, lacunes (representing the influence of cerebral small vessels) and degree of stenosis (representing the influence of extracranial large arteries) may identify patients who would not develop CH after CEA. This can obviate unnecessary invasive intravenous antihypertensive therapy on many post-CEA patients, different from the one-size-fits-all strategy that treating all patients with systolic BP > 140 or 160 mmHg (3, 22). Moreover, it will help clinicians decide who can safely return to ward or home instead of staying in intensive care unit; thus, this will lead to a reduction in hospital and patient costs.

Furthermore, all 6 patients with both a Fazekas score of 5 or 6 and number of lacunes ≥ 2 (2 of them with carotid near-occlusion, **Supplementary Table 2**) developed CH after CEA. Thus, our results gave a hint that clinicians may need to pay particular attention for those patients with both a higher Fazekas score (5 or 6 points) and more lacunes (≥ 2) during the surgical and perioperative periods, such as use of shunt or shortening of the cross-clamping time, more careful use of anticoagulants and antiplatelet therapy, and strict control of BP to minimize the occurrence of CH/CHS (2). Given the relatively small number of patients with severe WMHs (Fazekas score of 5 or 6, 9 of 77), this finding needs to be verified by future studies with a larger sample size.

In the present study, the incidence of CHS after CEA was 2.6%, and 12.5% of patients with CH developed CHS, which was consistent with previous reports (23, 24). Of the 16 CH patients, the 2 patients who further developed CHS had a higher systolic BP within 24 h after CEA than the remaining 14 patients. Post-operative hypertension has been demonstrated as an important risk factor for CHS by previous studies, both in CEA and CAS (1–3, 25, 26). The current study emphasized the effect of early post-operative BP during the progression from CH to CHS. Moulakakis et al. (27), Newman et al. (28) reported that post-endarterectomy hypertension was associated with higher post-operative pain scores, which may partially explain our findings. However, because of the small number of CHS patients, the mechanism of BP in CHS requires further exploration. Anyway, strict control of BP in the perioperative phase is essential in the prevention and management of CHS (2).

The study patients received CEA under general anesthesia. CEA is the standard treatment for patients with symptomatic carotid stenosis, and general anesthesia is the most preferable technique for CEA practiced by clinicians (29–31). Our findings may be applicable to most clinical situations. Theoretically, impaired cerebral autoregulation is a shared mechanism of CH for both CEA and CAS; thus, our finding of the association between cerebral SVD and CH may also apply to CAS. Some of general anesthetics may influence cerebral hemodynamics by vasodilating effects or disturbing blood flow-activity coupling (2, 32), while anesthesia protocols that may disturb CBF and autoregulation were not performed in the current study. Performing CEA under regional anesthetics does not impair cerebral hemodynamic, which may be a better choice for CH/CHS studies.

There are several limitations to our study. First, the sample size was relatively small for the low incidence of CHS. Since only 2 patients presented with CHS, statistical analysis was not performed for CHS patients. Our preliminary findings of the cutoff values of cerebral SVD for the prediction of CH need to be validated by further studies with larger sample sizes. Second, cerebrovascular reserve was not performed in our study. The pathogenesis underlying the relationship between cerebral SVD and CH cannot be directly verified in our study. Actually, cerebrovascular reserve studies are in progress in our unit. Third, our conclusions are applicable to patients undergoing CEA under general anesthesia, but cannot be directly extrapolated to patients undergoing carotid artery stenting or to those under local anesthesia. Whether our findings are applicable for CAS or CEA under regional anesthesia needs to be verified by future studies.

CONCLUSION

In conclusion, pre-operative WMHs and lacunes adversely affect CH after CEA. In patients with carotid stenosis, cerebral SVD may be an important risk factor for CH after CEA and can serve as a useful imaging marker for CH, especially for predicting patients who will not develop CH. When considering the risk of CH in patients undergoing CEA for carotid stenosis, pre-operative brain MRI could help clinicians make treatment decisions.

DATA AVAILABILITY STATEMENT

The raw data supporting the conclusions of this article will be made available by the authors, without undue reservation.

ETHICS STATEMENT

The studies involving human participants were reviewed and approved by the Medical Ethics Committee of the Peking Union Medical College Hospital. The patients/participants provided their written informed consent to participate in this study. Written informed consent was obtained from the individual(s) for the publication of any potentially identifiable images or data included in this article.

AUTHOR CONTRIBUTIONS

XF and TL: conception, design, and statistical analysis. XF, ZL, ML, and FF: analysis, interpretation, and final approval of the article. XF, ZL, TL, and HY: data collection. XF: writing the

article. XF, ZL, ML, FF, and JW: critical revision of the article. FF and CL: obtained funding. FF: overall responsibility. All authors contributed to the article and approved the submitted version.

FUNDING

This work was supported in part by the National Nature Science Foundation of China grant (82071899), the Fundamental Research Funds for the Central Universities (3332020009), and the Beijing Natural Science Foundation grant (L182067).

SUPPLEMENTARY MATERIAL

The Supplementary Material for this article can be found online at: https://www.frontiersin.org/articles/10.3389/fcvm.2021.734392/full#supplementary-material

REFERENCES

1. Wang GJ, Beck AW, DeMartino RR, Goodney PP, Rockman CB, Fairman RM. Insight into the cerebral hyperperfusion syndrome following carotid endarterectomy from the national vascular quality initiative. *J Vasc Surg.* (2017) 65:381–89. doi: 10.1016/j.jvs.2016.07.122
2. van Mook WN, Rennenberg RJ, Schurink GW, Van Oostenbrugge RJ, Mess WH, Hofman PA, et al. Cerebral hyperperfusion syndrome. *Lancet Neurol.* (2005) 4:877–88. doi: 10.1016/S1474-4422(05)70251-9
3. Lin YH, Liu HM. Update on cerebral hyperperfusion syndrome. *J Neurointerv Surg.* (2020) 12:788–93. doi: 10.1136/neurintsurg-2019-015621
4. Wardlaw JM, Smith C, Dichgans M. Small vessel disease: mechanisms and clinical implications. *Lancet Neurol.* (2019) 18:684–96. doi: 10.1016/S1474-4422(19)30079-1
5. Wardlaw JM, Smith EE, Biessels GJ, Cordonnier C, Fazekas F, Frayne R, et al. Neuroimaging standards for research into small vessel disease and its contribution to ageing and neurodegeneration. *Lancet Neurol.* (2013) 12:822–38. doi: 10.1016/S1474-4422(13)70124-8
6. Isaka Y, Nagano K, Narita M, Ashida K, Imaizumi M. High signal intensity on T2-weighted magnetic resonance imaging and cerebral hemodynamic reserve in carotid occlusive disease. *Stroke.* (1997) 28:354–7. doi: 10.1161/01.STR.28.2.354
7. Hu HH, Kuo TB, Wong WJ, Luk YO, Chern CM, Hsu LC, et al. Transfer function analysis of cerebral hemodynamics in patients with carotid stenosis. *J Cereb Blood Flow Metab.* (1999) 19:460–5. doi: 10.1097/00004647-199904000-00012
8. Ogasawara K, Yukawa H, Kobayashi M, Mikami C, Konno H, Terasaki K, et al. Prediction and monitoring of cerebral hyperperfusion after carotid endarterectomy by using single-photon emission computerized tomography scanning. *J Neurosurg.* (2003) 99:504–10. doi: 10.3171/jns.2003.99.3.0504
9. Barnett HJM, Taylor DW, Eliasziw M, Fox AJ, Ferguson GG, Haynes, et al. Benefit of carotid endarterectomy in patients with symptomatic moderate or severe stenosis. North American Symptomatic Carotid Endarterectomy Trial Collaborators. *N Engl J Med.* (1998) 339:1415–25. doi: 10.1056/NEJM199811123392002
10. Fazekas F, Chawluk JB, Alavi A, Hurtig HI, Zimmerman RA. MR signal abnormalities at 1.5T in Alzheimer's dementia and normal aging. *AJNR Am J Neuroradiol.* (1987) 8:421–26. doi: 10.2214/ajr.149.2.351
11. Huijts M, Duits A, van Oostenbrugge RJ, Kroon AA, de Leeuw PW, Staals J. Accumulation of MRI markers of cerebral small vessel disease is associated with decreased cognitive function. A study in first-ever lacunar stroke and hypertensive patients. *Front Aging Neurosci.* (2013) 5:72. doi: 10.3389/fnagi.2013.00072
12. Kim JJ, Fischbein NJ, Lu Y, Pham D, Dillon WP. Regional angiographic grading system for collateral flow: correlation with cerebral infarction in patients with middle cerebral artery occlusion. *Stroke.* (2004) 35:1340–44. doi: 10.1161/01.STR.0000126043.83777.3a
13. Bartlett ES, Walters TD, Symons SP, Fox AJ. Diagnosing carotid stenosis near-occlusion by using CT angiography. *AJNR Am J Neuroradiol.* (2006) 27:632–37. Available online at: http://www.ajnr.org/content/27/3/632.long
14. Johansson E, Gu T, Aviv RI, Fox AJ. Carotid near-occlusion is often overlooked when CT angiography is assessed in routine practice. *Eur Radiol.* (2020) 30:2543–51. doi: 10.1007/s00330-019-06636-4
15. Wardlaw JM, Smith C, Dichgans M. Mechanisms of sporadic cerebral small vessel disease: insights from neuroimaging. *Lancet Neurol.* (2013) 12:483–97. doi: 10.1016/S1474-4422(13)70060-7
16. Rutgers DR, Blankensteijn, JD, van der Grond J. Preoperative MRA flow quantification in CEA patients: flow differences between patients who develop cerebral ischemia and patients who do not develop cerebral ischemia during cross-clamping of the carotid artery. *Stroke.* (2000) 31:3021–28. doi: 10.1161/01.STR.31.12.3021
17. Timmerman N, Rots ML, van Koeverden ID, Haitjema S, van Laarhoven Cjhcm, Vuurens AM, et al. Cerebral small vessel disease in standard pre-operative imaging reports is independently associated with increased risk of cardiovascular death following carotid endarterectomy. *Eur J Vasc Endovasc Surg.* (2020) 59:872–80. doi: 10.1016/j.ejvs.2020.02.004
18. Farooq MU, Goshgarian C, Min J, Gorelick PB. Pathophysiology and management of reperfusion injury and hyperperfusion syndrome after carotid endarterectomy and carotid artery stenting. *Exp Transl Stroke Med.* (2016) 8:7. doi: 10.1186/s13231-016-0021-2
19. Streifler JY, Eliasziw M, Benavente OR, Alamowitch S, Fox AJ, Hachinski VC, et al. Prognostic importance of leukoaraiosis in patients with symptomatic internal carotid artery stenosis. *Stroke.* (2002) 33:1651–5. doi: 10.1161/01.STR.0000018010.38749.08
20. Patankar T, Widjaja E, Chant H, McCollum C, Baldwin R, Jeffries S, et al. Relationship of deep white matter hyperintensities and cerebral blood flow in severe carotid artery stenosis. *Eur J Neurol.* (2006) 13:10–6. doi: 10.1111/j.1468-1331.2006.01115.x
21. Grochowski C, Litak J, Kamieniak P, Maciejewski R. Oxidative stress in cerebral small vessel disease. Role of reactive species. *Free Radic Res.* (2018) 52:1–13. doi: 10.1080/10715762.2017.1402304
22. Fassaert LMM, de Borst GJ. Commentary on "Post-carotid endarterectomy hypertension. Part 2: association with peri-operative clinical, anaesthetic, and transcranial Doppler derived parameters. *Eur J Vasc Endovasc Surg.* (2018) 55:593. doi: 10.1016/j.ejvs.2018.01.031
23. Son S, Choi DS, Kim SK, Kang H, Park KJ, Choi NC, et al. Carotid artery stenting in patients with near occlusion: a single-center experience and comparison with recent studies. *Clin Neurol Neurosurg.* (2013) 115:1976–81. doi: 10.1016/j.clineuro.2013.06.001
24. Kirchoff-Torres KF, Bakradze E. Cerebral hyperperfusion syndrome after carotid revascularization and acute ischemic stroke. *Curr Pain Headache Rep.* (2018) 22:24. doi: 10.1007/s11916-018-0678-4
25. Manoilovic V, Budakov N, Budinski S, Milosevic D, Nikolic D, Manoilovic V. Cerebrovascular reserve predicts the cerebral hyperperfusion syndrome after carotid endarterectomy. *J Stroke Cerebrovasc Dis.* (2020) 29:105318. doi: 10.1016/j.jstrokecerebrovasdis.2020.105318
26. Lai ZC, Liu B, Chen Y, Ni L, Liu CW. Prediction of cerebral hyperperfusion syndrome with velocity blood pressure index. *Chin Med J.* (2015) 128:1611–7. doi: 10.4103/0366-6999.158317
27. Moulakakis KG, Mylonas SN, Sfyroeras GS, Andrikopoulos V. Hyperperfusion syndrome after carotid revascularization. *J Vasc Surg.* (2009) 49:1060–8. doi: 10.1016/j.jvs.2008.11.026

28. Newman JE, Bown MJ, Sayers RD, Thompson JP, Robinson TG, Williams B, et al. Post-carotid endarterectomy hypertension. Part 1: association with pre-operative clinical, imaging, and physiological parameters. *Eur J Vasc Endovasc Surg.* (2017) 54:551–63. doi: 10.1016/j.ejvs.2017.01.013
29. Kim Y, Lee S, Dua A. A modern series of carotid endarterectomy for symptomatic carotid stenosis. *J Vasc Surg.* (2021) 74:e59. doi: 10.1016/j.jvs.2021.06.099
30. Carnevale M, Koleilat I, Friedmann P, Aldailami H. Risk factors for cerebral hyperperfusion syndrome in patients undergoing transcarotid artery revascularization in the vascular quality initiative. *J Vasc Surg.* (2021) 74:e146–7. doi: 10.1016/j.jvs.2021.06.222
31. Greene NH, Minhaj MM, Zaky AF, Rozet I. Perioperative management of carotid endarterectomy: a survey of clinicians' backgrounds and practices. *J Cardiothorac Vasc Anesth.* (2014) 28:990–3. doi: 10.1053/j.jvca.2013.11.007
32. Kaisti KK, Langsjo JW, Aalto S, Oikonen V, Sipila H, Teras M, et al. Effects of sevoflurane, propofol and adjunct nitrous oxide on regional cerebral blood flow, oxygen consumption, and blood volume in humans. *Anesthesiology.* (2003) 99:603–13. doi: 10.1097/00000542-200309000-00015

Conflict of Interest: JW was employed by the company GE Healthcare.

The remaining authors declare that the research was conducted in the absence of any commercial or financial relationships that could be construed as a potential conflict of interest.

Publisher's Note: All claims expressed in this article are solely those of the authors and do not necessarily represent those of their affiliated organizations, or those of the publisher, the editors and the reviewers. Any product that may be evaluated in this article, or claim that may be made by its manufacturer, is not guaranteed or endorsed by the publisher.

Copyright © 2021 Fan, Lai, Lin, You, Wei, Li, Liu and Feng. This is an open-access article distributed under the terms of the Creative Commons Attribution License (CC BY). The use, distribution or reproduction in other forums is permitted, provided the original author(s) and the copyright owner(s) are credited and that the original publication in this journal is cited, in accordance with accepted academic practice. No use, distribution or reproduction is permitted which does not comply with these terms.

frontiers in Cardiovascular Medicine

ORIGINAL RESEARCH
published: 08 December 2021
doi: 10.3389/fcvm.2021.775307

Effect of Aneurysm and Patient Characteristics on Intracranial Aneurysm Wall Thickness

Jason M. Acosta[1], *Anne F. Cayron*[1,2,3], *Nicolas Dupuy*[4], *Graziano Pelli*[1], *Bernard Foglia*[1], *Julien Haemmerli*[4], *Eric Allémann*[2,3], *Philippe Bijlenga*[4], *Brenda R. Kwak*[1] *and Sandrine Morel*[1,4]*

[1] *Department of Pathology and Immunology, Faculty of Medicine, University of Geneva, Geneva, Switzerland,* [2] *School of Pharmaceutical Sciences, University of Geneva, Geneva, Switzerland,* [3] *Institute of Pharmaceutical Sciences of Western Switzerland, University of Geneva, Geneva, Switzerland,* [4] *Neurosurgery Division, Department of Clinical Neurosciences, Faculty of Medicine, Geneva University Hospitals and University of Geneva, Geneva, Switzerland*

Background: The circle of Willis is a network of arteries allowing blood supply to the brain. Bulging of these arteries leads to formation of intracranial aneurysm (IA). Subarachnoid hemorrhage (SAH) due to IA rupture is among the leading causes of disability in the western world. The formation and rupture of IAs is a complex pathological process not completely understood. In the present study, we have precisely measured aneurysmal wall thickness and its uniformity on histological sections and investigated for associations between IA wall thickness/uniformity and commonly admitted risk factors for IA rupture.

Methods: Fifty-five aneurysm domes were obtained at the Geneva University Hospitals during microsurgery after clipping of the IA neck. Samples were embedded in paraffin, sectioned and stained with hematoxylin-eosin to measure IA wall thickness. The mean, minimum, and maximum wall thickness as well as thickness uniformity was measured for each IA. Clinical data related to IA characteristics (ruptured or unruptured, vascular location, maximum dome diameter, neck size, bottleneck factor, aspect and morphology), and patient characteristics [age, smoking, hypertension, sex, ethnicity, previous SAH, positive family history for IA/SAH, presence of multiple IAs and diagnosis of polycystic kidney disease (PKD)] were collected.

Results: We found positive correlations between maximum dome diameter or neck size and IA wall thickness and thickness uniformity. PKD patients had thinner IA walls. No associations were found between smoking, hypertension, sex, IA multiplicity, rupture status or vascular location, and IA wall thickness. No correlation was found between patient age and IA wall thickness. The group of IAs with non-uniform wall thickness contained more ruptured IAs, women and patients harboring multiple IAs. Finally, PHASES and ELAPSS scores were positively correlated with higher IA wall heterogeneity.

Conclusion: Among our patient and aneurysm characteristics of interest, maximum dome diameter, neck size and PKD were the three factors having the most significant impact on IA wall thickness and thickness uniformity. Moreover, wall thickness heterogeneity was more observed in ruptured IAs, in women and in patients with multiple

OPEN ACCESS

Edited by:
Anne-Clémence Vion, INSERM U1087 L'unité de recherche de l'institut du thorax, France

Reviewed by:
Dan Rudic, Augusta University, United States
Rie Matsumori, Juntendo University, Japan

***Correspondence:**
Sandrine Morel
sandrine.morel@unige.ch

Specialty section:
This article was submitted to Atherosclerosis and Vascular Medicine, a section of the journal Frontiers in Cardiovascular Medicine

Received: *13 September 2021*
Accepted: *16 November 2021*
Published: *08 December 2021*

Citation:
Acosta JM, Cayron AF, Dupuy N, Pelli G, Foglia B, Haemmerli J, Allémann E, Bijlenga P, Kwak BR and Morel S (2021) Effect of Aneurysm and Patient Characteristics on Intracranial Aneurysm Wall Thickness. Front. Cardiovasc. Med. 8:775307. doi: 10.3389/fcvm.2021.775307

IAs. Advanced medical imaging allowing *in vivo* measurement of IA wall thickness would certainly improve personalized management of the disease and patient care.

Keywords: intracranial aneurysm, subarachnoid hemorrhage, risk factors, wall thickness uniformity, wall thickness

INTRODUCTION

Intracranial aneurysm (IA) resulting from the local outbulging of cerebral arteries is a disease with life-threatening complications. IAs are most often observed at bifurcations of cerebral arteries in the circle of Willis, which is a network of arteries localized at the basis of the brain and allowing its perfusion (**Figure 1A**). IAs have usually a saccular form (**Figure 1A**-right panel). Once an IA has formed, it can remain stable, grow or rupture. The most severe complication of an IA is its rupture leading to subarachnoid hemorrhage (SAH) (1). In Switzerland, a recent study demonstrated that SAH is lethal in 24% of cases and causes disability in more than 50% of patients (2). In the general population, the prevalence of IAs ranges from 2 to 3% (3), with some sources indicating it might even reach 9% (4, 5). Furthermore, IA prevalence is higher in 35–60 years old patients (6), in women (7) or in patients affected by polycystic kidney disease (PKD) (8, 9). Rupture probability of IAs has been estimated between 0.3 and 15% per 5 years (1, 10) with an annual rupture rate of 1% (11). Importantly, IAs are usually asymptomatic until rupture, making this illness a silent killer. Unruptured IAs are often unexpectedly found during cranial imaging (10). The discovery of unruptured IAs results in stress and anxiety for patients who are then confronted with the difficult decision to undergo prophylactic surgery or not. A precise evaluation of rupture probability is essential to help patients and physicians in this difficult choice. However, means to accurately estimate the likelihood of rupture are currently missing. Existing prediction tools such as PHASES (12), UIAT (13), and ELAPSS (14) scores consider various risk factors commonly linked with IA rupture, such as arterial hypertension, patient age, previous SAH, co-morbidities, IA size, location and morphology. Although these scores are based on readily available clinical data and correlate well with disease severity, they have several limitations. Indeed, retrospective studies showed that these scores do not perfectly reflect the likelihood of rupture, which may lead to overtreatment of unruptured IAs (15–22). Presently, no treatment is available to prevent IA rupture and prophylactic surgery presents important risks that must be considered (10). Indeed, endovascular coiling or surgical clipping is associated with 4.8% (23) and 6.7% (24) unfavorable outcomes, respectively.

The formation and rupture of IAs is a complex pathological process that despite extensive research (25–27), is still poorly understood. Considerable scientific evidence supports the notion that hemodynamic forces acting on the vessel wall induce vascular remodeling leading to IA formation, growth and rupture (28–31). Involved processes include inflammatory cell infiltration, smooth muscle cell (SMC) phenotypic switch, apoptosis, reorganization of extra cellular matrix (ECM), calcification and lipid accumulation (28–31). Numerous studies have tackled the mysteries of IA instability based on morphological dome aspects such as IA size and intraoperative appearance (32–34). Some studies have classified aneurysmal walls as "thick" or "thin" (35, 36), but to the best of our knowledge no study has performed a quantitative analysis of IA wall thickness or a rigorous description of IA wall thickness uniformity. We believe these two factors to be of importance for IA wall instability and rupture. In this study, we have precisely measured and defined aneurysmal wall thickness and thickness uniformity on histological sections. Potential links between such IA characteristics and patient and aneurysm descriptors commonly used in clinics to determine the rupture risk of IAs were investigated.

MATERIALS AND METHODS

Clinical Data

Patients were recruited at the Geneva University Hospitals following specific criteria. Inclusion criteria were as follows: (1) IA identified based on angiographic imaging [3D Magnetic Resonance Angiogram (3D-MRA), 3D Computed Tomography Angiogram (3D-CTA) or 3D Digital Subtraction Angiography (3D-DSA)]; (2) 18 years of age or older; and (3) patient having provided informed consent. Exclusion criteria were as follows: (1) lack of angiographic evidence for IA on 3D-MRA, 3D-CTA or 3D-DSA; (2) insufficient access to clinical data; (3) younger than 18 years of age; and 4) non-provision of informed consent. The study was approved by the Ethical Committee of the Geneva University Hospitals and by Swissethics (@neurIST protocol, ethics authorization PB_2018-00073, previously CER 07-056). All procedures were in accordance with the World Medical Association's Declaration of Helsinki.

Clinical data of recruited patients were collected with respect to IA and patient characteristics. IA characteristics were rupture status (ruptured or unruptured), vascular location, maximum dome diameter (**Figure 1B**), neck size (**Figure 1B**), and aspect (roughness, smoothness, presence of blebs and/or lobules [defined as (i) lobules have a diameter close to the IA diameter and (ii) blebs have a diameter much smaller than the IA diameter)], as previously described (27, 37, 38). Moreover, we calculated the bottleneck factor (ratio between maximum dome diameter and neck size), which is considered to be a potential predictor of IA rupture (39). Patient characteristics were age at discovery/rupture of IA, smoking status (defined as (i) never smoked more than 300 cigarettes and (ii) former (smoked more than 300 cigarettes and stopped at least 6 months ago) or current (smoked more than 300 cigarettes and continues smoking) smoker), hypertension (defined as arterial blood pressure >140/90 mmHg, regardless of treatment status),

sex, ethnicity, positive family history for IA or SAH, earlier SAH, presence of multiple IAs and diagnosis of PKD.

The PHASES (12) and ELAPSS (14) scores, used to evaluate IA rupture risk and growth respectively, were calculated for all patients.

Human Saccular IA Samples

Saccular IA samples were provided by the Division of Neurosurgery of the Geneva University Hospitals. All samples were obtained during microsurgery by resection of the IA dome (i.e., the bulging region of the IA) after clipping of the neck (**Figures 1C,D**). IAs were stored as previously described [Aneux Biobank (27)], fixed in formol, embedded in paraffin, sectioned at 5 μm and conserved at 4°C.

Aneurysm Wall Thickness Measurement

To measure aneurysm wall thickness, aneurysmal dome sections were stained with hematoxylin and eosin (**Figures 1E**, **2A,B**). Sections were scanned at 10× magnification in high resolution using the fully automated slide scanner Axio Scan.Z1 (Carl Zeiss Microscopy, Oberkochen, Germany). Using the software MATLAB 2019a (Mathworks, Massachusetts, USA), IA wall borders were precisely drawn (**Figures 2C,D**) and IA wall thickness was calculated every 0.4 μm all along the length of the resected aneurysm dome. For each sample, minimum and maximum IA wall thicknesses were extracted from all the data and the mean IA wall thickness was calculated.

Aneurysm Wall Thickness Uniformity Measurement

Based on the thickness measurements, a thickness topographic map of each dome was obtained. Thickness values were divided into 100 μm classes from 0 to 2,000 μm and frequencies of each thickness classes were determined (**Figures 2E,F**). Gaussian curves from this frequency distribution were obtained for each aneurysm (**Figures 2G,H**). Using the Gaussian Mixture Model (GMM) in the Excel software, each aneurysm Gaussian curve was decomposed into a maximum of five simple Gaussian functions, varying according to the mean thickness, amplitude and standard deviation (**Figures 2I,J**). To make the best possible match between the number of Gaussian and the GMM, the Chi-2 minimization simplex method was used. Based on the number of Gaussian curves, IA walls were classified as uniform (i.e., 1 Gaussian curve, example given in **Figure 2**- left side) or non-uniform (i.e., 2–5 Gaussian curves, example given in **Figure 2**- right side).

Statistical Analysis

Results are shown as individual values and as median ± interquartile range (IQR), as percentage or in correlations. Comparisons of medians were performed using a non-parametric Mann-Whitney *U*-test for two groups comparison and using Kruskal-Wallis and Dunn's multiple comparison tests for 4 groups comparison. Comparisons of percentages was performed using a Fisher exact test. For continuous variables with normal distribution, verified by the Kolmogonov-Smirnov test, Pearson correlations were performed to examine association between variables. For ordinal variables, Spearman correlations were performed to examine association between variables. Differences were considered statistically significant at values of $p < 0.05$.

RESULTS

Characteristics of the Studied Population

The studied population was composed of 55 patients with a mean age of 54 ± 11 years. Fifty-four patients were of Eurasian ethnicity and one was African. Our study group had a majority of females (75%) and smokers (63%: 47% current smokers and 16% former smokers). Forty-two percent of patients ($N = 23$) were diagnosed with hypertension, regardless of treatment status. Positive family history of IA or SAH was declared in 18% of the patients ($N = 10$). Previous SAH was present in 9% ($N = 5$) of the patients. Multiple-aneurysm cases concerned 49% of patients ($N = 27$). Six patients (11%) were affected by PKD. Eighteen IAs (33%) were ruptured and 37 (67%) were unruptured. The mean maximum dome diameter was 6.7 ± 3.6 mm. The mean aneurysm neck size was 3.9 ± 2.4 mm. The mean bottleneck factor was 1.7 ± 0.6. The majority of the aneurysms resected for this study were located at the middle cerebral artery (MCA, $N = 38$, 69%). The other vascular locations were internal carotid artery ($N = 1$), A2 artery ($N = 2$), posterior communicating artery ($N = 2$), anterior communicating artery ($N = 5$) and anterior cerebral artery ($N = 7$). Concerning aneurysm aspects, the ratio of rough/smooth domes was 0.3 rough and 0.7 smooth; 44% of domes included blebs, 27% included lobules and 55% of them included blebs and/or lobules.

Effects of IA Characteristics on IA Wall Thickness

Maximum dome diameter was positively correlated to mean (**Figure 3A**) and maximum (**Figure 3B**) IA wall thickness. A positive correlation was also observed between neck size and maximum IA wall thickness (**Figure 3E**). Bottleneck factor was positively correlated to mean (**Figure 3G**) and minimum (**Figure 3I**) IA wall thickness. No correlations were observed between maximum dome diameter and minimum IA wall thickness (**Figure 3C**), or between neck size and mean or minimum IA wall thickness (**Figures 3D,F**, respectively). Furthermore, no correlation was found between bottleneck factor and maximum IA wall thickness (**Figure 3H**). Finally, no associations were found between IA wall thickness (mean, maximum and minimum) and IA rupture status (**Figures 4A–C**), IA location (**Figures 4D–F**), IA aspect (**Figures 4G–I**) or morphology (**Figures 4J–L**).

Effects of IA Characteristics on IA Wall Thickness Uniformity

IA wall thickness uniformity was based on the number of Gaussian curves characterizing each aneurysm wall. For twelve IA domes, one Gaussian curve (example given in **Figure 2I**) characterized the aneurysm wall meaning that these walls had a uniform thickness. For forty-three IA domes, the IA wall thickness was depicted by 2–5 Gaussian curves (example given

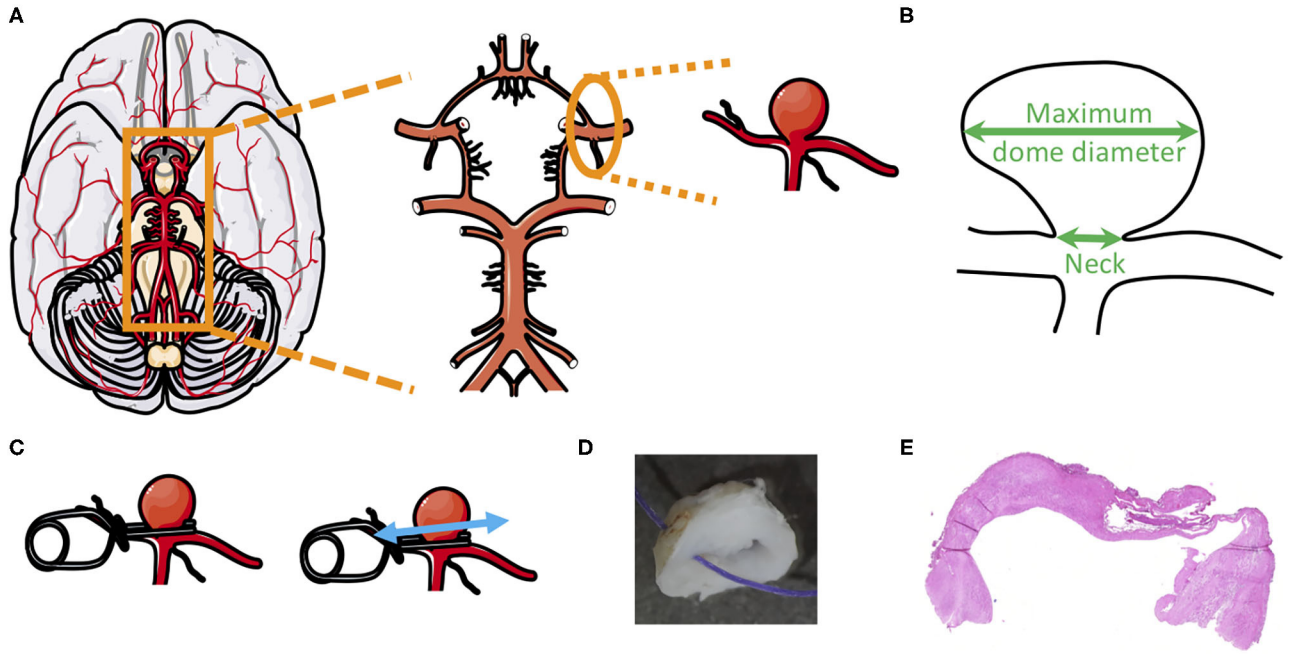

FIGURE 1 | Intracranial aneurysm dome, from the circle of Willis to histology. **(A)** Example of intracranial aneurysm location in the circle of Willis. **(B)** Schematic representation of an aneurysm dome to show where neck size and maximum dome diameter were measured. **(C–E)** After clipping of the IA neck **(C)**, the IA dome was resected and fixed in formol **(D)**, cutted and stained with hematoxylin and eosin **(E)** to allow IA wall thickness measurement.

in **Figure 2J**) implying that they had different degrees of non-uniform wall thickness. Maximum dome diameter (**Figure 5A**) and neck size (**Figure 5C**) were positively correlated with the number of Gaussian curves characterizing each IA wall. No correlation was found between the bottleneck factor and the number of Gaussian curves (**Figure 5E**). IA walls classified as uniform showed a lower maximum dome diameter in comparison with IA walls classified as non-uniform (**Figure 5B**). No difference with respect to neck size (**Figure 5D**) or bottleneck factor (**Figure 5F**) was shown between uniform and non-uniform IA walls. Mean (**Figure 5G**), maximum (**Figure 5H**) and minimum (**Figure 5I**) IA wall thickness were lower in uniform walls in comparison with walls with a non-uniform thickness. The proportion of unruptured IAs was higher in the IA group with uniform wall thickness ($N = 10/12$) in comparison with the IA group with non-uniform wall thickness ($N = 27/43$) (**Figure 5J**). This outcome was not induced by differences in maximum dome diameter, neck size, or bottleneck factor between unruptured IA domes with uniform wall thickness and those with non-uniform wall thickness (**Table 1**). In the group of IAs with uniform wall thickness, maximum dome diameter was not different between unruptured and ruptured IAs (**Table 1**). In the group of IAs with non-uniform wall thickness, maximum dome diameter was significantly higher in ruptured IAs in comparison with unruptured IAs ($p < 0.05$, **Table 1**). No differences for neck size and bottleneck factor were found between ruptured and unruptured IAs (**Table 1**). The distribution of IA domes with smooth/rough aspect or with presence or absence of blebs and/or lobules were not different between IA domes having a uniform or a non-uniform wall thickness (data not shown). In the group of IA domes with a uniform IA wall thickness, the proportion of IAs located on the MCA was higher than in the group of IA domes with a non-uniform wall thickness (83 *vs.* 65%, $p < 0.01$). Maximum dome diameter and bottleneck factor were not different between IA domes located in MCA or located at other locations, and were not different between IA domes with a uniform or non-uniform wall thickness (**Table 1**). In the group of IAs with uniform wall thickness, neck size was not different between MCA-located IA domes and non-MCA-located IA domes (**Table 1**). However, in the non-uniform wall thickness group, neck size was significantly higher ($p < 0.01$) in MCA-located IA domes in comparison with non-MCA-located IA domes (**Table 1**).

Effects of Patient Characteristics on IA Wall Thickness and Thickness Uniformity

None of the patient characteristics (age, sex, hypertension, smoking status, positive family history, or presence of multiple IAs) had an effect on mean, maximum or minimum IA wall thickness (data not shown). Although, no differences for mean (**Figure 6A**), maximum (**Figure 6B**) or minimum (**Figure 6C**) wall thickness were observed between men and women, the proportion of women was higher in the IA group with non-uniform wall thickness ($N = 34/43$, 79%) in comparison with the group of IAs with uniform wall thickness ($N = 7/12$, 58%) (**Figure 6D**). This observation was not induced by differences in

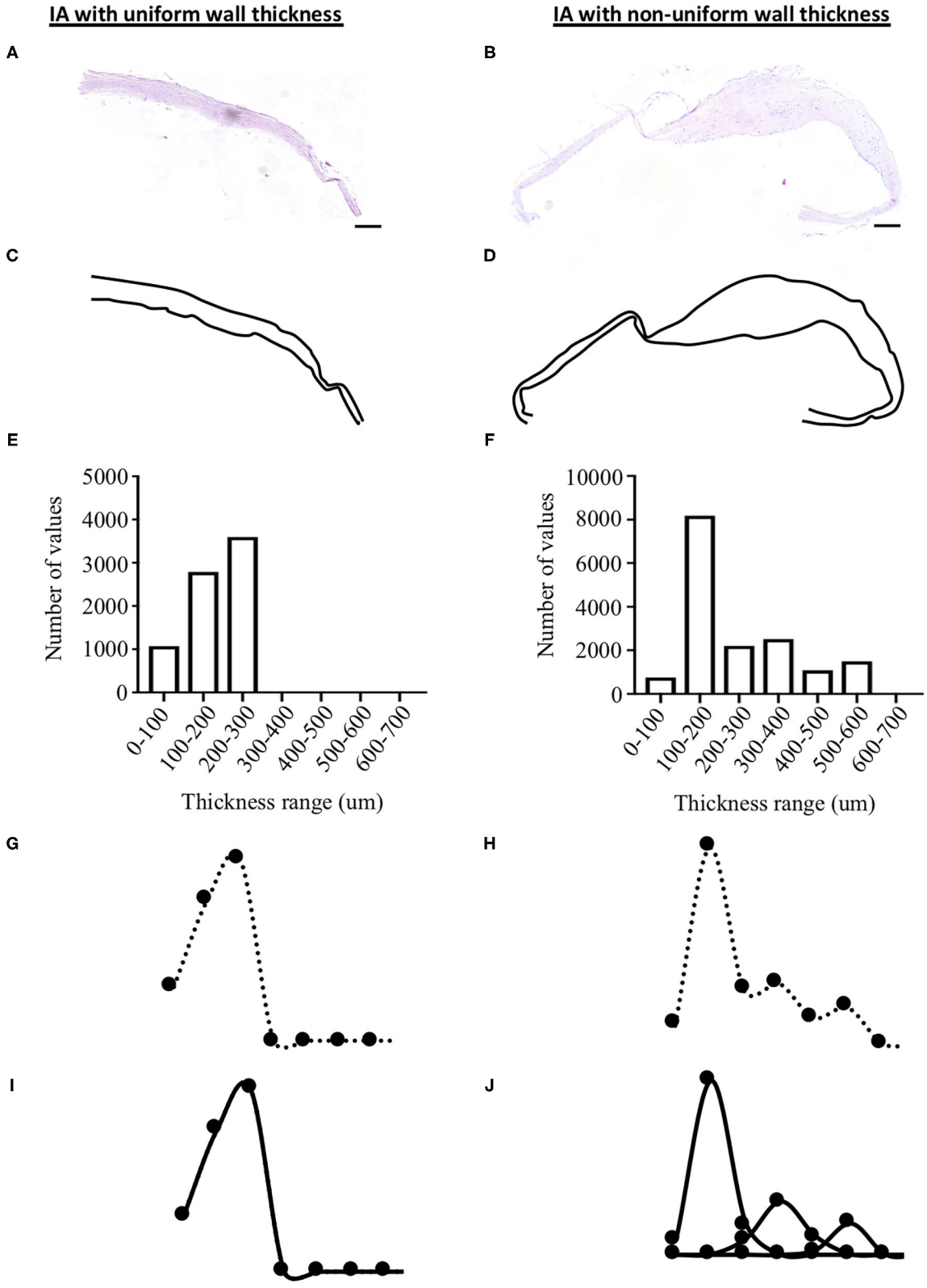

FIGURE 2 | Methods for the measurement of aneurysm wall thickness and thickness uniformity. IA wall thickness was measured on hematoxylin and eosin sections **(A,B)** after drawing the external border of the IA wall **(C,D)**. A thickness topographic map of each dome was obtained **(E,F)** allowing the calculation of a Gaussian curve from this frequency distribution **(G,H)**. Each Gaussian curve was decomposed **(I,J)** to classify IA wall as uniform (i.e., 1 Gaussian curve, left side of the figure) or non-uniform (i.e., 2–5 Gaussian curves, right side of the figure). Scale bar in **(A,B)** = 200 μm.

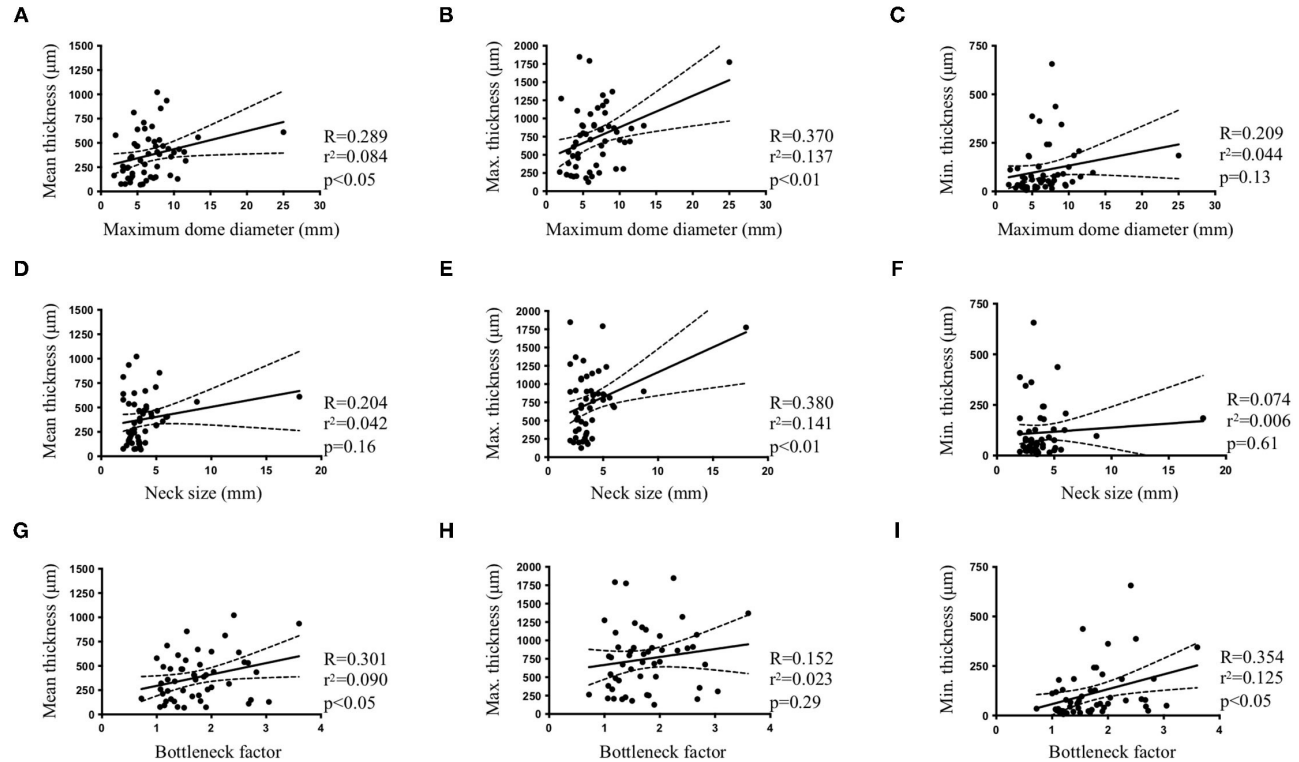

FIGURE 3 | Intracranial aneurysm characteristics and IA wall thickness. Pearson correlations between maximum dome diameter **(A–C)**, neck size **(D–F)** or bottleneck factor **(G–I)** and mean **(A,D,G)**, maximum [Max. **(B,E,H)**] or minimum [Min. **(C,F,I)**] IA wall thickness.

maximum dome diameter, neck size or bottleneck factor between women's IA domes with uniform wall thickness and those with non-uniform wall thickness (**Table 1**). Also, no significant differences were found for maximum dome diameter, neck size or bottleneck factor between men's IA domes in the uniform group and those in the non-uniform group (**Table 1**). Furthermore, no difference was found for maximum dome diameter, neck size or bottleneck factor when comparing men and women in uniform and non-uniform wall thickness groups (**Table 1**). Existence of multiple IAs did not affect the mean (**Figure 6E**), maximum (**Figure 6F**) or minimum (**Figure 6G**) IA wall thickness, but their proportion was higher in the group of IAs with non-uniform wall thickness (N = 24/43, 56%) in comparison with the group of IAs with uniform wall thickness (N = 3/12, 25%) (**Figure 6H**). No difference was found for maximum dome diameter, neck size or bottleneck factor when comparing patients with unique or multiple IAs in uniform and non-uniform wall thickness groups (**Table 1**). Mean (**Figure 6I**) and maximum (**Figure 6J**) wall thickness were significantly lower in IA walls of patients affected by PKD in comparison with non-PKD patients. No difference was found for minimum wall thickness between PKD and non-PKD patients (**Figure 6K**). The proportion of PKD patients was higher in the group of IAs with uniform wall thickness (N = 4/12, 33%) in comparison with the group of IAs with non-uniform wall thickness (N = 2/43, 5%) (**Figure 6L**). Although there was a tendency to a lower maximum dome diameter of the IAs of PKD patients, no significant differences were found for maximum dome diameter, neck size or bottleneck factor between PKD and non-PKD patients taking into account the uniformity or non-uniformity of the IA wall (**Table 1**). The age of the patients was not different between the uniform (48 (45–54) years old) and non-uniform (55 (45–65) years old) groups. The proportion of IA domes between uniform and non-uniform groups were not affected by smoking status (smokers: uniform = 67%, non-uniform = 63%), hypertension (yes: uniform = 42%, non-uniform = 42%) or positive family history (yes: uniform = 25%, non-uniform = 16%).

Clinical Prognosis Scores and IA Wall Thickness Uniformity

The PHASES score (12), based on population, hypertension status, age, size of the aneurysm, earlier SAH from another IA and site of aneurysm was calculated for 54 patients; IA size was missing for one patient resulting in omission of this patient for this comparison. The ELAPSS score (14), based on earlier SAH, location of the IA, age, population ethnicity, size and shape of the IA was calculated for 51 patients; IA size was missing for one patient and presence of irregularities was not described for 3 patients. Interestingly, the PHASES (**Figure 7A**) and ELAPSS (**Figure 7B**) scores were positively correlated with the number of Gaussian curves characterizing IA wall uniformity.

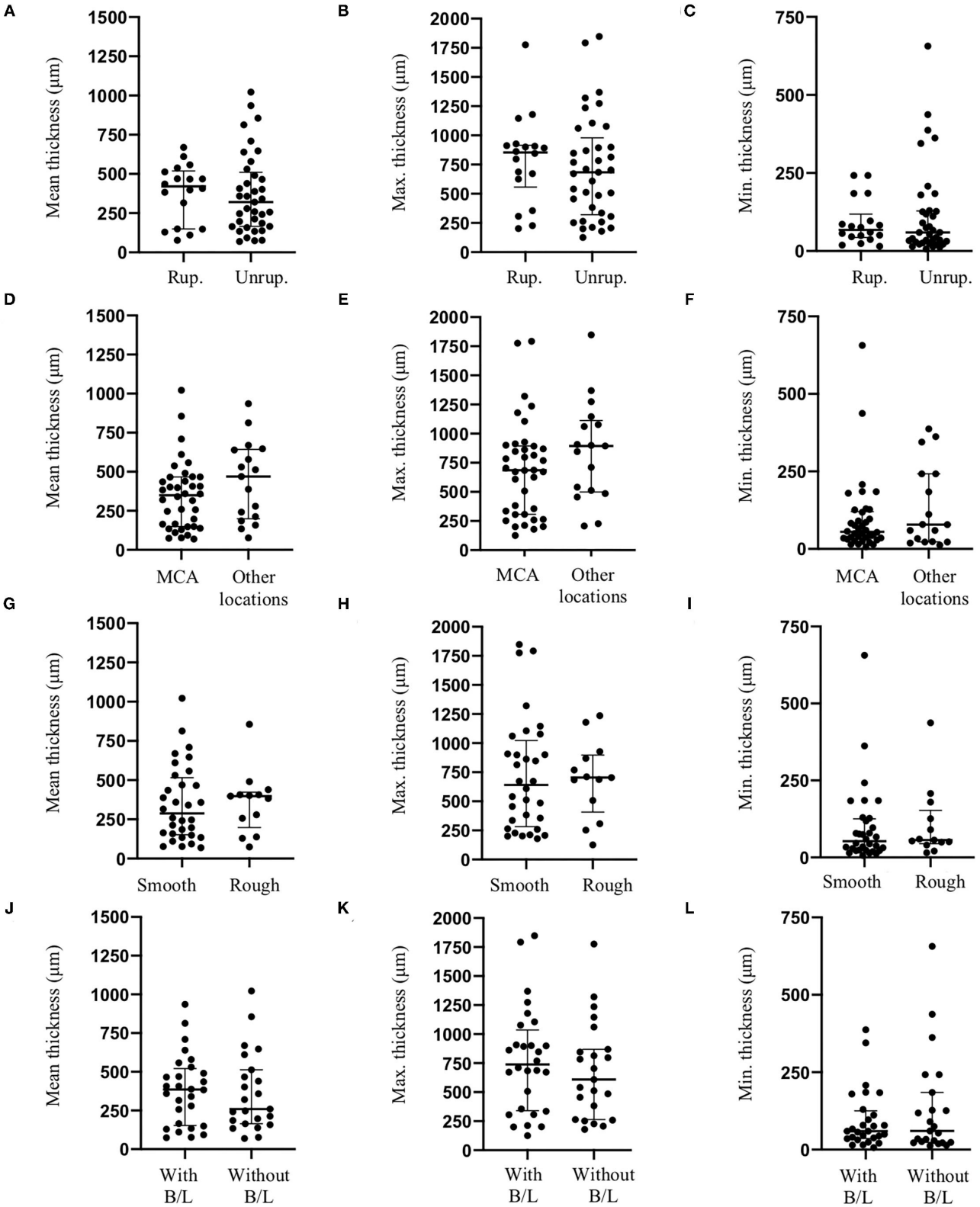

FIGURE 4 | Effects of intracranial aneurysm rupture status, location, aspect and morphology on IA wall thickness. Intracranial aneurysm rupture status [Rup.: Ruptured; Unrup.: Unruptured, **(A–C)**], location **(D–F)**, aneurysm aspect **(G–I)** or morphology [presence of blebs and/or lobules (B/L), **(J–L)**] did not affect mean **(A,D,G,J)**, maximum [Max., **(B,E,H,K)**] or minimum [Min., **(C,F,I,L)**] IA wall thickness.

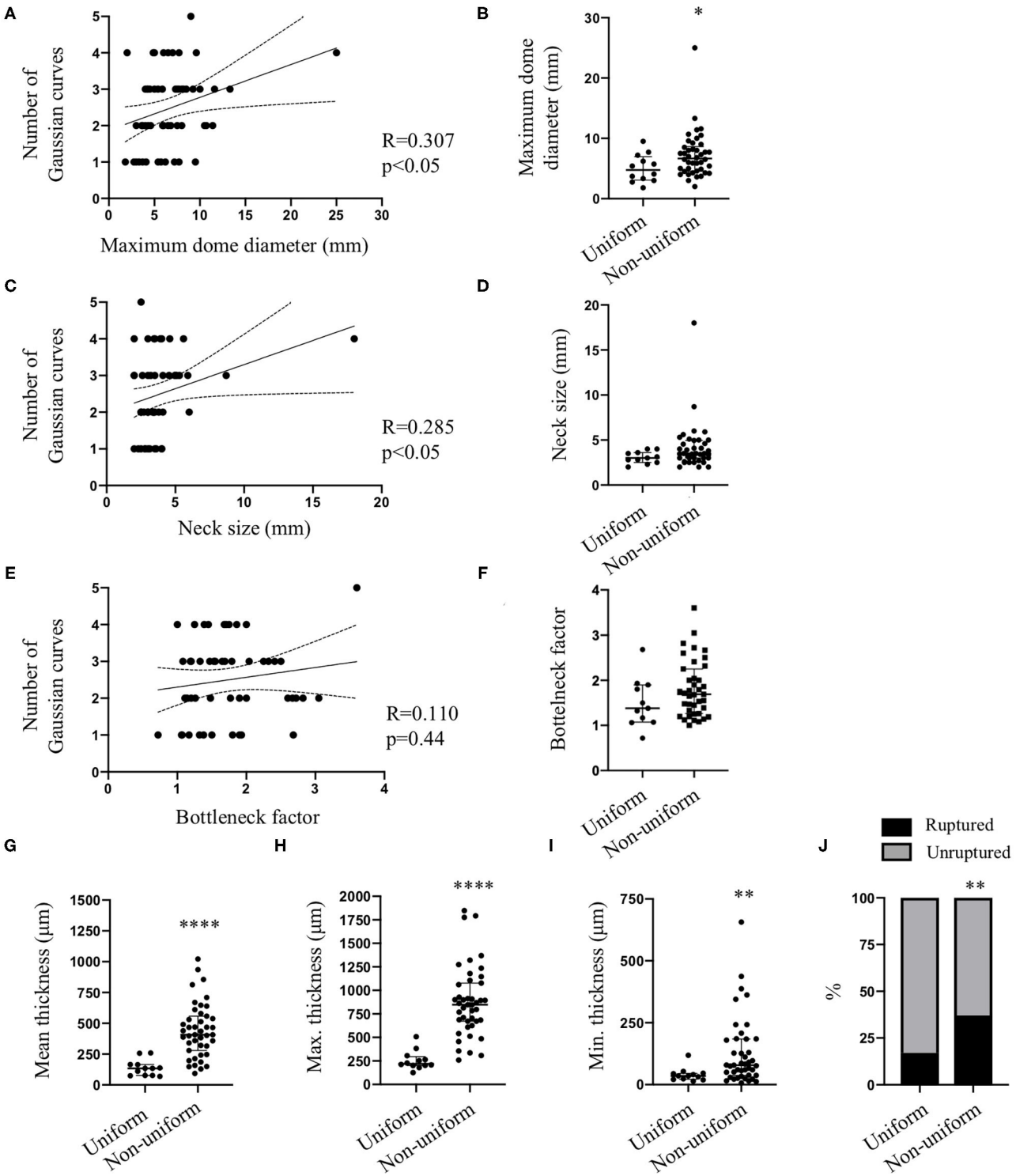

FIGURE 5 | Intracranial aneurysm characteristics and wall uniformity. Spearman correlations between maximum dome diameter **(A)**, neck size **(C)** or bottleneck factor **(E)** and number of Gaussian curves characterizing each intracranial aneurysm. Maximum dome diameter **(B)**, neck size **(D)**, and bottleneck factor **(F)** values in groups having a uniform or non-uniform IA wall thickness. Mean **(G)**, maximum [Max. **(H)**] and minimum [Min. **(I)**] wall thickness in groups having a uniform or non-uniform IA wall thickness. Data are shown as individual values and as median with interquartile range. $^{*}p < 0.05$, $^{**}p < 0.01$, $^{****}p < 0.0001$, non-parametric Mann-Whitney *U*-test. **(J)** Distribution of ruptured (black) and unruptured (gray) IA domes between uniform and non-uniform wall thickness groups. $^{**}p < 0.01$, Fisher's exact test.

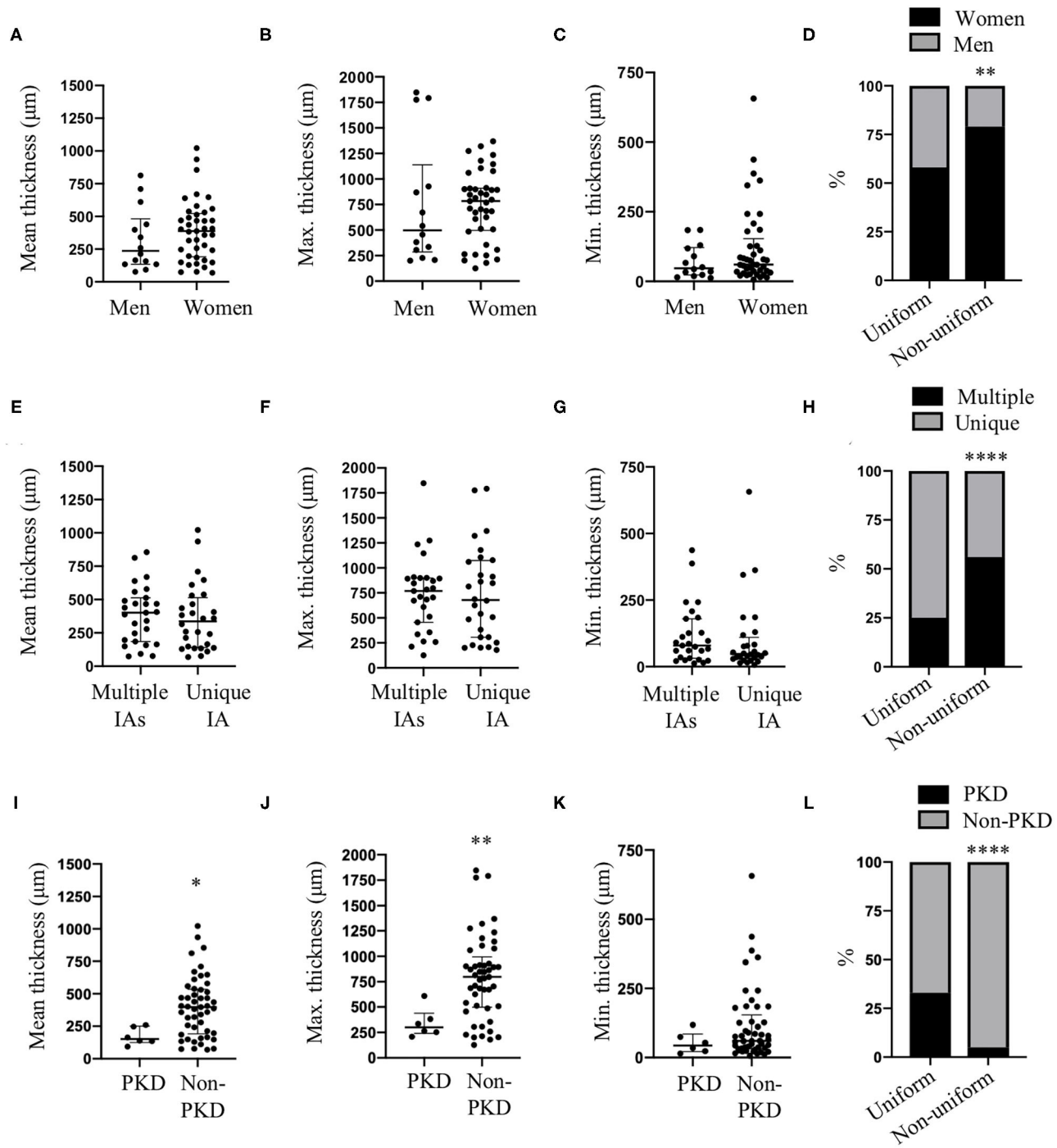

FIGURE 6 | Sex, IA multiplicity and PKD effects on IA wall thickness and uniformity. Mean **(A,E,I)**, maximum [Max. **(B,F,J)**] and minimum [Min. **(C,G,K)**] IA wall thickness in men and women **(A–C)**, for groups of multiple IAs and unique IA **(E–G)** and in patients diagnosed or not with PKD **(I–K)**. Data are shown as individual values and as median with interquartile range. *$p < 0.05$, **$p < 0.01$, non-parametric Mann-Whitney *U*-test. **(D)** Distribution of women (black) and men (gray) between uniform and non-uniform wall thickness groups. **(H)** Distribution of multiple IAs (black) and unique IA (gray) between uniform and non-uniform wall thickness groups. **(L)** Distribution of PKD (black) and non-PKD (gray) patients between uniform and non-uniform wall thickness groups. **$p < 0.01$, ****$p < 0.0001$, Fisher's exact test.

TABLE 1 | Maximum (Max.) dome diameter, neck size and bottleneck factor according to IA rupture status, IA location, IA multiplicity, patient sex, and PKD diagnosis in groups with uniform or non-uniform wall thickness.

			Uniform wall thickness	Non-uniform wall thickness
IA rupture status	Unruptured IA	Max. dome diameter	4.8 (3.2–7.3)	5.9 (4.2–8.0)
		Neck size	3.1 (2.8–3.8)	3.3 (2.7–5.0)
		Bottleneck factor	1.3 (1.1–1.8)	1.7 (1.2–2.0)
	Ruptured IA	Max. dome diameter	4.5 (2.8–6.2)	7.7 (6.8–10.7)
		Neck size	2.2 (2.0–2.3)	3.9 (3.4–4.9)
		Bottleneck factor	2.0 (1.4–2.7)	1.8 (1.5–2.7)
IA location	MCA	Max. dome diameter	5.6 (3.2–7.3)	7.7 (5.4–10.0)
		Neck size	3.0 (2.6–3.8)	4.3 (3.7–5.2)
		Bottleneck factor	1.5 (1.1–1.9)	1.6 (1.3–2.2)
	Other locations	Max. dome diameter	3.4 (2.8–4.1)	5.0 (4.3–7.0)
		Neck size	2.7 (2.0–3.5)	3.0 (2.5–3.5)
		Bottleneck factor	1.3 (1.2–1.4)	1.8 (1.2–2.2)
IA multiplicity	Unique IA	Max. dome diameter	5.4 (3.4–7.5)	7.7 (6.0–9.8)
		Neck size	3.2 (2.4–3.9)	3.5 (3.0–5.0)
		Bottleneck factor	1.4 (1.2–1.9)	1.9 (1.2–2.7)
	Multiple IAs	Max. dome diameter	3.3 (1.8–5.7)	5.7 (4.4–8.0)
		Neck size	3.0 (2.5–3.1)	3.5 (2.6–4.5)
		Bottleneck factor	1.1 (0.7–1.9)	1.7 (1.3–1.9)
Sex	Women	Max. dome diameter	5.7 (3.3–7.2)	7.2 (5.0–8.6)
		Neck size	3.1 (2.5–4.0)	3.5 (3.0–5.0)
		Bottleneck factor	1.8 (1.1–1.9)	1.8 (1.5–2.4)
	Men	Max. dome diameter	3.7 (2.9–6.8)	4.4 (4.9–8.4)
		Neck size	2.8 (2.2–3.3)	3.5 (2.8–4.9)
		Bottleneck factor	1.2 (1.1–1.4)	1.3 (1.2–1.9)
PKD diagnosis	PKD	Max. dome diameter	3.6 (2.1–6.4)	3.9 (3.7–4.0)
		Neck size	3.2 (2.6–3.9)	3.0 (2.5–3.5)
		Bottleneck factor	1.1 (0.9–1.6)	1.3 (1.1–1.5)
	Non-PKD	Max. dome diameter	5.6 (3.4–7.3)	6.9 (4.9–8.9)
		Neck size	3.0 (2.3–3.6)	3.5 (3.0–5.0)
		Bottleneck factor	1.5 (1.3–1.9)	1.7 (1.3–2.3)

Values are median (Interquartile range).

DISCUSSION

Formation, growth, remodeling, destabilization and rupture of IAs are complex pathological processes. Prediction tools such as PHASES (12) and ELAPSS (14) scores suggest age, smoking status, hypertension, or aneurysm location to be strong predictors of rupture risk. In 2017, a systematic review performed by Kleinloog et al. (40) including 102 studies and describing 144 risk factors for IA rupture found strong evidence that changes in some morphological factors, such as aspect ratio, size ratio or bottleneck factor, increase IA rupture risk. Previous studies on IA wall histological features focused on the effects of patients and aneurysms characteristics on wall cellular content and ECM protein organization (26, 27, 31, 41), but few investigated IA wall thickness or thickness uniformity (35, 36). As SAH is induced by a breach in the vessel wall, precise analyses of IA wall thickness and wall thickness uniformity are paramount in grasping what makes IAs prone to rupture. Through wall thickness assessment of IA domes from the Aneux biobank, we demonstrate in this study that maximum dome diameter, neck size and diagnosis of PKD are the main factors correlated with IA wall thickness and IA wall thickness uniformity. Interestingly, IAs with a non-uniform wall thickness are more often observed in the ruptured group, in women and in patients harboring multiple IAs. Finally, PHASES and ELAPSS scores are positively correlated with IA wall thickness heterogeneity.

One of our crucial findings is that IA wall thickness and thickness heterogeneity, measured in detail on histological sections, increase with maximum dome diameter, neck size or diagnosis of PKD. These results further support a previous study performed by Kadasi et al. (35) showing morphologically that large aneurysms (>7 mm) contained a larger proportion of thick wall than thin translucent wall. This size-pathogenesis interconnection was first put forward by Asari and Ohmoto (32) who characterized a group of entirely thick-walled IAs, all having a diameter over 9 mm. Aneurysm and neck size are important

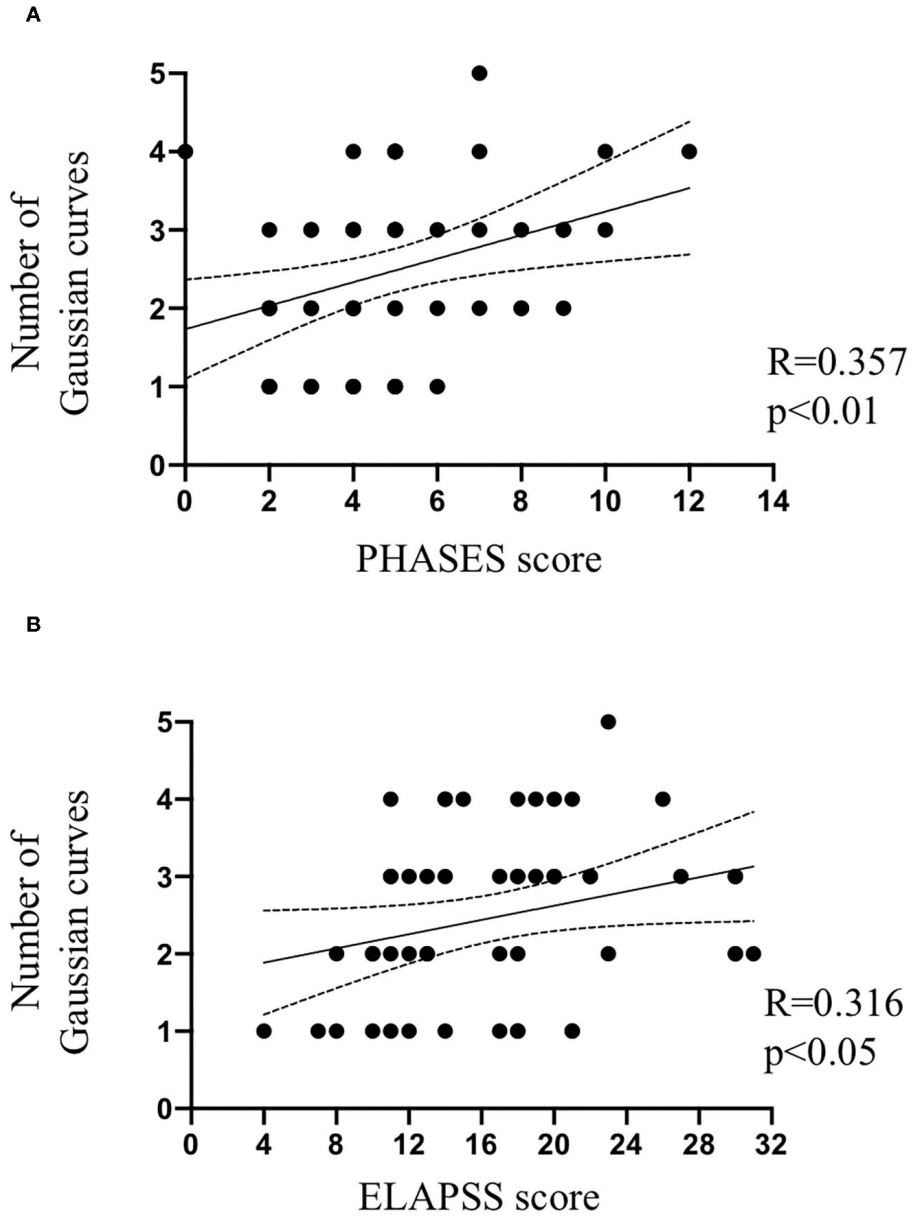

FIGURE 7 | IA wall uniformity and clinical scores. Spearman correlations between PHASES score **(A)** or ELAPSS score **(B)** and the number of Gaussian curves characterizing IA wall uniformity.

parameters modulating the impact of hemodynamic forces on the IA wall (30, 42, 43). Indeed, altered cyclic circumferential stretch was associated with reduced SMC viability and collagen expression (44). Otherwise, pathological levels and patterns of wall shear stress (WSS) have been linked to endothelial cell dysfunction, phenotypic changes in SMCs, remodeling of ECM, and activation of inflammatory pathways (42, 45). In a cohort of patients with small (<10 mm) or large/giant (>10 mm) aneurysms, Schnell et al. (43) demonstrated in 2014 that larger IAs were subjected to higher WSS than smaller IAs. More recently, Cebral et al. (46) showed that high average WSS and pressure were more likely associated with thin IA wall regions, and that hyperplastic regions had lower average WSS and pressure than normal regions. Important cellular sensors of WSS are primary cilia. Patients carrying a mutation of genes affecting the expression or function of primary cilia are more prone to develop IA than the general population (8, 9). In a previous study (47), we showed that the wall of unruptured IAs from PKD patients contained less collagen than the ones of non-PKD patients. In addition, PKD IAs displayed a more degraded vascular wall phenotype comparable to what was observed in ruptured IAs. Interestingly, we also showed that the expression of the junction protein Zonula Occludens-1 (ZO-1) was reduced in endothelial cells of PKD patients in comparison

with non-PKD patients. In subsequent *in vitro* experiments, we showed that the decreased expression of ZO-1 led to increased endothelial cell permeability suggesting that disturbed expression of ZO-1 in human IAs could underly the leakiness of the endothelium observed in PKD patients. Modification of IA wall composition in PKD patients may participate in the thinning of the aneurysmal wall observed in the present study. Altogether, these studies suggest that the association between IA wall thickness and morphological parameters may depend on local hemodynamic forces.

Whereas, smoking status, hypertension, aneurysm aspect, morphology, or location are risk factors used in current rupture prediction tools (12–14), we did not find any association between these parameters and IA wall thickness or thickness uniformity. Cigarette smoke is known to induce endothelial dysfunction, SMC phenotypic modulation or death, and promotes inflammation (48), which could all increase the risk of IA rupture. We have previously shown that the IA walls of smokers contained less SMCs than the ones of non-smokers and that this lower SMC content is similar to the one measured in ruptured IAs (27), strongly suggesting that reduced SMC content in the IA wall is associated with a higher risk of rupture (41). In the present study, IA wall thickness and thickness uniformity is not different between smokers and non-smokers indicating that although a lower presence of SMCs favors rupture, it does not necessarily lead to a thinner or non-uniform IA wall. Cardiovascular remodeling via SMCs migration, proliferation or hypertrophy has been shown to involve the renin-angiotensin system (49, 50). Ohkuma et al. (51), proposed that increased hemodynamic stress may activate local renin-angiotensin system resulting in arterial wall thickening, and demonstrated that the expression of angiotensin-converting enzyme, angiotensin type 1 receptor and angiotensin II were reduced in IA walls in comparison to control arteries. However, no difference in the expression of such proteins was found between patients with or without hypertension, suggesting that the local renin-angiotensin system is not activated in the case of IAs. This may explain why in our cohort no difference has been found between normotensive and hypertensive patients for IA wall thickness and thickness uniformity. Even if morphological observation of irregularities and presence of blebs and/or lobules were expected to have an impact on IA wall thickness and thickness uniformity in histological sections, no associations were found in our study. One important limitation concerning the analysis of the effects of these IA characteristics on wall thickness is that, due to IA neck clipping, we do not have access to the complete IA for histological investigations which can slightly skew the analysis. IA location is a central factor for aneurysm rupture risk (12, 13, 52). Here, IAs located in the MCA seemed to possess a more uniform wall thickness than IAs located elsewhere in the circle of Willis. The number of IAs in each sub-classification (i.e., smooth/rough aspect, presence or absence of blebs and/or lobules, locations and uniform/non-uniform wall thickness) lead to a low number of samples in some of the subgroups rendering statistical analyses underpowered. Another limitation to investigate a possible association between IA location and wall thickness is that some aneurysms are never treated by microsurgery preventing the inclusion of such domes for histological studies.

The prevalence of IAs is higher in women than in men, but the risk of IA rupture is not different between sexes (53, 54). In our study population, we did not find differences in IA mean, maximum or minimum wall thickness between men and women, but we showed that IA walls in females were more likely to be non-uniform in comparison to those of males. In the study performed by Kadasi et al. (35), it was shown that IA domes from women had a higher proportion of thin wall than IA domes from men. This disparity in IA wall uniformity might indicate a divergence in aneurysm remodeling between sexes, in which hormones and hemodynamic factors likely play a crucial role.

CONCLUSION

Intracranial aneurysm walls are subject to a myriad of complex cellular and biochemical mechanisms resulting in a heterogeneous wall that may greatly vary from one patient to another. Quantitative analysis of IA wall thickness and thickness uniformity is paramount to better understand this disease. Considering the ensemble of patient and aneurysm characteristics used in clinical scores, perhaps the most significant finding of our study is that higher values for PHASES or ELAPSS scores were associated with higher IA wall heterogeneity. Further improvement of advanced clinical imaging techniques allowing for detailed measurement of variations in IA wall thickness may greatly help in the decision to treat or not unruptured IAs.

DATA AVAILABILITY STATEMENT

The original contributions presented in the study are included in the article/**Supplementary Material**, further inquiries can be directed to the corresponding author.

ETHICS STATEMENT

The studies involving human participants were reviewed and approved by Ethical Committee of the Geneva University Hospitals and Swissethics. The patients/participants provided their written informed consent to participate in this study.

AUTHOR CONTRIBUTIONS

JA: acquisition of data, analysis of data, interpretation of analysis, and drafting of manuscript. AC: acquisition of data, analysis of data, interpretation of analysis, and revision of manuscript. ND, GP, BF, and JH: acquisition of data and revision of manuscript. EA: interpretation of analysis and revision of manuscript. PB: conceptualization of the study, acquisition of data, interpretation of analysis, and revision of manuscript. BK: conceptualization of the study, interpretation of analysis, and revision of manuscript. SM: design and conceptualization of the study, acquisition of data, analysis of data, interpretation of analysis, and drafting and revision of manuscript. All authors contributed to the article and approved the submitted version.

FUNDING

This study was supported by grants from the Fondation Privée des HUG [to PB, EA, and BK], the Swiss SystemsX.ch initiative, evaluated by the Swiss National Science Foundation [to PB and BK], and the Swiss Heart Foundation [to BK, PB, and EA].

ACKNOWLEDGMENTS

We thank Esther Sutter for excellent technical help with sample processing. We thank Nicolas Liaudet from the Bioimaging Core Facility, Faculty of Medicine, University of Geneva, for technical help for the measurement of IA wall thickness with the software MATLAB 2019a. We thank the medical staff from the Neurosurgery Division of the Geneva University Hospitals for providing us with human intracranial aneurysm domes.

SUPPLEMENTARY MATERIAL

The Supplementary Material for this article can be found online at: https://www.frontiersin.org/articles/10.3389/fcvm.2021.775307/full#supplementary-material

REFERENCES

1. Lawton MT, Vates GE. Subarachnoid hemorrhage. *N Engl J Med.* (2017) 377:257–66. doi: 10.1056/NEJMcp1605827
2. Schatlo B, Fung C, Stienen MN, Fathi AR, Fandino J, Smoll NR, et al. Incidence and outcome of aneurysmal subarachnoid hemorrhage: the swiss study on subarachnoid hemorrhage (Swiss SOS). *Stroke.* (2021) 52:344–7. doi: 10.1161/STROKEAHA.120.029538
3. Vlak MH, Algra A, Brandenburg R, Rinkel GJ. Prevalence of unruptured intracranial aneurysms, with emphasis on sex, age, comorbidity, country, and time period: a systematic review and meta-analysis. *Lancet Neurol.* (2011) 10:626–36. doi: 10.1016/S1474-4422(11)70109-0
4. Komotar RJ, Mocco J, Solomon RA. Guidelines for the surgical treatment of unruptured intracranial aneurysms: the first annual J. Lawrence pool memorial research symposium–controversies in the management of cerebral aneurysms. *Neurosurgery.* (2008) 62:183–93. doi: 10.1227/01.NEU.0000311076.64109.2E
5. Chalouhi N, Dumont AS, Randazzo C, Tjoumakaris S, Gonzalez LF, Rosenwasser R, et al. Management of incidentally discovered intracranial vascular abnormalities. *Neurosurg Focus.* (2011) 31:E1. doi: 10.3171/2011.9.FOCUS11200
6. Toth G, Cerejo R. Intracranial aneurysms: review of current science and management. *Vasc Med.* (2018) 23:276–88. doi: 10.1177/1358863X18754693
7. Rinkel GJ, Djibuti M, Algra A, van Gijn J. Prevalence and risk of rupture of intracranial aneurysms: a systematic review. *Stroke.* (1998) 29:251–6. doi: 10.1161/01.STR.29.1.251
8. Zhou S, Dion PA, Rouleau GA. Genetics of intracranial aneurysms. *Stroke.* (2018) 49:780–7. doi: 10.1161/STROKEAHA.117.018152
9. Liu M, Zhao J, Zhou Q, Peng Y, Zhou Y, Jiang Y. Primary cilia deficiency induces intracranial aneurysm. *Shock.* (2018) 49:604–11. doi: 10.1097/SHK.0000000000000961
10. Etminan N, Rinkel GJ. Unruptured intracranial aneurysms: development, rupture and preventive management. *Nat Rev Neurol.* (2016) 12:699–713. doi: 10.1038/nrneurol.2016.150
11. Matsushige T, Shimonaga K, Mizoue T, Hosogai M, Hashimoto Y, Takahashi H, et al. Lessons from vessel wall imaging of intracranial aneurysms: new era of aneurysm evaluation beyond morphology. *Neurol Med Chir.* (2019) 59:407–14. doi: 10.2176/nmc.ra.2019-0103
12. Greving JP, Wermer MJ, Brown RD, Jr., Morita A, Juvela S, et al. Development of the PHASES score for prediction of risk of rupture of intracranial aneurysms: a pooled analysis of six prospective cohort studies. *Lancet Neurol.* (2014) 13:59–66. doi: 10.1016/S1474-4422(13)70263-1
13. Etminan N, Brown RD Jr, Beseoglu K, Juvela S, Raymond J, Morita A, et al. The unruptured intracranial aneurysm treatment score: a multidisciplinary consensus. *Neurology.* (2015) 85:881–9. doi: 10.1212/WNL.0000000000001891
14. Backes D, Rinkel GJE, Greving JP, Velthuis BK, Murayama Y, Takao H, et al. ELAPSS score for prediction of risk of growth of unruptured intracranial aneurysms. *Neurology.* (2017) 88:1600–6. doi: 10.1212/WNL.0000000000003865
15. Bijlenga P, Gondar R, Schilling S, Morel S, Hirsch S, Cuony J, et al. PHASES score for the management of intracranial aneurysm: a cross-sectional population-based retrospective study. *Stroke.* (2017) 48:2105–12. doi: 10.1161/STROKEAHA.117.017391
16. Brinjikji W, Pereira VM, Khumtong R, Kostensky A, Tymianski M, Krings T, et al. PHASES and ELAPSS scores are associated with aneurysm growth: a study of 431 unruptured intracranial aneurysms. *World Neurosurg.* (2018) 114:e425–32. doi: 10.1016/j.wneu.2018.03.003
17. Foreman PM, Hendrix P, Harrigan MR, Fisher WS 3rd, Vyas NA, Lipsky RH, et al. PHASES score applied to a prospective cohort of aneurysmal subarachnoid hemorrhage patients. *J Clin Neurosci.* (2018) 53:69–73. doi: 10.1016/j.jocn.2018.04.014
18. Hernandez-Duran S, Mielke D, Rohde V, Malinova V. The application of the unruptured intracranial aneurysm treatment score: a retrospective, single-center study. *Neurosurg Rev.* (2018) 41:1021–8. doi: 10.1007/s10143-018-0944-2
19. Pagiola I, Mihalea C, Caroff J, Ikka L, Chalumeau V, Iacobucci M, et al. The PHASES score: to treat or not to treat? Retrospective evaluation of the risk of rupture of intracranial aneurysms in patients with aneurysmal subarachnoid hemorrhage. *J Neuroradiol.* (2019) 47:349–52. doi: 10.1016/j.neurad.2019.06.003
20. Ravindra VM, de Havenon A, Gooldy TC, Scoville J, Guan J, Couldwell WT, et al. Validation of the unruptured intracranial aneurysm treatment score: comparison with real-world cerebrovascular practice. *J Neurosurg.* (2018) 129:100–6. doi: 10.3171/2017.4.JNS17548
21. Sanchez van Kammen M, Greving JP, Kuroda S, Kashiwazaki D, Morita A, Shiokawa Y, et al. External validation of the ELAPSS score for prediction of unruptured intracranial aneurysm growth risk. *J Stroke.* (2019) 21:340–6. doi: 10.5853/jos.2019.01277
22. Smedley A, Yusupov N, Almousa A, Solbach T, Toma AK, Grieve JP. Management of incidental aneurysms: comparison of single centre multi-disciplinary team decision making with the unruptured incidental aneurysm treatment score. *Br J Neurosurg.* (2018) 32:536–40. doi: 10.1080/02688697.2018.1468019
23. Naggara ON, White PM, Guilbert F, Roy D, Weill A, Raymond J. Endovascular treatment of intracranial unruptured aneurysms: systematic review and meta-analysis of the literature on safety and efficacy. *Radiology.* (2010) 256:887–97. doi: 10.1148/radiol.10091982
24. Kotowski M, Naggara O, Darsaut TE, Nolet S, Gevry G, Kouznetsov E, et al. Safety and occlusion rates of surgical treatment of unruptured intracranial aneurysms: a systematic review and meta-analysis of the literature from 1990 to 2011. *J Neurol Neurosurg Psychiatry.* (2013) 84:42–8. doi: 10.1136/jnnp-2011-302068
25. Tulamo R, Frosen J, Hernesniemi J, Niemela M. Inflammatory changes in the aneurysm wall: a review. *J Neurointerv Surg.* (2018) 10(Suppl 1):i58–67. doi: 10.1136/jnis.2009.002055.rep
26. Texakalidis P, Sweid A, Mouchtouris N, Peterson EC, Sioka C, Rangel-Castilla L, et al. Aneurysm formation, growth, and rupture: the biology and physics of cerebral aneurysms. *World Neurosurg.* (2019) 130:277–84. doi: 10.1016/j.wneu.2019.07.093
27. Morel S, Diagbouga MR, Dupuy N, Sutter E, Braunersreuther V, Pelli G, et al. Correlating clinical risk factors and histological features in ruptured and unruptured human intracranial aneurysms: the Swiss aneuX study. *J Neuropathol Exp Neurol.* (2018) 77:555–66. doi: 10.1093/jnen/nly031

28. Frosen J, Cebral J, Robertson AM, Aoki T. Flow-induced, inflammation-mediated arterial wall remodeling in the formation and progression of intracranial aneurysms. *Neurosurg Focus.* (2019) 47:E21. doi: 10.3171/2019.5.FOCUS19234
29. Soldozy S, Norat P, Elsarrag M, Chatrath A, Costello JS, Sokolowski JD, et al. The biophysical role of hemodynamics in the pathogenesis of cerebral aneurysm formation and rupture. *Neurosurg Focus.* (2019) 47:E11. doi: 10.3171/2019.4.FOCUS19232
30. Rajabzadeh-Oghaz H, Siddiqui AH, Asadollahi A, Kolega J, Tutino VM. The association between hemodynamics and wall characteristics in human intracranial aneurysms: a review. *Neurosurg Rev*. (2021). doi: 10.1007/s10143-021-01554-w
31. Gade PS, Tulamo R, Lee KW, Mut F, Ollikainen E, Chuang CY, et al. Calcification in human intracranial aneurysms is highly prevalent and displays both atherosclerotic and nonatherosclerotic types. *Arterioscler Thromb Vasc Biol.* (2019) 39:2157–67. doi: 10.1161/ATVBAHA.119.312922
32. Asari S, Ohmoto T. Growth and rupture of unruptured cerebral aneurysms based on the intraoperative appearance. *Acta Med Okayama.* (1994) 48:257–62.
33. Mizoi K, Yoshimoto T, Nagamine Y. Types of unruptured cerebral aneurysms reviewed from operation video-recordings. *Acta Neurochir.* (1996) 138:965–9. doi: 10.1007/BF01411286
34. Inagawa T, Hirano A. Autopsy study of unruptured incidental intracranial aneurysms. *Surg Neurol.* (1990) 34:361–5. doi: 10.1016/0090-3019(90)90237-J
35. Kadasi LM, Dent WC, Malek AM. Cerebral aneurysm wall thickness analysis using intraoperative microscopy: effect of size and gender on thin translucent regions. *J Neurointerv Surg.* (2013) 5:201–6. doi: 10.1136/neurintsurg-2012-010285
36. Kadasi LM, Dent WC, Malek AM. Colocalization of thin-walled dome regions with low hemodynamic wall shear stress in unruptured cerebral aneurysms. *J Neurosurg.* (2013) 119:172–9. doi: 10.3171/2013.2.JNS12968
37. Gondar R, Gautschi OP, Cuony J, Perren F, Jagersberg M, Corniola MV, et al. Unruptured intracranial aneurysm follow-up and treatment after morphological change is safe: observational study and systematic review. *J Neurol Neurosurg Psychiatry.* (2016) 87:1277–82. doi: 10.1136/jnnp-2016-313584
38. Bijlenga P, Ebeling C, Jaegersberg M, Summers P, Rogers A, Waterworth A, et al. Risk of rupture of small anterior communicating artery aneurysms is similar to posterior circulation aneurysms. *Stroke.* (2013) 44:3018–26. doi: 10.1161/STROKEAHA.113.001667
39. Leemans EL, Cornelissen BMW, Said M, van den Berg R, Slump CH, Marquering HA, et al. Intracranial aneurysm growth: consistency of morphological changes. *Neurosurg Focus.* (2019) 47:E5. doi: 10.3171/2019.4.FOCUS1987
40. Kleinloog R, de Mul N, Verweij BH, Post JA, Rinkel GJE, Ruigrok YM. Risk factors for intracranial aneurysm rupture: a systematic review. *Neurosurgery.* (2018) 82:431–40. doi: 10.1093/neuros/nyx238
41. Frosen J, Piippo A, Paetau A, Kangasniemi M, Niemela M, Hernesniemi J, et al. Remodeling of saccular cerebral artery aneurysm wall is associated with rupture: histological analysis of 24 unruptured and 42 ruptured cases. *Stroke.* (2004) 35:2287–93. doi: 10.1161/01.STR.0000140636.30204.da
42. Diagbouga MR, Morel S, Bijlenga P, Kwak BR. Role of hemodynamics in initiation/growth of intracranial aneurysms. *Eur J Clin Invest.* (2018) 48:e12992. doi: 10.1111/eci.12992
43. Schnell S, Ansari SA, Vakil P, Wasielewski M, Carr ML, Hurley MC, et al. Three-dimensional hemodynamics in intracranial aneurysms: influence of size and morphology. *J Magn Reson Imaging.* (2014) 39:120–31. doi: 10.1002/jmri.24110
44. Liu P, Song Y, Zhou Y, Liu Y, Qiu T, An Q, et al. Cyclic mechanical stretch induced smooth muscle cell changes in cerebral aneurysm progress by reducing collagen type iV and collagen type vI levels. *Cell Physiol Biochem.* (2018) 45:1051–60. doi: 10.1159/000487347
45. Staarmann B, Smith M, Prestigiacomo CJ. Shear stress and aneurysms: a review. *Neurosurg Focus.* (2019) 47:E2. doi: 10.3171/2019.4.FOCUS19225
46. Cebral JR, Detmer F, Chung BJ, Choque-Velasquez J, Rezai B, Lehto H, et al. Local hemodynamic conditions associated with focal changes in the intracranial aneurysm wall. *AJNR Am J Neuroradiol.* (2019) 40:510–6. doi: 10.3174/ajnr.A5970
47. Diagbouga MR, Morel S, Cayron AF, Haemmerli J, Georges M, Hierck BP, et al. Primary cilia control endothelial permeability by regulating expression and location of junction proteins. *Cardiovasc Res.* (2021). doi: 10.1093/cvr/cvab165
48. Chalouhi N, Ali MS, Starke RM, Jabbour PM, Tjoumakaris SI, Gonzalez LF, et al. Cigarette smoke and inflammation: role in cerebral aneurysm formation and rupture. *Mediators Inflamm.* (2012) 2012:271582. doi: 10.1155/2012/271582
49. Kumar R, Singh VP, Baker KM. The intracellular renin-angiotensin system: implications in cardiovascular remodeling. *Curr Opin Nephrol Hypertens.* (2008) 17:168–73. doi: 10.1097/MNH.0b013e3282f521a8
50. Naftilan AJ. Role of the tissue renin-angiotensin system in vascular remodeling and smooth muscle cell growth. *Curr Opin Nephrol Hypertens.* (1994) 3:218–27. doi: 10.1097/00041552-199403000-00014
51. Ohkuma H, Suzuki S, Fujita S, Nakamura W. Role of a decreased expression of the local renin-angiotensin system in the etiology of cerebral aneurysms. *Circulation.* (2003) 108:785–7. doi: 10.1161/01.CIR.0000087339.31094.3C
52. Rousseau O, Karakachoff M, Gaignard A, Bellanger L, Bijlenga P, Constant Dit Beaufils P, et al. Location of intracranial aneurysms is the main factor associated with rupture in the iCAN population. *J Neurol Neurosurg Psychiatry.* (2021) 92:122–8. doi: 10.1136/jnnp-2020-324371
53. Hamdan A, Barnes J, Mitchell P. Subarachnoid hemorrhage and the female sex: analysis of risk factors, aneurysm characteristics, and outcomes. *J Neurosurg.* (2014) 121:1367–73. doi: 10.3171/2014.7.JNS132318
54. Amenta PS, Medel R, Pascale CL, Dumont AS. Elucidating sex differences in cerebral aneurysm biology and therapy: the time is now. *Hypertension.* (2016) 68:312–4. doi: 10.1161/HYPERTENSIONAHA.116.07606

Conflict of Interest: The authors declare that the research was conducted in the absence of any commercial or financial relationships that could be construed as a potential conflict of interest.

Publisher's Note: All claims expressed in this article are solely those of the authors and do not necessarily represent those of their affiliated organizations, or those of the publisher, the editors and the reviewers. Any product that may be evaluated in this article, or claim that may be made by its manufacturer, is not guaranteed or endorsed by the publisher.

Copyright © 2021 Acosta, Cayron, Dupuy, Pelli, Foglia, Haemmerli, Allémann, Bijlenga, Kwak and Morel. This is an open-access article distributed under the terms of the Creative Commons Attribution License (CC BY). The use, distribution or reproduction in other forums is permitted, provided the original author(s) and the copyright owner(s) are credited and that the original publication in this journal is cited, in accordance with accepted academic practice. No use, distribution or reproduction is permitted which does not comply with these terms.

frontiers in Cardiovascular Medicine

ORIGINAL RESEARCH
published: 24 January 2022
doi: 10.3389/fcvm.2022.793755

Association of Carotid Plaque Morphology and Glycemic and Lipid Parameters in the Northern Manhattan Study

David Della-Morte[1,2,3†], Chuanhui Dong[1†], Milita Crisby[4], Hannah Gardener[1], Digna Cabral[1], Mitchell S. V. Elkind[5], Jose Gutierrez[5], Ralph L. Sacco[1] and Tatjana Rundek[1]*

[1] Department of Neurology, The Evelyn McKnight Brain Institute, Miller School of Medicine, University of Miami, Miami, FL, United States, [2] Department of Systems Medicine, School of Medicine, University of Rome Tor Vergata, Rome, Italy, [3] Department of Human Sciences and Quality of Life Promotion, San Raffaele Roma Open University, Rome, Italy, [4] Department of Neurobiology, Karolinska Institute, Care Sciences and Society, Stockholm, Sweden, [5] Department of Neurology, Vagelos College of Physicians and Surgeons and Mailman School of Public Health, Columbia University, New York, NY, United States

OPEN ACCESS

Edited by:
Emma Gordon,
The University of Queensland, Australia

Reviewed by:
Aldo Bonaventura,
ASST Sette Laghi, Italy
Adriana Georgescu,
Institute of Cellular Biology and Pathology (ICBP), Romania
Ryan Temel,
University of Kentucky, United States

***Correspondence:**
David Della-Morte
ddellamorte@med.miami.edu

[†]These authors have contributed equally to this work

Specialty section:
This article was submitted to Atherosclerosis and Vascular Medicine, a section of the journal Frontiers in Cardiovascular Medicine

Received: 12 October 2021
Accepted: 04 January 2022
Published: 24 January 2022

Citation:
Della-Morte D, Dong C, Crisby M, Gardener H, Cabral D, Elkind MSV, Gutierrez J, Sacco RL and Rundek T (2022) Association of Carotid Plaque Morphology and Glycemic and Lipid Parameters in the Northern Manhattan Study. Front. Cardiovasc. Med. 9:793755. doi: 10.3389/fcvm.2022.793755

Low Gray-Scale Median (GSM) index is an ultrasonographic parameter of soft, lipid rich plaque morphology that has been associated with stroke and cardiovascular disease (CVD). We sought to explore the contribution of the modifiable and not-modifiable cardiovascular risk factors (RFs) to vulnerable plaque morphology measured by the low GSM index. A total of 1,030 stroke-free community dwelling individuals with carotid plaques present (mean age, 71.8 ± 9.1; 58% women; 56% Hispanic, 20% Non-Hispanic Black, 22% Non-Hispanic White) were assessed for minimum GSM (min GSM) using high-resolution B-mode carotid ultrasound. Multiple linear regression models were used to evaluate the association between RFs and minGSM after adjusting for sociodemographic characteristics. Within an individual, median plaque number was 2 (IQR: 1–3) and mean plaque number 2.3 (SD: 1.4). Mean minGSM was 78.4 ± 28.7 (IQR: 56–96), 76.3 ± 28.8 in men and 80 ± 28.5 in women; 78.7 ± 29.3 in Hispanics participants, 78.5 ± 27.2 in Non-Hispanic Black participants, and 78.2 ± 29 in Non-Hispanic white participants. In multivariable adjusted model, male sex ($\beta = -5.78$, $p = 0.007$), obesity BMI ($\beta = -6.92$, $p = 0.01$), and greater levels of fasting glucose ($\beta = -8.02$, $p = 0.02$) and LDL dyslipidemia ($\beta = -6.64$, $p = 0.005$) were positively associated with lower minGSM, while presence of glucose lowering medication resulted in a significant inverse association ($\beta = 7.68$, $p = 0.04$). Interaction (with p for interaction <0.1) and stratification analyses showed that effect of age on minGSM was stronger in men ($\beta = -0.44$, $p = 0.03$) than in women ($\beta = -0.20$, $p = 0.18$), and in individuals not taking glucose lowering medication ($\beta = -0.33$, $p = 0.009$). Our study has demonstrated an important contribution of glycemic and lipid metabolism to vulnerable, low density or echolucent plaque morphology, especially among men and suggested that use of glucose lowering medication was associated with more fibrose-stable plaque phenotype

(greater GSM). Further research is needed to evaluate effects of medical therapies in individuals with vulnerable, low density, non-stenotic carotid plaques and how these effects translate to prevention of cerebrovascular disease.

Keywords: carotid artery, plaque, atherosclerosis, ultrasonology, gray-scale median, vascular risk factors, glucose, lipids

INTRODUCTION

Carotid plaque assessed by high-resolution ultrasonography is a well-validated marker of atherosclerosis and risk of stroke (1). Plaque densitometry, measured by the ultrasonographic gray-scale median (GSM) index, is a parameter of plaque morphology and a helpful predictor of stroke and its outcomes (2, 3). The GSM index represents a marker of plaque vulnerability with the potential clinical use because of its simplicity and reliability of assessment, low cost, and ability to be measured from plaque images collected from a clinical B-mode ultrasonography (2). Low GSM plaque values correspond to soft, echolucent plaque with high lipid content and a thin fibrous cap, whereas high GSM index represents echodense plaques with high fibrous content and calcification (3, 4). Low GSM values have been associated with higher prevalence of symptomatic carotid stenosis, neurological symptoms (2), and cerebrovascular disease (5). Recently, lower GSM values, established by brain magnetic resonance diffusion-weighted imaging (DWI), was found helpful to predict new cerebral ischemic lesions after carotid endarterectomy (6). We previously reported on the impacts of traditional and less traditional vascular risk factors on atherosclerotic plaque phenotypes, including plaque area and densitometry (7). In the Prospective Investigation of the Vasculature in Uppsala Seniors (PIVUS) study, the low levels of high-density lipoproteins (HDL) cholesterol, increased body mass index (BMI), and decreased glutathione levels were associated with the echolucent carotid plaque, implying the role of metabolic factors in plaque composition (8). However, not all studies were consistent and some reported no association between risk factors and grayscale ultrasonographic plaque features in middle-aged adults free of known cardiovascular disease (9). Therefore, we sought to investigate contribution of vascular risk factors to the vulnerable plaque morphology measured by the low GSM index in an urban, multi-ethnic cohort.

MATERIALS AND METHODS

Study Populations

The Northern Manhattan Study (NOMAS) is an ongoing population-based study aimed to determine the incidence of stroke, cognitive decline, and the role of novel risk factors in a race/ethnically diverse community (10). The details of the NOMAS design have been described previously (11). Data were collected through interviews using standardized collection instruments, review of the medical records, and physical and neurological examinations (11). NOMAS was approved by the Institutional Review Boards of Columbia University Medical Center and the University of Miami. All participants gave written informed consent for participation in the study NOMAS subjects received carotid ultrasound at the time of baseline enrollment from 1999. There were no specific selection criteria for the participation in the carotid ancillary study. A sample of 1,790 stroke-free subjects has been enrolled into the NOMAS carotid ultrasound imaging substudy (1).

Vascular Risk Factors

Definitions of vascular risk factors in NOMAS were described previously (11). In brief, race/ethnicity was self-identified based on questions adapted from the 2000 US census and classified into four categories (White non-Hispanic, Black non-Hispanic, Hispanic, and non-Hispanic other race). Hypertension was defined as a SBP $\geq$ 140 mm Hg or a DBP $\geq$ 90 mm Hg or a patient's self-report of a history of hypertension or use of antihypertensive medications. Diabetes was defined as fasting blood glucose $\geq$ 126 mg/dL or the patient's self-report of such a history or use of insulin or hypoglycemic medications. Dyslipidemia was defined as total cholesterol >200 mg/dL or self-reported history of increased blood cholesterol levels or cholesterol-lowering medication use. We did not capture duration of comorbidities before enrollment to NOMAS. Therefore, if present diabetes and dyslipidemia at baseline of NOMAS enrollment, they would have been present for at least 6–8 years before the start of ultrasound ancillary study. Medication for these specific diseases in NOMAS are classified in specific classes of medications (e.g., for diabetes, insulin, and oral glucose lowering med; for dyslipidemia statin, fibrates, for hypertension, ACE inhibitors/ARBS, Ca^{2+} channel blockers, diuretics, and beta-blockers). Cigarette smoking was categorized as non-smoker, former, or current smoker (within the last year) and pack-years of smoking were calculated. Mild to moderate alcohol use was defined as current drinking of >1 drink per month and $\leq$2 drinks per day. Body mass index (BMI) was calculated in kg/m^2. Physical activity was defined as the frequency and duration of 14 different recreational activities during the 2-week period before the interview. Years of education were collected, and completion of high school was a proxy for socioeconomic status. Medical insurance status (Medicare or private insurance vs. Medicaid or uninsured) was used as a proxy of socioeconomic status.

Carotid Ultrasound

High-resolution B-mode carotid ultrasound (GE LogIQ 700, 9–13-MHz linear-array transducer) was performed by trained and certified sonographers as previously detailed (12). The left and right carotid bifurcations and the internal and common carotid arteries were examined for the presence of plaque.

Plaque was defined as an area of focal wall thickening 50% greater than surrounding wall thickness confirmed by marking and comparing plaque thickness with the thickness of the surrounding wall during scanning by electronic calipers (7). After image normalization using linear scaling, GSM of an operator-selected blood region inside the vessel lumen was mapped to 0 and the brightest region of the adventitia was mapped to 255 using M'Ath (Paris, France) (13). Both of these reference regions were ∼0.4 mm2 in area and were selected on the first image of the image sequence. The reference GSM values calculated on the first frame were applied to that and all subsequent images. GSM was expressed for each plaque. The minimal GSM (minGSM) values of all carotid plaques insonated within an individual were averaged and considered a measure of echolucent or vulnerable plaque morphology (14).

Statistical Analysis

Among a total of 3,298 subjects enrolled in NOMAS, 1,790 stroke-free subjects represent the sample size needed to reach a significant α level. Sample characteristics were summarized as means with standard deviation (SD) for continuous variables and reported as frequencies with percentages for categorical variables. Student *t*-test, or *F*-test when more than two groups, was used to compare group mean differences in minGSM, whereas Pearson correlation analyses were conducted to examine the correlation between minGSM and each continuous variable. A multiple linear regression model fully adjusted for sociodemographic was constructed to evaluate association of risk factors with minGSM and collinearity was evaluated using variance inflation factor (VIF). As a secondary and sensitivity analysis, a stepwise linear regression was performed to identify risk factors associated with minGSM independently. Two-way interactions between the significant factors were also conducted by inclusions of interaction terms of them in the regression models and stratification analyses were followed if the interactions with a $p < 0.10$. All analyses were done using SAS version 9.4 (SAS Institute, Cary, N.C.).

RESULTS

Among 1,790 stroke-free subjects, 1,030 subjects had at least one carotid plaque. Plaques were non-stenotic (<1% of subjects had carotid stenosis >50% on carotid ultrasound). The associations between demographic and clinical characteristics with minGSM are shown in **Table 1**. The mean age in the whole sample was 71.8 ± 9.1years; 58% were women; 56% Caribbean Hispanics, 20% Non-Hispanic Black, and 22% Non-Hispanic White. Mean minGSM was 78.4 ± 28.7 in all subjects (IQR: 56–96), 76.3 ± 28.8 in men and 80 ± 28.5 in women; 78.7 ± 29.3 in Hispanic, 78.5 ± 27.2 in Non-Hispanic black, and 78.2 ± 29 in Non-Hispanic white participants. In univariate analysis, male sex ($p = 0.04$), increased BMI ≥ 30 ($p = 0.005$) and fasting glucose level ($p = 0.02$) were significantly and inversely associated with minGSM, while lower HDL cholesterol ($p = 0.05$) was positively associated with minGSM (**Table 1**). In the fully adjusted model, minGSM-correlates were observed for age (β = −0.42, $p = 0.001$), male sex (β = −5.78, $p = 0.007$), BMI ≥ 30 (β = −6.29,

TABLE 1 | Demographic and clinical characteristic of study sample.

Characteristics	Sample		Min. GSM	*P*-value
	N	%	Mean ± SD	
All	1,030	100%	78.4 ± 28.7	
Sex				0.04
Female	598	58%	80.0 ± 28.5	
Male	432	42%	76.3 ± 28.8	
Race/ethnicity				
Non-Hispanic White	223	22%	78.2 ± 29.0	**Ref**
Non-Hispanic Black	211	20%	78.5 ± 27.2	0.995
Hispanic	575	56%	78.7 ± 29.3	0.852
Non-Hispanic other	21	2%	74.1 ± 22.6	0.454
High school completion				0.77
No	515	50%	78.2 ± 28.8	
Yes	515	50%	78.7 ± 28.5	
Private insurance/medicare				0.89
No	234	23%	78.2 ± 30.1	
Yes	796	77%	78.5 ± 28.3	
Moderate alcohol drinking				0.89
No	614	60%	78.3 ± 28.0	
Yes	416	40%	78.6 ± 29.6	
Physical activity				0.46
No	444	43%	77.7 ± 28.5	
Yes	581	56%	79.0 ± 28.9	
Smoking				
Never	444	43%		**Ref**
Former	399	33%		0.983
Current	187	69%		0.048
BMI, Kg/m^2				
<25	278	27%	81.3 ± 29.6	**Ref**
25–29	464	45%	78.7 ± 28.5	0.18
≥30	86	28%	75.1 ± 27.8	0.005
BS, mg/dL				
<100	662	66%	79.3 ± 29	**Ref**
100–125	165	17%	79.6 ± 28.6	0.909
>125	170	17%	74.2 ± 27.1	0.036
SBP, mmHg				
<120	127	12%	79.8 ± 29.6	**Ref**
120–139	313	30%	78.9 ± 28.2	0.808
≥140	589	57%	77.9 ± 28.7	0.636
DBP, mmHg				
<80	508	49%	79.8 ± 29	**Ref**
80–89	224	22%	76.2 ± 27.5	0.081
≥90	297	29%	77.7 ± 29	0.224
LDL, mg/dL				
<130	512	52%	79.4 ± 29.6	**Ref**
130–149	205	21%	79.2 ± 28.5	0.867
≥150	276	28%	75.7 ± 27.4	0.088

(Continued)

TABLE 1 | Continued

Characteristics	Sample		Min. GSM	*P*-value
	N	%	Mean ± SD	
HDL, mg/dL				
≥40 for M, ≥50 for f	473	47%	78.2 ± 28.9	**Ref**
≥30 for M, ≥40 for f	338	34%	79.3 ± 27.2	0.725
<30 for M, <40 for f	191	19%	77.2 ± 31.2	0.586
TC, mg/dL				
<200	478	48%	77.4 ± 29.6	**Ref**
200–239	351	35%	80 ± 28.2	0.171
Antihypertension medication				0.35
No	576	56%	79.2 ± 29.8	
Yes	454	44%	77.5 ± 27.2	
Lipid-lowering medication				0.25
No	839	81%	78.9 ± 28.8	
Yes	191	19%	76.3 ± 28.3	
Glucose-lowering medication				0.90
No	870	84%	78.5 ± 28.8	
Yes	160	16%	78.2 ± 27.8	
Hypertension				0.88
No	282	27%	78.5 ± 29.0	
Yes	748	73%	78.4 ± 28.5	
Hypercholesterolemia				0.19
No	690	67%	79.3 ± 28.9	
Yes	340	33%	76.8 ± 28.1	
Diabetes				0.09
No	798	77%	79.2 ± 28.8	
Yes	232	23%	75.8 ± 28.0	
	Mean	**SD**	**Correlation**	***P*-value**
Age, years	71.8	9.1	−0.049	0.11
BMI, Kg/m^2	28.0	4.9	−0.068	0.03
SBP, mmHg	143.8	20.4	−0.043	0.17
DBP, mmHg	82.8	10.8	−0.053	0.09
Fasting Glucose, mg/dL	104.6	43.3	−0.075	0.02
LDL, mg/dL	129.7	36.4	−0.038	0.23
HDL, mg/dL	46.5	14.4	0.061	0.05

TABLE 2 | Association of demographic and categorical vascular risk factors with min GSM.

Variable	Beta	SE	*P*-value	VIF
Age	**−0.42**	**0.13**	**0.001**	**1.42**
Male sex	**−5.78**	**2.15**	**0.007**	**1.23**
Hispanic vs. non-Hispanic white	2.15	3.02	0.478	2.47
non-Hispanic black vs. non-Hispanic white	−0.91	3.10	0.768	1.75
Non-Hispanic other vs. non-Hispanic white	−3.38	6.77	0.618	1.12
High school completion (yes vs. no)	−0.61	2.40	0.800	1.57
Private insurance/medicare (yes vs. no)	4.92	2.57	0.056	1.28
Smoker current vs. never smoker	−4.68	2.83	0.098	1.29
Smoker former vs. never smoker	2.62	2.05	0.236	1.27
Moderate alcohol drinking (yes vs. no)	0.32	2.05	0.877	1.08
Physical activity (yes vs. no)	1.62	2.01	0.419	1.07
BMI overweight	−2.72	2.42	0.263	1.59
BMI obese	**−6.92**	**2.84**	**0.015**	**1.72**
Fasting glucose border	0.46	0.67	0.862	1.10
Fasting glucose diabetic	**−8.02**	**3.64**	**0.028**	**1.20**
SBP border	−0.74	3.45	0.830	2.68
SBP hypertension	0.49	3.48	0.888	3.20
DBP border	−2.89	2.63	0.272	1.28
DBP hypertension	−2.76	2.55	0.280	1.53
LDL border	−2.19	2.56	0.394	1.19
LDL dyslipidemia	**−6.64**	**2.34**	**0.005**	**1.22**
HDL border	2.26	2.32	0.330	1.35
HDL dyslipidemia	0.19	2.94	0.949	1.42
Glucose-lowering medication (yes vs. no)	**7.68**	**3.70**	**0.038**	**1.91**
Antihypertension medication (yes vs. no)	−0.80	2.15	0.709	1.23
Lipid-lowering medication (yes vs. no)	−2.51	2.73	0.359	1.12

Fully adjusted model: age, sex, race/ethnicity, high school completion and vascular risk factors (moderate alcohol use, moderate-heavy physical activity, BMI, systolic blood pressure, diastolic blood pressure, anti-hypertensive medication use, diabetes, LDL, HDL, cholesterol-lowering medication use). VIF, variance inflation factor. The bold values are significant, with a p-value < 0.05.

TABLE 3 | Effect of age on minGSM by sex and antidiabetic medication use and their interactions.

Variable	Beta	SE	*P*-value	*p* for interaction
Sex				
Male	−0.44	0.18	0.02	0.04
Female	−0.20	0.15	0.18	
Glucose-lowering use				
Yes	0.23	0.33	0.48	0.07
No	−0.33	0.12	0.009	

$p = 0.01$), diabetes (β = −8.02, $p = 0.02$), dyslipidemia (β = −6.64, $p = 0.005$), and lipid lowering medication use (β = 7.68, $p = 0.04$). All factors had a VIF < 3.5, suggesting that there was no high correlation between these factors (**Table 2**). Similarly, in multivariable adjusted model with stepwise selection, age, male sex, current smoking, obesity, diabetes, dyslipidemia, and antidiabetic medication use, were significantly associated with minGSM (**Supplementary Table 1**). Interaction (with p for interaction <0.1) and stratification analyses showed that effect of age on minGSM was stronger in men (β = −0.44, $p = 0.03$) than in women (β = −0.20, $p = 0.18$), and in individuals without taking glucose lowering medication (β = −0.33, $p = 0.009$; **Table 3**; **Figure 1**).

DISCUSSION

In this study, we reported significant associations between glycemic and lipidic parameters with unfavorable carotid plaque

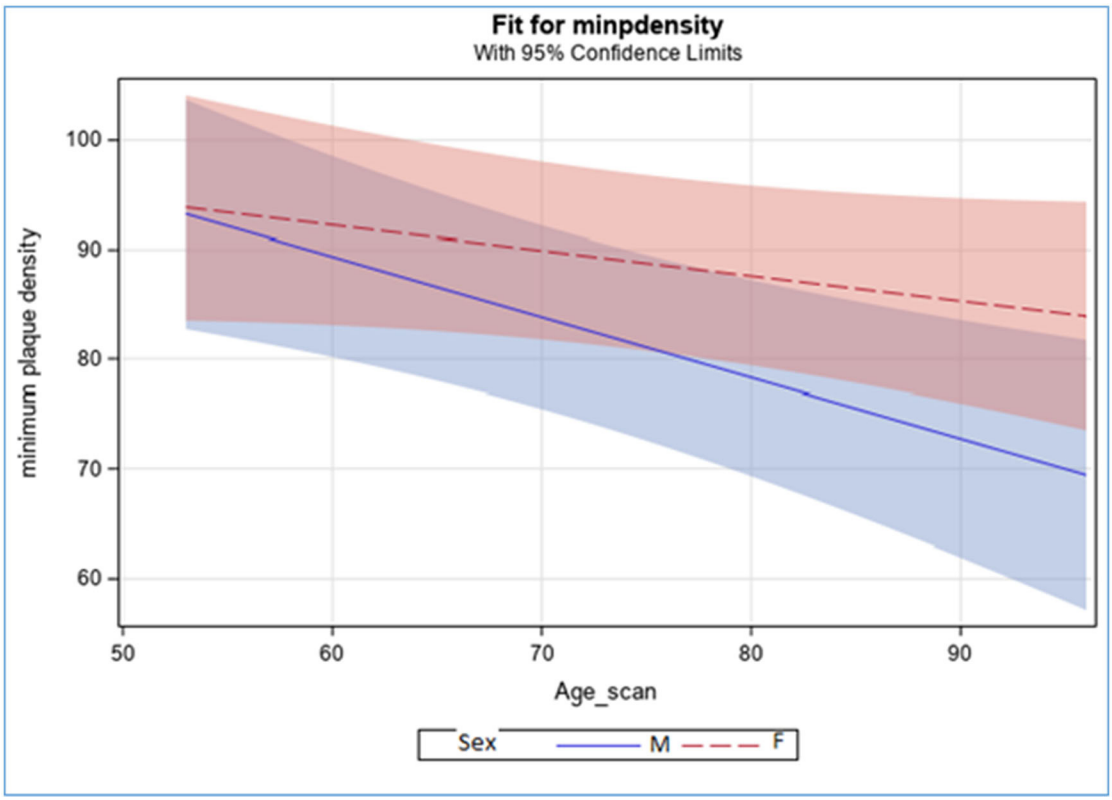

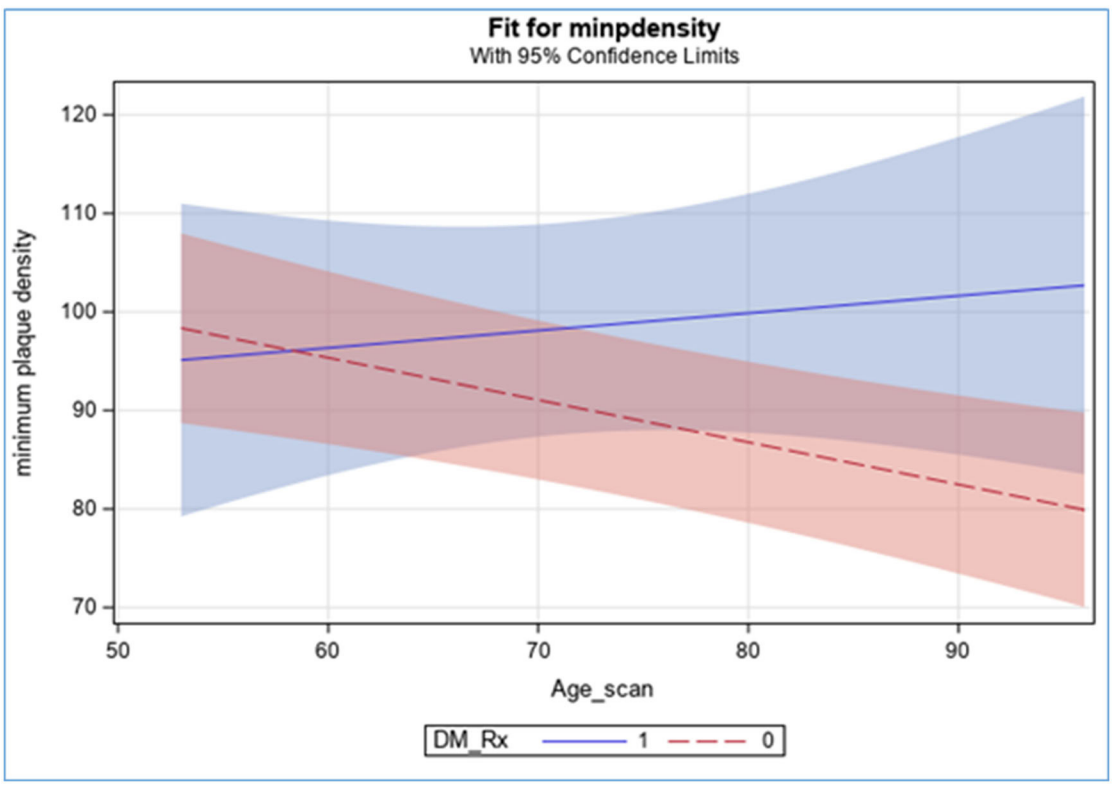

FIGURE 1 | Effect of age on minGSM by sex and antidiabetic medications.

morphology measured by the ultrasonographic GSM index. Our results suggest that along age and male sex, increased levels of fasting glucose, LDL cholesterol, and greater BMI are particularly critical for vulnerable plaque morphology, while glucose lowering medication use was protective. Moreover, the effects of these factors were more pronounced in older men than in older women, and in older patients treated for diabetes. No differences in vulnerable plaque morphology or the effects of risk factors on plaque morphology were noted between race-ethnic groups of participants. Our results indicate an atherosclerotic plaque phenotype that may explain a greater prevalence of extracranial atherosclerotic stroke in men than in women. Smoking did not affect echolucent plaque phenotype in our study. Aggressive treatments of metabolic factors and glycemic control provide opportunities for effective prevention of stroke and other atherosclerotic events. The carotid GSM index may be utilized as an effective non-invasive imaging biomarker to monitor vulnerable atherosclerotic plaque morphology and success of preventive interventions.

The relevance of low GSM values in carotid plaque has been established in a meta-analysis including 7,557 subjects with a mean follow-up of 37.2 months, where echolucent carotid plaques were associated with an increased risk of ipsilateral stroke regardless of the degree of stenosis (15). Moreover, in the Imaging in Carotid Angioplasty and Risk of Stroke (ICAROS) study, lower GSM was associated with poor outcome after intervention and low GSM improved stratification of patients for carotid endarterectomy or stenting (16). Lowest GSM has been characterized with a presence of lipid core, inflammation, neovascularity, and foam cells (17). Age and male sex are the main risk factors for the vulnerable atherosclerotic plaque morphology. In Evaluation of Rosuvastatin (METEOR) study, older age (mean 84 $\pm$ 29) was associated with more echolucent plaques (18). Age-related changes in arterial hemodynamic and increased arterial stiffness lead to an increase prevalence of atheromatous plaques and decrease in fibrous plaques morphology, characterized by higher macrophage and less smooth muscle cells content. This process seems to be accelerated in men, as suggested in our study as well as in the Tromsø Study (19). In patients with recent ischemic event, older men had carotid plaque with lower GSM values compared to women of same age (20), consistent with our findings. Sex seems to be a critical determinant of atherogenic lipoprotein levels with glycemic control and LDL cholesterol playing a central role (21). Glycated LDL after oxidation increases their permeation in the endothelial space generating atherosclerotic process, especially in a state of vascular inflammation that is higher in older men than women (20). Moreover, a histopathological study has demonstrated that atherosclerotic carotid plaques obtained from men had a greater prevalence of plaque hemorrhage and more vascular inflammation (22). Here, we extend these observations to a large multi-ethnic stroke-free population.

Alteration in glycemic metabolism and dyslipidemia plays an important role in the development of heterogeneous plaque morphology. They are directly related to change in BMI that is considered an independent risk factor for carotid plaque destabilization (23). In the Atherosclerosis Risk in Young Adults (ARYA) Study, high BMI was associated with lower GSM values independently of other RFs and phenotypes of atherosclerosis (24). Hyperglycemia and high LDL cholesterol levels change the structure of plaque to rise its susceptibility to ulceration and to become more prone to rupture and consequently cause embolic vascular events. We previously reported that this unfavorable plaque morphology can be reversed by reducing the levels of LDL cholesterol using a high-dose atorvastatin intervention in 30 days (25).

The association between low GSM and type 2 diabetes has been established (26). A combined analysis of 5 longitudinal studies with a total of 3,263 patients with uncontrolled diabetes but without apparent CVD demonstrated that presence of low-GSM echolucent plaques at baseline were the most powerful prognostic factor for the occurrence of CVD, even after adjustment for traditional risk factors (9). In our study, there was a significant association with fasting glucose even in those without diabetes, and a protective effect of lipid lowering medication especially among older patients. These evidences indicate that increased levels of glucose may trigger the mechanisms leading to echolucent plaque, which can be reverted by reducing glucose levels. Soft plaques are more present in diabetic patients and higher levels of glycated hemoglobin (HbA1c), further suggesting the role of glucose homeostasis in the development of unstable plaques (27).

Recently, in The Multi-Ethnic Study of Atherosclerosis (MESA), total plaque area, but not grayscale plaque features, was associated with risk factors and predicted incident coronary heart disease events (9). However, significant relationships with risk factors were observed after adjustment for Non-Hispanic Black (vs. Non-Hispanic White participants) who had plaques with the lower GSM values (9). Discrepancy between our study and MESA are mostly due to the differences in study designs, inclusion criteria, and ultrasound methods and definition of atherosclerosis.

Limitations of our study need to be acknowledged. The cross-sectional nature of the current findings does not allow inference of temporal effects or causality. Our study mainly included well-known atherosclerotic risk factors, whereas other factors of possible importance for atherosclerosis such as diet or endothelial function were not considered. Moreover, GSM analysis represents a mean value of whole atherosclerotic area and does not reflect the presence of particular regional plaque components. However, a lack of regional plaque analyses may have underestimated plaque vulnerability and therefore attenuated true associations. The major strengths of our study include a well-characterized multi-ethnic population representative of an urban community and standardized and carful assessments of carotid plaque presence and echogenic morphology.

In conclusion, it is important to highlight the usefulness of GSM analysis as ultrasound markers in the clinical practice, since based on its low cost, and lack of radiation can be repeated routinely in diabetic and dyslipidemic patients to evaluate, non-invasively, the risk for vascular diseases. By

understanding the impact of metabolic risk factors, such as increased levels of lipids and glycemia, on high-risk plaque morphology in multi-ethnic communities is of great importance for intensive interventions aimed at reversal of unfavorable plaque morphology and successful prevention of stroke and cardiovascular disease.

DATA AVAILABILITY STATEMENT

The original contributions presented in the study are included in the article/**Supplementary Material**, further inquiries can be directed to the corresponding author/s.

ETHICS STATEMENT

The studies involving human participants were reviewed and approved by Institutional Review Boards of Columbia University Medical Center and the University of Miami. The patients/participants provided their written informed consent to participate in this study.

AUTHOR CONTRIBUTIONS

DD-M, CD, MC, and TR: conceptualization, validation, data curation, and project administration. DD-M, CD, and MC: writing—original draft. CD: formal analysis. ME, JG, RS, and TR: writing—review and editing. DD-M and TR: funding acquisition. All authors have assisted with manuscript preparation and approved the final manuscript.

FUNDING

This work was supported by the National Institute of Neurologic Disorders and Stroke Grants: R01NS040807 and R0129993, and the Evelyn F. McKnight Brain Institute.

SUPPLEMENTARY MATERIAL

The Supplementary Material for this article can be found online at: https://www.frontiersin.org/articles/10.3389/fcvm.2022.793755/full#supplementary-material

REFERENCES

1. Rundek T, Arif H, Boden-Albala B, Elkind MS, Paik MC, Sacco RL. Carotid plaque, a subclinical precursor of vascular events: the Northern Manhattan Study. *Neurology.* (2008) 70:1200–7. doi: 10.1212/01.wnl.0000303969.63165.34
2. Sztajzel R, Momjian-Mayor I, Comelli M, Momjian S. Correlation of cerebrovascular symptoms and microembolic signals with the stratified gray-scale median analysis and color mapping of the carotid plaque. *Stroke.* (2006) 37:824–9. doi: 10.1161/01.STR.0000204277.86466.f0
3. Spence JD. Uses of ultrasound in stroke prevention. *Cardiovasc Diagn Ther.* (2020) 10:955–64. doi: 10.21037/cdt.2019.12.12
4. Rundek T, Spence JD. Ultrasonographic measure of carotid plaque burden. *JACC Cardiovasc Imaging.* (2013) 6:129–30. doi: 10.1016/j.jcmg.2012.08.015
5. Aizawa K, Elyas S, Adingupu DD, Casanova F, Gooding KM, Shore AC, et al. Echogenicity of the common carotid artery intima-media complex in stroke. *Ultrasound Med Biol.* (2016) 42:1130–7. doi: 10.1016/j.ultrasmedbio.2016.01.006
6. Zhou F, Hua Y, Ji X, Jia L, Zhang K, Li Q, et al. Ultrasound-based carotid plaque characteristics help predict new cerebral ischemic lesions after endarterectomy. *Ultrasound Med Biol.* (2021) 47:244–51. doi: 10.1016/j.ultrasmedbio.2020.09.025
7. Kuo F, Gardener H, Dong C, Cabral D, Della-Morte D, Blanton SH, et al. Traditional cardiovascular risk factors explain the minority of the variability in carotid plaque. *Stroke.* (2012) 43:1755–60. doi: 10.1161/STROKEAHA.112.651059
8. Andersson J, Sundstrom J, Kurland L, Gustavsson T, Hulthe J, Elmgren A, et al. The carotid artery plaque size and echogenicity are related to different cardiovascular risk factors in the elderly: the Prospective Investigation of the Vasculature in Uppsala Seniors (PIVUS) study. *Lipids.* (2009) 44:397–403. doi: 10.1007/s11745-009-3281-y
9. Mitchell C, Korcarz CE, Gepner AD, Kaufman JD, Post W, Tracy R, et al. Ultrasound carotid plaque features, cardiovascular disease risk factors and events: the Multi-Ethnic Study of Atherosclerosis. *Atherosclerosis.* (2018) 276:195–202. doi: 10.1016/j.atherosclerosis.2018.06.005
10. Sacco RL, Boden-Albala B, Gan R, Chen X, Kargman DE, Shea S, et al. Stroke incidence among white, black, and Hispanic residents of an urban community: the Northern Manhattan Stroke Study. *Am J Epidemiol.* (1998) 147:259–68. doi: 10.1093/oxfordjournals.aje.a009445
11. White H, Boden-Albala B, Wang C, Elkind MS, Rundek T, Wright CB, et al. Ischemic stroke subtype incidence among whites, blacks, and Hispanics: the Northern Manhattan Study. *Circulation.* (2005) 111:1327–31. doi: 10.1161/01.CIR.0000157736.19739.D0
12. Rundek T, Hundle R, Ratchford E, Ramas R, Sciacca R, Di Tullio MR, et al. Endothelial dysfunction is associated with carotid plaque: a cross-sectional study from the population based Northern Manhattan Study. *BMC Cardiovasc Disord.* (2006) 6:35. doi: 10.1186/1471-2261-6-35
13. Ferguson GG, Eliasziw M, Barr HW, Clagett GP, Barnes RW, Wallace MC, et al. The North American Symptomatic Carotid Endarterectomy Trial: surgical results in 1415 patients. *Stroke.* (1999) 30:1751–8. doi: 10.1161/01.STR.30.9.1751
14. Dong C, Della-Morte D, Cabral D, Wang L, Blanton SH, Seemant C, et al. Sirtuin/uncoupling protein gene variants and carotid plaque area and morphology. *Int J Stroke.* (2015) 10:1247–52. doi: 10.1111/ijs.12623
15. Gupta A, Kesavabhotla K, Baradaran H, Kamel H, Pandya A, Giambrone AE, et al. Plaque echolucency and stroke risk in asymptomatic carotid stenosis: a systematic review and meta-analysis. *Stroke.* (2015) 46:91–7. doi: 10.1161/STROKEAHA.114.006091
16. Biasi GM, Froio A, Diethrich EB, Deleo G, Galimberti S, Mingazzini P, et al. Carotid plaque echolucency increases the risk of stroke in carotid stenting: the Imaging in Carotid Angioplasty and Risk of Stroke (ICAROS) study. *Circulation.* (2004) 110:756–62. doi: 10.1161/01.CIR.0000138103.91187.E3
17. Salem MK, Bown MJ, Sayers RD, West K, Moore D, Nicolaides A, et al. Identification of patients with a histologically unstable carotid plaque using ultrasonic plaque image analysis. *Eur J Vasc Endovasc Surg.* (2014) 48:118–25. doi: 10.1016/j.ejvs.2014.05.015
18. Peters SA, Lind L, Palmer MK, Grobbee DE, Crouse JR, 3rd, O'Leary DH, et al. Increased age, high body mass index and low HDL-C levels are related to an echolucent carotid intima-media: the METEOR study. *J Intern Med.* (2012) 272:257–66. doi: 10.1111/j.1365-2796.2011.02505.x
19. Joakimsen O, Bonaa KH, Stensland-Bugge E, Jacobsen BK. Age and sex differences in the distribution and ultrasound morphology of carotid atherosclerosis: the Tromso Study. *Arterioscler Thromb Vasc Biol.* (1999) 19:3007–13. doi: 10.1161/01.ATV.19.12.3007
20. Skowronska M, Piorkowska A, Czlonkowska A. Differences in carotid artery atherosclerosis between men and women in the early phase after ischemic event. *Neurol Neurochir Pol.* (2018) 52:162–7. doi: 10.1016/j.pjnns.2017.09.002
21. Williams K, Tchernof A, Hunt KJ, Wagenknecht LE, Haffner SM, Sniderman AD. Diabetes, abdominal adiposity, and atherogenic dyslipoproteinemia in women compared with men. *Diabetes.* (2008) 57:3289–96. doi: 10.2337/db08-0787

22. Vrijenhoek JE, Den Ruijter HM, De Borst GJ, de Kleijn DP, De Vries JP, Bots ML, et al. Sex is associated with the presence of atherosclerotic plaque hemorrhage and modifies the relation between plaque hemorrhage and cardiovascular outcome. *Stroke.* (2013) 44:3318–23. doi: 10.1161/STROKEAHA.113.002633
23. Rovella V, Anemona L, Cardellini M, Scimeca M, Saggini A, Santeusanio G, et al. The role of obesity in carotid plaque instability: interaction with age, gender, and cardiovascular risk factors. *Cardiovasc Diabetol.* (2018) 17:46. doi: 10.1186/s12933-018-0685-0
24. Eikendal AL, Groenewegen KA, Bots ML, Peters SA, Uiterwaal CS, den Ruijter HM. Relation between adolescent cardiovascular risk factors and carotid intima-media echogenicity in healthy young adults: the Atherosclerosis Risk in Young Adults (ARYA) Study. *J Am Heart Assoc.* (2016) 5:e002941. doi: 10.1161/JAHA.115.002941
25. Della-Morte D, Moussa I, Elkind MS, Sacco RL, Rundek T. The short-term effect of atorvastatin on carotid plaque morphology assessed by computer-assisted gray-scale densitometry: a pilot study. *Neurol Res.* (2011) 33:991–4. doi: 10.1179/1743132811Y.0000000039
26. Katakami N, Matsuoka TA, Shimomura I. Clinical utility of carotid ultrasonography: application for the management of patients with diabetes. *J Diabetes Investig.* (2019) 10:883–98. doi: 10.1111/jdi.13042
27. Huang XW, Zhang YL, Meng L, Qian M, Zhou W, Zheng RQ, et al. The relationship between HbA(1)c and ultrasound plaque textures in atherosclerotic patients. *Cardiovasc Diabetol.* (2016) 15:98. doi: 10.1186/s12933-016-0422-5

Conflict of Interest: The authors declare that the research was conducted in the absence of any commercial or financial relationships that could be construed as a potential conflict of interest.

Publisher's Note: All claims expressed in this article are solely those of the authors and do not necessarily represent those of their affiliated organizations, or those of the publisher, the editors and the reviewers. Any product that may be evaluated in this article, or claim that may be made by its manufacturer, is not guaranteed or endorsed by the publisher.

Copyright © 2022 Della-Morte, Dong, Crisby, Gardener, Cabral, Elkind, Gutierrez, Sacco and Rundek. This is an open-access article distributed under the terms of the Creative Commons Attribution License (CC BY). The use, distribution or reproduction in other forums is permitted, provided the original author(s) and the copyright owner(s) are credited and that the original publication in this journal is cited, in accordance with accepted academic practice. No use, distribution or reproduction is permitted which does not comply with these terms.

frontiers in Cardiovascular Medicine

REVIEW
published: 10 February 2022
doi: 10.3389/fcvm.2022.815668

Why Are Women Predisposed to Intracranial Aneurysm?

*Milène Fréneau, Céline Baron-Menguy, Anne-Clémence Vion and Gervaise Loirand**

Université de Nantes, CHU Nantes, CNRS, INSERM, l'institut du thorax, Nantes, France

Intracranial aneurysm (IA) is a frequent and generally asymptomatic cerebrovascular abnormality characterized as a localized dilation and wall thinning of intracranial arteries that preferentially arises at the arterial bifurcations of the circle of Willis. The devastating complication of IA is its rupture, which results in subarachnoid hemorrhage that can lead to severe disability and death. IA affects about 3% of the general population with an average age for detection of rupture around 50 years. IAs, whether ruptured or unruptured, are more common in women than in men by about 60% overall, and more especially after the menopause where the risk is double-compared to men. Although these data support a protective role of estrogen, differences in the location and number of IAs observed in women and men under the age of 50 suggest that other underlying mechanisms participate to the greater IA prevalence in women. The aim of this review is to provide a comprehensive overview of the current data from both clinical and basic research and a synthesis of the proposed mechanisms that may explain why women are more prone to develop IA.

Keywords: intracranial aneurysm, cerebral artery, circle of Willis, sex difference, gender, endothelium, estrogens

OPEN ACCESS

Edited by:
Masayo Koide,
University of Vermont, United States

Reviewed by:
Junkoh Yamamoto,
University of Occupational and Environmental Health Japan, Japan
Seana Gall,
University of Tasmania, Australia

****Correspondence:***
Gervaise Loirand
gervaise.loirand@univ-nantes.fr

Specialty section:
This article was submitted to Atherosclerosis and Vascular Medicine, a section of the journal Frontiers in Cardiovascular Medicine

Received: *15 November 2021*
Accepted: *11 January 2022*
Published: *10 February 2022*

Citation:
Fréneau M, Baron-Menguy C, Vion A-C and Loirand G (2022) Why Are Women Predisposed to Intracranial Aneurysm? Front. Cardiovasc. Med. 9:815668. doi: 10.3389/fcvm.2022.815668

INTRODUCTION

Intracranial aneurysm (IA) is defined as a localized dilation of cerebral arteries which preferentially forms at arterial bifurcation of the circle of Willis. IAs are thought to result from an abnormal thickening of the artery wall at sites where hemodynamic stress is high (1). Unruptured IAs are generally silent but become symptomatic when they rupture, causing subarachnoid hemorrhage, with mortality rates of about 30–40% and severe neurological dysfunction and disability in a great part of subarachnoid hemorrhage survivors (2–4).

Cellular and molecular mechanisms leading to IA formation and rupture are not fully elucidated, but risk factors such as familial history of IA, high blood pressure, cigarette smoking, alcohol consumption, and female sex have been clearly identified. Indeed, in contrast to most neurocardiovascular diseases, the incidence of IA is higher in women than in men, whereas most of the risk factors that include cigarette smoking, hypertension, atherosclerosis, and alcohol consumption are all more common among men (5–13).

Women are found to suffer two times as often from unruptured IAs as men. Whereas, the overall prevalence of unruptured IAs in study population is reported about 3%−4%, it reaches 6% in women, with a woman-to-man prevalence ratio of 1.57 (14). This woman-to-man prevalence ratio changes with age, from 1.1 in populations with mean age of 50 years to 2.2 for populations over the age of 50 years (14). In addition, the follow-up of a cohort of patients diagnosed with either ruptured or unruptured IAs showed that female gender is an independent risk factors for the formation of new IAs (7).

Despite these clinical data, studies that are specifically designed to explain and understand the reasons for this female predisposition to IA remain few. Clinical analyses primarily addressed the role of sex hormones, and preclinical studies performed in rodent models of IA have mainly focused on the effects of ovariectomy and/or estrogen treatments, and *in vitro* on hormone actions in vascular cell models. The synthesis of published data supports a possible role of sex-specific hormonal mechanisms in the pathogenesis of IA. Nevertheless, the particular features of IA in women suggest that the greater predisposition of women to IA relies on complex and probably multiple mechanisms, including a role for hemodynamic forces.

GENDER DIFFERENCE IN IA FEATURES

IA Number and Localization

There is no statistical difference between men and women regarding the size and the laterality of unruptured IAs (15–17). However, together with a higher susceptibility to IA formation compared to men, women are more likely to develop multiple IAs (17–22). Also, women exhibit about two times the rate of bilateral IAs than men (16, 17). In addition, the number of IAs rises in women of increasing age (19). Both female sex and postmenopausal state are found as independent risk factors for the formation of multiple IAs (19).

In women, unruptured IA aspect has been shown to change with age: women of premenopausal age have a higher numbers of aneurysm lobes, whereas those in women of postmenopausal have larger size (23).

A gender difference in the anatomical distribution of IA is also clearly demonstrated. In women, unruptured IA localizes preferentially on the internal carotid artery (ICA; 54% vs. 38% in men), whereas in men, IA affects more frequently the anterior cerebral artery (ACA; 29% vs. 15% in women) and anterior communicating artery (**Figure 1**) (15). No difference according to the gender has been observed in the frequency of IA in the middle cerebral artery and posterior circulation (posterior cerebral, basilar and vertebral, artery) (15).

IA Growth and Rupture

As for IA formation, women are at increased risk for IA growth (7, 24). More particularly, female sex is shown to be an independent risk factor for the growth of unruptured IA in elderly patients (age $\geq$ 70 years) (25). However, the growth rate of an IA itself does not differ by sex (7).

Once an IA is formed, female sex does not represent a risk factor for its subsequent rupture (7). As a whole, no difference in the size of ruptured aneurysms between women and men has been detected (15, 20, 22, 26). However, some differences exist between ruptured IA in men and women. IA rupture and aneurysmal subarachnoid hemorrhage more frequently affect women than men but the gender distribution varied with age (15, 18, 27–29). Indeed, in young people, incidence of aneurysmal subarachnoid hemorrhage is slightly higher in men, and the increased risk of aneurysmal subarachnoid hemorrhage in women only appears after the fourth and fifth decades (28, 30–32). Accordingly, among patients with ruptured IAs, the mean age of women is higher (60–70 years) than that of men (50–60 years) (15, 16, 20, 26).

The location of aneurysmal subarachnoid hemorrhage also differs between women and men. According to the preferential location of IA on internal carotid artery in women, the posterior communicating artery is also the most common site of IA rupture in women, whereas anterior communicating artery aneurysm ruptures are overrepresented in men (16, 18, 20, 26, 33–35). This is in agreement with the majority of anterior communicating artery aneurysms in men and their higher risk of rupture than IAs at other locations (18, 36). Regarding this specific IA location, women exhibit a lower rate of ruptured anterior communicating artery aneurysms than men in whom these IAs are larger (16, 33). This greater IA size may thus participate to the higher proportion of men with ruptured anterior communicating artery.

For both women and men, outcomes varied according to the location of aneurysmal subarachnoid hemorrhage but the overall outcomes after IA rupture are similar in women and men (16, 20, 26, 33).

POSSIBLE CAUSES OF THE GENDER DIFFERENCE IN IA FORMATION AND RUPTURE

Anatomical and Hemodynamic Parameters

Both IA formation and rupture did not occur on same arteries in women and men. ICA and ACA have been identified as the main sites of IA formation and rupture in women and men, respectively. Indeed, there is a female preponderance of IA in all intracranial arteries except the ACA. It is well admitted that hemodynamic stress, such as high blood pressure or strong wall shear stress, may participate to IA formation and growth (37), which may suggest that gender difference in the arterial geometry and consequent arterial wall shear stress could participate in the different preferential location of IA in women and men.

Analysis of the anatomical variations in the circle of Willis in more than one hundred of patients with IA by magnetic resonance angiography suggested a correlation between the sex-linked difference in IA distribution (preferential ICA aneurysm in women) and a sex-linked difference in anatomical variations of the circle of Willis (38). Beyond these anatomical variations, measurement of the diameter of arteries of the circle of Willis revealed that ICA, ACA, posterior cerebral artery and basilar artery were significantly smaller in women than in men, with the greatest difference found for ICA (39, 40). In contrast, the diameter of posterior communicating artery has been found to be either larger or similar in women compared to men. Since a smaller arterial diameter results in higher blood flow velocity and shear stress, arteries in women are expected to be submitted to stronger wall shear stress and tension than in men. Examination of the dimension and geometry of the terminal bifurcation of the ICA confirmed that the diameter of the parent artery and the branches is smaller in women than in men, but the bifurcation angle is the same in both sexes (41). Modeling of bifurcations and computational fluid dynamic simulations allowed to demonstrate that the maximum wall shear stress in the ICA bifurcation in the

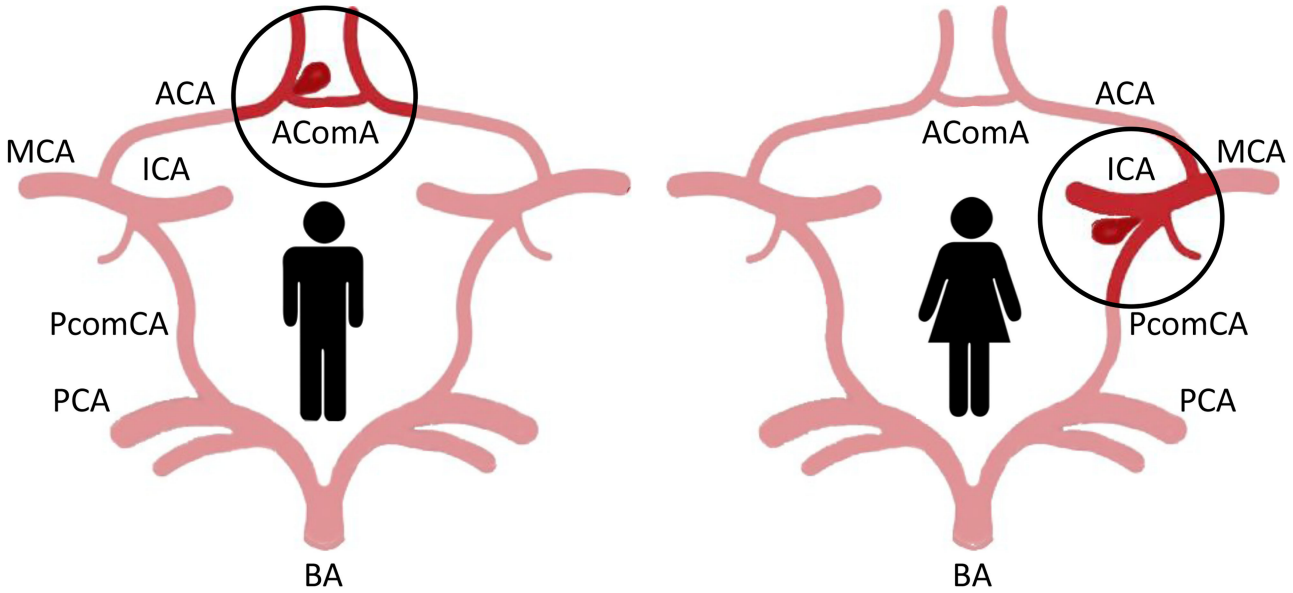

FIGURE 1 | Major localization of IA in the circle of Willis of men and women. In men, IA affects more frequently the anterior cerebral artery (ACA) and anterior communicating artery (AComA; left). In women, IA localizes preferentially on the internal carotid artery (ICA), in particular at the bifurcation with the posterior communicating artery (PComA; right) (MCA, middle cerebral artery; BA, basilar artery; PCA, posterior cerebral artery).

female was 50% higher than in men (41). In addition, the area of increased wall shear stress at the ICA bifurcation is larger in women compared to men (**Figure 2**). Such differences between men and women, although less pronounced, were also found at the bifurcation of the MCA into two main branches (41).

Regarding the wall tension generated by pressure, blood flow modeling of circle of Willis circulation has demonstrated that peak pressure is higher when artery diameter is smaller and the angle of the bifurcations is asymmetric (42).

All these observations thus support the idea that the gender difference in the diameter and geometry of bifurcations of arteries of the circle of Willis results in higher shear stress and peak pressure in women that may induce more severe endothelial damage and favors IA formation in women, particularly at ICA bifurcation and ICA posterior communicating artery junction. Moreover, it has been described that the larger the diameter of an IA relative to the native artery diameter, the higher the risk of rupture (43). With smaller diameter intracranial arteries in women, it can be thus considered that at equal IA size, the risk of rupture will be higher in women than in men.

Hormones

Hormones are a fundamental part of sex differences and hormonal changes in the course of female life participate in sex differences in neurocardiovascular disease prevalence. Although the female preponderance of both unruptured and ruptured IAs in the general population is clear, and even more pronounced in familial forms of IA (44, 45), an important additional factor to be considered is the age. The change in the preponderance of IAs between men and women starts after the first two decades of life and became significant after the age of 55, with the peak in female prevalence of IA in the sixth decade (5, 14, 20, 28, 30–32). These changes are contemporary with the fall in estrogen levels occurring during and after menopause, which suggests the possible protective effect of estrogens on IA formation and rupture. This hypothesis is further supported by the greater risk of IA in association with earlier age at menopause (46). In contrast, women who used oral contraceptive pills and hormone replacement therapy are less likely to have cerebral aneurysms (47). The decline in estrogen concentration in peri- and post-menopause periods can thus be responsible of changes in cerebral artery structure and functions that favor the formation and/or the rupture of IAs.

Animal models of aneurysm provided a useful way to address the sex difference in IAs, in particular to understand the role of estrogens thanks to the use of ovariectomized females and/or estrogen supplementation. Estrogen effects are mediated by the activation of two nuclear estrogen receptors, ERα and ERβ, acting as transcription factors which control gene expression, and through a more recently described membrane G protein-coupled estrogen receptor (GPER) (48). Several studies have demonstrated the presence of functional ERα and ERβ in human and animal vascular smooth muscle and endothelial cells. However, vascular effects of estrogens are predominantly mediated by ERα (48).

In rodent models of IA, the incidence of IA is higher in female animals than in males and was further significantly increased in ovariectomized females, despite similar or even lower systolic blood pressure in females (6, 49–51). Surgically or pharmacologically induced-estrogen deficiency also aggravated IA lesions and significantly increased rupture of IAs (49, 52). In ovariectomized hypertensive rats, the increased incidence of

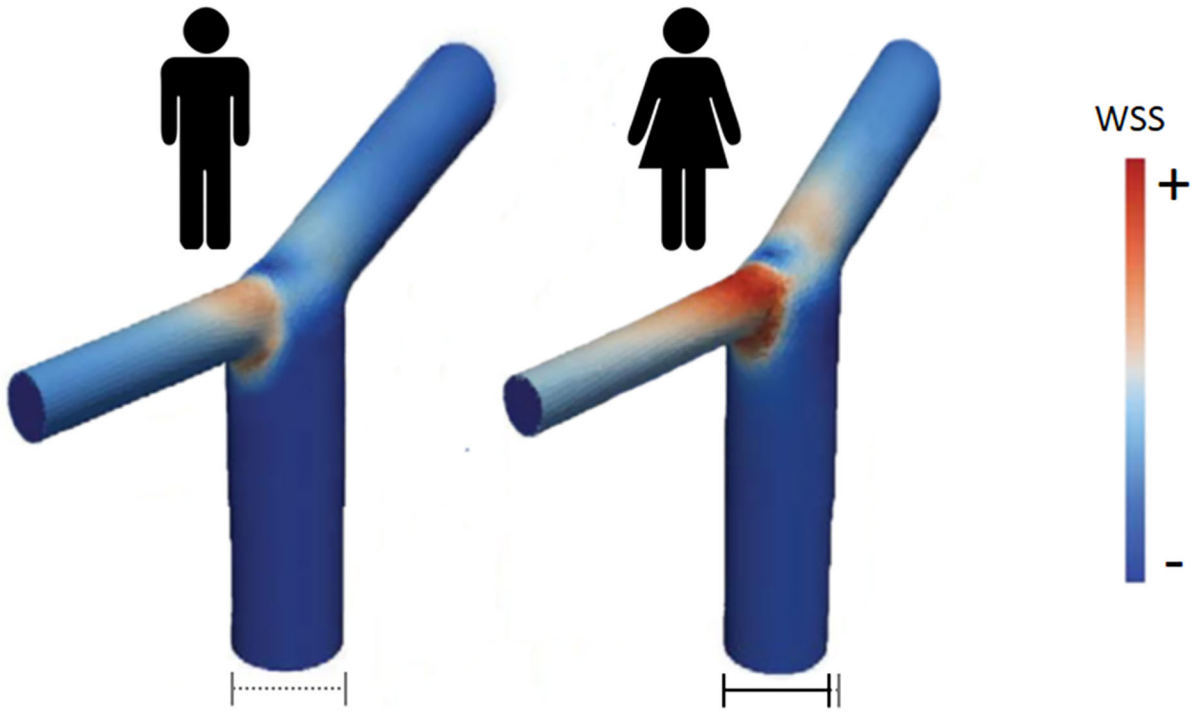

FIGURE 2 | Wall shear stress intensity in ICA bifurcation in men (left) and women (right). According to computational fluid dynamics simulations, area of high WSS is larger and of stronger intensity in women than in men [adapted from Lindekleiv et al. (41)].

carotid ligation-induced IA can be reversed by bazedoxifene, a selective estrogen receptor modulator, without change in blood pressure. This effect is associated with a restoration of ERα and ERβ expression in cerebral arteries that were downregulated by ovariectomy (53).

Estrogen treatment and specific estrogen ERβ agonist, but not ERα agonist, reversed the increased incidence of IA in ovariectomized female mice, which suggests that the protective effect of estrogens on IA was mediated by ERβ activation (50, 54). This role of ERβ was further confirmed by showing that the effect of the ERβ agonist was not observed in ERβ knockout mice and that non-ovariectomized ERβ knockout mice displayed an increased incidence of IA compared to non-ovariectomized control mice (50). With a protective effect of estrogens on IA mostly attributed to ERβ, the cerebral circulation stands out from the rest of the arteries in which the protective effect of estrogens is mediated by ERα.

MOLECULAR MECHANISMS OF ESTROGEN PROTECTION TO IA FORMATION

Although the exact pathogenesis of IA formation, growth, and rupture remains to be established, current knowledge suggests that endothelial dysfunction induced by hemodynamic injury at bifurcation of intracranial artery could be the initial step of IA formation (55–58). This first event then triggers a vascular inflammation process, with neutrophil and macrophage infiltration, oxidative stress, fragmentation of the internal elastic lamina, and degradation of the extracellular matrix by metalloproteinase, endothelial, and smooth muscle cell apoptosis (56, 59). All these interconnected processes lead to the structural degradation and remodeling of the arterial wall responsible for the weakening and fragility of the arterial wall. Protecting effects of estrogens can thus result from an inhibitory action on one or more components involved in IA formation.

Estrogen Effect on Endothelial NO Synthase and Cerebral Artery Vasoreactivity

Endothelial dysfunction, with abnormal endothelial cell morphology and a loss of endothelial nitric oxide synthase (eNOS) expression, is a key early step of IA formation (**Figure 3**). In a rat model of IA, ovariectomy significantly decreased eNOS mRNA and protein expression, especially in the cerebral vascular wall of animals with saccular aneurysms (51). In contrast, estradiol treatment has been shown to increase the expression of eNOS in endothelial cells *in vitro* (51). Thus, estrogen deficiency promotes endothelial dysfunction whereas conversely, estrogen would protect against endothelial damage in the early phase of IA formation.

The *in vitro* effect of estrogen on eNOS expression in endothelial cell culture is mediated by ERα (51). ERα has

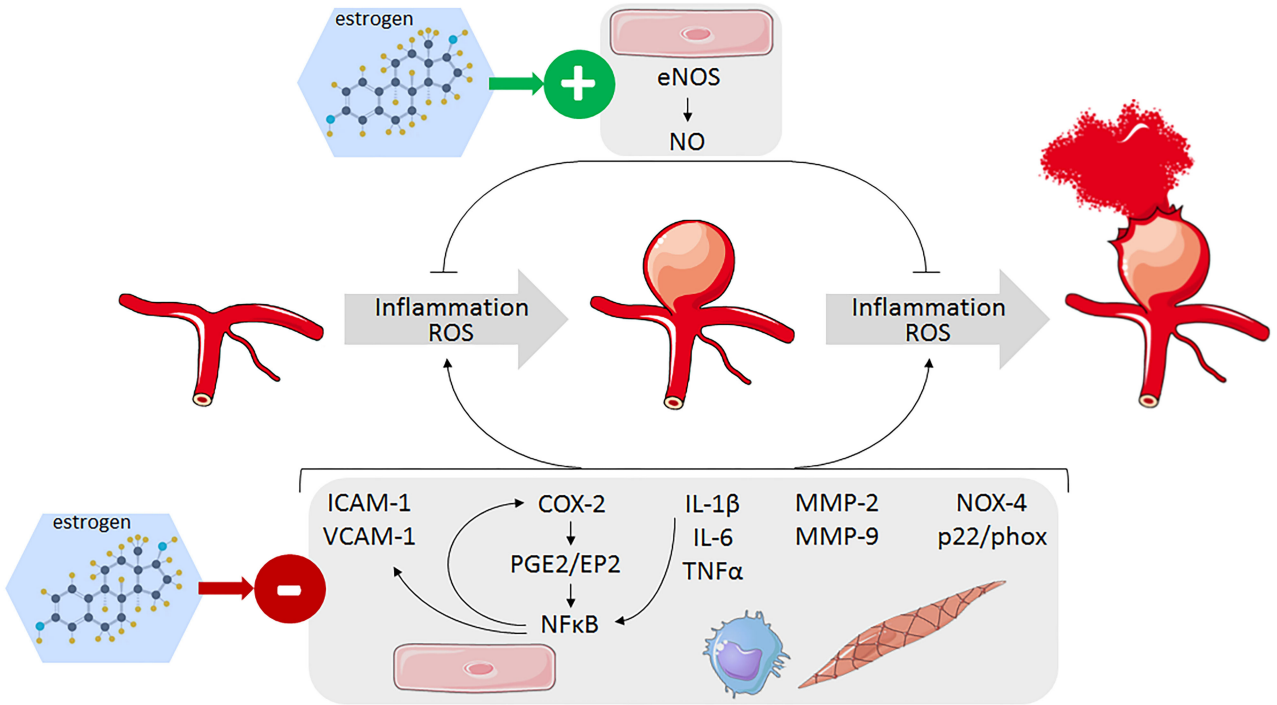

FIGURE 3 | Identified pathways involved in the protective effect of estrogens against IA formation and rupture leading to decrease inflammation and oxidative stress in the arterial wall of cerebral arteries. Endothelial cells (pink), monocytes/macrophages (blue), and smooth muscle cells (light brow).

been also shown to induce eNOS phosphorylation through phosphoinositide-3 (PI-3) kinase/Akt cascade leading to a rapid NO production in intact cerebral arteries from ovariectomized rats *ex vivo* and causing a long-term increase in NO production in the cerebral circulation of ovariectomized rats chronically treated with estrogen *in vivo* (60). This effect of ERα therefore seems to contradict the causal link established between the rise in NO production mediated by ERβ and the beneficial effect of estrogen on IA (50). Indeed, the protective effect of ERβ agonist on IA incidence in ovariectomized mice is completely abolished by the inhibition of eNOS by L-NAME treatment, which supports the fact that ERβ-induced NO production by eNOS mediates the beneficial effect of estrogens against IA formation (50). The *in vivo* role of ERα thus remains to be clarified but it has been shown that ovariectomy induces a loss of ERα expression in the vascular wall of mouse cerebral arteries with in contrast, an increase in ERβ expression (51), which may contribute to the discrepancy in the respective role of these two receptors in estrogen effects on NO production.

With regard to vasoreactivity, *ex vivo*, 17β-estradiol and agonists of ERα relax pressurized rat middle cerebral arteries from both male and female animals through a direct effect on smooth muscle cells (61). A relaxing effect of ERβ agonists was observed only in female rat arteries and was also due to an action on smooth muscle cells. ERβ agonists also induce relaxation of human cerebral artery in a NO-independent manner likely through an action on smooth muscle, whereas ERα receptor agonists have only a minimal effect (61).

In agreement with this relaxing effect of estrogens, ovariectomy enhanced the contractile response of rat cerebral arteries to vasoconstrictors, in association with an alteration of NO-dependent relaxing effect (62, 63). Tamoxifen or 17β-estradiol treatment, presumably through ERα, normalized cerebral artery reactivity to phenylephrine in ovariectomized rats (62, 63).

In summary, estrogens preserve normal endothelial function and have a limiting action on cerebral artery contraction and cerebrovascular tone through both endothelial-mediated NO dependent-relaxing effect and a direct relaxing action on smooth muscle, which participate to their protective effect on IA. Whereas, studies in ovariectomized rodent models of IA support a major role of ERβ, the observed changes in ERα and ERβ expression in cerebral artery wall of ovariectomized animals support a differential role of these receptors in the modulation of eNOS expression and activity, with a major of ERα before menopause and of ERβ after menopause.

Estrogen Effect on Cerebral Artery Inflammation

The mechanisms linking high wall shear stress to the activation of proinflammatory signaling pathway at arterial bifurcation are not fully elucidated, but the transcription factor nuclear factor kappa B (NF-κB) is shown to play a critical role in IA formation and rupture (**Figure 3**). Its activation leads to an increase in

the expression of vascular cell adhesion molecule-1 (VCAM-1), intercellular adhesion molecule-1 (ICAM-1), and monocyte chemoattractant protein-1 (MCP-1), which are responsible for the recruitment and adhesion of inflammatory cells to the endothelium where they produce proinflammatory cytokines such as tumor necrotizing factor alpha (TNFα), interleukin (IL)-1β, and IL-6 (56, 64–67). These cytokines then perpetuate local inflammation and neutrophil and macrophage infiltration in the cerebral artery wall, which produced damaging matrix metalloproteinases (MMP-2/9), and reactive oxygen species (ROS) (55). Whereas, the general vasculo-protector effects of estrogens are quite well documented, only a limited number of studies specifically addressed the anti-inflammatory action of estrogens on cerebral arteries and on IA.

Estrogens have been shown to limit proinflammatory cytokine expression and effects in cerebral arteries (**Figure 3**). Ovariectomy in female animals increased expression of TNFα and accumulation of neutrophils and macrophages in the arterial wall (49). Estrogen deficiency was also shown to upregulate IL-17A, which in turn downregulates E-cadherin and favors macrophage infiltration in the IA wall (52). Bazedoxifene decreases IL-1β mRNA expression in cerebral arteries which was upregulated by ovariectomy (53). Recently, a bioactive phytoestrogen daidzein, which reverses the increased IA incidence in ovariectomized mice via ERβ, was shown to decrease IL-6 mRNA level in cerebral arteries and, to a lesser extent, IL-1β and TNFα mRNAs (68). IL-6 level in the serum is increased and involved in the formation and rupture of IA in estrogen-deficient mice but not in control mice, which suggests that estrogen-induced repression of IL-6 expression participates to the beneficial effect of estrogen on IA (67).

Estrogen not only reduces IL-1β expression, but also suppresses exogenous IL-1β-mediated induction of cyclooxygenase 2 (COX-2)/prostaglandin E2 (PGE2) pathway in cerebral blood vessels of ovariectomized rats (69). IL-1β induces COX-2 expression through the activation of NF-κB, and the observed inhibitory effect of estrogen has been ascribed to an inhibition of NF-κB activity (70). This result is particularly interesting as it has been proposed that COX-2/PGE2/NF-κB pathway in cerebral artery endothelium is responsible for high wall shear stress-induced endothelial cell damage and may be the link between hemodynamic stress and IA formation (71). The inflammatory PGE2 formation is catalyzed from arachidonic acid by the sequential action of COX-2 and prostaglandin E synthase-1 (PGES-1). COX-2 and prostaglandin E receptor 2 (EP2) mRNA expression was induced *in vitro* in endothelial cell cultures exposed to shear stress. In a mouse model of IA induced by elevated hemodynamic stress, expression of COX2 and EP2 is increased in the endothelial cell layer at early stage of IA formation. Inhibition or knockout of COX-2 or EP2 resulted in decreased NF-κB expression and a reduction of incidence of IA formation (71, 72). The induction of COX-2/PGE2/EP2 signaling activates NF-κB, thus creating a self-amplified feedback loop that prevents the resolution of this initial process and contributes to generate the chronic inflammation in the cerebral arterial wall enabling for IA formation and progression. The observed inhibitory action of estrogen on NF-κB (69) might thus limit the shear stress-induced amplification loop of the COX-2/PGE2/NF-κB pathway and the perpetuation of inflammation in cerebral artery wall.

Estrogen Effect on Cerebral Artery Oxidative Stress

Vascular oxidative stress and increased production of reactive oxygen species (ROS) are considered as the common mechanisms of vascular dysfunction and arterial disease, including IA (73) (**Figure 3**). Oxidative stress is mainly caused by an imbalance of ROS production by prooxidative enzymes (nicotinamide adenine dinucleotide phosphate (NADPH) oxidase, xanthine oxidase or the mitochondrial respiratory chain) and antioxidant mechanisms (superoxide dismutase, glutathione peroxidase, heme oxygenase, catalase, and so on.). The resulting rise in ROS concentration reduces bioactive endothelial NO and inhibits eNOs, which favors monocyte and macrophage recruitment creating a proinflammatory environment which leads to the activation of MMPs, phenotypic conversion of vascular smooth muscle cells and apoptosis, and finally a harmful arterial wall remodeling.

Excessive production of ROS has been demonstrated in aneurysmal walls in rodent models of IA, in association with an increased expression of heme oxygenase-1 and NADPH oxidase subunits (NOX4, p22phox, p47phox), mainly in macrophages and smooth muscle cells, whereas superoxide dismutase 1 was downregulated (51, 74). Free radical scavenger treatment or p47phox deletion markedly reduced IA formation and inhibited enlargement and medial degradation of IA (74). Estrogen deficiency in a rat model of IA increased the expression of NOX4 and p22phox in IA walls, and in contrast, 17β-estradiol inhibited NOX4 and p22phox expression in cerebral endothelial cell culture, suggesting that NADPH oxidase regulation by estrogen might participate to the gender difference in IA prevalence (51).

Additional indirect evidence supporting a role of ROS in the sex difference in IA has been provided by the differential effect of cigarette smoking on IA in men and women. Smoking is a well-known risk factor of IA formation and rupture, which mainly acts by inducing ROS accumulation (75). However, cigarette smoking has a more severe impact on IA, particularly on IA rupture, in smoking women than in men (76, 77). A recent study showed that relatively young women (between 30 and 60 years) with a positive smoking history have a four-fold increased risk for having an incidental unruptured IA (78). These results are consistent with an antiestrogenic effect of cigarette smoking (20), which should become even more apparent after the menopause when endogenous estrogen production is decreased and thus have a greater impact on the risk of postmenopausal IA.

Estrogen Effect on Cerebral Artery Matrix and Elastic Mechanical Properties

Vascular remodeling is an important process in the pathogenesis of IA characterized by the degradation of the internal elastic lamina of aneurysmal walls and dynamic modification of extracellular matrix components such as elastin, collagens, and proteoglycan leading to weakening of the arterial wall (79, 80).

Arterial wall undergoes postmenopausal extracellular matrix changes similar to those occurring in the skin and bones, including a decrease in collagen and water content that leads to thinning and loss of elasticity offering a favorable ground to IA (81, 82). These changes particularly affect the media, which is the layer richest in collagen and elastin of the arterial wall. In contrast, thanks to the positive effect of estrogens on connective tissue and its turnover, hormone replacement has morphological effect on the carotid arteries in postmenopausal women, preserving the thickness of the arterial media layer (83).

In rats with IA, an imbalance between MMP-9 and MMP-2 and their inhibitors TIMP-1 and TIMP-2 is responsible for extracellular matrix degradation in the arterial walls leading to the progression and rupture of IA (84, 85)(**Figure 3**). In the same experimental model, the reduction in the incidence of IA rupture produced by treatment with the ER modulator bazedoxifene is associated with a significant decrease of MMP-9 expression that, on the contrary, was upregulated by ovariectomy (53). Estradiol administration has been also shown to inhibit the formation of lipid peroxidation products and restore middle cerebral arterial viscoelasticity and compliance in aged female rats (86, 87). In a rabbit model of IA induced by carotid ligation, estrogen deficiency, in combination with hypertension, increases vessel length and tortuosity in the circle of Willis, probably by lowering the tolerance of vascular tissue to hemodynamic stresses caused by carotid ligation, making it more vulnerable to flow-induced aneurysmal remodeling (88).

POTENTIAL ROLE OF 15-HYDROXYPROSTAGLANDIN DEHYDROGENASE (15-PGDH)

The key role of COX-2/PGE2/NF-κB pathway in IA pathogenesis and its participation in the sex difference of the disease was further supported by the sex difference in the effect of aspirin on IA and the potential role of the PGE2 degrading enzyme 15-PGDH. Interestingly, frequent use of aspirin decreased the risk of IA rupture more significantly in men than in women (89, 90). This difference in aspirin effect was reproduced in male and female mice in an experimental model of IA (89). The beneficial effect of aspirin in mice is associated with a decreased expression of inflammatory molecules in cerebral arteries, which has been ascribed to its inhibitory action of COX-2 (89). In an attempt to identify the mechanisms involved in the differential effect of aspirin on IA in male and female, gene expression analysis in cerebral arteries has revealed a lower expression of 15-PGDH and higher levels of proinflammatory molecules (COX-2, CD-68, MMP-9, MCP-1, and NF-κB) in treated females than in treated males. 15-PGDH is the main enzyme of prostaglandin degradation that stops the biological activity of PGE2 by converting it to 15-keto-PGE2, an endogenous peroxisome proliferator-activated receptor γ (PPARγ) agonist. Thus, even if the activity of COX-2 is reduced by aspirin, the low level of 15-PGDH in female could contribute to maintaining, at least in part the activity of the PGE2/NF-κB pathway. Indeed, expression of COX-2, CD-68, MMP-9, MCP-1, and NF-κB was higher in cerebral arteries of aspirin-treated female mice than in treated males, and this difference and also the increased risk of IA rupture between males and females were completely equalized by treatment a 15-PGDH activator (89). This observation further supports the essential role of 15-PGDH-mediating PGE2 degradation in the protective effect of aspirin. It also suggests that the low expression of 15-PGDH in cerebral artery in female might favor high shear stress-induced COX-2/PGE2/NF-κB pathway activation and the resulting maintained inflammation in arterial wall, thus participating to the increased propensity to IA rupture. Moreover, the low catalytic activity of 15-PGDH also limits the activation of PPARγ shown to decrease IA formation and rupture (91, 92).

CONCLUSION

Experimental works driven over the past decades to understand the well-known higher prevalence of IA women compared with men have gathered knowledge that allows us to propose different mechanisms that would be involved. One of them lies in the anatomic difference of the circle of Willis between men and women, with diameters and geometry of bifurcation of the arteries leading to higher hemodynamic stresses in women, driving more severe endothelial damage which favors IA formation. In addition, cigarette smoking appears to have a greater impact on IA in women than in men, an effect that could be related to the low level of 15-PGDH described in cerebral artery in female, and as a consequence, a stronger prooxidative damaging action of smoking in women. However, although these unmodifiable and modifiable risk factors predispose women to IA, they are counteracted by the protective effects of estrogens, acting on multiple steps of IA formation including, endothelial dysfunction, inflammation, and oxidative stress. The loss of these estrogen-mediated protecting mechanisms at menopause thus plays a major role in the critical increase in IA prevalence in women over the age of 50 years.

It is obvious that multiple combined mechanisms are responsible for the gender differences of IA disease. As in any disease, sex differences in IA may be linked to sex hormones but also to nonhormonal factors dependent of the genes present in the X and Y chromosomes. Currently, the vast majority of studies, in humans and animal models, have focused on the role of sex hormones, more particularly of estrogens, and further research is needed to determine the part of each of these mechanisms in the female susceptibility to IA. Moreover, beside biological sex influences on IA pathophysiology, the psycho-sociocultural construct of gender can further participate to the difference between men and women. Societal, cultural, behavioral, and psychological factors may add to or modulate the biological factors involved in men and women differences toward IA formation and rupture.

Regarding IA patient care, despite the significant data that demonstrate the negative impact of female sex on IA incidence and rupture, this important variable is surprisingly largely neglected in clinical practice. However, even if the

mechanisms involved are not elucidated, the current data would nevertheless make it possible to propose ways to improve the management of women suspected or diagnosed with IA. First, it would be relevant to consider women as a high-risk group. Second, given the strong impact of hemodynamic and oxidative stress on IA in women, the implementation of intensive strategies to lower blood pressure and promote cigarette smoking cessation seems to be strongly warranted in women.

There is no doubt that our understanding of the mechanisms underlying sex differences in IA will improve further in the coming years and contribute to a better understanding of the pathophysiology of IA. The challenge will then be to transform this knowledge into means to improve the prevention of IA formation, progression, and rupture, and more globally for a better care of IA patients, both women and men.

AUTHOR CONTRIBUTIONS

GL participated in the preparation of conceptualization, literature search, and writing—original draft preparation. A-CV and GL provided funding acquisition. MF, CB-M, A-CV, and GL involved in writing, designing, and making of the figures—draft revision. All authors have read and agreed to the published version of the manuscript.

FUNDING

This work benefited funding from Fondation pour la Recherche Médicale, (DPC20171138968), Fondation Recherche Cardio-Vasculaire - Institut de France (Coeur de Femmes), and Programme d'Investissements d'Avenir ANR-16-IDEX-0007 (NExT Junior Talent, ICARA project, co-funded by Région Pays de la Loire and Nantes Métropole).

REFERENCES

1. Alfano JM, Kolega J, Natarajan SK, Xiang J, Paluch RA, Levy EI, et al. Intracranial aneurysms occur more frequently at bifurcation sites that typically experience higher hemodynamic stresses. *Neurosurgery*. (2013) 73:497–505. doi: 10.1227/NEU.0000000000000016
2. Frosen J, Tulamo R, Paetau A, Laaksamo E, Korja M, Laakso A, et al. Saccular intracranial aneurysm: pathology and mechanisms. *Acta Neuropathol.* (2012) 123:773–86. doi: 10.1007/s00401-011-0939-3
3. Suarez JI, Tarr RW, Selman WR. Aneurysmal subarachnoid hemorrhage. *N Engl J Med.* (2006) 354:387–96. doi: 10.1056/NEJMra052732
4. Van Gijn J, Kerr RS, Rinkel GJ. Subarachnoid haemorrhage. *Lancet.* (2007) 369:306–18. doi: 10.1016/S0140-6736(07)60153-6
5. Harrod CG, Batjer HH, Bendok BR. Deficiencies in estrogen-mediated regulation of cerebrovascular homeostasis may contribute to an increased risk of cerebral aneurysm pathogenesis and rupture in menopausal and postmenopausal women. *Med Hypotheses.* (2006) 66:736–56. doi: 10.1016/j.mehy.2005.09.051
6. Jamous MA, Nagahiro S, Kitazato KT, Satomi J, Satoh K. Role of estrogen deficiency in the formation and progression of cerebral aneurysms. Part I: experimental study of the effect of oophorectomy in rats. *J Neurosurg.* (2005) 103:1046–51. doi: 10.3171/jns.2005.103.6.1046
7. Juvela S. Risk of subarachnoid hemorrhage from a de novo aneurysm. *Stroke.* (2001) 32:1933–4. doi: 10.1161/01.STR.32.8.1933
8. Juvela S, Porras M, Heiskanen O. Natural history of unruptured intracranial aneurysms: a long-term follow-up study. *J Neurosurg.* (1993) 79:174–82. doi: 10.3171/jns.1993.79.2.0174
9. Longstreth, WT, Jr., Koepsell, TD, Yerby, MS, Van Belle, G. Risk factors for subarachnoid hemorrhage. *Stroke.* (1985). 16:377–85. doi: 10.1161/01.STR.16.3.377
10. Longstreth WT, Nelson LM, Koepsell TD, Van Belle G. Subarachnoid hemorrhage and hormonal factors in women. A population-based case-control study. *Ann Intern Med.* (1994) 121:168–73. doi: 10.7326/0003-4819-121-3-199408010-00002
11. Mhurchu, C.N., Anderson, C., Jamrozik, K., Hankey, G., Dunbabin, D., Australasian Cooperative Research on Subarachnoid Hemorrhage Study, G. Hormonal factors and risk of aneurysmal subarachnoid hemorrhage: an international population-based, case-control study. *Stroke*. (2001) 32:606–12. doi: 10.1161/01.STR.32.3.606
12. Stirone C, Duckles SP, Krause DN. Multiple forms of estrogen receptor-alpha in cerebral blood vessels: regulation by estrogen. *Am J Physiol Endocrinol Metab.* (2003) 284:E184–92. doi: 10.1152/ajpendo.00165.2002
13. Stober T, Sen S, Anstatt T, Freier G, Schimrigk K. Direct evidence of hypertension and the possible role of post-menopause oestrogen deficiency in the pathogenesis of berry aneurysms. *J Neurol.* (1985) 232:67–72. doi: 10.1007/BF00313903
14. Vlak MH, Algra A, Brandenburg R, Rinkel GJ. Prevalence of unruptured intracranial aneurysms, with emphasis on sex, age, comorbidity, country, and time period: a systematic review and meta-analysis. *Lancet Neurol.* (2011) 10:626–36. doi: 10.1016/S1474-4422(11)70109-0
15. Ghods AJ, Lopes D, Chen M. Gender differences in cerebral aneurysm location. *Front Neurol.* (2012) 3:78. doi: 10.3389/fneur.2012.00078
16. Hamdan A, Barnes J, Mitchell P. Subarachnoid hemorrhage and the female sex: analysis of risk factors, aneurysm characteristics, and outcomes. *J Neurosurg.* (2014) 121:1367–73. doi: 10.3171/2014.7.JNS132318
17. Krzyzewski RM, Klis KM, Kucala R, Polak J, Kwinta BM, Starowicz-Filip A, et al. Intracranial aneurysm distribution and characteristics according to gender. *Br J Neurosurg.* (2018) 32:541–3. doi: 10.1080/02688697.2018.1518514
18. Aarhus M, Helland CA, Wester K. Differences in anatomical distribution, gender, and sidedness between ruptured and unruptured intracranial aneurysms in a defined patient population. *Acta Neurochir (Wien).* (2009) 151:1569–74. doi: 10.1007/s00701-009-0316-3
19. Ellamushi HE, Grieve JP, Jager HR, Kitchen ND. Risk factors for the formation of multiple intracranial aneurysms. *J Neurosurg.* (2001) 94:728–32. doi: 10.3171/jns.2001.94.5.0728
20. Kongable GL, Lanzino G, Germanson TP, Truskowski LL, Alves WM, Torner JC, et al. Gender-related differences in aneurysmal subarachnoid hemorrhage. *J Neurosurg.* (1996) 84:43–8. doi: 10.3171/jns.1996.84.1.0043
21. Ostergaard JR, Hog E. Incidence of multiple intracranial aneurysms. Influence of arterial hypertension and gender. *J Neurosurg.* (1985) 63:49–55. doi: 10.3171/jns.1985.63.1.0049
22. Park SK, Kim JM, Kim JH, Cheong JH, Bak KH, Kim CH. Aneurysmal subarachnoid hemorrhage in young adults: a gender comparison study. *J Clin Neurosci.* (2008) 15:389–92. doi: 10.1016/j.jocn.2007.04.007
23. Dharmadhikari S, Atchaneeyasakul K, Ambekar S, Saini V, Haussen DC, Yavagal D. Association of Menopausal Age with Unruptured Intracranial Aneurysm Morphology. *Interv Neurol.* (2020) 8:109–15. doi: 10.1159/000496701
24. Backes D, Rinkel GJ, Laban KG, Algra A, Vergouwen MD. Patient- and Aneurysm-Specific Risk Factors for Intracranial Aneurysm Growth: A Systematic Review and Meta-Analysis. *Stroke.* (2016) 47:951–7. doi: 10.1161/STROKEAHA.115.012162
25. Kubo Y, Koji T, Kashimura H, Otawara Y, Ogawa A, Ogasawara K. Female sex as a risk factor for the growth of asymptomatic unruptured cerebral saccular aneurysms in elderly patients. *J Neurosurg.* (2014) 121:599–604. doi: 10.3171/2014.5.JNS132048
26. Horiuchi T, Tanaka Y, Hongo K. Sex-related differences in patients treated surgically for aneurysmal subarachnoid hemorrhage. *Neurol Med Chir*. (2006) 46:328–32; discussion 32. doi: 10.2176/nmc.46.328

27. De Marchis GM, Schaad C, Fung C, Beck J, Gralla J, Takala J, et al. Gender-related differences in aneurysmal subarachnoid hemorrhage: a hospital based study. *Clin Neurol Neurosurg.* (2017) 157:82–7. doi: 10.1016/j.clineuro.2017.04.009
28. De Rooij NK, Linn FH, Van Der Plas JA, Algra A, Rinkel GJ. Incidence of subarachnoid haemorrhage: a systematic review with emphasis on region, age, gender and time trends. *J Neurol Neurosurg Psychiatry.* (2007) 78:1365–72. doi: 10.1136/jnnp.2007.117655
29. Eden SV, Meurer WJ, Sanchez BN, Lisabeth LD, Smith MA, Brown DL, et al. Gender and ethnic differences in subarachnoid hemorrhage. *Neurology.* (2008) 71:731–5. doi: 10.1212/01.wnl.0000319690.82357.44
30. Bonita R, Thomson S. Subarachnoid hemorrhage: epidemiology, diagnosis, management, and outcome. *Stroke.* (1985) 16:591–4. doi: 10.1161/01.STR.16.4.591
31. Risselada R, De Vries LM, Dippel DW, Van Kooten F, Van Der Lugt A, Niessen WJ, et al. Incidence, treatment, and case-fatality of non-traumatic subarachnoid haemorrhage in the Netherlands. *Clin Neurol Neurosurg.* (2011) 113:483–7. doi: 10.1016/j.clineuro.2011.02.015
32. Turan N, Heider RA, Zaharieva D, Ahmad FU, Barrow DL, Pradilla G. Sex differences in the formation of intracranial aneurysms and incidence and outcome of subarachnoid hemorrhage: review of experimental and human studies. *Transl Stroke Res.* (2016) 7:12–9. doi: 10.1007/s12975-015-0434-6
33. Lin B, Chen W, Ruan L, Chen Y, Zhong M, Zhuge Q, et al. Sex differences in aneurysm morphologies and clinical outcomes in ruptured anterior communicating artery aneurysms: a retrospective study. *BMJ Open.* (2016) 6:e009920. doi: 10.1136/bmjopen-2015-009920
34. Lindner SH, Bor AS, Rinkel GJ. Differences in risk factors according to the site of intracranial aneurysms. *J Neurol Neurosurg Psychiatry.* (2010) 81:116–8. doi: 10.1136/jnnp.2008.163063
35. Rehman S, Chandra RV, Zhou K, Tan D, Lai L, Asadi H, et al. Sex differences in aneurysmal subarachnoid haemorrhage (aSAH): aneurysm characteristics, neurological complications, and outcome. *Acta Neurochir (Wien).* (2020) 162:2271–82. doi: 10.1007/s00701-020-04469-5
36. Forget TR, Benitez R, Veznedaroglu E, Sharan A, Mitchell W, Silva M, et al. A review of size and location of ruptured intracranial aneurysms. *Neurosurgery.* (2001) 49:1322-5; discussion 5–6. doi: 10.1097/00006123-200112000-00006
37. Diagbouga MR, Morel S, Bijlenga P, Kwak BR. Role of hemodynamics in initiation/growth of intracranial aneurysms. *Eur J Clin Invest.* (2018) 48:e12992. doi: 10.1111/eci.12992
38. Horikoshi T, Akiyama I, Yamagata Z, Sugita M, Nukui H. Magnetic resonance angiographic evidence of sex-linked variations in the circle of willis and the occurrence of cerebral aneurysms. *J Neurosurg.* (2002) 96:697–703. doi: 10.3171/jns.2002.96.4.0697
39. Mujagic S, Moranjkic M, Mesanovic N, Osmanovic S. The inner diameter of arteries of the Circle ofWillis regarding gender and age on magnetic resonance angiography. *Acta Medica Saliniana.* (2013) 42:6–12. doi: 10.5457/342
40. Shatri J, Bexheti D, Bexheti S, Kabashi S, Krasniqi S, Ahmetgjekaj I, et al. Influence of gender and age on average dimensions of arteries forming the circle of Willis study by magnetic resonance angiography on Kosovo's population. *Open Access Maced J Med Sci.* (2017) 5:714–9. doi: 10.3889/oamjms.2017.160
41. Lindekleiv HM, Valen-Sendstad K, Morgan MK, Mardal KA, Faulder K, Magnus JH, et al. Sex differences in intracranial arterial bifurcations. *Gend Med.* (2010) 7:149–55. doi: 10.1016/j.genm.2010.03.003
42. Alnaes MS, Isaksen J, Mardal KA, Romner B, Morgan MK, Ingebrigtsen T. Computation of hemodynamics in the circle of Willis. *Stroke.* (2007) 38:2500–5. doi: 10.1161/STROKEAHA.107.482471
43. Rahman M, Smietana J, Hauck E, Hoh B, Hopkins N, Siddiqui A, et al. Size ratio correlates with intracranial aneurysm rupture status: a prospective study. *Stroke.* (2010) 41:916–20. doi: 10.1161/STROKEAHA.109.574244
44. Leblanc R. Familial cerebral aneurysms. *A bias for women Stroke.* (1996) 27:1050–4. doi: 10.1161/01.STR.27.6.1050
45. Sijtsma LC, Rinkel GJ, Ruigrok YM. Sex-related clustering of intracranial aneurysms within families. *Stroke.* (2015) 46:1107–9. doi: 10.1161/STROKEAHA.115.008798
46. Ding C, Toll V, Ouyang B, Chen M. Younger age of menopause in women with cerebral aneurysms. *J Neurointerv Surg.* (2013) 5:327–31. doi: 10.1136/neurintsurg-2012-010364
47. Chen M, Ouyang B, Goldstein-Smith L, Feldman L. Oral contraceptive and hormone replacement therapy in women with cerebral aneurysms. *J Neurointerv Surg.* (2011) 3:163–6. doi: 10.1136/jnis.2010.003855
48. Fontaine C, Morfoisse F, Tatin F, Zamora A, Zahreddine R, Henrion D, et al. The impact of estrogen receptor in arterial and lymphatic vascular diseases. *Int J Mol Sci.* (2020) 21. doi: 10.3390/ijms21093244
49. Oka M, Ono I, Shimizu K, Kushamae M, Miyata H, Kawamata T, et al. The bilateral ovariectomy in a female animal exacerbates the pathogenesis of an intracranial aneurysm. *Brain Sci.* (2020) 10. doi: 10.3390/brainsci10060335
50. Tada Y, Makino H, Furukawa H, Shimada K, Wada K, Liang EI, et al. Roles of estrogen in the formation of intracranial aneurysms in ovariectomized female mice. *Neurosurgery.* (2014) 75:690–5; discussion 5. doi: 10.1227/NEU.0000000000000528
51. Tamura T, Jamous MA, Kitazato KT, Yagi K, Tada Y, Uno M, et al. Endothelial damage due to impaired nitric oxide bioavailability triggers cerebral aneurysm formation in female rats. *J Hypertens.* (2009) 27:1284–92. doi: 10.1097/HJH.0b013e328329d1a7
52. Hoh BL, Rojas K, Lin L, Fazal HZ, Hourani S, Nowicki KW, et al. Estrogen deficiency promotes cerebral aneurysm rupture by up regulation of Th17 cells and interleukin-17A which downregulates E-cadherin. *J Am Heart Assoc.* (2018) 7. doi: 10.1161/JAHA.118.008863
53. Maekawa H, Tada Y, Yagi K, Miyamoto T, Kitazato KT, Korai M, et al. Bazedoxifene, a selective estrogen receptor modulator, reduces cerebral aneurysm rupture in Ovariectomized rats. *J Neuroinflammation.* (2017) 14:197. doi: 10.1186/s12974-017-0966-7
54. Jamous MA, Nagahiro S, Kitazato KT, Tamura T, Kuwayama K, Satoh K. Role of estrogen deficiency in the formation and progression of cerebral aneurysms. Part II: experimental study of the effects of hormone replacement therapy in rats. *J Neurosurg.* (2005) 103:1052–7. doi: 10.3171/jns.2005.103.6.1052
55. Chalouhi N, Hoh BL, Hasan D. Review of cerebral aneurysm formation, growth, and rupture. *Stroke.* (2013) 44:3613–22. doi: 10.1161/STROKEAHA.113.002390
56. Frosen J, Cebral J, Robertson AM, Aoki T. Flow-induced, inflammation-mediated arterial wall remodeling in the formation and progression of intracranial aneurysms. *Neurosurg Focus.* (2019) 47:E21. doi: 10.3171/2019.5.FOCUS19234
57. Hashimoto T, Meng H, Young WL. Intracranial aneurysms: links among inflammation, hemodynamics and vascular remodeling. *Neurol Res.* (2006) 28:372–80. doi: 10.1179/016164106X14973
58. Jamous MA, Nagahiro S, Kitazato KT, Tamura T, Aziz HA, Shono M, et al. Endothelial injury and inflammatory response induced by hemodynamic changes preceding intracranial aneurysm formation: experimental study in rats. *J Neurosurg.* (2007) 107:405–11. doi: 10.3171/JNS-07/08/0405
59. Aoki T, Nishimura M. Targeting chronic inflammation in cerebral aneurysms: focusing on NF-kappaB as a putative target of medical therapy. *Expert Opin Ther Targets.* (2010) 14:265–73. doi: 10.1517/14728221003586836
60. Stirone C, Boroujerdi A, Duckles SP, Krause DN. Estrogen receptor activation of phosphoinositide-3 kinase, akt, and nitric oxide signaling in cerebral blood vessels: rapid and long-term effects. *Mol Pharmacol.* (2005) 67:105–13. doi: 10.1124/mol.104.004465
61. Warfvinge K, Krause DN, Maddahi A, Edvinsson JCA, Edvinsson L, Haanes KA. Estrogen receptors alpha, beta and GPER in the CNS and trigeminal system - molecular and functional aspects. *J Headache Pain.* (2020) 21:131. doi: 10.1186/s10194-020-01197-0
62. Thorin E, Pham-Dang M, Clement R, Mercier I, Calderone A. Hyper-reactivity of cerebral arteries from ovariectomized rats: therapeutic benefit of tamoxifen. *Br J Pharmacol.* (2003) 140:1187–92. doi: 10.1038/sj.bjp.0705547
63. Tsang SY, Yao X, Chan FL, Wong CM, Chen ZY, Laher I, et al. Estrogen and tamoxifen modulate cerebrovascular tone in ovariectomized female rats. *Hypertension.* (2004) 44:78–82. doi: 10.1161/01.HYP.0000131659.27081.19
64. Aoki T, Kataoka H, Ishibashi R, Nozaki K, Egashira K, Hashimoto N. Impact of monocyte chemoattractant protein-1 deficiency on cerebral aneurysm formation. *Stroke.* (2009) 40:942–51. doi: 10.1161/STROKEAHA.108.532556
65. Aoki T, Kataoka H, Shimamura M, Nakagami H, Wakayama K, Moriwaki T, et al. NF-kappaB is a key mediator of cerebral aneurysm formation. *Circulation.* (2007) 116:2830–40. doi: 10.1161/CIRCULATIONAHA.107.728303

66. Jayaraman T, Berenstein V, Li X, Mayer J, Silane M, Shin YS, et al. Tumor necrosis factor alpha is a key modulator of inflammation in cerebral aneurysms. *Neurosurgery*. (2005) 57:558–64; discussion-64. doi: 10.1227/01.NEU.0000170439.89041.D6
67. Wajima D, Hourani S, Dodd W, Patel D, Jones C, Motwani K, et al. Interleukin-6 promotes murine estrogen deficiency-associated cerebral aneurysm rupture. *Neurosurgery*. (2020) 86:583–92. doi: 10.1093/neuros/nyz220
68. Yokosuka K, Rutledge C, Kamio Y, Kuwabara A, Sato H, Rahmani R, et al. Roles of Phytoestrogen in the Pathophysiology of Intracranial Aneurysm. *Stroke*. (2021) 52:2661–70. doi: 10.1161/STROKEAHA.120.032042
69. Ospina JA, Brevig HN, Krause DN, Duckles SP. Estrogen suppresses IL-1beta-mediated induction of COX-2 pathway in rat cerebral blood vessels. *Am J Physiol Heart Circ Physiol*. (2004) 286:H2010–9. doi: 10.1152/ajpheart.00481.2003
70. Ospina JA, Duckles SP, Krause DN. 17beta-estradiol decreases vascular tone in cerebral arteries by shifting COX-dependent vasoconstriction to vasodilation. *Am J Physiol Heart Circ Physiol*. (2003) 285:H241–50. doi: 10.1152/ajpheart.00018.2003
71. Aoki T, Nishimura M, Matsuoka T, Yamamoto K, Furuyashiki T, Kataoka H, et al. PGE(2) -EP(2) signalling in endothelium is activated by haemodynamic stress and induces cerebral aneurysm through an amplifying loop via NF-kappaB. *Br J Pharmacol*. (2011) 163:1237–49. doi: 10.1111/j.1476-5381.2011.01358.x
72. Sheinberg DL, Mccarthy DJ, Elwardany O, Bryant JP, Luther E, Chen SH, et al. Endothelial dysfunction in cerebral aneurysms. *Neurosurg Focus*. (2019) 47:E3. doi: 10.3171/2019.4.FOCUS19221
73. Starke RM, Chalouhi N, Ali MS, Jabbour PM, Tjoumakaris SI, Gonzalez LF, et al. The role of oxidative stress in cerebral aneurysm formation and rupture. *Curr Neurovasc Res*. (2013) 10:247–55. doi: 10.2174/15672026113109990003
74. Aoki T, Nishimura M, Kataoka H, Ishibashi R, Nozaki K, Hashimoto N. Reactive oxygen species modulate growth of cerebral aneurysms: a study using the free radical scavenger edaravone and p47phox(-/-) mice. *Lab Invest*. (2009) 89:730–41. doi: 10.1038/labinvest.2009.36
75. Starke RM, Thompson JW, Ali MS, Pascale CL, Martinez Lege A, Ding D, et al. Cigarette Smoke Initiates Oxidative Stress-Induced Cellular Phenotypic Modulation Leading to Cerebral Aneurysm Pathogenesis. *Arterioscler Thromb Vasc Biol*. (2018) 38:610–21. doi: 10.1161/ATVBAHA.117.310478
76. Bonita R. Cigarette smoking, hypertension and the risk of subarachnoid hemorrhage: a population-based case-control study. *Stroke*. (1986) 17:831–5. doi: 10.1161/01.STR.17.5.831
77. Lindekleiv H, Sandvei MS, Njolstad I, Lochen ML, Romundstad PR, Vatten L, et al. Sex differences in risk factors for aneurysmal subarachnoid hemorrhage: a cohort study. *Neurology*. (2011) 76:637–43. doi: 10.1212/WNL.0b013e31820c30d3
78. Ogilvy CS, Gomez-Paz S, Kicielinski KP, Salem MM, Akamatsu Y, Waqas M, et al. Cigarette smoking and risk of intracranial aneurysms in middle-aged women. *J Neurol Neurosurg Psychiatry*. (2020) 91:985–90. doi: 10.1136/jnnp-2020-323753
79. Chalouhi N, Ali MS, Jabbour PM, Tjoumakaris SI, Gonzalez LF, Rosenwasser RH, et al. Biology of intracranial aneurysms: role of inflammation. *J Cereb Blood Flow Metab*. (2012) 32:1659–76. doi: 10.1038/jcbfm.2012.84
80. Frosen J, Piippo A, Paetau A, Kangasniemi M, Niemela M, Hernesniemi J, et al. Remodeling of saccular cerebral artery aneurysm wall is associated with rupture: histological analysis of 24 unruptured and 42 ruptured cases. *Stroke*. (2004) 35:2287–93. doi: 10.1161/01.STR.0000140636.30204.da
81. Brincat MP, Calleja-Agius J, Baron YM. The skin carotid and intervertebral disc: making the connection! *Climacteric*. (2007) 10 Suppl 2:83–7. doi: 10.1080/13697130701591998
82. Calleja-Agius J, Brincat M. The effect of menopause on the skin and other connective tissues. *Gynecol Endocrinol*. (2012) 28:273–7. doi: 10.3109/09513590.2011.613970
83. Baron YM, Galea R, Brincat M. Carotid artery wall changes in estrogen-treated and -untreated postmenopausal women. *Obstet Gynecol*. (1998) 91:982–6. doi: 10.1097/00006250-199806000-00021
84. Aoki T, Kataoka H, Morimoto M, Nozaki K, Hashimoto N. Macrophage-derived matrix metalloproteinase-2 and−9 promote the progression of cerebral aneurysms in rats. *Stroke*. (2007) 38:162–9. doi: 10.1161/01.STR.0000252129.18605.c8
85. Aoki T, Kataoka H, Moriwaki T, Nozaki K, Hashimoto N. Role of TIMP-1 and TIMP-2 in the progression of cerebral aneurysms. *Stroke*. (2007) 38:2337–45. doi: 10.1161/STROKEAHA.107.481838
86. Qin Z, Li G, Liu N, Zhao C, Zhao H. Effect of estrogen administration on middle cerebral arterial viscoelastic properties in aged female rats. *Acta Cir Bras*. (2016) 31:661–7. doi: 10.1590/S0102-865020160100000004
87. Wang SJ, Zhao SJ, Wang YS, Yu T, Luo M. Effects of estrogen intervention on the biomechanical characteristics of serum SOD, MDA, and middle cerebral artery in aged female rats. *Clin Exp Obstet Gynecol*. (2015) 42:295–9. doi: 10.12891/ceog1756.2015
88. Tutino VM, Mandelbaum M, Takahashi A, Pope LC, Siddiqui A, Kolega J, et al. Hypertension and Estrogen Deficiency Augment Aneurysmal Remodeling in the Rabbit Circle of Willis in Response to Carotid Ligation. *Anat Rec (Hoboken)*. (2015) 298:1903–10. doi: 10.1002/ar.23205
89. Chalouhi N, Starke RM, Correa T, Jabbour PM, Zanaty M, Brown RD, et al. Differential sex response to aspirin in decreasing aneurysm rupture in humans and mice. *Hypertension*. (2016) 68:411–7. doi: 10.1161/HYPERTENSIONAHA.116.07515
90. Hasan DM, Mahaney KB, Brown RD, Meissner I, Piepgras DG, Huston J, et al. Aspirin as a promising agent for decreasing incidence of cerebral aneurysm rupture. *Stroke*. (2011) 42:3156–62. doi: 10.1161/STROKEAHA.111.619411
91. Hasan DM, Starke RM, Gu H, Wilson K, Chu Y, Chalouhi N, et al. Smooth muscle peroxisome proliferator-activated receptor gamma plays a critical role in formation and rupture of cerebral aneurysms in mice *in vivo*. *Hypertension*. (2015) 66:211–20. doi: 10.1161/HYPERTENSIONAHA.115.05332
92. Shimada K, Furukawa H, Wada K, Korai M, Wei Y, Tada Y, et al. Protective role of peroxisome proliferator-activated receptor-gamma in the development of intracranial aneurysm rupture. *Stroke*. (2015) 46:1664–72. doi: 10.1161/STROKEAHA.114.007722

Conflict of Interest: The authors declare that the research was conducted in the absence of any commercial or financial relationships that could be construed as a potential conflict of interest.

Publisher's Note: All claims expressed in this article are solely those of the authors and do not necessarily represent those of their affiliated organizations, or those of the publisher, the editors and the reviewers. Any product that may be evaluated in this article, or claim that may be made by its manufacturer, is not guaranteed or endorsed by the publisher.

Copyright © 2022 Fréneau, Baron-Menguy, Vion and Loirand. This is an open-access article distributed under the terms of the Creative Commons Attribution License (CC BY). The use, distribution or reproduction in other forums is permitted, provided the original author(s) and the copyright owner(s) are credited and that the original publication in this journal is cited, in accordance with accepted academic practice. No use, distribution or reproduction is permitted which does not comply with these terms.

frontiers in Cardiovascular Medicine

MINI REVIEW
published: 15 February 2022
doi: 10.3389/fcvm.2022.793072

Imaging Modalities for Intracranial Aneurysm: More Than Meets the Eye

Clémence Maupu, Héloïse Lebas and Yacine Boulaftali*

INSERM, U1148-LVTS, University of Paris, Paris, France

Intracranial aneurysms (IA) are often asymptomatic and have a prevalence of 3 to 5% in the adult population. The risk of IA rupture is low, however when it occurs half of the patients dies from subarachnoid hemorrhage (SAH). To avoid this fatal evolution, the main treatment is an invasive surgical procedure, which is considered to be at high risk of rupture. This risk score of IA rupture is evaluated mainly according to its size and location. Therefore, angiography and anatomic imaging of the intracranial aneurysm are crucial for its diagnosis. Moreover, it has become obvious in recent years that several other factors are implied in this complication, such as the blood flow complexity or inflammation. These recent findings lead to the development of new IA imaging tools such as vessel wall imaging, 4D-MRI, or molecular MRI to visualize inflammation at the site of IA in human and animal models. In this review, we will summarize IA imaging techniques used for the patients and those currently in development.

Keywords: intracranial aneurysm, vessel wall imaging, imaging technique, hemodynamic imaging, inflammation imaging

OPEN ACCESS

Edited by:
Margreet R. De Vries, Leiden University Medical Center, Netherlands

Reviewed by:
Philipp Berg, Otto von Guericke University Magdeburg, Germany

****Correspondence:***
Héloïse Lebas
heloise.lebas@inserm.fr

Specialty section:
This article was submitted to Atherosclerosis and Vascular Medicine, a section of the journal Frontiers in Cardiovascular Medicine

Received: *11 October 2021*
Accepted: *17 January 2022*
Published: *15 February 2022*

Citation:
Maupu C, Lebas H and Boulaftali Y (2022) Imaging Modalities for Intracranial Aneurysm: More Than Meets the Eye. Front. Cardiovasc. Med. 9:793072. doi: 10.3389/fcvm.2022.793072

Intracranial aneurysms (IA) are pathological focal dilatations of intracranial arteries mainly located at bifurcations of the circle of Willis. IAs are found approximatively in 3.2% of the adult population and are being detected mostly incidentally. Unruptured IAs are commonly asymptomatic but their rupture has severe consequences. Indeed, IA rupture leads to aneurysmal subarachnoid hemorrhage (SAH) which affects 6 in 100,000 persons per year and leads to death for 27–44% of patients (1, 2). Even if the majority of IAs do not evolve toward their rupture, 1 in 200 to 400 will (3). Therefore, there is a need to identify those IAs at risk of rupture in order to treat them and decrease this risk.

In the past few decades, several pathophysiological processes leading to IA rupture were identified as irregular IA shape, an altered hemodynamic stress within the IA and vessel wall inflammation (4). Those findings led to the development of a variety of new imaging tools which provide a better characterization of IAs and enable clinicians to identify those at risk of rupture.

This review will summarize the classical methods of imaging aneurysms and the latest development in the field. It should be noted that this review intend to provide a comprehensive overview of the imaging modalities and discuss their relevance in the field of aneurysmal pathology.

MORPHOLOGICAL IMAGING

Imaging is a crucial diagnostic tool for the aneurysm's detection and characterization. Indeed, IA imaging can provide detailed information such as its location, size, morphology and geometry, determining the therapeutic strategy (surgical intervention or conservative management) (3). In routine clinical practice, IA are detected and imaged based on their morphology.

Digital subtraction angiography (DSA), a fluoroscopy technique using iodine contrast, is used to produce images of intracranial blood vessels without surrounding tissues as they are removed by digital subtraction (5). Thanks to its high spatial resolution, specificity and sensitivity, DSA is the gold standard for IA imaging and can determine its morphological characteristics such as its size, neck diameter and delineation (3, 6, 7). The development of 3D rotational angiography (3DRA) improved the spatial resolution of DSA, as 3D reconstruction helps to avoid imaging errors related to the superposition of vascular structures, allowing the visualization of small IAs (<3mm) (8). However DSA remains invasive and rare complications exist due to the use of intra-arterial devices and iodine-containing contrast agents during the catheter angiography [neurological: 0.1–1%; severe allergic reaction: 0.05–0.1%] (9).

Several non-invasive imaging techniques have been developed such as computational tomography angiography (CTA). CTA specificity and sensitivity are nearly as good as DSA [sensitivity for IA > 3 mm: 93.3–97.2%; specificity: 87.8–100%] (3, 6, 7). However, CTA is a poor choice for detection of small IAs localized near the skull bone as ionizing ray are almost equally absorbed by calcium and iodinated contrast agents [sensitivity = 61%] (10). Thus, a match mask bone elimination (MMBE) technique has been developed, removing non-specific signal induced by bones, but it requires a longer exposure to ionizing ray and is sensitive to patient movement (11). The advent of dual energy CTA (DE-CTA) subsequently improved material differentiation thereby reducing artifacts created by bony structures without the drawback of the MMBE method (12, 13).

Unlike CTA and DSA, magnetic resonance angiography (MRA) is performed without X-rays. MRA sequences, such as time-of-flight MRA (TOF-MRA) or non-enhanced magnetization-prepared rapid acquisition gradient echo (MPRAGE), do not require contrast agents and is thus considered the least invasive method to date. Non-contrast enhanced MRA gained interest in the last decade due to the well-known health risk of iodinated agents (14). TOF-MRA at 1.5 and 3 Tesla (T) are the most common MRA performed to visualize IAs with a greater sensitivity and accuracy for 3T [Sensitivity: 1.5T = 53.6% vs. 3T = 76.6%; accuracy: 1.5T = 84% vs. 3T = 91.9%] (15, 16). This MRA method relies on the magnetic properties of circulating blood (17). Although this allows for the elimination of contrast agents, some artifacts can be observed especially when the blood flow is turbulent or low, which constitute a limiting factor as those flow disturbances are common in large or coiled aneurysms (17, 18). To alleviate this issue, gadolinium-enhanced MRA (GE-MRA) can be performed as it is flow-independent (18–20). Both TOF- and GE-MRA have 95% sensitivity compared to DSA (6). Recently, 7T MRA has been evaluated in the study of IA. 7T MRI remains infrequent but studies agree on its high potential for the detection of IAs as well as their anatomical description and is a great tool for IA follow-up (21–23). The combination of 7T 3D-TOF and MPRAGE has been demonstrated to delineate unruptured IAs as well as DSA (22). Finally, intracranial black blood vessel imaging (MR-IBBVI), a new MRA sequence based on blood signal suppression, has been compared to TOF-MRA and DSA. Its sensitivity and specificity is higher than TOF-MRA regardless of aneurysm size [Sensitivity: MR-IBBVI = 94.5% vs. TOF-MRA = 62.7%; specificity: MR-IBBVI = 94.5% vs. TOF MRA = 92%; both compared with DSA] (24).

All these IA morphology imaging, with their benefits and disadvantages, summarized in **Table 1**, have a millimeter spatial resolution which is sufficient for IA detection and morphological characterization and the risk of rupture. However, vessel wall remodeling, which is a main feature of IAs evolving toward rupture, can not be observed with classical imaging mentioned above and there is currently no imaging technique to visualize the elastic lamina disruption or the thinning of the media. Optical coherence tomography (OCT), which is already widely used in ophthalmology, is being optimized for intracranial usage. OCT is based on the differential reflective properties of tissues to near infra-red light. A catheter is introduced in the targeted vessel and 2D cross-sectional images are acquired with a high resolution (1 to 15 μm) (31, 33). It has already been demonstrated that OCT allows the visualization of layers disruption in IA as the delimitations between intima and media layers are no longer visible compared to healthy vessel wall (31, 34). Moreover, the good position of intrasaccular devices can be monitored through OCT in real-time during the surgical procedure (35, 36). The development of such imaging would significantly complement the existing IA rupture risk stratification tools based on IA morphology enabled by current imaging.

HEMODYNAMIC IMAGING

All the above-mentioned imaging procedures are performed to assess the morphologic characteristics of IAs, evaluating its rupture risk. However, these parameters seem to be insufficient to accurately predict this evolution toward rupture (37). Indeed,

Abbreviations: AWE, Aneurysm wall enhancement; CAWE, Circumferential aneurysm wall enhancement; CFD, Computational fluid dynamics; CSF, Cerebrospinal fluid signal; CTA, Computational tomography angiography; DE-CTA, Dual energy computational tomography angiography; DSA, Digital subtraction angiography; FAWE, Focal aneurysm wall enhancement; GE-MRA, Gadolinium-enhanced magnetic resonance angiography; IA, Intracranial aneurysm; MMBE, Match mask bone elimination; MPRAGE, Magnetization-prepared rapid acquisition gradient echo; MRA, Magnetic resonance angiography; MRI, Magnetic resonance imaging; MR-IBBVI, Magnetic resonance- intracranial black blood vessel imaging; OCT, Optical coherence tomography; OSI, Oscillatory shear index; PIV, Particule image velocimetry; RRT, Relative residence time; SAH, Subarachnoid hemorrhage; T, Tesla; TOF-MRA, Time-of-flight magnetic resonance angiography; VWI, Vessel wall imaging; WSS, Wall shear stress; 3DRA, 3-dimensional rotational angiography.

TABLE 1 | IA morphology imaging techniques.

IA morphology imaging			
Features imaged	**Principle**	**Observations**	**References**
Rotational angiography (3DRA)			
Arteries' lumen without surrounding tissues	Angiography principle: pre and post contrast rotational acquisition	- High spatial resolution; best specificity, sensitivity, depiction of small IA (<3 mm) - Iodinated agent needed - Invasive imaging (catheterization)	(5, 25)
Computational tomography angiography (CTA)			
Classical CTA: Arteries' lumen in hypersignal with surrounding tissues	Tomography principle	- Iodinated agent needed - Artifacts due to bones signal but software to remove bony structures exists - Non-invasive	(26–28)
Dual-energy CTA: Arteries' lumen in hypersignal with improved contrast of surrounding tissues	Same principle as classical CTA. Differs by the type of scanner used which emit X-rays of different energies	- Iodinated agent needed - Bones signal removed directly - Non-invasive	(12, 28)
Magnetic resonance angiography (MRA)			
Time of flight (TOF): arteries' lumen in hypersignal	Principle of flow-related enhancement MRI. Under repetitive radiofrequency pulses, static tissues undergo a magnetic saturation unlike the circulating blood	- Ionizing radiation and contrast agent free - Less invasive technic - Abnormal blood flow related artifacts - Lowest spatial resolution when compared to CTA and DSA	(29)
Gadolinium-enhanced: arteries' lumen in hypersignal at the bolus passage	MRI sequences sensitive to gadolinium	- Ionizing radiation free - Lowest resolution when compared to CTA and DSA	(30)
Optical coherence tomography (OCT)			
Layers disruption in 2D-cross-sectional imaging of arteries	The differential reflective properties of tissues to near infra-red light	- Catheterization needed - High spatial resolution (μm)	(31, 32)

it has been described that hemodynamics stressors are a major cause of IA formation, growth and rupture (38, 39). The main hemodynamic parameters studied are the wall shear stress (WSS defined as the frictional force tangent to vessel wall induced by blood flow), the oscillatory shear index (OSI defined as the direction and intensity flow changes during a cardiac cycle), relative residence time (RRT express the distribution of blood flow over time at the aneurysm wall) and flow patterns (40). Nowadays, a high WSS is commonly accepted to be involved in the formation of IAs, but its role in rupture is less certain as a high or a low WSS can both lead to a destructive remodeling of the aneurysm wall. Indeed, a high WSS is believed to be at the origin of a mural cell-mediated pathological response whereas a low WSS is the source of an inflammatory cell-mediated pathological response (39, 41). However, IA rupture is associated with a higher OSI, a prolonged RTT and complex flow patterns and yet, these hemodynamics parameters are not accessible *via* the current clinical imaging methods described in morphological imaging section of this review (40–43).

Computational fluid dynamics (CFD), widely used to study hemodynamic parameters, is performed on high-resolution 3D data sets (44). CFD uses static characteristics of IAs (size, location, aspect ratio, size ratio) to calculate WSS, OSI, flow velocity and RRT (39, 45). Thus, CFD is highly influenced by the choice of imaging modality, albeit no imaging modality, so far, has been described as the gold standard to CFD calculations (46, 47). Although CFD is an effective method to calculate hemodynamic parameters and has led to a better understanding of IAs, varying degrees of errors are observed due to some limitations (e.g., considers blood as a Newtonian fluid, arteries as rigid, no standardized protocol) and should be overcome in order to provide important information to clinicians (45, 46, 48).

3DRA is considered the gold standard for the detection and definition of static aneurysm characteristics, however, there are no such clear-cut opinions for dynamic features. In clinical practice, a combination of 2D and 3DRA are used to assess cerebrovascular blood flow. 2D-DSA gives flux information during the contrast-agent passage and 3DRA provides static anatomic information (49, 50). This has led to the development of 4D-DSA, also named time-resolved 3DRA, combining 2D-DSA and 3DRA. This method uses the 3D images obtained with conventional 3DRA and retains the temporal information of these acquisitions, allowing visualization of the influx and efflux of the contrast agent at any angle (51). Vanrossomme et al. reviewed several studies which successfully detected and quantified IA wall deformation between different frames with high spatial and temporal resolutions [35–165 ms and 0.2 mm] (52). Concerning hemodynamics, 4D-DSA applications have mostly been studied in arteriovenous malformations (50) and only one study assessed qualitatively the capacity of this imaging to detect IA flow pattern [excellent visualization in 27.7% of IA and fair visualization in 72.3% of IA] (53). Additionally,

Lang et al. demonstrated that 4D-DSA is as reliable as 3DRA for CFD analysis as there is no significant differences in the flow velocity or WSS calculated (54). Moreover, with its high spatial resolution [voxel volume = 0.008 mm^3] (51) 4D-DSA allows the same anatomic characterization of IAs than the gold standard 3DRA (54). Thus, 4D-DSA still needs to be improved to achieve a direct quantification of blood hemodynamics but its spatial resolution could allow, in addition to a morphological characterization of IAs, a robust CFD analysis.

Conventionally, to visualize blood flow with magnetic resonance imaging (MRI), a phase-contrast method is performed to access unidirectional flow in a 2D space (55). This 2D phase-contrast MRI has evolved to 3D time-resolved phase-contrast MRI, also called 4D-MRI. This flow imaging quantifies direct blood flow velocity in 3D, allowing flow pattern modeling and quantification of WSS, OSI and vorticity (55–58). In 2020, two complete state-of-the-art reviews on the 4D-MRI's ability to study IA hemodynamics have been published (56, 58). To summarize, 4D-MRI, mostly compared to CFD, reliably depicts intra-aneurysmal flow pattern in different IA morphologies. However, this 4D-imaging still has great limitations, in particular in terms of spatial and temporal resolution which has consequences on the calculation of hemodynamic parameters (depending on magnetic field and acquisition protocol, 4D-MRI = ranging from $0.43 \times 0.43 \times 0.43$ to $1 \times 1 \times 1.6$ mm^3 voxels vs. CFD = 0.1-mm voxels) (56, 58). For instance, the WSS values had a lower magnitude when derived from 4D-MRI even if the localization of these WSS are similar (59). Another limit to the use of 4D-MRI in clinic is the long time of acquisition (depending on magnetic field and acquisition protocol, 5–30 min) (58). To overcome this limitation, an accelerated high spatiotemporal resolution 4D-7T-MRI have been proposed, providing accurate quantitative flow values with a 10 min acquisition (vs. 20 min) (60). Moreover, 4D-MRI has also been validated *in vitro* by comparing its hemodynamic measurements to those obtain by particle image velocimetry (PIV) (61). PIV is an optical imaging method which tracks particle displacement throughout a fluid field illuminated by a laser (62). As an increasingly popular *in vitro* tool to analyze fluid dynamics and validate medical flux imaging modality, PIV has been used to assess flow pattern in patient IA models with ultra-high spatial and temporal resolution [4Mpixel, 100 images/sec] (63).

Compared to classical CTA, with a longer acquisition time or several acquisitions over a given period, 4D-CTA records the influx and efflux of the contrast product and morphological changes of IA within a cardiac cycle when the acquisition is ECG-gated (64). 4D-CTA is mostly used in the evaluation of hemorrhagic/ischemic stroke and vascular malformations and has been proposed to replace the gold standard 3D-DSA for follow-up imaging since it produces accurate IA geometrics and reliable CFD results when compared to 3DRA (65).

Aside from these classical hemodynamic parameters, the notion of aneurysmal pulsatility arose. Aneurysm pulsation is an important dynamic parameter of IA since increased wall motion is assumed to be linked to a reduced stability of the aneurysm wall and, consequently, to the rupture (52, 66). This pulsation, composed of the global pulsation of the aneurysm and the movement of focal parts (blebs), must be differentiated from the physiological cerebrovascular movement during the cardiac cycle. As those pulsations are quick and of low magnitude, the development of an accurate imaging modality is a real challenge (52, 66). A study performed on 7T MRI quantifying volume pulsation showed insufficient accuracy due to multiple imaging artifacts (67). The most used imaging technique to study aneurysmal pulsation is 4D-CTA (52, 66). This imaging achieves a spatial resolution going up to the same order as the studied IA movements [high-resolution CT scans = 0.25 mm; standard scan = 0.6–0.8 mm] (52). Also, its ability to measure aneurysm pulsation in IAs larger than 5 mm *in vivo* have been reported (68). These above-mentioned imaging techniques have been summarized in **Table 2**.

INFLAMMATION IMAGING

Over the past decades, a growing amount of evidence seems to involve vessel wall inflammation in the pathogenesis of IA (73). Indeed, several histological studies demonstrated that inflammatory cells (mainly T-cells and macrophages) infiltration and complement activation are associated with IA rupture (74, 75). In line with this observation, vessel wall inflammation detection could help to identify IA at high risk of rupture. In order to develop new tools to visualize inflammation *in vivo*, non-invasive inflammation imaging has been developed over the past few years.

As macrophage infiltration is a typical feature observed in aneurysmal vessel wall, macrophage imaging emerged thanks to the development of ferumoxytol. Ferumoxytol is a superparamagnetic form of iron oxide, engulfed by macrophages and detectable using MRI. Therefore, MRI after ferumoxytol infusion can reflect macrophage activity and associated inflammation within aneurysmal vessel wall. A first histological study analyzed unruptured aneurysm tissues from patients displaying ferumoxytol-induced hyposignal (72h after ferumoxytol infusion) and observed both macrophage infiltration and iron particle uptake by IA vessel wall (69). Intriguingly, they observed a noticeably different level of ferumoxytol uptake among patients, some considered with "early uptake" (visible 24h after infusion) or "late uptake" (visible 72h after infusion) (76). The authors showed that IA with "early uptake" had a similar level of macrophage infiltration compared to ruptured IA, and it was significantly higher in "early uptake" IAs vs. "late uptake" IAs. Finally, all of the "early uptake" IAs managed conservatively evolved to rupture within 6 months while no "late uptake" IAs did. Thus, this study by Hasan et al. suggested that ferumoxytol-MRI could identify unstable IAs at high risk of rupture within 6 months. However, since iron is abundant in red blood cells, subtraction of pre- and post-ferumoxytol infusion images is required to detect ferumoxytol engulfed by macrophages. These pre- and post- infusion images performed independently make this analysis technically difficult and time-consuming therefore, a simpler diagnostic method is desirable (70, 77).

Vessel wall imaging (VWI) has recently emerged as a promising diagnostic tool to image intracranial vessel wall

TABLE 2 | IA hemodynamics and inflammation imaging techniques.

IA hemodynamics imaging			
Features imaged	**Principle**	**Observations**	**References**
Computational fluid dynamics (CFD)			
Allows calculation of WSS, OSI, flow velocity and RTT	*In silico* blood flow simulation on high resolution 3D anatomical images of IAs	- Most advanced method for visualizing hemodynamic characteristics - Numerous approximations: blood as a Newtonian fluid, arteries as rigid entities	(46)
4D digital subtraction angiography (4D-DSA)			
Influx and efflux of the contrast product and therefore of the blood flow pattern and arteries' lumen in hypersignal	Same principle as 3DRA. Differs in the images processing	- As reliable as 3DRA for CFD analysis - High spatial resolution - Iodinated agent needed - Most invasive imaging (catheterization)	(50, 51)
4D-magnetic resonance angiography (4D-MRA)			
Characterization and quantification of WSS, blood flow pattern and velocity	Principle of a flow-sensitive MRI (Phase contrast-MRI). Under bipolar gradient, blood emit a signal directly proportional to its speed	- Direct quantification of blood flow velocity - No contrast agent - Long time acquisition	(55, 56)
4D-computational tomography angiography (4D-CTA)			
Blood flow pattern and arteries' lumen in hypersignal	Same principle as classical CTA. Differs in protocol of acquisition to have temporal information	- Promising technic to study aneurysm pulsation - Longer exposition to ionizing ray compared to CTA	(64)
IA inflammation imaging			
Macrophage imaging			
Inflamed arteries' wall in hyposignal	Property of ferumoxytol to be engulfed by macrophages and detectable using specific MRI sequences	- Risk of allergic reaction to ferumoxytol - Technically difficult and time consuming	(69, 70)
Vessel wall imaging (VWI)			
Inflamed arteries' wall in hypersignal	MRI sequences which suppress both blood and cerebrospinal fluid signal	- High negative predictive value; moderate positive predictive value - Stagnant flow artifact - Lack of reproducibility	(71, 72)

inflammation through MRI. This technique, also known as black blood MRI, provides only signals from the vessel wall thanks to the suppression of both blood and cerebrospinal fluid signal (CSF). The acquisition of VWI demands high resolution, therefore a 3T or higher magnet strength is required. Briefly, VWI generally consist in T1-weighted pre- and post- contrast sequences along with blood and CSF suppression obtained with a 3D turbo spin-echo sequence with variable flip angle refocusing pulses (71). VWI sequence names differ among MRI constructors: VISTA (volume isotropic turbo spin-echo acquisition; Phillips healthcare, Eindhoven, Netherlands), SPACE (sampling perfection with application-optimized contrasts by using different flip angle evolutions; Siemens Healthinners, Erlangen, Germany) or CUBE (GE Healthcare, Milwaukee, WI, USA) (78).

Thanks to blood signal suppression, VWI has been used to study aneurysm wall structure, thickness and wall enhancement. Aneurysm wall enhancement (AWE) is mainly qualitatively assessed and can be classified as focal or circumferential. Radio-histological correlation studies revealed that focal AWE (FAWE) is associated with fresh intraluminal thrombus at the rupture site (79). This finding can provide useful information for the surgical treatment of ruptured IA before treating the patient by microsurgical clipping or endovascular coiling. FAWE can also be observed in unruptured IA and colocalized with hemodynamic factors in favor to a higher rupture risk (80). Moreover, FAWE is observed in areas of morphological changes in the IA vessel wall, supporting the hypothesis that FAWE could be a marker of instability (80). On the other hand, circumferential AWE (CAWE) is thought to be due to wall thickening with abundant inflammatory cell infiltration and neovascularization (78, 81, 82).

In cases of subarachnoid hemorrhage and multiple aneurysms, several criteria are used to determine which one underwent rupture (*i.e.* hemorrhage localization, IA size, location, shape, aspect ratio). As vessel wall inflammation is a risk factor of IA rupture, AWE is nearly always observed in ruptured IAs (83). Along with this observation, some studies performed on patients presenting multiple IAs, demonstrated that VWI can identify the ruptured IA which is characterized by a thick vessel wall enhancement (84, 85). Thus, VWI can be a useful diagnostic tool in identifying ruptured IA and its site of rupture (79).

With regard to unruptured IA, current research is deciphering the clinical interpretation of AWE. It has been proposed that AWE could be a biomarker of vessel wall inflammation in unstable IAs prone to evolve toward rupture (86). Indeed, some studies performed on unruptured IAs demonstrated a correlation between AWE and common risk factors of IA rupture such as

a larger size (≥7 mm), an irregular shape, a high aspect ratio (depth/neck width) and its localization in the anterior cerebral, posterior communicating and posterior cerebral arteries (87–91). A correlation between AWE intensity and the severity of PHASES and ELAPSS scores has also been demonstrated (92).

Finally, a meta-analysis performed on 6 studies analyzed VWI and aneurysm instability. The authors concluded that unstable aneurysms (defined as ruptured, symptomatic, or growing on serial imaging) had statistically higher odds to display AWE. There was still a significant correlation between AWE and IA instability after the removal of ruptured aneurysms (93). Moreover, these meta-analyses highlighted that the absence of wall enhancement on VWI is strongly associated with IA stability (negative predictive value: 96.2%). Very recently, another meta-analysis added 6 more studies, including a longitudinal prospective study, and confirmed these positive and negative predictive value (94, 95). Therefore, VWI and AWE could be a useful risk stratification tools in assessing IAs stability.

Despite potential clinical applications of VWI, it is important to highlight potential limitations of this new diagnostic tool. The meta-analysis demonstrated a moderate specificity (62.7%) and positive predictive value (55.8%) of AWE in identifying unstable aneurysms, meaning that a part of IAs with AWE on VWI are considered to be stable (93). Moreover, flow artifacts within the sac, contrast extravasation and stagnant flow could mimic AWE, leading to false-positive signals (96, 97). In addition, there is no consensus on the definition of AWE as some studies included both FAWE and CAWE whereas others only studied CAWE. Most studies qualitatively assessed AWE inducing a lack of reproducibility, therefore quantitative AWE measurement should be considered (91). Finally, there is a heterogeneity concerning the definition of unstable IA qualified as growth, morphology changes, symptomatic and/or rupture (97). The different inflammation imaging methods have been summarized in **Table 2**.

Imaging in Animal Model of IAs

Understanding of IA pathophysiology has been largely enabled by the use of small animal models (rat, mouse, rabbit) in which induced IA can mimic aspects of the human pathology. As such, induced IA are smaller than those found in humans thus, the above-mentioned imaging techniques are not widely used to analyze IA's dynamic and static characteristics (98). In fact, only a few studies use them other than as IA detection tools, for instance to detect macrophage infiltration or to perform CFD analysis on 3DRA images (77, 99). To the best of our knowledge, only 2 studies managed to follow aneurysmal remodeling in mice over 3 months using really high-field MRI (9,4T) (100, 101). Regarding IA's hemodynamics, Doppler ultrasound imaging can be used to measure blood flow velocity in rabbit models of internal carotid aneurysm (99, 102, 103).

CONCLUSION AND PERSPECTIVES

As IA pathophysiology becomes better understood, new factors contributing to IA progression and rupture are discovered, such as altered hemodynamic parameters or inflammation within IA vessel wall. Novel imaging technique must be developed to visualize these important characteristics and provide essential information's to clinicians for a better IA management. One can speculate that the combination of different imaging techniques that rely on morphological, hemodynamic and inflammatory markers will allow clinicians to accurately assess the risk of aneurysm rupture and adopt the best care strategy.

AUTHOR CONTRIBUTIONS

HL and CM did the literature research and wrote the first draft of the review. YB, HL, and CM contributed to the idea of the manuscript. YB provided critical feedback. All authors reviewed the manuscript and approved the submitted version.

FUNDING

This work was funded by a predoctoral fellowship from the Doctoral School Hématologie – Oncogenèse – Biothérapies ED 561 (to CM) and by the European Research Council grant 759880 (to YB).

ACKNOWLEDGMENTS

We would like to thank Dr. David S. Paul for editing this manuscript.

REFERENCES

1. Etminan N, Chang H-S, Hackenberg K, de Rooij NK, Vergouwen MDI, Rinkel GJE, et al. Worldwide incidence of aneurysmal subarachnoid hemorrhage according to region, time period, blood pressure, and smoking prevalence in the population: a systematic review and meta-analysis. *JAMA Neurol.* (2019) 76:588–97. doi: 10.1001/jamaneurol.2019.0006
2. Nieuwkamp DJ, Setz LE, Algra A, Linn FH, de Rooij NK, Rinkel GJ. Changes in case fatality of aneurysmal subarachnoid haemorrhage over time, according to age, sex, and region: a meta-analysis. *Lancet Neurol.* (2009) 8:635–42. doi: 10.1016/S1474-4422(09)70126-7
3. Thompson BG, Brown RD, Amin-Hanjani S, Broderick JP, Cockroft KM, Connolly ES, et al. Guidelines for the management of patients with unruptured intracranial aneurysms: a guideline for healthcare professionals from the American heart association/American stroke association. *Stroke.* (2015) 46:2368–400. doi: 10.1161/STR.0000000000000070
4. Texakalidis P, Sweid A, Mouchtouris N, Peterson EC, Sioka C, Rangel-Castilla L, et al. Aneurysm formation, growth, and rupture: the biology and physics of cerebral aneurysms. *World Neurosurg.* (2019) 130:277–84. doi: 10.1016/j.wneu.2019.07.093
5. Harrington D, Boxt L, Murray P. Digital subtraction angiography: overview of technical principles. *Am J Roentgenol.* (1982) 139:781–6. doi: 10.2214/ajr.139.4.781
6. Turan N, Heider RA, Roy AK, Miller BA, Mullins ME, Barrow DL, et al. Current perspectives in imaging modalities for the assessment of unruptured intracranial aneurysms: a comparative analysis and review. *World Neurosurg.* (2018) 113:280–92. doi: 10.1016/j.wneu.2018.01.054

7. Howard BM, Hu R, Barrow JW, Barrow DL. Comprehensive review of imaging of intracranial aneurysms and angiographically negative subarachnoid hemorrhage. *Neurosurg Focus.* (2019) 47:E20. doi: 10.3171/2019.9.FOCUS19653
8. Wong SC, Nawawi O, Ramli N, Abd Kadir KA. Benefits of 3D rotational DSA compared with 2D DSA in the evaluation of intracranial aneurysm. *Acad Radiol.* (2012) 19:701–7. doi: 10.1016/j.acra.2012.02.012
9. Alakbarzade V, Pereira AC. Cerebral catheter angiography and its complications. *Pract Neurol.* (2018) 18:393–8. doi: 10.1136/practneurol-2018-001986
10. White PM, Wardlaw JM, Easton V. Can noninvasive imaging accurately depict intracranial aneurysms? A systematic review. *Radiology.* (2000) 217:361–70. doi: 10.1148/radiology.217.2.r00nv06361
11. Venema HW, Hulsmans FJ, den Heeten GJ, CT. angiography of the circle of Willis and intracranial internal carotid arteries: maximum intensity projection with matched mask bone elimination-feasibility study. *Radiology.* (2001) 218:893–8. doi: 10.1148/radiology.218.3.r01mr30893
12. Postma AA, Hofman PAM, Stadler AAR, van Oostenbrugge RJ, Tijssen MPM, Wildberger JE. Dual-energy CT of the brain and intracranial vessels. *Am J Roentgenol.* (2012) 199:S26–33. doi: 10.2214/AJR.12.9115
13. Zhang L-J, Wu S-Y, Niu J-B, Zhang Z-L, Wang HZ, Zhao Y-E, et al. Dual-Energy CT angiography in the evaluation of intracranial aneurysms: image quality, radiation dose, and comparison with 3D rotational digital subtraction angiography. *Am J Roentgenol.* (2010) 194:23–30. doi: 10.2214/AJR.08.2290
14. Edelman RR, Koktzoglou I. Non-contrast MR angiography: an update. *J Magn Reson Imaging.* (2019) 49:355–73. doi: 10.1002/jmri.26288
15. Gibbs GF, Huston J, Bernstein MA, Riederer SJ. Brown RD. Improved image quality of intracranial aneurysms: 30-T versus 15-T time-of-flight MR angiography. *AJNR Am J Neuroradiol.* (2004) 25:84–7.
16. Kwak Y, Son W, Kim Y-S, Park J, Kang D-H. Discrepancy between MRA and DSA in identifying the shape of small intracranial aneurysms. *J Neurosurg.* (2020) 134:1887–93. doi: 10.3171/2020.4.JNS20128
17. Yanamadala V, Sheth SA, Walcott BP, Buchbinder BR, Buckley D, Ogilvy CS. Non-contrast 3D time-of-flight magnetic resonance angiography for visualization of intracranial aneurysms in patients with absolute contraindications to CT or MRI contrast. *J Clin Neurosci.* (2013) 20:1122–6. doi: 10.1016/j.jocn.2012.12.005
18. Cirillo M, Scomazzoni F, Cirillo L, Cadioli M, Simionato F, Iadanza A, et al. Comparison of 3D TOF-MRA and 3D CE-MRA at 3T for imaging of intracranial aneurysms. *Eur J Radiol.* (2013) 82:e853–9. doi: 10.1016/j.ejrad.2013.08.052
19. Levent A, Yuce I, Eren S, Ozyigit O, Kantarci M. Contrast-enhanced and time-of-flight MR angiographic assessment of endovascular coiled intracranial aneurysms at 1.5 T. *Interv Neuroradiol.* (2014) 20:686–92. doi: 10.15274/INR-2014-10064
20. Nael K, Villablanca JP, Saleh R, Pope W, Nael A, Laub G, et al. Contrast-enhanced MR angiography at 3T in the evaluation of intracranial aneurysms: a comparison with time-of-flight MR angiography. *AJNR Am J Neuroradiol.* (2006) 27:2118–21. doi: 10.1097/01.rli.0000242835.00032.f5
21. Wrede KH, Dammann P, Mönninghoff C, Johst S, Maderwald S, Sandalcioglu IE. et al. Non-enhanced MR imaging of cerebral aneurysms: 7 tesla versus 15 tesla. *PLoS ONE.* (2014) 9:e84562. doi: 10.1371/journal.pone.0084562
22. Wrede KH, Matsushige T, Goericke SL, Chen B, Umutlu L, Quick HH, et al. Non-enhanced magnetic resonance imaging of unruptured intracranial aneurysms at 7 tesla: comparison with digital subtraction angiography. *Eur Radiol.* (2017) 27:354–64. doi: 10.1007/s00330-016-4323-5
23. Stamm AC, Wright CL, Knopp MV, Schmalbrock P. Heverhagen JT. Phase contrast and time-of-flight magnetic resonance angiography of the intracerebral arteries at 15, 3 and 7 T. *Magn Reson Imaging.* (2013) 31:545–9. doi: 10.1016/j.mri.2012.10.023
24. Songsaeng D, Sakarunchai I, Mongkolnaowarat S, Harmontree S, Pornpunyawut P, Suwanbundit A, et al. Detection and measurement of intracranial aneurysm compared between magnetic resonance intracranial black blood vessel imaging and gold standard cerebral digital subtraction angiography. *J Neurosci Rural Pract.* (2020) 11:545–51. doi: 10.1055/s-0040-1714042
25. Anxionnat R, Bracard S, Ducrocq X, Trousset Y, Launay L, Kerrien E, et al. Intracranial aneurysms: clinical value of 3D digital subtraction angiography in the therapeutic decision and endovascular treatment. *Radiology.* (2001) 218:799–808. doi: 10.1148/radiology.218.3.r01mr09799
26. Foley WD, Karcaaltincaba M. Computed tomography angiography: principles and clinical applications. *J Comput Assist Tomogr.* (2003) 27:S23–30. doi: 10.1097/00004728-200305001-00006
27. Lell MM, Anders K, Uder M, Klotz E, Ditt H, Vega-Higuera F, et al. New techniques in CT angiography. *RadioGraphics.* (2006) 26:S45–62. doi: 10.1148/rg.26si065508
28. Fleischmann D, Chin AS, Molvin L, Wang J, Hallett R. Computed tomography angiography. *Radiol Clin North Am.* (2016) 54:1–12. doi: 10.1016/j.rcl.2015.09.002
29. Saloner D. The AAPM/RSNA physics tutorial for residents. An introduction to MR angiography. *RadioGraphics.* (1995) 15:453–65. doi: 10.1148/radiographics.15.2.7761648
30. Maki JH, Chenevert TL, Prince MR. Contrast-enhanced MR angiography. *Abdom Imaging.* (1998) 23:469–84. doi: 10.1007/s002619900384
31. Hoffmann T, Glaßer S, Boese A, Brandstädter K, Kalinski T, Beuing O, et al. Experimental investigation of intravascular OCT for imaging of intracranial aneurysms. *Int J CARS.* (2016) 11:231–41. doi: 10.1007/s11548-015-1275-1
32. Popescu DP, Choo-Smith L-P, Flueraru C, Mao Y, Chang S, Disano J, et al. Optical coherence tomography: fundamental principles, instrumental designs and biomedical applications. *Biophys Rev.* (2011) 3:155. doi: 10.1007/s12551-011-0054-7
33. Fujimoto JG, Pitris C, Boppart SA, Brezinski ME. Optical coherence tomography: an emerging technology for biomedical imaging and optical biopsy. *Neoplasia.* (2000) 2:9–25. doi: 10.1038/sj.neo.7900071
34. Liu Y, Zheng Y, An Q, Song Y, Leng B. Optical coherence tomography for intracranial aneurysms: a new method for assessing the aneurysm structure. *World Neurosurg.* (2019) 123:e194–201. doi: 10.1016/j.wneu.2018.11.123
35. King RM, Marosfoi M, Caroff J, Ughi GJ, Groth DM, Gounis MJ, et al. High frequency optical coherence tomography assessment of homogenous neck coverage by intrasaccular devices predicts successful aneurysm occlusion. *J Neurointerv Surg.* (2019) 11:1150–4. doi: 10.1136/neurintsurg-2019-014843
36. Vardar Z, King RM, Kraitem A, Langan ET, Peterson LM, Duncan BH, et al. High-resolution image-guided WEB aneurysm embolization by high-frequency optical coherence tomography. *J Neurointerv Surg.* (2021) 13:669–73. doi: 10.1136/neurintsurg-2020-016447
37. Xiang J, Natarajan SK, Tremmel M, Ma D, Mocco J, Hopkins LN, et al. Hemodynamic-morphologic discriminants for intracranial aneurysm rupture. *Stroke.* (2011) 42:144–52. doi: 10.1161/STROKEAHA.110.592923
38. Cebral J, Ollikainen E, Chung BJ, Mut F, Sippola V, Jahromi BR, et al. Flow conditions in the intracranial aneurysm lumen are associated with inflammation and degenerative changes of the aneurysm wall. *AJNR Am J Neuroradiol.* (2017) 38:119–26. doi: 10.3174/ajnr.A4951
39. Soldozy S, Norat P, Elsarrag M, Chatrath A, Costello JS, Sokolowski JD, et al. The biophysical role of hemodynamics in the pathogenesis of cerebral aneurysm formation and rupture. *Neurosurg Focus.* (2019) 47:E11. doi: 10.3171/2019.4.FOCUS19232
40. Sheikh MAA, Shuib AS, Mohyi MHH. A review of hemodynamic parameters in cerebral aneurysm. *Interdiscipl Neurosurg.* (2020) 22:100716. doi: 10.1016/j.inat.2020.100716
41. Sforza DM, Putman CM, Cebral JR. Hemodynamics of cerebral aneurysms. *Annu Rev Fluid Mech.* (2009) 41:91–107. doi: 10.1146/annurev.fluid.40.111406.102126
42. Jiang P, Liu Q, Wu J, Chen X, Li M, Li Z, et al. A novel scoring system for rupture risk stratification of intracranial aneurysms: a hemodynamic and morphological study. *Front Neurosci.* (2018) 12:596. doi: 10.3389/fnins.2018.00596
43. Byrne G, Mut F, Cebral J. Quantifying the large-scale hemodynamics of intracranial aneurysms. *AJNR Am J Neuroradiol.* (2014) 35:333–8. doi: 10.3174/ajnr.A3678
44. Murayama Y, Fujimura S, Suzuki T, Takao H. Computational fluid dynamics as a risk assessment tool for aneurysm rupture. *Neurosurg Focus.* (2019) 47:E12. doi: 10.3171/2019.4.FOCUS19189

45. Wu T, Zhu Q. Advancement in the haemodynamic study of intracranial aneurysms by computational fluid dynamics. *Brain Hemorrhages.* (2021) 2:71–5. doi: 10.1016/j.hest.2020.12.002
46. Berg P, Saalfeld S, Voß S, Beuing O, Janiga G. A review on the reliability of hemodynamic modeling in intracranial aneurysms: why computational fluid dynamics alone cannot solve the equation. *Neurosurg Focus.* (2019) 47:E15. doi: 10.3171/2019.4.FOCUS19181
47. Ren Y, Chen G-Z, Liu Z, Cai Y, Lu G-M, Li Z-Y. Reproducibility of image-based computational models of intracranial aneurysm: a comparison between 3D rotational angiography, CT angiography and MR angiography. *Biomed Eng Online.* (2016) 15:50. doi: 10.1186/s12938-016-0163-4
48. Saqr KM, Rashad S, Tupin S, Niizuma K, Hassan T, Tominaga T, et al. What does computational fluid dynamics tell us about intracranial aneurysms? A meta-analysis and critical review. *J Cereb Blood Flow Metab.* (2020) 40:1021–39. doi: 10.1177/0271678X19854640
49. Castillo M. Digital subtraction angiography (DSA): basic principles. In: Ramalho JN, Castillo M (eds), *Vascular Imaging of the Central Nervous System*. Oxford, UK: John Wiley & Sons, Ltd., (2013). p. 207–220. doi: 10.1002/9781118434550.ch14
50. Ruedinger KL, Schafer S, Speidel MA, Strother CM. 4D-DSA: development and current neurovascular applications. *AJNR Am J Neuroradiol.* (2021) 42:214–20. doi: 10.3174/ajnr.A6860
51. Davis B, Royalty K, Kowarschik M, Rohkohl C, Oberstar E, Aagaard-Kienitz B, et al. 4D digital subtraction angiography: implementation and demonstration of feasibility. *Am J Neuroradiol.* (2013) 34:1914–21. doi: 10.3174/ajnr.A3529
52. Vanrossomme AE, Eker OF, Thiran J-P, Courbebaisse GP, Zouaoui Boudjeltia K. Intracranial aneurysms: wall motion analysis for prediction of rupture. *AJNR Am J Neuroradiol.* (2015) 36:1796–802. doi: 10.3174/ajnr.A4310
53. Kato N, Yuki I, Hataoka S, Dahmani C, Otani K, Abe Y, et al. 4D digital subtraction angiography for the temporal flow visualization of intracranial aneurysms and vascular malformations. *J Stroke Cerebrov Dis.* (2020) 29:105327. doi: 10.1016/j.jstrokecerebrovasdis.2020.105327
54. Lang S, Hoelter P, Birkhold AI, Schmidt M, Endres J, Strother C, et al. Quantitative and qualitative comparison of 4D-DSA with 3D-DSA using computational fluid dynamics simulations in cerebral aneurysms. *AJNR Am J Neuroradiol.* (2019) 40:1505–10. doi: 10.3174/ajnr.A6172
55. Markl M, Frydrychowicz A, Kozerke S, Hope M, Wieben O. 4D flow MRI. *J Magn Reson Imaging.* (2012) 36:1015–36. doi: 10.1002/jmri.23632
56. Castle-Kirszbaum M, Maingard J, Lim RP, Barras CD, Kok HK, Chandra RV, et al. Four-dimensional magnetic resonance imaging assessment of intracranial aneurysms: a state-of-the-art review. *Neurosurgery.* (2020) 87:453–65. doi: 10.1093/neuros/nyaa021
57. Turski P, Scarano A, Hartman E, Clark Z, Schubert T, Rivera L, et al. Neurovascular 4DFlow MRI (Phase Contrast MRA): emerging clinical applications. *Neurovasc Imaging.* (2016) 2:8. doi: 10.1186/s40809-016-0019-0
58. Youn SW, Lee J. From 2D to 4D phase-contrast MRI in the neurovascular system: will it be a quantum jump or a fancy decoration? *J Magn Reson Imaging.* (2020) 55:347–72. doi: 10.1002/jmri.27430
59. Szajer J, Ho-Shon K. A comparison of 4D flow MRI-derived wall shear stress with computational fluid dynamics methods for intracranial aneurysms and carotid bifurcations - a review. *Magn Reson Imaging.* (2018) 48:62–9. doi: 10.1016/j.mri.2017.12.005
60. Gottwald LM, Töger J, Bloch KM, Peper ES, Coolen BF, Strijkers GJ, et al. High spatiotemporal resolution 4D flow MRI of intracranial aneurysms at 7T in 10 minutes. *Am J Neuroradiol.* (2020) 41:1201–8. doi: 10.3174/ajnr.A6603
61. Medero R, Ruedinger K, Rutkowski D, Johnson K, Roldán-Alzate A. In vitro assessment of flow variability in an intracranial aneurysm model using 4D flow MRI and tomographic PIV. *Ann Biomed Eng.* (2020) 48:2484–93. doi: 10.1007/s10439-020-02543-8
62. Ruedinger KL, Medero R, Roldán-Alzate A. Fabrication of low-cost patient-specific vascular models for particle image velocimetry. *Cardiovasc Eng Technol.* (2019) 10:500–7. doi: 10.1007/s13239-019-00417-2
63. Medero R, Hoffman C, Roldán-Alzate A. Comparison of 4D flow MRI and particle image velocimetry using an *in vitro* carotid bifurcation model. *Ann Biomed Eng.* (2018) 46:2112–22. doi: 10.1007/s10439-018-02109-9
64. Kortman HGJ, Smit EJ, Oei MTH, Manniesing R, Prokop M, Meijer FJA. 4D-CTA in neurovascular disease: a review. *AJNR Am J Neuroradiol.* (2015) 36:1026–33. doi: 10.3174/ajnr.A4162
65. Cancelliere NM, Najafi M, Brina O, Bouillot P, Vargas MI, Lovblad K-O, et al. 4D-CT angiography versus 3D-rotational angiography as the imaging modality for computational fluid dynamics of cerebral aneurysms. *J Neurointerv Surg.* (2020) 12:626–30. doi: 10.1136/neurintsurg-2019-015389
66. Stam LB, Aquarius R, de Jong GA, Slump CH, Meijer FJA, Boogaarts HD, et al. review on imaging techniques and quantitative measurements for dynamic imaging of cerebral aneurysm pulsations. *Sci Rep.* (2021) 11:2175. doi: 10.1038/s41598-021-81753-z
67. Kleinloog R, Zwanenburg JJM, Schermers B, Krikken E, Ruigrok YM, Luijten PR, et al. Quantification of intracranial aneurysm volume pulsation with 7T MRI. *AJNR Am J Neuroradiol.* (2018) 39:713–9. doi: 10.3174/ajnr.A5546
68. Gu Y, Zhang Y, Luo M, Zhang H, Liu X, Miao C. Risk factors for asymptomatic intracranial small aneurysm rupture determined by electrocardiographic-gated 4D computed tomographic (CT) angiography. *Med Sci Monit.* (2020) 26:e921835-1–e921835-8. doi: 10.12659/MSM.921835
69. Hasan DM, Mahaney KB, Magnotta VA, Kung DK, Lawton MT, Hashimoto T, et al. Macrophage imaging within human cerebral aneurysms wall using ferumoxytol-enhanced MRI: a pilot study. *ATVB.* (2012) 32:1032–8. doi: 10.1161/ATVBAHA.111.239871
70. Shimizu K, Kushamae M, Aoki T. Macrophage imaging of intracranial aneurysms. *Neurol Med Chir(Tokyo).* (2019) 59:257–63. doi: 10.2176/nmc.st.2019-0034
71. Leao DJ, Agarwal A, Mohan S, Bathla G. Intracranial vessel wall imaging: applications, interpretation, and pitfalls. *Clin Radiol.* (2020) 75:730–9. doi: 10.1016/j.crad.2020.02.006
72. Mandell DM, Mossa-Basha M, Qiao Y, Hess CP, Hui F, Matouk C, et al. Intracranial vessel wall MRI: principles and expert consensus recommendations of the American society of neuroradiology. *AJNR Am J Neuroradiol.* (2017) 38:218–29. doi: 10.3174/ajnr.A4893
73. Chalouhi N, Ali MS, Jabbour PM, Tjoumakaris SI, Gonzalez LF, Rosenwasser RH, et al. Biology of intracranial aneurysms: role of inflammation. *J Cereb Blood Flow Metab.* (2012) 32:1659–76. doi: 10.1038/jcbfm.2012.84
74. Tulamo R, Frösen J, Junnikkala S, Paetau A, Pitkäniemi J, Kangasniemi M, et al. Complement activation associates with saccular cerebral artery aneurysm wall degeneration and rupture. *Neurosurgery.* (2006) 59:1069–76. doi: 10.1227/01.NEU.0000245598.84698.26
75. Frösen J, Piippo A, Paetau A, Kangasniemi M, Niemelä M, Hernesniemi J, et al. Remodeling of saccular cerebral artery aneurysm wall is associated with rupture: histological analysis of 24 unruptured and 42 ruptured cases. *Stroke.* (2004) 35:2287–93. doi: 10.1161/01.STR.0000140636.30204.da
76. Hasan D, Chalouhi N, Jabbour P, Dumont AS, Kung DK, Magnotta VA, et al. Early change in ferumoxytol-enhanced magnetic resonance imaging signal suggests unstable human cerebral aneurysm: a pilot study. *Stroke.* (2012) 43:3258–65. doi: 10.1161/STROKEAHA.112.673400
77. Aoki T, Saito M, Koseki H, Tsuji K, Tsuji A, Murata K, et al. Macrophage imaging of cerebral aneurysms with ferumoxytol: an exploratory study in an animal model and in patients. *J Stroke Cerebrovasc Dis.* (2017) 26:2055–64. doi: 10.1016/j.jstrokecerebrovasdis.2016.10.026
78. Matsushige T, Shimonaga K, Mizoue T, Hosogai M, Hashimoto Y, Takahashi H, et al. Lessons from vessel wall imaging of intracranial aneurysms: new era of aneurysm evaluation beyond morphology. *Neurol Med Chir.* (2019) 59:407–14. doi: 10.2176/nmc.ra.2019-0103
79. Matsushige T, Shimonaga K, Mizoue T, Hosogai M, Hashimoto Y, Kaneko M, et al. Focal aneurysm wall enhancement on magnetic resonance imaging indicates intraluminal thrombus and the rupture point. *World Neurosurg.* (2019) 127:e578–84. doi: 10.1016/j.wneu.2019.03.209
80. Larsen N, Flüh C, Saalfeld S, Voß S, Hille G, Trick D, et al. Multimodal validation of focal enhancement in intracranial aneurysms as a surrogate marker for aneurysm instability. *Neuroradiology.* (2020) 62:1627–35. doi: 10.1007/s00234-020-02498-6
81. Zhong W, Su W, Li T, Tan X, Chen C, Wang Q, et al. Aneurysm wall enhancement in unruptured intracranial aneurysms: a histopathological evaluation. *J Am Heart Assoc.* (2021) 10:e018633. doi: 10.1161/JAHA.120.018633

82. Shimonaga K, Matsushige T, Ishii D, Sakamoto S, Hosogai M, Kawasumi T, et al. Clinicopathological insights from vessel wall imaging of unruptured intracranial aneurysms. *Stroke.* (2018) 49:2516–9. doi: 10.1161/STROKEAHA.118.021819
83. Wang X, Zhu C, Leng Y, Degnan AJ, Lu J. Intracranial aneurysm wall enhancement associated with aneurysm rupture: a systematic review and meta-analysis. *Acad Radiol.* (2019) 26:664–73. doi: 10.1016/j.acra.2018.05.005
84. Matouk CC, Mandell DM, Günel M, Bulsara KR, Malhotra A, Hebert R, et al. Vessel wall magnetic resonance imaging identifies the site of rupture in patients with multiple intracranial aneurysms: proof of principle. *Neurosurgery.* (2013) 72:492–6. doi: 10.1227/NEU.0b013e31827d1012
85. Kondo R, Yamaki T, Mouri W, Sato S, Saito S, Nagahata M, et al. Magnetic resonance vessel wall imaging reveals rupture site in subarachnoid hemorrhage with multiple cerebral aneurysms. *No Shinkei Geka.* (2014) 42:1147–50.
86. Hu P, Yang Q, Wang D-D, Guan S-C, Zhang H-Q. Wall enhancement on high-resolution magnetic resonance imaging may predict an unsteady state of an intracranial saccular aneurysm. *Neuroradiology.* (2016) 58:979–85. doi: 10.1007/s00234-016-1729-3
87. Liu P, Qi H, Liu A, Lv X, Jiang Y, Zhao X, et al. Relationship between aneurysm wall enhancement and conventional risk factors in patients with unruptured intracranial aneurysms: a black-blood MRI study. *Interv Neuroradiol.* (2016) 22:501–5. doi: 10.1177/1591019916653252
88. Lv N, Karmonik C, Chen S, Wang X, Fang Y, Huang Q, et al. Wall enhancement, hemodynamics, and morphology in unruptured intracranial aneurysms with high rupture risk. *Transl Stroke Res.* (2020) 11:882–9. doi: 10.1007/s12975-020-00782-4
89. Lv N, Karmonik C, Chen S, Wang X, Fang Y, Huang Q, et al. Relationship between aneurysm wall enhancement in vessel wall magnetic resonance imaging and rupture risk of unruptured intracranial aneurysms. *Neurosurgery.* (2019) 84:E385–91. doi: 10.1093/neuros/nyy310
90. Wang G-X, Li W, Lei S, Ge X-D, Yin J-B, Zhang D. Relationships between aneurysmal wall enhancement and conventional risk factors in patients with intracranial aneurysm: a high-resolution MRI study. *J Neuroradiol.* (2019) 46:25–8. doi: 10.1016/j.neurad.2018.09.007
91. Zhang Y, Fu Q, Wang Y, Cheng J, Ren C, Guan S, et al. Qualitative and quantitative wall enhancement analyses in unruptured aneurysms are associated with an increased risk of aneurysm instability. *Front Neurosci.* (2020) 14:580205. doi: 10.3389/fnins.2020.580205
92. Bae H, Suh S-I, Yoon WK, Roh H, Kim C, Kwon T-H. Correlation of aneurysmal wall enhancement of unruptured intracranial aneurysms on high-resolution vessel-wall imaging with clinical indices and surgical findings. *Neurosurgery.* (2021) 89:420–7. doi: 10.1093/neuros/nyab178
93. Texakalidis P, Hilditch CA, Lehman V, Lanzino G, Pereira VM, Brinjikji W. Vessel wall imaging of intracranial aneurysms: systematic review and meta-analysis. *World Neurosurg.* (2018) 117:453–8.e1. doi: 10.1016/j.wneu.2018.06.008
94. Vergouwen MDI, Backes D, van der Schaaf IC, Hendrikse J, Kleinloog R, Algra A, et al. Gadolinium enhancement of the aneurysm wall in unruptured intracranial aneurysms is associated with an increased risk of aneurysm instability: a follow-up study. *AJNR Am J Neuroradiol.* (2019) 40:1112–6. doi: 10.3174/ajnr.A6105
95. Molenberg R, Aalbers MW, Appelman APA, Uyttenboogaart M, Dijk JMC. Intracranial aneurysm wall enhancement as an indicator of instability: a systematic review and meta-analysis. *Eur J Neurol.* (2021) 28:3837–48. doi: 10.1111/ene.15046
96. Kalsoum E, Chabernaud Negrier A, Tuilier T, Benaïssa A, Blanc R, Gallas S, et al. Blood flow mimicking aneurysmal wall enhancement: a diagnostic pitfall of vessel wall MRI using the postcontrast 3D turbo spin-echo MR imaging sequence. *AJNR Am J Neuroradiol.* (2018) 39:1065–7. doi: 10.3174/ajnr.A5616
97. Samaniego EA, Roa JA, Hasan D. Vessel wall imaging in intracranial aneurysms. *J NeuroIntervent Surg.* (2019) 11:1105–12. doi: 10.1136/neurintsurg-2019-014938
98. Tutino VM, Rajabzadeh-Oghaz H, Veeturi SS, Poppenberg KE, Waqas M, Mandelbaum M, et al. Endogenous animal models of intracranial aneurysm development: a review. *Neurosurg Rev.* (2021) 44:2545–70. doi: 10.1007/s10143-021-01481-w
99. Zeng Z, Kallmes DF, Durka MJ, Ding Y, Lewis D, Kadirvel R, et al. Hemodynamics and anatomy of elastase-induced rabbit aneurysm models: similarity to human cerebral aneurysms? *Am J Neuroradiol.* (2011) 32:595–601. doi: 10.3174/ajnr.A2324
100. Tutino VM, Rajabzadeh-Oghaz H, Chandra AR, Gutierrez LC, Schweser F, Preda M. et al. 94T magnetic resonance imaging of the mouse circle of willis enables serial characterization of flow-induced vascular remodeling by computational fluid dynamics. *Curr Neurovasc Res.* (2018) 15:312–25. doi: 10.2174/1567202616666181127165943
101. Rajabzadeh-Oghaz H, Chandra AR, Gutierrez LC, Schweser F, Ionita C, Siddiqui A, et al. High-resolution MRI of the mouse cerebral vasculature to study hemodynamic-induced vascular remodeling. *Proc SPIE.* (2019) 10953:1–8. doi: 10.1117/12.2511772
102. Lyu Y, Luo J, Zhang Y, Wang C, Li A, Zhou Y, et al. An effective and simple way to establish elastase-induced middle carotid artery fusiform aneurysms in rabbits. *Biomed Res Int.* (2020) 2020:6707012. doi: 10.1155/2020/6707012
103. Kainth D, Salazar P, Safinia C, Chow R, Bachour O, Andalib S, et al. A modified method for creating elastase-induced aneurysms by ligation of common carotid arteries in rabbits and its effect on surrounding arteries. *J Vasc Interv Neurol.* (2017) 9:26–35.

Conflict of Interest: The authors declare that the research was conducted in the absence of any commercial or financial relationships that could be construed as a potential conflict of interest.

Publisher's Note: All claims expressed in this article are solely those of the authors and do not necessarily represent those of their affiliated organizations, or those of the publisher, the editors and the reviewers. Any product that may be evaluated in this article, or claim that may be made by its manufacturer, is not guaranteed or endorsed by the publisher.

Copyright © 2022 Maupu, Lebas and Boulaftali. This is an open-access article distributed under the terms of the Creative Commons Attribution License (CC BY). The use, distribution or reproduction in other forums is permitted, provided the original author(s) and the copyright owner(s) are credited and that the original publication in this journal is cited, in accordance with accepted academic practice. No use, distribution or reproduction is permitted which does not comply with these terms.

frontiers in Cardiovascular Medicine

ORIGINAL RESEARCH
published: 11 March 2022
doi: 10.3389/fcvm.2022.819274

Interaction Analysis of Abnormal Lipid Indices and Hypertension for Ischemic Stroke: A 10-Year Prospective Cohort Study

Lai Wei[1†], Junxiang Sun[2†], Hankun Xie[1†], Qian Zhuang[2], Pengfei Wei[2], Xianghai Zhao[2], Yanchun Chen[2], Jiayi Dong[1], Mengxia Li[1], Changying Chen[1], Song Yang[2] and Chong Shen[1*]*

[1] Department of Epidemiology, School of Public Health, Nanjing Medical University, Nanjing, China, [2] Department of Cardiology, Affiliated Yixing People's Hospital of Jiangsu University, People's Hospital of Yixing City, Yixing, China

OPEN ACCESS

Edited by:
Anne-Clémence Vion,
INSERM U1087 L'unité de recherche de l'institut du thorax, France

Reviewed by:
Chongke Zhong,
Soochow University, China
Jianjun Mu,
First Affiliated Hospital of Xi'an Jiaotong University, China

***Correspondence:**
Chong Shen
sc@njmu.edu.cn
Song Yang
staff052@yxph.com

[†] These authors have contributed equally to this work

Specialty section:
This article was submitted to Atherosclerosis and Vascular Medicine, a section of the journal Frontiers in Cardiovascular Medicine

Received: 21 November 2021
Accepted: 18 February 2022
Published: 11 March 2022

Citation:
Wei L, Sun J, Xie H, Zhuang Q, Wei P, Zhao X, Chen Y, Dong J, Li M, Chen C, Yang S and Shen C (2022) Interaction Analysis of Abnormal Lipid Indices and Hypertension for Ischemic Stroke: A 10-Year Prospective Cohort Study. Front. Cardiovasc. Med. 9:819274. doi: 10.3389/fcvm.2022.819274

Background: Dyslipidemia and hypertension are two important independent risk factors for ischemic stroke (IS); however, their combined effect on IS remains uncertain.

Objectives: This present study aimed to evaluate the interaction effect of hypertension and abnormal lipid indices on IS in a 10-year prospective cohort in Chinese adults.

Methods: The cohort study of 4,128 participants was conducted in May 2009 and was followed up to July 2020. All qualified participants received a questionnaire survey, physical examination, and blood sample detection. Cox regression was used to evaluate the association of dyslipidemia and hypertension with IS, and calculate the hazard ratio (HR) and 95% confidence interval (CI). The relative excess risk of interaction (RERI) and the HR (95%CI) of interaction terms were used to examine additive and multiplicative interactions.

Results: In the hypertensive population, Non-HDL-C ≥190 mg/dl, LDL-C/HDL-C ≥2 and HDL-C ≥60 mg/dl were statistically associated with IS, and after adjusting for covariates, HRs (95%CIs) were 1.565 (1.007–2.429), 1.414 (1.034–1.933) and 0.665 (0.450–0.983), respectively. While in the non-hypertension population, no significant association of Non-HDL-C ≥190 mg/dl, LDL-C/HDL-C ≥2, and HDL-C ≥60 was detected with IS ($P > 0.05$). There was a significant association between TC/HDL-C ≥ 3.6 and the decreased risk of IS in the non-hypertension population, and the HR (95%CI) was 0.479 (0.307–0.750). Whereas, a similar association was not observed in the hypertensive population. HDL-C ≥ 60 mg/dl, Non-HDL-C ≥ 190 mg/dl, TC/HDL-C ≥ 3.6, and TG/HDL-C ≥ 1 have additive and multiplicative interactions with hypertension ($P < 0.05$). The RERIs (95% CIs) of the additive interaction are −0.93 (−1.882–0.044), 1.394 (0.38–2.407), 0.752 (0.354–1.151) and 0.575 (0.086–1.065), respectively. The HRs (95% CIs) of the multiplicative interaction terms were 0.498 (0.272–0.911), 4.218 (1.230–14.464), 2.423 (1.437–4.086) and 1.701 (1.016–2.848), respectively.

Conclusion: High concentration of HDL-C reduces the impact of hypertension on IS, while the high concentration of Non-HDL-C, TC/HDL-C, and TG/HDL-C positively interact with hypertension affecting the incidence of IS. This study provides useful evidence for the combined effects of dyslipidemia and hypertension in predicting IS.

Keywords: lipids, hypertension, ischemic stroke, interaction, cohort study, dyslipidemia

INTRODUCTION

Stroke is a major public health issue worldwide, with a high incidence rate, recurrence rate, disability rate, and mortality rate in the population (1). The global lifetime stroke risk from 25 years onward was estimated to be 24.9%, with China having the highest risk of stroke (39.3%), in 2016 (2). In China, stroke has also caused the highest number of disability-adjusted life years of all diseases and has been ranked third among the leading causes of death after malignant tumors and heart disease (3, 4). Moreover, due to changes in lifestyle and population structure and insufficient control over major risk factors, the burden it has brought to public health will be worsened in the future (5). Ischemic stroke (IS), the main subtype of stroke, accounts for almost 78% of stroke cases in China and takes up most of the health burden that stroke caused (6). IS usually occurs suddenly with acute signs and symptoms, which calls for emergency treatment. If emergency care is not provided timely, it will cause severe damage to blood vessels and nerves in the brain, resulting in irreversible complications, lifelong disabilities, or even death. However, the existing treatment for IS requires a strict time window, and the effect of its treatments is not satisfactory. The function damage to the brain will basically not recover fully after the stroke. Consequent side effects and a high risk of recurrence will continuously impact the prognosis and survivors' quality of life. Thus, it is key to focus on the management of risk factors to prevent IS.

IS is a multi-factorial disorder (7) of which prevention may require an improved understanding of modifiable risk factors. Several risk factors increase the IS incidence, such as hypertension, diabetes mellitus, hyperlipidemia, obesity, smoking, drinking, physical inactivity, and a family history of stroke (8, 9). Although each risk factor may contribute significantly to the development of IS, its occurrence is the result of a combination of multiple risk factors (10). According to GBD, over 90% of the global stroke burden is caused by the combined impact of modifiable risk factors (11).

Numerous studies have demonstrated that hypertension and dyslipidemia are two important independent risk factors that can be controlled and modified to prevent IS (12–15). Dyslipidemia is generally believed to play a critical role in the pathogenesis of IS, which can be represented by abnormal changes of traditional and non-traditional lipid indices. Traditional lipid indices, usually referring to total cholesterol (TC), triglycerides (TGs), low-density lipoprotein cholesterol (LDL-C), and high-density lipoprotein cholesterol (HDL-C), were identified to have predictive effects on the risk of cardiovascular disease and stroke (16–18). While compared with the traditional lipid indices, non-traditional lipid indices (non-HDL-C, TG/HDL-C, TC/HDL-C, and LDL-C/HDL-C) could serve as a more powerful predictor for vascular risk in stroke and CVD (19). Hypertension has a high co-occurrence rate with dyslipidemia, especially in the middle-aged and elderly population (20). A large cohort study in a French population showed a significantly higher risk of CVD in people under 55 years of age who suffered from comorbid hypertension and dyslipidemia (21). Therefore, exploring the possible interaction effect between hypertension and dyslipidemia on IS is of great significance for preventing and treating IS. However, few studies have examined the interaction of these two risk factors regarding IS. This present study aimed to evaluate the interaction effect of hypertension and abnormal lipid indices on IS in a 10-year prospective cohort in Chinese adults.

METHODS

Study Design and Ethics Approval

This study adopted a prospective cohort design and a total of 4,128 individuals over 18 years old were recruited by a cluster sampling approach from 6 villages for baseline investigation in Guanlin Town and Xushe Town, Yixing City, Jiangsu Province from May to October 2009. The first field follow-up survey proceeded from May to October in 2014. After excluding 30 baseline stroke patients, the remaining 4,098 patients were followed up to July 27th, 2020 for stroke onset. For more information of this cohort, please refer to our previous published literature (22).

The Ethics Committee approved this study of Nanjing Medical University (#200803307). All participants or their caregivers provided signed informed consent before being included in this study.

Data Collection and Related Covariates Definition

Population baseline investigation included questionnaire survey, physical examination, blood sample collection, etc. All the personnel involved in on-site investigations have received standardized training, and only after passing the assessment could they start their investigation.

Participants' demographic characteristics, smoking status, drinking status, and disease history were obtained from a validated questionnaire at the time of enrollment. Height, weight, and blood pressure were measured by standardized instruments, which were performed in duplicates to reduce random errors. Smoking was defined as cigarettes consumption greater than $\geq$ cigarettes per week, lasting at least 3 months a year. Drinking

was defined as alcohol consumption ≥2 times per week, lasting at least 6 months per year. Body mass index (BMI) was obtained by dividing weight (kg) by the square of height (m^2). Hypertension was defined as average systolic blood pressure (SBP) ≥ 140 mmHg or diastolic blood pressure (DBP) ≥ 90 mmHg, or currently receiving antihypertensive medication to lower blood pressure. The blood pressure of all subjects was measured 3 times with an interval of 30 s. If the difference between any two systolic or diastolic blood pressures is more than 8 mmHg, the fourth measurement is performed. Diabetes was defined as fasting plasma glucose (FPG) ≥7.0 mmol/l or a self-reported diabetes history. Received lipid-lowering treatment was defined as patients self-reported taking lipid-lowering medications or other lipid-lowering treatment measures.

All participants underwent 8-h overnight fasting and blood sampling to detect FPG and lipid indices, including total cholesterol (TC), triglycerides (TG), high-density lipoprotein cholesterol (HDL-C), and low-density lipoprotein cholesterol (LDL-C). Non-HDL-C, TC/HDL-C, TG/HDL-C, LDL-C/HDL-C, and remnant-cholesterol (RC) were derived from detected lipids. The non-HDL-C value was calculated as the difference value of TC minus HDL-C. RC was calculated by TC minus LDL-C minus HDL-C. Baseline dyslipidemia was defined by meeting any of the following conditions: (1) TC ≥ 6.2 mmol/l (240 mg/dl), TG ≥ 2.3 mmol/l (200 mg/dl), LDL-C ≥ 4.1 mmol/l (160 mg/dl), HDL-C < 1.04 mmol/l (40 mg/dl) or HDL-C ≥ 1.55 mmol/l (60 mg/dl); (2) Self-reported diagnosis of dyslipidemia; (3) Currently taking lipid-lowering drugs. As per Chinese Guidelines for the Management of Dyslipidemia in Adults (2016), the cut-off points of TC, TG, LDL-C, HDL-C, and non-HDL-C were 240 mg/dl, 200 mg/dl, 160 mg/dl, 40–60 mg/dl, and 190 mg/dl, respectively. While for indices like RC, TC/HDL-C, TG/HDL-C, and LDL-C/HDL-C, there are no definite clinical diagnostic criteria, so the median of these indicators, which were 30 mg/dl, 3.6, 1, and 2, were defined as the cut-off point value in this study.

Outcome Ascertainment

Outcome events of stroke in this cohort were collected through the local register system of disease and death of the Center for Disease Control and Prevention (CDC). International Classification of Diseases, Tenth Revision, Clinical Modification (ICD-10-CM) was used to identify for stroke (I60∼I64), IS (I63), and hemorrhagic stroke (I60, I61, I62, and I64). All the monitored stroke onset events were further inspected by certified neurologists and cardiologists through reviewing the medical records system and relevant files of Yixing People's Hospital.

Statistical Analysis

Mann-Whitney *U* test was used to examine the differences of all the quantitative variables among groups of dyslipidemia presented as median (interquartile range). Chi-square (χ^2) test was performed to compare the frequency distributions of qualitative variables. Cox proportional hazards regression models were used to estimate the HRs and 95% confidence intervals (CIs) of IS after adjustment for age, gender, smoking, drinking, BMI, hypertension, diabetes, and received lipid-lowering treatment. Heterogeneity was tested for inter-subgroup associations using Cochran's Q test. The interaction effect was evaluated using the relative excess risk of interaction (RERI) for additive interactions and the HR (95% CI) of multi-factor interaction terms for multiplicative interactions. All statistical analyses were conducted using SAS software version 9.4 (SAS Institute, Inc, Cary, NC), and test results were considered significant at the two-sided 0.05 level.

RESULTS

Baseline Characteristics of the Cohort Study Population

Descriptive characteristics of the 4,098 participants at baseline are presented in **Table 1**. The participants were followed up for a median duration of 10.76 years, with 272 participants who developed IS. All participants were categorized into four groups according to the presence of dyslipidemia and hypertension at baseline. The proportion of people with only dyslipidemia, hypertension, and co-morbidity were 26.2, 20.8, and 27.6%, respectively. The median age is 59.20 years, with females accounting for 59.5% of the total population. Smokers and drinkers accounted for 24.3 and 21.5%, respectively. The prevalence of dyslipidemia, hypertension, and diabetes in the population was 53.9, 48.4, and 11.2%, respectively, at baseline. Participants with dyslipidemia or hypertension were more likely to have higher levels of BMI and higher proportions of drinkers and diabetes than their counterparts without dyslipidemia and hypertension ($P < 0.05$). The sex ratio and the proportion of smokers were approximately the same among four groups (**Table 1**).

Association of Dyslipidemia and Hypertension With IS

As of July 27th, 2020, the median follow-up time was 10.76 years. There were 272 new IS with a prevalence density of 65.41 per 10,000 person-years during the follow-up period. The incidence density was higher among hypertensive patients, those with dyslipidemia, and both together, at 43.48 per 10,000 person-years, 91.52 per 10,000 person-years, and 92.28 per 10,000 person-years, respectively, compared to those with normal lipids and no hypertension. The corresponding HRs (95%) CIs are 1.603 (1.097–2.343), 1.025 (0.677–1.553) and 1.627 (1.129–2.343), respectively (**Table 2**).

Association Between Blood Lipids and the Risk of IS

Non-HDL-C ≥ 190 mg/dl was associated with an increased risk of IS in the whole population, but the correlation was not statistically significant after adjusting the covariates (**Supplementary Table S1**). The HR (95%CI) before and after adjustment were 1.529 (1.028–2.275) and 1.128 (0.751–1.694), respectively. The remaining lipid indices showed no statistically significant association with IS among the total population (**Supplementary Table S1**).

TABLE 1 | Baseline characteristics of the study population.

Characteristics	All subjects (*N* = 4,098)	Non-dyslipidemia and non-hypertension (*N* = 1,038)	Only dyslipidemia (*N* = 1,075)	Only hypertension (*N* = 853)	Dyslipidemia and hypertension (*N* = 1,132)	Z/χ^2	p^a
Age (years)	59.20 (52.75, 67.00)	56.78 (49.78, 63.81)	57.80 (51.77, 64.78)	61.75 (54.76, 69.77)	61.62 (54.74, 69.39)	144.538	<0.001
Gender (%)						2.541	0.468
Male	1,661 (40.5)	408 (39.3)	444 (41.3)	334 (39.2)	475 (42.0)		
Female	2,437 (59.5)	630 (60.7)	631 (58.7)	519 (60.8)	657 (58.0)		
Smokers (%)	995 (24.3)	258 (24.9)	266 (24.7)	191 (22.4)	280 (24.7)	2.095	0.553
Drinkers (%)	883 (21.5)	212 (20.4)	256 (23.8)	157 (18.4)	258 (22.8)	10.059	0.018
Diabetes (%)	461 (11.2)	80 (7.7)	112 (10.4)	86 (10.1)	183 (16.2)	42.362	<0.001
BMI (kg/m^2)	24.00 (21.93, 26.40)	23.35 (21.51, 25.71)	23.50 (21.47, 26.02)	24.30 (22.33, 26.80)	24.88 (22.37, 27.28)	99.665	<0.001
TC (mg/dl)	185.33 (162.93, 210.42)	178.19 (159.07, 198.46)	189.96 (164.09, 220.85)	177.99 (160.23, 200.77)	197.30 (171.43, 229.34)	231.087	<0.001
TG (mg/dl)	116.81 (79.65, 176.99)	93.81 (69.91, 130.97)	128.32 (76.11, 224.78)	107.96 (79.65, 146.02)	162.39 (95.58, 253.98)	452.728	<0.001
HDL-C (mg/dl)	51.35 (43.63, 59.85)	50.19 (45.95, 54.83)	59.07 (39.00, 66.02)	50.19 (45.95, 54.83)	55.21 (39.77, 65.25)	81.570	<0.001
LDL-C (mg/dl)	102.32 (84.94, 120.08)	99.61 (86.49, 114.29)	100.77 (81.85, 122.78)	102.32 (87.84, 117.18)	105.41 (84.94, 129.34)	36.332	<0.001
Non-HDL-C (mg/dl)	133.59 (111.58, 157.14)	128.57 (108.88, 147.10)	135.52 (111.20, 162.55)	128.57 (109.65, 149.42)	143.24 (115.83, 173.26)	141.155	<0.001
RC (mg/dl)	29.34 (13.90, 43.63)	27.41 (13.42, 38.61)	32.05 (13.51, 49.03)	26.64 (12.74, 38.42)	32.82 (15.44, 51.74)	77.174	<0.001
TC/HDL-C	3.64 (3.06, 4.22)	3.59 (3.13, 4.00)	3.62 (2.90, 4.48)	3.61 (3.14, 4.00)	3.87 (3.06, 4.68)	57.117	<0.001
TG/HDL-C	0.99 (0.63, 1.63)	0.83 (0.60, 1.15)	1.11 (0.54, 2.15)	0.93 (0.68, 1.27)	1.44 (0.67, 2.49)	266.166	<0.001
LDL-C/HDL-C	2.02 (1.64, 2.39)	2.01 (1.69, 2.32)	1.94(1.48, 2.39)	2.05 (1.74, 2.34)	2.07 (1.62, 2.57)	26.279	<0.001
Taking lipid lowering drugs	19 (0.5)	0 (0.0)	3 (0.3)	0 (0.0)	16 (0.5)	31.729	<0.001

All continuous variables are tested for normality (Shapiro-Wilk test and Kolmogorov–Smirnov test), and none of them obey normal distribution. Values are presented as median (interquartile range) or n (%).
BMI, body mass index; TC, total cholesterol; TG, triglycerides; HDL-C, high-density lipoprotein cholesterol; LDL-C, low-density lipoprotein cholesterol; Non-HDL-C, non-high-density lipoprotein cholesterol; RC, remnant cholesterol.
[a]: For each quantitative variable, the P-value is obtained by the Mann-Whitney U test; for each categorical variable, the P-value is obtained through Pearson's χ^2 test.

TABLE 2 | Association of dyslipidemia and hypertension with IS.

Dyslipidemia	Hypertension	IS cases	Follow-up time (person-years)	Incidence density (/10,000 person-years)	HR(95%CI)[a]	*P*[a]
No	No	42	10,749.9	39.07	Ref	-
	Yes	78	8,522.4	91.52	1.603 (1.097–2.343)	0.015
Yes	No	48	11,040.22	43.48	1.025 (0.677–1.553)	0.907
	Yes	104	11,270.54	92.28	1.627 (1.129–2.343)	0.009

IS, Ischemic stroke.

[a]: Adjusted for age, gender, BMI, cigarette smoking, alcohol consumption, T2DM at baseline, and use of lipid-lowering drugs.

Stratification Analysis of the Association Between Blood Lipids and the Risk of IS by Hypertension

In the hypertensive population, Non-HDL-C $\geq$ 190 mg/dl and LDL-C/HDL-C $\geq$ 2 were significantly associated with increased risk of IS, after adjusting for covariates, HRs (95%CIs) were 1.565 (1.007–2.429) and 1.414 (1.034–1.933), respectively. HDL-C $\geq$ 60 mg/dl was significantly associated with reduced risk of IS with adjusted HR (95%CI) of 0.665 (0.450–0.983). While in the non-hypertension population, no significant association of Non-HDL-C $\geq$ 190 mg/dl, LDL-C/HDL-C $\geq$ 2, and HDL-C $\geq$ 60 was detected with IS ($P > 0.05$).

Additionally, there was a significant association between TC/HDL-C $\geq$ 3.6 and the decreased risk of IS in the non-hypertension population, and the HR (95%CI) was 0.479 (0.307–0.750). However, a similar association was not observed in the hypertensive population.

Further analysis of heterogeneity test results indicated that the association of HDL-C $\geq$ 60 mg/dl, Non-HDL-C $\geq$ 190 mg/dl, TC/HDL-C $\geq$ 3.6, and TG/HDL-C $\geq$ 1 and IS are heterogeneous between hypertension and non-hypertension groups ($P_{\text{heterogeneity}} < 0.05$). See **Table 3** for details.

Interaction Analysis of Abnormal Blood Lipid Indices and Hypertension for IS

We further analyzed the interaction between those indices which had heterogeneous associations with IS among different blood pressure statuses and hypertension. The results showed that HDL-C $\geq$ 60 mg/dl (vs HDL-C $<$ 60 mg/dl), Non-HDL-C $\geq$ 190 mg/dl (vs. Non-HDL-C $<$ 190 mg/dl), TC/HDL-C $\geq$ 3.6 (vs TC/HDL-C $<$ 3.6), and TG/HDL-C $\geq$ 1 (vs. TG/HDL-C $<$ 1) have additive and multiplicative interactions with hypertension. The RERIs (95% CIs) of the additive interaction are −0.93 (−1.882–0.044), 1.394 (0.38–2.407), 0.752 (0.354–1.151) and 0.575 (0.086–1.065), respectively. The HRs (95% CIs) of the multiplicative interaction terms were 0.498 (0.272–0.911), 4.218 (1.230–14.464), 2.423 (1.437–4.086) and 1.701 (1.016–2.848), respectively. In the analysis of the interaction between total dyslipidemia and hypertension, the association was not statistically significant. The RERI (95% CI) of the additive interaction was −0.002 (−0.635–0.632), while the HR (95% CI) of the multiplicative interaction term was 0.990 (0.595–1.645). See **Table 4** for details.

DISCUSSION

This study indicated that higher HDL-C levels will reduce the impact of hypertension on the risk of developing IS, while higher levels of Non-HDL-C, TC/HDL-C, and TG/HDL-C have a positive interaction effect with hypertension on the incidence of IS in Chinese adults.

Dyslipidemia is one of the major and modifiable risk factors for IS (23, 24). In China, the prevalence of adult dyslipidemia has increased significantly, from 18.6 in 2002 to 40.4% in 2012. Yet the awareness, treatment, and control rates of dyslipidemia are still low, at 31.0, 19.5, and 8.9%, respectively (12, 25, 26). Several studies have reported the association between cardiovascular disease and dyslipidemia, involving the conventional lipid indices such as TC, TG, LDL-C, HDL-C, and the lipid ratios such as TC/HDL-C, TG/HDL-C, and LDL-C/HDL-C. Two large prospective cohort studies both confirmed that high TC, TG, and LDL-C levels or low HDL-C levels increase the risk of CVD (27, 28). However, recent studies have also found a "U" or "J" shaped association between cholesterol levels (including TC, LDL-C, HDL-C) and CVD, with both high and low TC, LDL-C, and HDL-C levels contributing to adverse cardiovascular events (29–34). To comprehensively consider the effects of different lipid components on CVD risk, non-HDL-C, TC/HDL-C, TG/HDL-C, and LDL-C/HDL-C were proposed. Due to the ease of calculation of non-HDL-C and its strong predictive power for CVD, non-HDL-C was recommended as an independent risk factor for CVD (35, 36). Previous epidemiological studies have also demonstrated that higher levels of TC/HDL-C, TG/HDL-C, and LDL-C/HDL-C are associated with an increased risk of developing CVD.

In this study, stratification analysis showed that Non-HDL-C, LDL-C/HDL-C, and HDL-C were associated with IS in the hypertensive population and TC/HDL-C in the non-hypertensive population. These statistically significant indices are derived indices of HDL-C, which may indicate the important influence of HDL-C in the occurrence and development of IS. Besides, analyses of the association of dyslipidemia with IS demonstrated that, compared to LDL-C, non-HDL-C had a stronger relationship with IS risk in the hypertension stratified analysis. This finding may provide more evidence for non-HDL-C as a better predictor for atherogenesis risk than LDL-C in the hypertensive population. However, in the whole population analysis, none of the lipid indices showed a statistical

TABLE 3 | Hypertension status stratified analyses of abnormal lipid indices and the risk of IS.

Lipid indices	Group	Non-hypertension		Hypertension		$P^{b}_{heterogeneity}$
		HR (95% CI)[a]	P^{a}	HR (95% CI)[a]	P^{a}	
TC	<240 mg/dl	reference	-	reference	-	
	≥240 mg/dl	0.445 (0.176–1.123)	0.086	1.224 (0.801–1.868)	0.350	0.052
TG	<200 mg/dl	reference	-	reference	-	
	≥200 mg/dl	0.714 (0.373–1.368)	0.310	1.254 (0.891–1.765)	0.194	0.133
HDL-C	40–60mg/dl	reference	-	reference	-	
	<40 mg/dl	0.884 (0.477–1.639)	0.695	1.157 (0.778–1.720)	0.471	0.472
	>60 mg/dl	1.411 (0.883–2.253)	0.150	0.665 (0.450–0.983)	0.041	0.016
LDL-C	<160 mg/dl	reference	-	reference	-	
	≥160 mg/dl	0.401 (0.056–2.880)	0.364	1.000 (0.542–1.847)	0.999	0.385
Non-HDL-C	<190 mg/dl	reference	-	reference	-	
	≥190 mg/dl	0.319 (0.098–1.036)	0.057	1.565 (1.007–2.429)	0.046	0.013
RC	<30 mg/dl	reference	-	reference	-	
	≥30 mg/dl	0.749 (0.488–1.148)	0.184	1.071 (0.795–1.442)	0.651	0.179
TC/HDL-C	<3.6	reference	-	reference	-	
	≥3.6	0.479 (0.307–0.750)	0.001	1.303 (0.955–1.778)	0.094	<0.001
TG/HDL-C	<1	reference	-	reference	-	
	≥1	0.698 (0.447–1.090)	0.114	1.259 (0.925–1.714)	0.143	0.033
LDL-C/HDL-C	<2	reference	-	reference	-	
	≥2	0.800 (0.523–1.223)	0.302	1.414 (1.034–1.933)	0.030	0.126

TC, total cholesterol; TG, triglycerides; HDL-C, high-density lipoprotein cholesterol; LDL-C, low-density lipoprotein cholesterol; Non-HDL-C, non-high-density lipoprotein cholesterol; RC, remnant cholesterol.

[a]: Adjusted for age, gender, BMI, cigarette smoking, alcohol consumption, T2DM at baseline, and use of lipid-lowering drugs.

[b]: $P_{heterogeneity}$ stands for the P value of the heterogeneity test.

TABLE 4 | Analysis of the additive and multiplicative interaction of abnormal blood lipids and hypertension on IS.

Interaction terms	Additive interaction		Multiplicative interaction	
	RERI (95% CI)[a]	p^{a}	HR (95% CI)[a]	p^{a}
HDL-C (≥60 mg/dl) * HT	−0.963 (−1.882– −0.044)	0.040	0.498 (0.272–0.911)	0.024
Non-HDL-C (≥190 mg/dl) * HT	1.394 (0.38–2.407)	0.007	4.218 (1.230–14.464)	0.022
TC/HDL-C (≥3.6) * HT	0.752 (0.354–1.151)	0.001	2.423 (1.437–4.086)	0.001
TG/HDL-C (≥1) * HT	0.575 (0.086–1.065)	0.021	1.701 (1.016–2.848)	0.044
Dyslipidemia*HT	−0.002 (−0.635–0.632)	0.996	0.990 (0.595–1.645)	0.968

TC, total cholesterol; TG, triglycerides; HDL-C, high-density lipoprotein cholesterol; Non-HDL-C, non-high-density lipoprotein cholesterol; RERI, relative excess risk due to interaction.

[a]: Adjusted for age, gender, BMI, cigarette smoking, alcohol consumption, T2DM at baseline, and use of lipid-lowering drugs.

association with IS. There are two main reasons. First, the cohort population and the number of patients with IS are relatively small, especially in performing subgroup analysis. So, it may be difficult to observe a statistically significant association, but the association trend can still be observed. Second, hypertension has a greater effect on the onset of IS, and the etiologic effect of dyslipidemia is relatively small. In the present study population, the prevalence of hypertension was as high as ∼50%, so the effect of dyslipidemia may be masked.

Hypertension is another critical and controllable risk factor for IS. It can occur simultaneously with dyslipidemia and act synergistically to affect the risk of CVD according to previous research (21, 37). So, in this study, we analyze different results of the additive model and multiplicative models to evaluate the interaction between blood lipid indices and hypertension comprehensively. Our results suggested that HDL-C ≥ 60 mg/dl negatively affected IS in the hypertension group, from which we could infer that higher HDL-C levels may help reduce the impact of hypertension on IS risk. The underlying mechanism of this finding could be related to endothelial dysfunction in cerebral blood vessels. Atherosclerosis involving impairment of endothelial function and vascular contractility is an essential pathological basis for the development of IS (38). Hypertension-induced abnormalities in the cerebrovascular structure are

known to play an important part in the pathogenesis of IS (39). Previous studies have shown that endothelium-mediated vasodilation is undermined in patients with essential hypertension (40–42). This abnormality is associated with attenuated endothelial Nitric Oxide (NO) activity and may be caused by selective abnormalities in NO synthesis (43). However, HDL particles could increase NO production by stimulating endothelial nitric oxide synthase (eNOS) activity and enhance endothelium- and NO-dependent relaxation in wild-type mice (44), which may help to explain, to some extent, the atheroprotective role of HDL-C in reducing the effect of hypertension on IS.

Non-HDL-C, TC/HDL-C, and TG/HDL-C, closely related to HDL-C, are all lipid indices derived from HDL-C but measure other lipids in the blood as well. Thus, these non-traditional lipid parameters may depict a more accurate and more comprehensive lipid profile than traditional ones. In the present study, non-HDL-C, TC/HDL-C, and TG/HDL-C had a positive interaction with hypertension for IS, implying that the abnormal imbalance of circulating lipids may amplify the effect of hypertension on IS. The pathophysiological mechanisms that could possibly explain the interaction between dyslipidemia and hypertension can be summarized as follows. First, LDL-C and hypercholesterolemia have been shown to make a difference in the interference for NO signaling activities resulting in the decrease of NO production and bioavailability, which consequently reduce endothelial vasolidaiton and enhance vasoconstructive activation. Therefore, dyslipidemia exacerbates the development of hypertensive status (45, 46). Moreover, subsequent vascular changes in function and structure caused by hypertension, such as altered hemodynamics at arterial bifurcations, as well as proinflammatory activities and oxidative stress, may worsen the harm produced by dyslipidemia (47). These can be supported by an animal study, which suggests that hypertension and hypercholesterolemia synergistically reduce endothelial function and increase oxidative stress in blood vessels in pigs, possibly exacerbating atherosclerosis due to dyslipidemia (48). In addition, previous research also indicated that the elevated LDL-C level indirectly increased the calcium influx into cells and stimulated vascular smooth muscle cell contraction (47).

With a follow-up of up to 10.75 years, this study systematically and prospectively investigated the interaction between lipid indices and hypertension on IS development. However, the following limitations exist. First, the sample size of this study was relatively small, which may reduce the efficacy of the test. Second, the study did not collect information on physical activity, whereas previous studies have shown that active physical activity reduces the risk of CVD morbidity and mortality by improving CVD risk factors. In addition, because the lipid data in this analysis were collected only at baseline, it was impossible to assess the effect of changes in lipid levels on CVD morbidity and mortality during follow-up. Therefore, a prospective cohort study with larger sample size, more comprehensive baseline information, and repeated lipid measurements during follow-up is urgently needed to validate the results of this study.

CONCLUSION

This large prospective cohort study is the first for all we know to evaluate the combined effects of abnormal lipid parameters and hypertension on IS. The current results demonstrate that higher HDL-C levels may help reduce the impact of hypertension on IS risk and higher levels of non-HDL-C, TC/HDL-C, and TG/HDL-C, additively interacting with hypertension, increase the risk for developing IS. This study provides useful evidence for the combined effects of dyslipidemia and hypertension in predicting IS in Chinese adults. Therefore, the combination of non-traditional lipid indices and hypertension could aid in the screening process to identify high-risk populations before IS and may lead to more effective prevention of IS in clinical practice. Furthermore, because of the high comorbidity of dyslipidemia and hypertension and the interaction effect on IS, it is essential to implement lipids-control measures to prevent and treat IS in patients with hypertension in China. Targeting both dyslipidemia and hypertension in the clinical context could help build optimal therapeutic interventions for the prevention and management of IS.

DATA AVAILABILITY STATEMENT

The raw data supporting the conclusions of this article will be made available by the authors, without undue reservation.

ETHICS STATEMENT

The studies involving human participants were reviewed and approved by Nanjing Medical University. The patients/participants provided their written informed consent to participate in this study.

AUTHOR CONTRIBUTIONS

LW: data analysis and manuscript preparation. JS and QZ: data acquisition and sorting. HX and CC: manuscript preparation. PW, XZ, YC, and ML: data acquisition. JD: data analysis. SY: study design and manuscript preparation. CS: study design, data interpretation, and manuscript preparation. All authors have read and approved the final manuscript.

FUNDING

This work was supported by the National Natural Science Foundation of China (Grant No. 81872686, No.82173611, and No. 81573232), the Priority Academic Program for the Development of Jiangsu Higher Education Institutions (Public Health and Preventive Medicine), and the Flagship Major Development of Jiangsu Higher Education Institutions. The Funders had no role in the design and conduct of the study; collection, management, analysis, and interpretation of the data; preparation, review, or approval of the manuscript; and decision to submit the manuscript for publication.

ACKNOWLEDGMENTS

We would like to thank Solim Essomandan Clemence Bafei for helping to edit the English language. We sincerely thank all patients and healthy volunteers who participated in this study.

SUPPLEMENTARY MATERIAL

The Supplementary Material for this article can be found online at: https://www.frontiersin.org/articles/10.3389/fcvm.2022.819274/full#supplementary-material

REFERENCES

1. Al Kasab S, Lynn MJ, Turan TN, Derdeyn CP, Fiorella D, Lane BF, et al. Impact of the new American heart association/American stroke association definition of stroke on the results of the stenting and aggressive medical management for preventing recurrent stroke in intracranial stenosis trial. *J Stroke Cerebrovasc Dis.* (2017) 26:108–15. doi: 10.1016/j.jstrokecerebrovasdis.2016.08.038
2. Feigin VL, Nguyen G, Cercy K, Johnson CO, Alam T, Parmar PG, et al. Global, regional, and country-specific lifetime risks of stroke, 1990 and 2016. *N Engl J Med.* (2018) 379:2429–37. doi: 10.1056/NEJMoa1804492
3. Wang YJ, Li ZX, Gu HQ, Zhai Y, Jiang Y, Zhao XQ, et al. China stroke statistics 2019: a report from the national center for healthcare quality management in neurological diseases, China national clinical research center for neurological diseases, the Chinese stroke association, national center for chronic and non-communicable disease control and prevention, chinese center for disease control and prevention and institute for global neuroscience and stroke collaborations. *Stroke Vasc Neurol.* (2020) 5:211–39. doi: 10.1136/svn-2020-000457
4. Wu S, Wu B, Liu M, Chen Z, Wang W, Anderson CS, et al. Stroke in China: advances and challenges in epidemiology, prevention, and management. *Lancet Neurol.* (2019) 18:394–405. doi: 10.1016/S1474-4422(18)30500-3
5. Lou H, Dong Z, Zhang P, Shao X, Li T, Zhao C, et al. Interaction of diabetes and smoking on stroke: a population-based cross-sectional survey in China. *BMJ Open.* (2018) 8:e017706. doi: 10.1136/bmjopen-2017-017706
6. Wang W, Jiang B, Sun H, Ru X, Sun D, Wang L, et al. Prevalence, incidence, and mortality of stroke in China: results from a nationwide population-based survey of 480 687 adults. *Circulation.* (2017) 135:759–71. doi: 10.1161/CIRCULATIONAHA.116.025250
7. Goldstein LB, Adams R, Alberts MJ, Appel LJ, Brass LM, Bushnell CD, et al. Primary prevention of ischemic stroke: a guideline from the American heart association/American stroke association stroke council: cosponsored by the atherosclerotic peripheral vascular disease interdisciplinary working group; cardiovascular nursing council; clinical cardiology council; nutrition, physical activity, and metabolism council; and the quality of care and outcomes research interdisciplinary working group: the American academy of neurology affirms the value of this guideline. *Stroke.* (2006) 37:1583–633. doi: 10.1161/01.STR.0000223048.70103.F1
8. Cui Q, Naikoo NA. Modifiable and non-modifiable risk factors in ischemic stroke: a meta-analysis. *Afr Health Sci.* (2019) 19:2121–9. doi: 10.4314/ahs.v19i2.36
9. O'Donnell MJ, Xavier D, Liu L, Zhang H, Chin SL, Rao-Melacini P, et al. Risk factors for ischaemic and intracerebral haemorrhagic stroke in 22 countries (the INTERSTROKE study): a case-control study. *Lancet.* (2010) 376:112–23. doi: 10.1016/S0140-6736(10)60834-3
10. Wang J, Wen X, Li W, Li X, Wang Y, Lu W. Risk factors for stroke in the Chinese population: a systematic review and meta-analysis. *J Stroke Cerebrovasc Dis.* (2017) 26:509–17. doi: 10.1016/j.jstrokecerebrovasdis.2016.12.002
11. Feigin VL, Roth GA, Naghavi M, Parmar P, Krishnamurthi R, Chugh S, et al. Global burden of stroke and risk factors in 188 countries, during 1990-2013: a systematic analysis for the Global Burden of Disease Study 2013. *Lancet Neurol.* (2016) 15:913–24. doi: 10.1016/S1474-4422(16)30073-4
12. Sun L, Clarke R, Bennett D, Guo Y, Walters RG, Hill M, et al. Causal associations of blood lipids with risk of ischemic stroke and intracerebral hemorrhage in Chinese adults. *Nat Med.* (2019) 25:569–74. doi: 10.1038/s41591-019-0366-x
13. Gorgui J, Gorshkov M, Khan N, Daskalopoulou SS. Hypertension as a risk factor for ischemic stroke in women. *Can J Cardiol.* (2014) 30:774–82. doi: 10.1016/j.cjca.2014.01.007
14. Hindy G, Engström G, Larsson SC, Traylor M, Markus HS, Melander O, et al. Role of blood lipids in the development of ischemic stroke and its subtypes: a mendelian randomization study. *Stroke.* (2018) 49:820–7. doi: 10.1161/STROKEAHA.117.019653
15. Cipolla MJ, Liebeskind DS, Chan SL. The importance of comorbidities in ischemic stroke: impact of hypertension on the cerebral circulation. *J Cereb Blood Flow Metab.* (2018) 38:2129–49. doi: 10.1177/0271678X18800589
16. Jain M, Jain A, Yerragondu N, Brown RD, Rabinstein A, Jahromi BS, et al. The triglyceride paradox in stroke survivors: a prospective study. *Neurosci J.* (2013) 2013:870608. doi: 10.1155/2013/870608
17. Tirschwell DL, Smith NL, Heckbert SR, Lemaitre RN, Longstreth WT Jr, et al. Association of cholesterol with stroke risk varies in stroke subtypes and patient subgroups. *Neurology.* (2004) 63:1868–75. doi: 10.1212/01.WNL.0000144282.42222.DA
18. Gorelick PB, Mazzone T. Plasma lipids and stroke. *J Cardiovasc Risk.* (1999) 6:217–21. doi: 10.1177/204748739900600405
19. Park JH, Lee J, Ovbiagele B. Nontraditional serum lipid variables and recurrent stroke risk. *Stroke.* (2014) 45:3269–74. doi: 10.1161/STROKEAHA.114.006827
20. Lu S, Bao MY, Miao SM, Zhang X, Jia QQ, Jing SQ, et al. Prevalence of hypertension, diabetes, and dyslipidemia, and their additive effects on myocardial infarction and stroke: a cross-sectional study in Nanjing, China. *Ann Transl Med.* (2019) 7:436. doi: 10.21037/atm.2019.09.04
21. Thomas F, Bean K, Guize L, Quentzel S, Argyriadis P, Benetos A. Combined effects of systolic blood pressure and serum cholesterol on cardiovascular mortality in young (<55 years) men and women. *Eur Heart J.* (2002) 23:528–35. doi: 10.1053/euhj.2001.2888
22. Dong J, Yang S, Zhuang Q, Sun J, Wei P, Zhao X, et al. The associations of lipid profiles with cardiovascular diseases and death in a 10-year prospective cohort study. *Front Cardiovasc Med.* (2021) 8:745539. doi: 10.3389/fcvm.2021.745539
23. Kostis JB. The importance of managing hypertension and dyslipidemia to decrease cardiovascular disease. *Cardiovasc Drugs Ther.* (2007) 21:297–309. doi: 10.1007/s10557-007-6032-4
24. Turer CB, Brady TM, de Ferranti SD. Obesity, hypertension, and dyslipidemia in childhood are key modifiable antecedents of adult cardiovascular disease: a call to action. *Circulation.* (2018) 137:1256–9. doi: 10.1161/CIRCULATIONAHA.118.032531
25. Song PK, Man QQ, Li H, Pang SJ, Jia SS, Li YQ, et al. Trends in lipids level and dyslipidemia among chinese adults, 2002-2015. *Biomed Environ Sci.* (2019) 32:559–70. doi: 10.3967/bes2019.074
26. Zhang M, Deng Q, Wang L, Huang Z, Zhou M, Li Y, et al. Prevalence of dyslipidemia and achievement of low-density lipoprotein cholesterol targets in Chinese adults: a nationally representative survey of 163,641 adults. *Int J Cardiol.* (2018) 260:196–203. doi: 10.1016/j.ijcard.2017.12.069
27. Bowe B, Xie Y, Xian H, Balasubramanian S, Zayed MA, Al-Aly Z. High density lipoprotein cholesterol and the risk of all-cause mortality among U.S. Veterans. *Clin J Am Soc Nephrol.* (2016) 11:1784–93. doi: 10.2215/CJN.00730116
28. Gu X, Li Y, Chen S, Yang X, Liu F, Li Y, et al. Association of lipids with ischemic and hemorrhagic stroke: a prospective cohort study among 267 500 Chinese. *Stroke.* (2019) 50:3376–84. doi: 10.1161/STROKEAHA.119.026402
29. Castañer O, Pintó X, Subirana I, Amor AJ, Ros E, Hernáez Á, et al. Remnant cholesterol, Not LDL cholesterol, is associated with incident cardiovascular disease. *J Am Coll Cardiol.* (2020) 76:2712–24. doi: 10.1016/j.jacc.2020.10.008
30. Yokokawa H, Yasumura S, Tanno K, Ohsawa M, Onoda T, Itai K, et al. Serum low-density lipoprotein to high-density lipoprotein ratio as a predictor of future acute myocardial infarction among men in a 2.7-year cohort study of a Japanese northern rural population. *J Atheroscler Thromb.* (2011) 18:89–98. doi: 10.5551/jat.5215

31. Ingelsson E, Schaefer EJ, Contois JH, McNamara JR, Sullivan L, Keyes MJ, et al. Clinical utility of different lipid measures for prediction of coronary heart disease in men and women. *JAMA*. (2007) 298:776–85. doi: 10.1001/jama.298.7.776
32. Sung KC, Ryu S, Wild SH, Byrne CD. An increased high-density lipoprotein cholesterol/apolipoprotein A-I ratio is associated with increased cardiovascular and all-cause mortality. *Heart*. (2015) 101:553–8. doi: 10.1136/heartjnl-2014-306784
33. Ding D, Li X, Qiu J, Li R, Zhang Y, Su D, et al. Serum lipids, apolipoproteins, and mortality among coronary artery disease patients. *Biomed Res Int*. (2014) 2014:709756. doi: 10.1155/2014/709756
34. Zhong GC, Huang SQ, Peng Y, Wan L, Wu YQ, Hu TY, et al. HDL-C is associated with mortality from all causes, cardiovascular disease and cancer in a J-shaped dose-response fashion: a pooled analysis of 37 prospective cohort studies. *Eur J Prev Cardiol*. (2020) 27:1187–203. doi: 10.1177/2047487320914756
35. Catapano AL, Graham I, De Backer G, Wiklund O, Chapman MJ, Drexel H, et al. 2016 ESC/EAS guidelines for the management of dyslipidaemias. *Eur Heart J*. (2016) 37:2999–3058. doi: 10.1093/eurheartj/ehw272
36. Averna M, Stroes E. How to assess and manage cardiovascular risk associated with lipid alterations beyond LDL. *Atheroscler Suppl*. (2017) 26:16–24. doi: 10.1016/S1567-5688(17)30021-1
37. Agbor-Etang BB, Setaro JF. Management of hypertension in patients with ischemic heart disease. *Curr Cardiol Rep*. (2015) 17:119. doi: 10.1007/s11886-015-0662-0
38. Rajendran P, Rengarajan T, Thangavel J, Nishigaki Y, Sakthisekaran D, Sethi G, et al. The vascular endothelium and human diseases. *Int J Biol Sci*. (2013) 9:1057–69. doi: 10.7150/ijbs.7502
39. Yu JG, Zhou RR, Cai GJ. From hypertension to stroke: mechanisms and potential prevention strategies. *CNS Neurosci Ther*. (2011) 17:577–84. doi: 10.1111/j.1755-5949.2011.00264.x
40. Hirooka Y, Imaizumi T, Masaki H, Ando S, Harada S, Momohara M, et al. Captopril improves impaired endothelium-dependent vasodilation in hypertensive patients. *Hypertension*. (1992) 20:175–80. doi: 10.1161/01.HYP.20.2.175
41. Linder L, Kiowski W, Bühler FR, Lüscher TF. Indirect evidence for release of endothelium-derived relaxing factor in human forearm circulation *in vivo*. Blunted response in essential hypertension. *Circulation*. (1990) 81:1762–7. doi: 10.1161/01.CIR.81.6.1762
42. Panza JA, Quyyumi AA, Brush JE Jr, Epstein SE. Abnormal endothelium-dependent vascular relaxation in patients with essential hypertension. *N Engl J Med*. (1990) 323:22–7. doi: 10.1056/NEJM199007053230105
43. Cardillo C, Kilcoyne CM, Quyyumi AA, Cannon RO 3rd, Panza JA. Selective defect in nitric oxide synthesis may explain the impaired endothelium-dependent vasodilation in patients with essential hypertension. *Circulation*. (1998) 97:851–6. doi: 10.1161/01.CIR.97.9.851
44. Yuhanna IS, Zhu Y, Cox BE, Hahner LD, Osborne-Lawrence S, Lu P, et al. High-density lipoprotein binding to scavenger receptor-BI activates endothelial nitric oxide synthase. *Nat Med*. (2001) 7:853–7. doi: 10.1038/89986
45. Pereira AC, Sposito AC, Mota GF, Cunha RS, Herkenhoff FL, Mill JG, et al. Endothelial nitric oxide synthase gene variant modulates the relationship between serum cholesterol levels and blood pressure in the general population: new evidence for a direct effect of lipids in arterial blood pressure. *Atherosclerosis*. (2006) 184:193–200. doi: 10.1016/j.atherosclerosis.2005.03.035
46. Liao JK, Shin WS, Lee WY, Clark SL. Oxidized low-density lipoprotein decreases the expression of endothelial nitric oxide synthase. *J Biol Chem*. (1995) 270:319–24. doi: 10.1074/jbc.270.1.319
47. Chapman MJ, Sposito AC. Hypertension and dyslipidaemia in obesity and insulin resistance: pathophysiology, impact on atherosclerotic disease and pharmacotherapy. *Pharmacol Ther*. (2008) 117:354–73. doi: 10.1016/j.pharmthera.2007.10.004
48. Rodriguez-Porcel M, Lerman LO, Herrmann J, Sawamura T, Napoli C, Lerman A. Hypercholesterolemia and hypertension have synergistic deleterious effects on coronary endothelial function. *Arterioscler Thromb Vasc Biol*. (2003) 23:885–91. doi: 10.1161/01.ATV.0000069209.26507.BF

Conflict of Interest: The authors declare that the research was conducted in the absence of any commercial or financial relationships that could be construed as a potential conflict of interest.

Publisher's Note: All claims expressed in this article are solely those of the authors and do not necessarily represent those of their affiliated organizations, or those of the publisher, the editors and the reviewers. Any product that may be evaluated in this article, or claim that may be made by its manufacturer, is not guaranteed or endorsed by the publisher.

Copyright © 2022 Wei, Sun, Xie, Zhuang, Wei, Zhao, Chen, Dong, Li, Chen, Yang and Shen. This is an open-access article distributed under the terms of the Creative Commons Attribution License (CC BY). The use, distribution or reproduction in other forums is permitted, provided the original author(s) and the copyright owner(s) are credited and that the original publication in this journal is cited, in accordance with accepted academic practice. No use, distribution or reproduction is permitted which does not comply with these terms.

frontiers in Cardiovascular Medicine

ORIGINAL RESEARCH
published: 16 March 2022
doi: 10.3389/fcvm.2022.769717

1α,25-Dihydroxyvitamin D3 Promotes Angiogenesis After Cerebral Ischemia Injury in Rats by Upregulating the TGF-β/Smad2/3 Signaling Pathway

Yajie Zhang[1,2†], Yingfeng Mu[2†], Hongmei Ding[2], Bo Du[2], Mingyue Zhou[1,2], Qingqing Li[1,2], Shitong Gong[1,2], Fuchi Zhang[3], Deqin Geng[2] and Yanqiang Wang[4*]*

[1] Department of Neurology, Xuzhou Medical University, Xuzhou, China, [2] Department of Neurology, The Affiliated Hospital of Xuzhou Medical University, Xuzhou, China, [3] Department of Neurology, The Third Hospital of Huai'an, Huai'an, China, [4] Department of Neurology II, The Affiliated Hospital of Weifang Medical University, Weifang, China

Stroke is a disease with high morbidity, disability and mortality, which seriously endangers the life span and quality of life of people worldwide. Angiogenesis and neuroprotection are the key to the functional recovery of penumbra function after acute cerebral infarction. In this study, we used the middle cerebral artery occlusion (MCAO) model to investigate the effects of 1α,25-dihydroxyvitamin D3 (1,25-D3) on transforming growth factor-β (TGF-β)/Smad2/3 signaling pathway. Cerebral infarct volume was measured by TTC staining. A laser speckle flow imaging system was used to measure cerebral blood flow (CBF) around the ischemic cortex of the infarction, followed by platelet endothelial cell adhesion molecule-1 (PECAM-1/CD31) and isolectin-B4 (IB4) immunofluorescence. The expression of vitamin D receptor (VDR), TGF-β, Smad2/3, p-Smad2, p-Smad3, and vascular endothelial growth factor (VEGF) was analyzed by western blot and RT-qPCR. Results showed that compared with the sham group, the cerebral infarction volume was significantly increased while the CBF was reduced remarkably in the MCAO group. 1,25-D3 reduced cerebral infarction volume, increased the recovery of CBF and expressions of VDR, TGF-β, p-Smad2, p-Smad3, and VEGF, significantly increased $IB4^+$ tip cells and $CD31^+$ vascular length in the peri-infarct area compared with the DMSO group. The VDR antagonist pyridoxal-5-phosphate (P5P) partially reversed the neuroprotective effects of 1,25-D3 described above. In summary, 1,25-D3 plays a neuroprotective role in stroke by activating VDR and promoting the activation of TGF-β, which in turn up-regulates the TGF-β/Smad2/3 signaling pathway, increases the release of VEGF and thus promotes angiogenesis, suggesting that this signaling pathway may be an effective target for ischemic stroke treatment. 1,25-D3 is considered to be a neuroprotective agent and is expected to be an effective drug for the treatment of ischemic stroke and related diseases.

Keywords: 1α,25-dihydroxyvitamin D3, vitamin D receptor, TGF-β/Smad2/3 signaling pathway, vascular endothelial growth factor, cerebral ischemia-reperfusion, angiogenesis

OPEN ACCESS

Edited by:
Yacine Boulaftali, Institut National de la Santé et de la Recherche Médicale (INSERM), France

Reviewed by:
Yansheng Feng, The University of Texas Health Science Center at San Antonio, United States
Shereen Nizari, University College London, United Kingdom

***Correspondence:**
Yanqiang Wang
wangqiangdoctor@126.com
Deqin Geng
gengdeqin@126.com

[†] These authors have contributed equally to this work and share first authorship

Specialty section:
This article was submitted to Atherosclerosis and Vascular Medicine, a section of the journal Frontiers in Cardiovascular Medicine

Received: *02 September 2021*
Accepted: *21 February 2022*
Published: *16 March 2022*

Citation:
Zhang Y, Mu Y, Ding H, Du B, Zhou M, Li Q, Gong S, Zhang F, Geng D and Wang Y (2022) 1α,25-Dihydroxyvitamin D3 Promotes Angiogenesis After Cerebral Ischemia Injury in Rats by Upregulating the TGF-β/Smad2/3 Signaling Pathway. Front. Cardiovasc. Med. 9:769717. doi: 10.3389/fcvm.2022.769717

INTRODUCTION

For past two decades, thrombolytic therapy has been the standard treatment for acute ischemic stroke. Intravenous thrombolysis can be used to treat acute stroke only when it can be determined that the time after the onset of symptoms is less than 4.5 h (1, 2). Although its efficacy has been demonstrated in clinical trials, the number of patients benefited by this procedure is unfortunately low, around 5% of all stroke patients, a fact ascribed to the narrow time window for t-PA administration and because delayed thrombolytic therapy and blood reperfusion have been associated with a high risk of hemorrhagic transformation and oxidative stress, thus causing additional damage (3). A recent clinical study showed that in patients with acute stroke whose onset time was unknown, the incidence of intracranial hemorrhage was also significantly increased at 90 days after intravenous injection of alteplase under the guidance of diffusion-weighted imaging and FLAIR (fluid attenuated inversion recovery) mismatch in the ischemic area compared with the placebo group (4). Endovascular thrombectomy (EVT) has been shown to be a highly effective treatment in high-resource countries. Infrastructure and support are needed for EVT in the developing world (5). Therefore, it is particularly important to seek more therapeutic measures for ischemic stroke.

1α,25-dihydroxyvitamin D3 (1,25-D3) is widely expressed in human organs and tissues and exerts the steroid effect in the whole body. Its neuroprotective effect has been paid more and more attention by scholars. 1,25-D3 produces a wide range of biological activities once binding to vitamin D receptor (VDR), including inhibition of proliferation, affecting angiogenesis, regulating immune activity, and endocrine activity (6–8). Observational studies have shown that patients with lower serum 1,25-D3 levels experience infarct volume and worse functional outcomes after stroke, indicating that 1,25-D3 may play a protective role during cerebral ischemia, but whether it can promote brain function recovery in terms of angiogenesis has not been reported (9).

After the brain encounters ischemia and hypoxia, cells around the ischemic core suffer irreversible necrosis (10, 11). The injury around the infarction is selective and progressive, thus ensuring the survival of cells around the infarction and angiogenesis is an effective target for brain protection. Angiogenesis is the key for functional recovery of ischemic penumbra after acute cerebral infarction (12–14). Vascular endothelial growth factor (VEGF) is essential for angiogenesis and neovascularization, and the release of VEGF is regulated by neurotrophic factors including transforming growth factor β (TGF-β) (15). In recent years, more and more attention has been paid to the link between TGF-β signaling pathway and angiogenesis. TGF-β participates in angiogenesis by regulating the stability of capillaries (16). Maharaj et al. demonstrated that activated TGF-β acts on endothelial cells and pericytes to induce the production and the release of VEGF (17). VEGF and TGF-β are involved in the regulation of endothelial cell stability, ependymal cell function and periventricular permeability (17). Patients with scleroderma can lessen angiogenesis by inhibiting TGF-β signaling pathway (18). Nanda et al. have confirmed that after TGF-β signal damage, angiogenesis decreases in non-atherosclerotic ischemic injury model, which weakens the ability of neovascularization to mature (19). A lot of evidence confirmed the crucial role of TGF-β signaling pathway in angiogenesis (20, 21).

We investigated the effects of 1,25-D3 on angiogenesis and explore the possible mechanism after ischemia. We found that 1,25-D3 protected against ischemic injury and improved stroke outcome 3 days after MCAO. 1,25-D3 promotes angiogenesis by activating VDR, up-regulating TGF-β/Smad2/3 signaling pathway and inducing the release of VEGF. Therefore, our study highlights the potential of 1,25-D3 in stroke treatment.

MATERIALS AND METHODS

Ethics Statement

All animal experiments were conducted in accordance with the National Institute of Health Guide for the Care and Use of Laboratory Animals of Laboratory Animals. All the experimental procedures involved in this study were approved by the Animal Ethics Committee of Xuzhou Medical University (protocol: 202007A102).

Animals

Male Sprague-Dawley (SD) rats were provided by the Experimental Animal Center of Xuzhou Medical University. All rats were kept in pathogen-free conditions and housed under a light-dark cycle for 12 h (20 ± 1°C, and 55 ± 10% humidity), with access to food and water *ad libitum*.

Chemicals and Reagents

1,25-D3 and VDR antagonist pyridoxal-5-phosphate (P5P) were purchased from Med chem Express. 2,3,5-triphenyltetrazolium chloride (TTC) was purchased from Sigma-Aldrich. The primary antibodies: anti-VDR antibody (14526-1-AP) and anti-β-actin antibody (20536-1-AP) were purchased from Proteintech. Anti-VEGF antibody (ab1316) and anti-platelet endothelial cell adhesion molecule-1 (PECAM-1/CD31) antibody (ab222783) were purchased from Abcam. Anti- isolectin-B4 (IB4) antibody (DL-1207) was purchased from Vector Laboratories. The primary antibodies of anti-TGF-β (3711S), anti-Smad2/3 (8685T), anti-p-Smad2 (18338T) and anti-p-Smad3 (9250T) were purchased from Cell Signaling Technology. MCAO threads (2636-100, diameter of the head of nylon filament: 0.36 ± 0.02 mm) were purchased from Beijing Shadong Biotechnology. Reverse transcription kit, SYBRGreen® PremixExTaq™ II kits were purchased from Takara.

Establishment of the Middle Cerebral Artery Occlusion/Reperfusion (MCAO) and Grouping

A total of 120 male Sprague-Dawley rats weighing 250 to 280 g were used in this study. Rats were randomly assigned resulting in five groups, each consisting of 24 rats:sham group,

middle cerebral artery ischemia-reperfusion group (MCAO), MCAO + dimethyl sulfoxide group (DMSO), MCAO + 1,25-D3 group (1,25-D3) and MCAO + 1,25-D3 + VDR antagonist (P5P, Pyridoxal-5-Phosphate) group (1,25-D3 + P5P). Rats from all the groups were subjected to a 90-min middle cerebral artery occlusion followed by reperfusion as previously described (10). The neurological function was scored according to the neurological deficit score established by Longa et al. (22). Grade 0: no neurological deficit; Grade I: mild focal neurological deficit (inability to fully extend the ischemic forelimb); Grade II: moderate focal neurological deficit (circling to the ischemic scar); Grade III: severe focal neurological deficit (dumping to the ischemic scar); Grade IV: lethargic and unable to walk spontaneously. Neurological severity scores of I to III were considered successful modeling, otherwise the corresponding number of rats was eliminated and supplemented. Rats of the 1,25-D3 group were administered intravenously with 1,25-D3 at a dose of 5 mg/kg (dissolved in 2% DMSO) 30 min before reperfusion, and the 1,25-D_3 + P5P group was administered intravenously with 1,25-D3 at a dose of 5 mg/kg (dissolved in 2% DMSO) and P5P at a dose of 0.4 mg/kg (dissolved in 0.9% NaCl). The same volume of DMSO was given in the DMSO group intravenously. The drug was given once a day for 3 consecutive days.

Cerebral Infarction Volume Assessment

After anesthesia, the brains were refrigerated at −20°C for 20 min and then consecutively sliced into coronal slices, each slice being about 2 mm thick. Then they were placed into 2%TTC and incubated at 37°C for 20 min. After staining, the brain slices were fixed overnight in 10% paraformaldehyde and photographed by camera. Image J was used to calculate the percentage of cerebral infarction volume. The percentage of cerebral infarct volume in rats (%) = (volume of the normal cerebral hemisphere - volume of the non-infarct cerebral hemisphere on the infarct side)/volume of the normal cerebral hemisphere *100%.

Cerebral Blood Flow Measurement

Cortical cerebral blood flow (CBF) was monitored by a laser speckle flow imaging technique 3 days after reperfusion. All procedures were performed under double-blind conditions. Briefly, rats were anesthetized and disinfected using iodophor, and the skull was exposed. The fascia attached to the skull was removed as much as possible and 0.9% saline was added to maintain the liquid level. Images and quantification of cerebral blood flow in the penumbra can be accessed by the laser speckle flow imaging technique (RFLSI III, RWD, China).

Immunofluorescence

The rats in each group were sacrificed 3 days after reperfusion and fixed for immunofluorescence of CD31 and IB4. Sections were incubated with 5% BSA for 1 h and then overnight with anti-CD31 antibody (1:200) at 4°C. After washing with PBST (0.1% Triton X-100 in 0.1 M PBS), fluorescent secondary antibody (1:500) and IB4 were incubated at room temperature for 1 h, then incubated with DAPI. Ultra-high resolution inverted fluorescence microscope (Stellaris5, Leica) was used for observation, and appropriate fluorescent light source was selected, and photos were taken. The vascular length and tip cell count was quantified by Image J.

Western Blot Analysis

The fresh tissue around the cerebral infarction was cryopreserved with liquid nitrogen, homogenized, centrifuged, and the total protein was extracted. The protein concentration was detected by BCA protein assay kit (Beyotime Biotechnology) and the 5 ug/ul system was prepared. Protein was boiled at 100°C for 5 min, then separated by SDS-PAGE and transferred to NC membrane

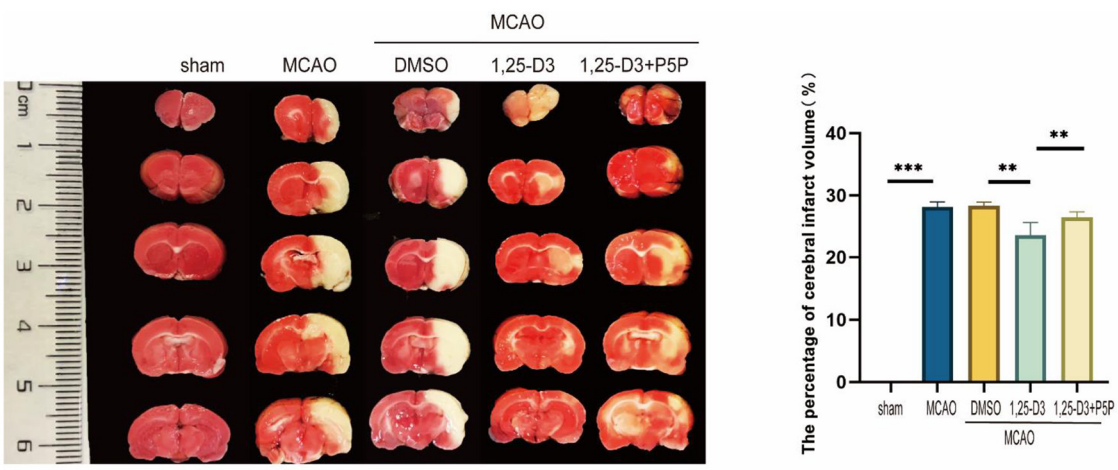

FIGURE 1 | 1,25-D3 reduced the volume of infarct regions in rats 3 days after stroke. Data were represented as Mean ± SEM, $n = 5$ per group, $^{*}p < 0.05$, $^{**}p < 0.005$, $^{***}p < 0.001$. MCAO, middle cerebral artery occlusion; DMSO, dimethyl sulfoxide; P5P, antagonist of VDR; 1,25-D3, 1α,25-dihydroxyvitamin D3.

(Cytiva). After incubated with 5% skimmed milk at room temperature for 2 h, incubated with the primary antibodies at 4°C overnight (1:1,000), incubated with the secondary antibodies at room temperature for 1 h (1: 10,000), and developed by ECL colorimetric method. The Image J was used to measure the gray value of the strip. The expression of the target protein band is expressed by the gray value of the target protein band/β-actin gray value.

Quantitative Real-Time PCR

Total RNA was extracted from peri-infarct tissues by Trizol. Complementary deoxyribonucleic acid (cDNA) was reverse

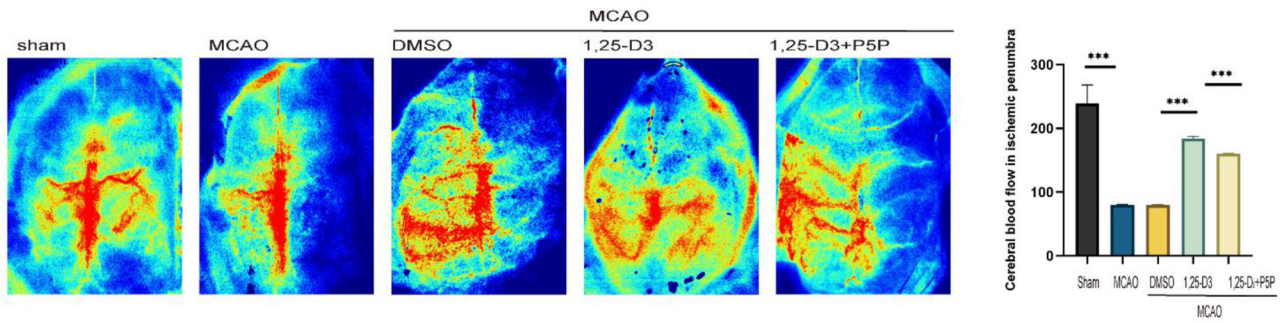

FIGURE 2 | 1,25-D3 increased cerebral blood flow of peri-infarcted cortex 3 days after stroke, and P5P partially reversed the neuroprotective effect. Data were represented as Mean ± SEM, $n = 5$ per group, $^{*}p < 0.05$, $^{**}p < 0.005$, $^{***}p < 0.001$. MCAO, middle cerebral artery occlusion; DMSO, dimethyl sulfoxide; P5P, antagonist of VDR; 1,25-D3, 1α,25-dihydroxyvitamin D3.

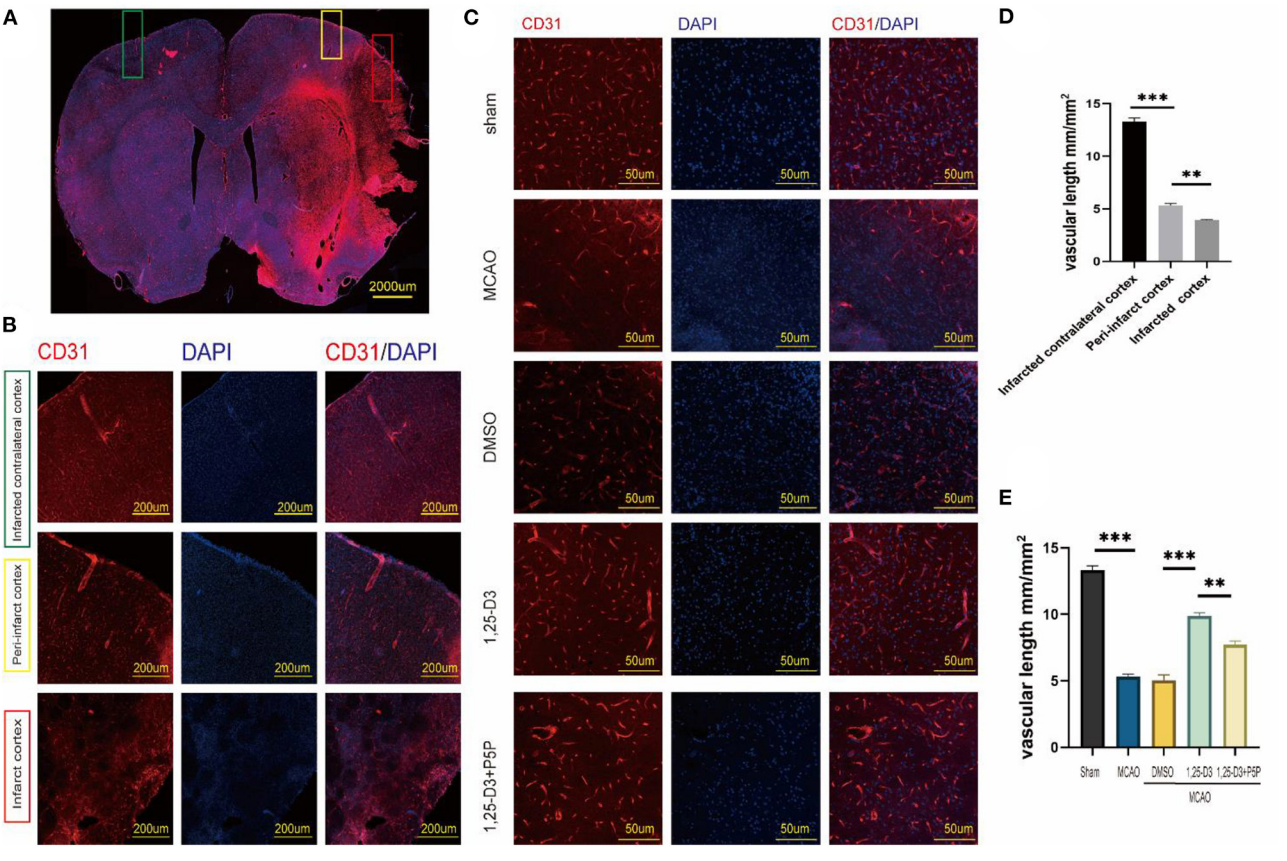

FIGURE 3 | 1,25-D3 increased the microvascular length and density and alleviated impairments induced by cerebral ischemic reperfusion 3 days after MCAO. **(A,B,D)** *In situ* expression of CD31 (red) and 4',6-diamidino-2-phenylindole (DAPI; blue) in different region of MCAO group (100× magnification 100). **(C,E)** *In situ* expression of CD31 (red) and 4',6-diamidino-2-phenylindole (DAPI; blue) in the peri-infarct region of sham, MCAO, DMSO, 1,25-D3 and 1,25-D3 + P5P groups (400× magnification 400). Data were represented as Mean ± SEM, $n = 5$ per group. $^{*}p < 0.05$, $^{**}p < 0.005$, $^{***}p < 0.001$. MCAO, middle cerebral artery occlusion; 1,25-D3, 1α,25-dihydroxyvitamin D3.

transcribed and used as a template for the reaction by fluorescence quantitative real-time PCR apparatus. The target gene fragment was amplified according to the steps of the Power SYBR Green PCR Master Mix kit (Takara). Real-time PCR reaction conditions were as follows: pre-denaturation at 95°C for 10 s, denaturation at 95°C for 5 s, annealing and extension at 60°C for 20 s, a total of 40 cycles. After the reaction was complete, the dissolution curve program was run to detect the specificity of the amplified products. The following primers were used: TGF-β1_*fwd* 5'-3': TGAGTGGCTGTCTTTTGACG, TGF-β1_*rev* 5'-3': GGTTCATGTCATGGATGGTG. TGF-β2_*fwd* 5'-3': GTGATTTCCATCTACAACAGTACC, TGF-β2_*rev* 5'-3': TATAAACCTCCTTGGCGTAGTAC; TGF-β3_*fwd* 5'-3': CCCAACCCCAGCTCCAAGCG; TGF-β3_*rev* 5'-3': AGCCACTCGCGCACAGTGTC; VDR_*fwd* 5'-3': CCACCGGCAGAAACGTGTAT; VDR_rev 5'-3': TGCCTTGTGAGAGGCTCTAGGA; VEGF_*fwd* 5'-3': CCGTCCTGTGTGCCCCTAATG; VEGF_*rev* 5'-3': CGCATGATCTGCATAGTGACGTTG; GAPDH_*fwd* 5'-3': GCATCTTCTTGTGCAGTGCC and GAPDH_*rev* 5'-3': TACGGCCAAAT CCGTTCACA.

Statistical Analysis

GraphPad Prism 5 (Graph Pad Software Inc, La Jolla, CA) was used to generate graphs and perform statistical analysis. Normal distribution was determined by the Kolmogorov-Smirnov test. One-way ANOVA was used for comparison among multiple groups, and Turkey's *post hoc* test was used for further pairwise comparison. Data were expressed as Mean ± SEM. Differences were considered statistically significant at $p < 0.05$.

RESULTS

1,25-D3 Significantly Reduced the Volume of Infarct Regions, Alleviated Brain Injury in Rats With Stroke

In order to confirm the effect of 1,25-D3 on stroke, we analyzed the volume of cerebral infarction 3 days after MCAO. Compared with sham group, the volume of cerebral infarction in MCAO group was significantly increased. There was no significant difference in cerebral infarction volume in DMSO and MCAO group. The cerebral infarct volume was decreased in 1,25-D3 group compared with the DMSO group. While it was more in 1,25-D3 + P5P group than 1,25-D3 group (**Figure 1**). It is suggested that 1,25-D3 treatment can significantly reduce the cerebral infarct volume and reduce the brain injury in stroke rats. VDR antagonist P5P partially reversed the neuroprotective effect of 1,25-D3.

1,25-D3 Promoted the Recovery of CBF After Ischemia-Reperfusion

We analyzed the CBF of peri-infarcted cortex in different groups of rats 3 days after ischemia-reperfusion using a laser speckle imaging system. The results showed that compared with the sham group, the CBF around the infarct cortex was significantly decreased in the MCAO group. Compared

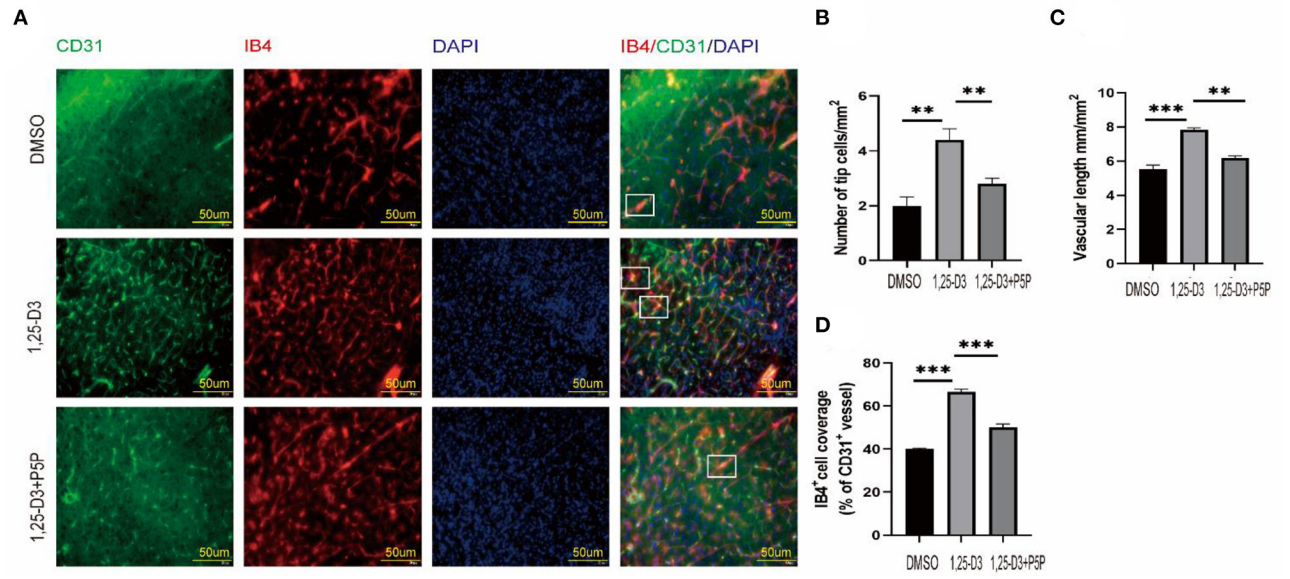

FIGURE 4 | 1,25-D3 increased neovascularization and improved vascular function 3 days after stroke. **(A)** *In situ* expression of CD31 (green), IB4 (red) and 4',6-diamidino-2-phenylindole (DAPI; blue) in the peri-infarct region of DMSO, 1,25-D3 and 1,25-D3 + P5P groups (400× magnification 400). Levels of $IB4^+$ tip cells **(B)**, $CD31^+$vascular length (mm/mm^2 of brain tissue) **(C),** and $IB4^+$cell coverage (area ratio of $IB4^+$ and $CD31^+$) **(D)** in the peri-infarct region of DMSO, 1,25-D3 and 1,25-D3 + P5P groups. Data were represented as Mean ± SEM. Data were represented as Mean ± SEM, $n = 5$ per group, $^*p < 0.05$, $^{**}p < 0.005$, $^{***}p < 0.001$. MCAO, middle cerebral artery occlusion; DMSO, dimethyl sulfoxide; P5P, antagonist of VDR; 1,25-D3, 1α,25-dihydroxyvitamin D3.

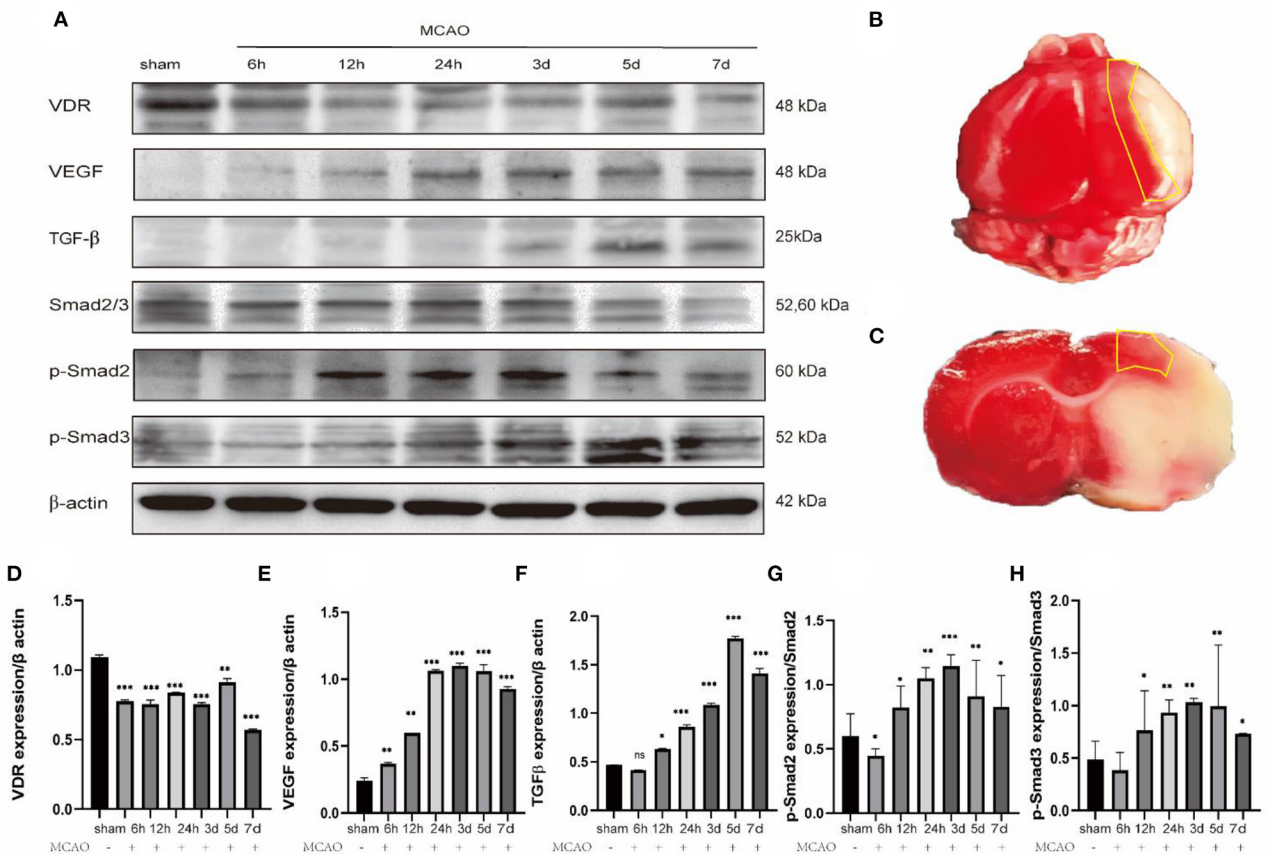

FIGURE 5 | Changes in the expression of relevant proteins at different time after ischemia reperfusion. **(A,D–H)** Western blots shows the expression levels of VDR, VEGF, TGF-β, Smad2/3, p-Smad2, p-Smad3 differ at different time after ischemia reperfusion in the ischemic penumbra cortex. Data were represented as Mean ± SEM, n =3 per group. $^{*}p < 0.05$, $^{**}p < 0.005$, $^{***}p < 0.001$. **(B,C)** The yellow box selection indicates the area of the ischemic penumbra.

with the DMSO group, the CBF at the infarct margin was increased in the 1,25-D3 group, which was decreased in the 1,25-D3 + P5P group (**Figure 2**). Namely, 1,25-D3 increased CBF recovery in ischemia-reperfusion rats, while VDR antagonist P5P partially reversed the neuroprotective effect of 1,25-D3.

1,25-D3 Increased Neovascularization and Improves Vascular Function After Stroke

The results of CD31 staining suggested that the length of vessel at various positions after ischemia-reperfusion differ. The microvascular length was longer than that in the infarct core area (**Figures 3A,B,D**). Comparison of different groups showed that the microvascular length was lower in the MCAO group than in the sham group, higher in the 1,25-D3 group than in the DMSO group. In addition, the microvascular length in 1,25-D3+P5P group was lower than in the 1,25-D3 group, suggesting that P5P can partially reduce the microvascular increase induced by 1,25-D3 (**Figures 3C,E**).

To further understand the role of 1,25-D3 in neovascular development, we used IB4 fluorescence staining to look for neovascular sprouting as it is a marker of angiogenesis after we have confirmed that 1,25-D3 could increase CD31-labeled microvascular density after ischemia-reperfusion. IB4 staining showed that 1,25-D3 increased IB4^{+} tip cells in the peri-infarct area while P5P reversed the improvement of vascular development induced by 1,25-D3 (**Figure 4**).

1,25-D3 Promotes the Expression of VDR, VEGF, and TGF-β/Smad2/3 Signal Pathway Proteins in MCAO Rats

In order to explore the angiogenic effects of 1,25-D3 on TGF-β/Smad2/3 signaling pathway, we analyzed the expression of VEGF, TGF-β/Smad2/3 and VDR at different time points: 6 h, 12 h, 24 h, 3 d, 5 d, 7 d after reperfusion. We found that compared with the sham group, the expression of VDR decreased gradually at 6 h after ischemia-reperfusion. VEGF increased gradually at 12 h after stroke, reaching the peak at 3 d and then decreased slowly. The expression of TGF-β increased gradually at 12 h after stroke and reached the peak at 5 d. The phosphorylation levels of Smad2 and Smad3 increased at 12 h after reperfusion, reached the peak at day 3 after reperfusion, and then decreased gradually (**Figure 5**). We chose 3 days after reperfusion as the time point to measure the expression of angiogenesis-related proteins induced by 1,25-D3. Results showed that the expression

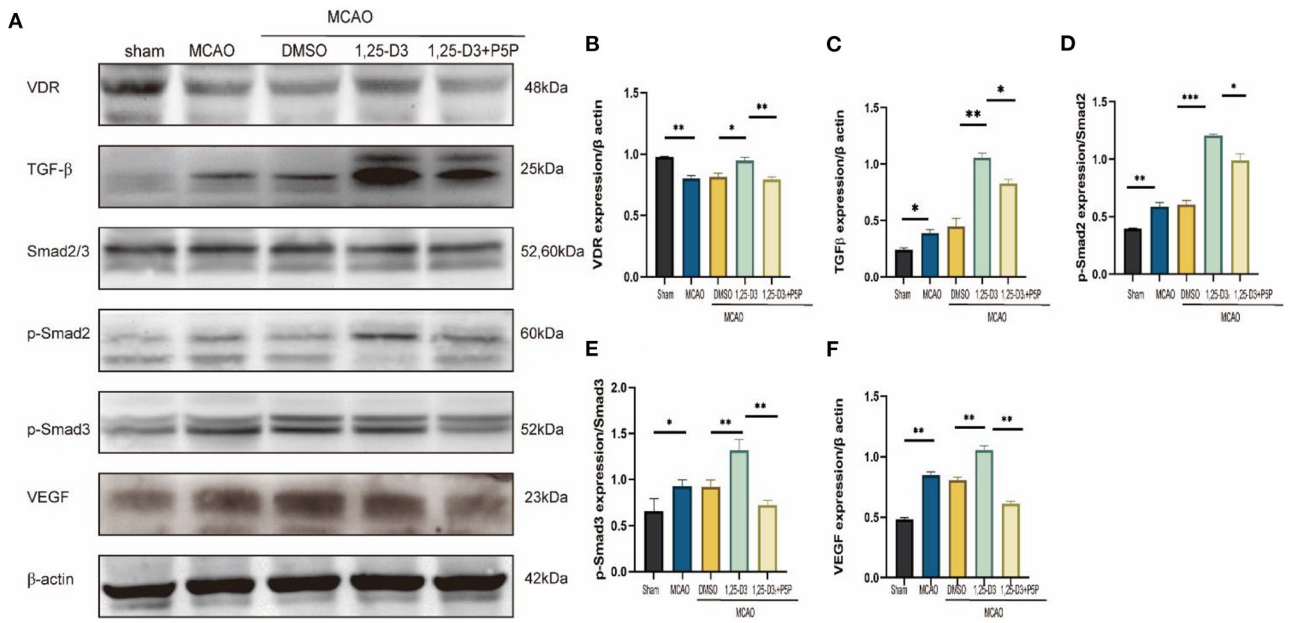

FIGURE 6 | 1,25-D3 promoted the expression of VDR, TGF-β, p-Smad2, p-Smad3, and VEGF induced by cerebral ischemic reperfusion 3 days after MCAO. **(A)** Western blot showed the expression of VDR, TGF-β, Smad2/3, p-Smad2, p-Smad3, VEGF in the ischemic penumbra cortex. Quantification of VDR **(B)**, TGF-β **(C)**, p-Smad2 **(D)**, p-Smad3 **(E)**, VEGF **(F)** in **(A)**. Data were represented as Mean ± SEM, $n = 3$ per group, $^{*}p < 0.05$, $^{**}p < 0.005$, $^{***}p < 0.001$. MCAO, middle cerebral artery occlusion; DMSO, dimethyl sulfoxide; P5P, antagonist of VDR; 1,25-D3, 1α,25-dihydroxyvitamin D3.

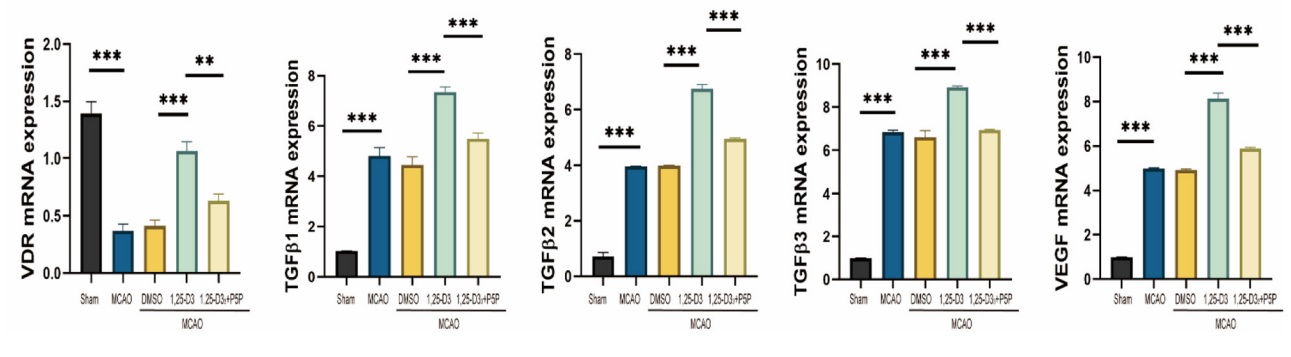

FIGURE 7 | The expression of VDR, VEGF and TGF-β1, TGF-β2, TGF-β3 mRNA in MCAO rats increased after pretreatment with 1,25-D3. Data were represented as Mean ± SEM, $n = 5$ per group, $^{*}p < 0.05$, $^{**}p < 0.005$, $^{***}p < 0.001$. MCAO, middle cerebral artery occlusion; DMSO, dimethyl sulfoxide; P5P, antagonist of VDR; 1,25-D3, 1α,25-dihydroxyvitamin D3.

of VDR, TGF-β, p-Smad2/Smad2, p-Smad3/Smad3, and VEGF in the periinfarcted cortex was significantly higher than DMSO group 3 days after stroke. The effect can be partially reversed by P5P. These results were confirmed by western blotting (**Figure 6**).

The Expression of VDR, VEGF, and TGF-β1, TGF-β2, TGF-β3 mRNA in MCAO Rats Was Increased After Pretreatment With 1,25-D3

RT-qPCR analysis reveals the expression of VDR, TGF-β1, TGF-β2, TGF-β3, and VEGF mRNA levels in the peri-infarct cortex after 1,25-D3 treatment. The results showed that compared with the sham group, the expression of VDR mRNA decreased in MCAO rats. 1,25-D3 activated the VDR, TGF-β1, TGF-β2, TGF-β3 and VEGF mRNA level induced by ischemia, while the increase was partially reversed by P5P treatment (**Figure 7**). Therefore, 1,25-D3 promotes angiogenesis after stroke by activating VDR, thus promotes the activation of TGF-β subtypes and the expression of VEGF mRNA.

DISCUSSION

The strength and novelty of present study was that we demonstrated a salutary effect of 1,25-D3 on angiogenesis after ischemia stroke. 1,25-D3 activated VDR then up-regulated TGF-β/Smad2/3 signaling pathway and enhanced VEGF production,

which contribute to promoting angiogenesis and improving stroke outcomes in rats after stroke.

We confirmed that 1,25-D3 reduces infarct volume and has a neuroprotective effect after cerebral ischemia injury in rats by TTC staining. Since our group previously demonstrated that 1,25-D3 reduces infarct size and attenuates neuronal cell death via PPAR-γ during cerebral ischemia (10). What is more, we find that 1,25-D3 can increase the CBF. As shown by CD31 and IB4 staining, micro-vascular density and length in the peri-infarct cortex was significantly higher in the 1,25-D3 group than in the DMSO and 1,25-D3 + P5P group, which has accompanied by increase in the number of new vessel sprouts, thereby playing a role in promoting angiogenesis. Compensatory angiogenesis and new capillaries improve blood perfusion around the ischemic area, providing a suitable microenvironment for nerve cell repair and promoting the recovery of neurological function after ischemic stroke (23). However, compensatory angiogenesis is often insufficient (24, 25). In order to explore the possible mechanism of promoting angiogenesis, we analyzed the expression of VDR, VEGF, TGF-β, and Smad2/3 at different time points after ischemia-reperfusion. At the end, we found that the expression of the corresponding proteins differs at different time points after ischemia-reperfusion. In western blot and RT-qPCR, we were surprised to find that 1,25-D3 could promote the expression of VDR, VEGF and TGF-β signaling pathway proteins 3 days after infarction. Because of this, we speculate that the proangiogenic effect of 1,25-D3 may be related to the TGF-β/Smad2/3 signaling pathway. Previous studies have shown that 1,25-D3 can promote the activation of PPAR-γ, while PPAR-γ and TGF-β are involved in the regulation of angiogenesis in the central nervous system (26, 27). Our results showed that reduction of VDR expression was strongly up-regulated by 1,25-D3 in rats under the condition of ischemia-reperfusion. VDR affects downstream proteins by inducing TGF-β/Smad2/3 signaling pathway. In response to 1,25-D3, the TGF-β/Smad2/3 signaling pathway is enhanced and acts as its activator to regulate downstream signaling (28–30). A large body of literature suggests that TGF-β, its receptors, and mediators of its downstream signaling are attractive targets for therapeutic interventions (20, 31, 32). TGF-β exerts its effects on effects mainly by upregulating the expression of proteins through TGF-β/Smad2/3 signaling (30, 33–35).

Lack of 1,25-D3 is a decisive causative factor in several neurodegenerative and neuropsychiatric disorders (36, 37). Once 1,25-D3 linked to the VDR, abundant biological effects can be exerted (8, 38). Mounting evidences have shown that 1,25-D3 plays a critical role in the process of stroke, including regulating the expression of neurotrophic factors and hormonal (36, 39, 40). It is involved in immune cell differentiation, gut microbiota modulation, gene transcription, blood-brain barrier integrity and so on (36, 39, 41). Further studies are needed to validate TGF-β isoforms, and their receptor subtypes involved in the TGF-β/Smad2/3 pathway.

In conclusion, we have demonstrated that 1,25-D3 promotes angiogenesis of the cortex around the ischemic boundary zone. Our results suggest that 1,25-D3 promotes angiogenesis by up-regulating TGF-β/Smad2/3 signaling pathway via VDR activation, thereby alleviating ischemia/reperfusion injury and improving stroke outcomes in rats.

Our study has several limitations to be resolved in the future. In this study, we show the effect of 1,25-D3 act on TGF-β/Smad2/3 in stroke. While TGF-β has several subtypes as TGF-β1 TGF-β2, TGF-β3 and so on. Future work should extend to the mechanism study for detail. In addition, no VDR overexpression group was set up in this study, and the effect of VDR was verified only by the antagonist group, thus plasmid construction will be performed in the next assay. Moreover, few studies address the effect of 1,25-D3 response on long-term outcome during late stage of stroke. Therefore, future studies are required to determine the potential impact of 1,25-D3 during stroke recovery.

DATA AVAILABILITY STATEMENT

The original contributions presented in the study are included in the article/**Supplementary Material**, further inquiries can be directed to the corresponding author/s.

ETHICS STATEMENT

The animal study was reviewed and approved by the Animal Ethics Committee of Xuzhou Medical University (protocol: 202007A102).

AUTHOR CONTRIBUTIONS

Main manuscript text was written by YZ and YM. YZ, YM, HD, BD, MZ, QL, SG, and FZ performed the experiments and data analysis. DG and YW designed the study and revised the manuscript. All authors approved the final version of this manuscript.

FUNDING

This work was supported by the National Natural Science Foundation of China (No. 81870943) and the Shandong Provincial Nature Fund Joint Special Fund Project (ZR2018LH006).

SUPPLEMENTARY MATERIAL

The Supplementary Material for this article can be found online at: https://www.frontiersin.org/articles/10.3389/fcvm.2022.769717/full#supplementary-material

REFERENCES

1. Hayashi T, Abe K, Suzuki H, Itoyama Y. Rapid induction of vascular endothelial growth factor gene expression after transient middle cerebral artery occlusion in rats. *Stroke.* (1997) 28:2039–44. doi: 10.1161/01.STR.28.10.2039
2. Catanese L, Tarsia J, Fisher M. Acute ischemic stroke therapy overview. *Circ Res.* (2017) 120:541–58. doi: 10.1161/CIRCRESAHA.116.309278
3. Gonzalez-Nieto D, Fernandez-Serra R, Perez-Rigueiro J, Panetsos F, Martinez-Murillo R, Guinea GV. Biomaterials to neuroprotect the stroke brain: a large opportunity for narrow time windows. *Cells.* (2020) 9:1074. doi: 10.3390/cells9051074
4. Thomalla G, Simonsen CZ, Boutitie F. MRI-Guided thrombolysis for stroke with unknown time of onset. *New Engl J Med.* (2018) 379:611–22. doi: 10.1056/NEJMoa1804355
5. Broderick JP, Hill MD. Advances in acute stroke treatment 2020. *Stroke.* (2021) 52:729–34. doi: 10.1161/STROKEAHA.120.033744
6. Brozyna AA, Jozwicki W, Slominski AT. Decreased VDR expression in cutaneous melanomas as marker of tumor progression: new data and analyses. *Anticancer Res.* (2014) 34:2735–43. doi: 10.1093/annonc/mdu137
7. Chen J, Tang Z, Slominski AT, Li W, Zmijewski MA, Liu Y, et al. Vitamin D and its analogs as anticancer and anti-inflammatory agents. *Eur J Med Chem.* (2020) 207:112738. doi: 10.1016/j.ejmech.2020.112738
8. Mori T, Horibe K, Koide M, Uehara S, Yamamoto Y, Kato S, et al. The Vitamin D receptor in osteoblast-lineage cells is essential for the proresorptive activity of 1alpha,25(OH)2D3 *in vivo*. *Endocrinology.* (2020) 161:bqaa178. doi: 10.1210/endocr/bqaa178
9. Daubail B, Jacquin A, Guilland JC, Hervieu M, Osseby GV, Rouaud O, et al. Serum 25-hydroxyvitamin D predicts severity and prognosis in stroke patients. *Eur J Neurol.* (2013) 20:57–61. doi: 10.1111/j.1468-1331.2012.03758.x
10. Guo T, Wang Y, Guo Y, Wu S, Chen W, Liu N, et al. 1, 25-D3 protects from cerebral ischemia by maintaining BBB permeability via PPAR-γ activation. *Front Cell Neurosci.* (2018) 12:480. doi: 10.3389/fncel.2018.00480
11. Amani H, Mostafavi E, Alebouyeh MR, Arzaghi H, Akbarzadeh A, Pazoki-Toroudi H, et al. Would colloidal gold nanocarriers present an effective diagnosis or treatment for ischemic stroke? *Int J Nanomed.* (2019) 14:8013–31. doi: 10.2147/IJN.S210035
12. Rosenstein JM, Mani N, Silverman WF, Krum JM. Patterns of brain angiogenesis after vascular endothelial growth factor administration *in vitro* and *in vivo*. *Proc Natl Acad Sci USA.* (1998) 95:7086–91. doi: 10.1073/pnas.95.12.7086
13. Wang Z, Tsai LK, Munasinghe J, Leng Y, Fessler EB, Chibane F, et al. Chronic valproate treatment enhances postischemic angiogenesis and promotes functional recovery in a rat model of ischemic stroke. *Stroke.* (2012) 43:2430–6. doi: 10.1161/STROKEAHA.112.652545
14. Wesley UV, Sutton IC, Cunningham K, Jaeger JW, Phan AQ, Hatcher JF, et al. Galectin-3 protects against ischemic stroke by promoting neuro-angiogenesis via apoptosis inhibition and Akt/Caspase regulation. *J Cereb Blood Flow Metab.* (2021) 41:857–73. doi: 10.1177/0271678X20931137
15. Fang L, Li Y, Wang S, Li Y, Chang HM, Yi Y, et al. TGF-beta1 induces VEGF expression in human granulosa-lutein cells: a potential mechanism for the pathogenesis of ovarian hyperstimulation syndrome. *Exp Mol Med.* (2020) 52:450–60. doi: 10.1038/s12276-020-0396-y
16. Lai TH, Chen HT, Wu WB. TGFbeta1 induces *in-vitro* and *ex-vivo* angiogenesis through VEGF production in human ovarian follicular fluid-derived granulosa cells during *in-vitro* fertilization cycle. *J Reprod Immunol.* (2021) 145:103311. doi: 10.1016/j.jri.2021.103311
17. Maharaj AS, Walshe TE, Saint-Geniez M, Venkatesha S, Maldonado AE, Himes NC, et al. VEGF and TGF-beta are required for the maintenance of the choroid plexus and ependyma. *J Exp Med.* (2008) 205:491–501. doi: 10.1084/jem.20072041
18. Liakouli V, Elies J, El-Sherbiny YM, Scarcia M, Grant G, Abignano G, et al. Scleroderma fibroblasts suppress angiogenesis via TGF-beta/caveolin-1 dependent secretion of pigment epithelium-derived factor. *Ann Rheum Dis.* (2018) 77:431–40. doi: 10.1136/annrheumdis-2017-212120
19. Nanda V, Downing KP, Ye J, Xiao S, Kojima Y, Spin JM, et al. CDKN2B regulates TGFbeta signaling and smooth muscle cell investment of hypoxic neovessels. *Circ Res.* (2016) 118:230–40. doi: 10.1161/CIRCRESAHA.115.307906
20. Kim R, Song BW, Kim M, Kim WJ, Lee HW, Lee MY, et al. Regulation of alternative macrophage activation by MSCs derived hypoxic conditioned medium, via the TGF-beta1/Smad3 pathway. *Bmb Rep.* (2020) 53:600–4. doi: 10.5483/BMBRep.2020.53.11.177
21. Ashrafizadeh M, Najafi M, Orouei S, Zabolian A, Saleki H, Azami N, et al. Resveratrol modulates transforming growth factor-beta (TGF-beta) signaling pathway for disease therapy: a new insight into its pharmacological activities. *Biomedicines.* (2020) 8:261. doi: 10.3390/biomedicines8080261
22. Longa EZ, Weinstein PR, Carlson S, Cummins R. Reversible middle cerebral artery occlusion without craniectomy in rats. *Stroke.* (1989) 20:84–91. doi: 10.1161/01.STR.20.1.84
23. Wlodarczyk L, Szelenberger R, Cichon N, Saluk-Bijak J, Bijak M, Miller E. Biomarkers of angiogenesis and neuroplasticity as promising clinical tools for stroke recovery evaluation. *Int J Mol Sci.* (2021) 22:3949. doi: 10.3390/ijms22083949
24. Mao Y, Liu X, Song Y, Zhai C, Zhang L. VEGF-A/VEGFR-2 and FGF-2/FGFR-1 but not PDGF-BB/PDGFR-β play important roles in promoting immature and inflammatory intraplaque angiogenesis. *Plos ONE.* (2018) 13:e201395. doi: 10.1371/journal.pone.0201395
25. Navarro-Sobrino M, Hernandez-Guillamon M, Fernandez-Cadenas I, Ribo M, Romero IA, Couraud PO, et al. The angiogenic gene profile of circulating endothelial progenitor cells from ischemic stroke patients. *Vasc Cell.* (2013) 5:3. doi: 10.1186/2045-824X-5-3
26. Madani NA, Nasseri MS, Saberi PM, Golmohammadi S, Nazarinia D, Aboutaleb N. Donepezil attenuates injury following ischaemic stroke by stimulation of neurogenesis, angiogenesis, and inhibition of inflammation and apoptosis. *Inflammopharmacology.* (2021) 29:153–66. doi: 10.1007/s10787-020-00769-5
27. Kanazawa M, Takahashi T, Ishikawa M, Onodera O, Shimohata T, Del ZG. Angiogenesis in the ischemic core: a potential treatment target? *J Cereb Blood Flow Metab.* (2019) 39:753–69. doi: 10.1177/0271678X19834158
28. Zhou Q, Qin S, Zhang J, Zhon L, Pen Z, Xing T. 1,25(OH)2D3 induces regulatory T cell differentiation by influencing the VDR/PLC-gamma1/TGF-beta1/pathway. *Mol Immunol.* (2017) 91:156–64. doi: 10.1016/j.molimm.2017.09.006
29. Lv Y, Han X, Yao Q, Zhang K, Zheng L, Hong W, et al. 1α,25-dihydroxyvitamin D3 attenuates oxidative stress-induced damage in human trabecular meshwork cells by inhibiting TGFβ-SMAD3-VDR pathway. *Biochem Bioph Res Co.* (2019) 516:75–81. doi: 10.1016/j.bbrc.2019.06.027
30. Peng L, Yin J, Wang S, Ge M, Han Z, Wang Y, et al. TGF-beta2/Smad3 signaling pathway activation through enhancing VEGF and CD34 ameliorates cerebral ischemia/reperfusion injury after isoflurane post-conditioning in rats. *Neurochem Res.* (2019) 44:2606–18. doi: 10.1007/s11064-019-02880-8
31. Zhu H, Gui Q, Hui X, Wang X, Jiang J, Ding L, et al. TGF-beta1/Smad3 signaling pathway suppresses cell apoptosis in cerebral ischemic stroke rats. *Med Sci Monit.* (2017) 23:366–76. doi: 10.12659/MSM.899195
32. Yang L, Wu L, Zhang X, Hu Y, Fan Y, Ma J. 1,25(OH)2D3/VDR attenuates high glucoseinduced epithelialmesenchymal transition in human peritoneal mesothelial cells via the TGFbeta/Smad3 pathway. *Mol Med Rep.* (2017) 15:2273–9. doi: 10.3892/mmr.2017.6276
33. Zhang W, Zhang X, Zhang Y, Qu C, Zhou X, Zhang S. Histamine induces microglia activation and the release of proinflammatory mediators in rat brain via H1R or H4R. *J Neuroimmune Pharm.* (2020) 15:280–91. doi: 10.1007/s11481-019-09887-6
34. Tu JH, Xu Y, Dai Y, Dang L. Effect of alprostadil on myocardial fibrosis in rats with diabetes mellitus via TGF-beta1/Smad signaling pathway. *Eur Rev Med Pharmacol Sci.* (2019) 23:9633–41. doi: 10.26355/eurrev_201911_19457
35. Zhou XL, Fang YH, Wan L, Xu QR, Huang H, Zhu RR, et al. Notch signaling inhibits cardiac fibroblast to myofibroblast transformation by antagonizing TGF-beta1/Smad3 signaling. *J Cell Physiol.* (2019) 234:8834–45. doi: 10.1002/jcp.27543
36. Nissou MF, Guttin A, Zenga C, Berger F, Issartel JP, Wion D. Additional clues for a protective role of vitamin D in neurodegenerative diseases: 1,25-dihydroxyvitamin D3 triggers an anti-inflammatory response in brain pericytes. *J Alzheimers Dis.* (2014) 42:789–99. doi: 10.3233/JAD-140411

37. Bao Z, Wang X, Li Y, Feng F. Vitamin D alleviates cognitive dysfunction by activating the VDR/ERK1/2 signaling pathway in an Alzheimer's disease mouse model. *Neuroimmunomodulat.* (2021) 27:178–85. doi: 10.1159/000510400
38. Jamali N, Song YS, Sorenson CM, Sheibani N. 1,25(OH)2D3 regulates the proangiogenic activity of pericyte through VDR-mediated modulation of VEGF production and signaling of VEGF and PDGF receptors. *FASEB Bioadv.* (2019) 1:415–34. doi: 10.1096/fba.2018-00067
39. Won S, Sayeed I, Peterson BL, Wali B, Kahn JS, Stein DG. Vitamin D prevents hypoxia/reoxygenation-induced blood-brain barrier disruption via vitamin D receptor-mediated NF-kB signaling pathways. *PloS ONE.* (2015) 10:e122821. doi: 10.1371/journal.pone.0122821
40. Haussler MR, Jurutka PW, Mizwicki M, Norman AW. Vitamin D receptor (VDR)-mediated actions of 1α,25(OH)2vitamin D3: Genomic and non-genomic mechanisms. *Best Pract Res Cl En.* (2011) 25:543–59. doi: 10.1016/j.beem.2011.05.010
41. Battistini C, Ballan R, Herkenhoff ME, Saad S, Sun J. Vitamin D modulates intestinal microbiota in inflammatory Bowel diseases. *Int J Mol Sci.* (2020) 22:362. doi: 10.3390/ijms22010362

Conflict of Interest: The authors declare that the research was conducted in the absence of any commercial or financial relationships that could be construed as a potential conflict of interest.

Publisher's Note: All claims expressed in this article are solely those of the authors and do not necessarily represent those of their affiliated organizations, or those of the publisher, the editors and the reviewers. Any product that may be evaluated in this article, or claim that may be made by its manufacturer, is not guaranteed or endorsed by the publisher.

Copyright © 2022 Zhang, Mu, Ding, Du, Zhou, Li, Gong, Zhang, Geng and Wang. This is an open-access article distributed under the terms of the Creative Commons Attribution License (CC BY). The use, distribution or reproduction in other forums is permitted, provided the original author(s) and the copyright owner(s) are credited and that the original publication in this journal is cited, in accordance with accepted academic practice. No use, distribution or reproduction is permitted which does not comply with these terms.

frontiers in Cardiovascular Medicine

REVIEW
published: 16 March 2022
doi: 10.3389/fcvm.2022.802783

Noble Gases Therapy in Cardiocerebrovascular Diseases: The Novel Stars?

Jiongshan Zhang[1,2], *Wei Liu*[3,4], *Mingmin Bi*[5], *Jinwen Xu*[3,4], *Hongzhi Yang*[1,2*] and *Yaxing Zhang*[3,4*†]

[1] Department of Traditional Chinese Medicine, The Third Affiliated Hospital, Sun Yat-sen University, Guangzhou, China, [2] Institute of Integrated Traditional Chinese and Western Medicine, Sun Yat-sen University, Guangzhou, China, [3] Department of Physiology, School of Basic Medical Sciences, Guangzhou University of Chinese Medicine, Guangzhou, China, [4] Research Centre for Integrative Medicine (Key Laboratory of Chinese Medicine Pathogenesis and Therapy Research), Guangzhou University of Chinese Medicine, Guangzhou, China, [5] Department of Otorhinolaryngology, The Seventh Affiliated Hospital, Sun Yat-sen University, Shenzhen, China

OPEN ACCESS

Edited by:
Anne-Clémence Vion, INSERM U1087 L'unité de recherche de l'institut du thorax, France

Reviewed by:
Jerzy Beltowski, Medical University of Lublin, Poland
Jack Lancaster, University of Pittsburgh, United States

***Correspondence:**
Yaxing Zhang
zhangyaxing@gzucm.edu.cn
Hongzhi Yang
yanghzhi@mail.sysu.edu.cn

†Lead Contact

Specialty section:
This article was submitted to Atherosclerosis and Vascular Medicine, a section of the journal Frontiers in Cardiovascular Medicine

Received: *27 October 2021*
Accepted: *18 January 2022*
Published: *16 March 2022*

Citation:
Zhang J, Liu W, Bi M, Xu J, Yang H and Zhang Y (2022) Noble Gases Therapy in Cardiocerebrovascular Diseases: The Novel Stars? Front. Cardiovasc. Med. 9:802783. doi: 10.3389/fcvm.2022.802783

Cardiocerebrovascular diseases (CCVDs) are the leading cause of death worldwide; therefore, to deeply explore the pathogenesis of CCVDs and to find the cheap and efficient strategies to prevent and treat CCVDs, these are of great clinical and social significance. The discovery of nitric oxide (NO), as one of the endothelium-derived relaxing factors and its successful utilization in clinical practice for CCVDs, provides new ideas for us to develop drugs for CCVDs: "gas medicine" or "medical gases." The endogenous gas molecules such as carbon monoxide (CO), hydrogen sulfide (H_2S), sulfur dioxide (SO_2), methane (CH_4), and hydrogen (H_2) have essential biological effects on modulating cardiocerebrovascular homeostasis and CCVDs. Moreover, it has been shown that noble gas atoms such as helium (He), neon (Ne), argon (Ar), krypton (Kr), and xenon (Xe) display strong cytoprotective effects and therefore, act as the exogenous pharmacologic preventive and therapeutic agents for CCVDs. Mechanistically, besides the competitive inhibition of N-methyl-D-aspartate (NMDA) receptor in nervous system by xenon, the key and common mechanisms of noble gases are involved in modulation of cell death and inflammatory or immune signals. Moreover, gases interaction and reduction in oxidative stress are emerging as the novel biological mechanisms of noble gases. Therefore, to investigate the precise actions of noble gases on redox signals, gases interaction, different cell death forms, and the emerging field of gasoimmunology, which focus on the effects of gas atoms/molecules on innate immune signaling or immune cells under both the homeostatic and perturbed conditions, these will help us to uncover the mystery of noble gases in modulating CCVDs.

Keywords: helium (He), neon (Ne), argon (Ar), krypton (Kr), xenon (Xe), cardiovascular diseases, cerebrovascular disease, gasoimmunology

INTRODUCTION

Cardiovascular diseases (CVDs) are a group of disorders of heart and blood vessels, CVDs include primary hypertension, pulmonary arterial hypertension, abdominal aortic aneurysm, coronary heart disease (CHD) (especially myocardial ischemia, which is primarily mediated by the buildup of atherosclerotic plaque in the blood vessels that supply oxygen and nutrients to the heart, coronary artery vasospasm, and coronary microvascular dysfunction) (1–4), congenital heart disease, valvular heart disease (e.g., rheumatic heart disease), myocarditis and inflammatory cardiomyopathy, diabetic cardiomyopathy, and other conditions, ultimately cardiac arrhythmias and/or heart failure; additionally, cerebrovascular diseases (CBVDs), a range of conditions influencing brain and cerebral arteries, e.g., ischemic stroke, also belong to CVDs; therefore, CVDs also refer to as cardiocerebrovascular diseases (CCVDs) (5–13). Heart attack and stroke are the representative diseases of CCVDs (14). CCVDs are the leading cause of death globally and the statistical data from the WHO indicate that CCVDs take an estimated 17.9 million lives each year (15). Therefore, to deeply explore the pathogenesis of CCVDs and to find the cheap and efficient strategies to prevent/treat CCVDs, these are of great clinical and social significance.

The discovery of nitric oxide (NO), as one of the endothelium-derived relaxing factors (for which the Nobel Prize in Physiology or Medicine was awarded in 1998) and its successful clinical application in CCVDs, opens a new direction for the scientists to discover drugs for treating CCVDs: "medical gases" or "gas medicine" (16–18). For example, the endogenous gases, including carbon monoxide (CO), hydrogen sulfide (H_2S), sulfur dioxide (SO_2), methane (CH_4), and hydrogen (H_2, which is primarily produced by intestinal flora), have been shown to prevent or treat CCVDs in animals or in human body (19–32). Recently, noble gas family has emerged as the novel exogenous pharmacologic preventive and therapeutic agents for CCVDs (33–38). The aim of this comprehensive review is to summarize and discuss the current understanding of the biological effects and mechanisms of noble gases on CCVDs.

BASIC CHARACTERISTICS OF NOBLE GASES

The noble gases refer to the gas atoms corresponding to all the group 18 elements on the periodic table of the elements. This family constitutes six naturally occurring gases: helium (He), neon (Ne), argon (Ar), krypton (Kr), xenon (Xe), and the radioactive radon (Rn) (38) (**Figure 1**). Xe was first shown to possess anesthetic properties in 1951, whereas none of the other five noble gases show anesthetic properties under normobaric conditions (38, 39). At normal temperature and normal pressure,

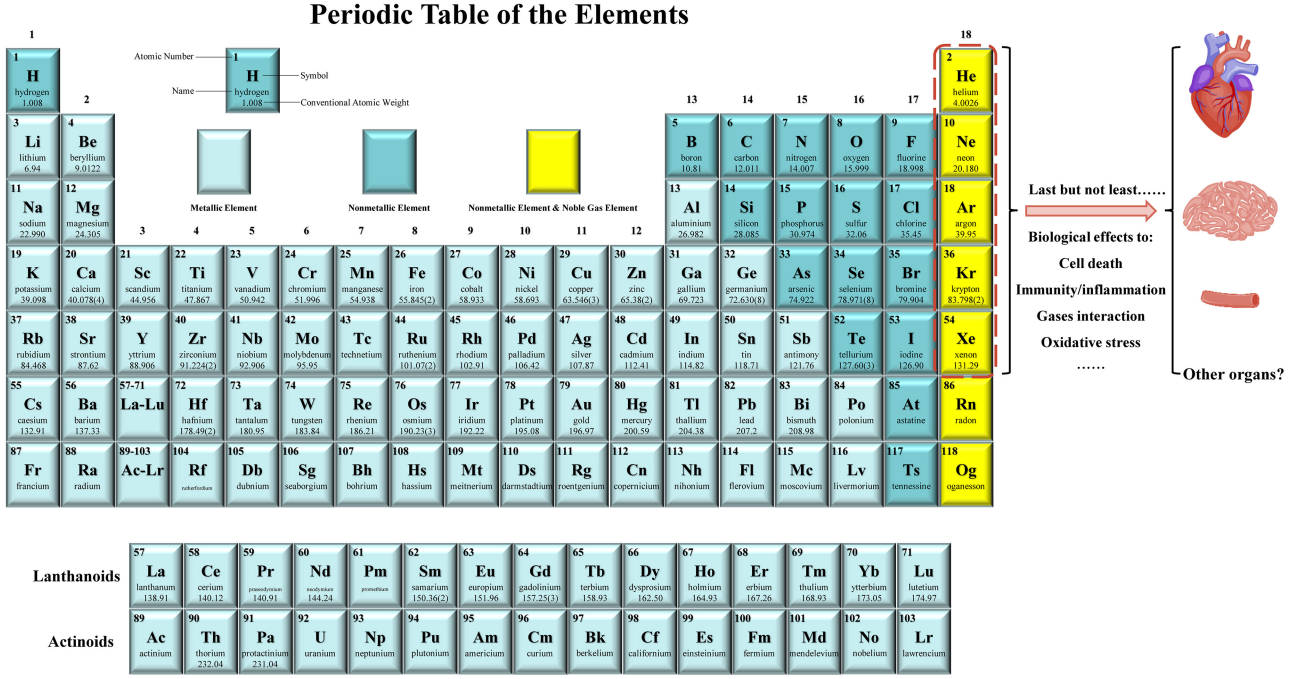

FIGURE 1 | Noble gases have emerged as the novel preventive and therapeutic agents for cardiocerebrovascular diseases (CCVDs). The noble gas family includes helium (He), neon (Ne), argon (Ar), krypton (Kr), xenon (Xe), and the radioactive radon (Rn). They are monatomic gases at the far right of the periodic table and are chemically inert. Last but not least, it has been shown that most of noble gases have essential biological effects, including modulation of cell death, immunity/inflammation, gases interaction, and oxidative stress. They have been acted as protectants for alleviating the injuries of heart, brain, blood vessels (e.g., endothelial cells), liver, kidney, and intestine in animal models or in human body. Therefore, noble gases therapy provides a novel idea for the prevention and treatment of CCVDs.

noble gases are odorless, colorless, and monatomic gases that are characterized by a filled outer shell of valence electrons, making them "inert" or at least less capable of interaction with other compounds; therefore, they are also known as "inert gases" (34–36, 38). However, some of these noble gases have strong biological activities such as the properties of neuroprotection and cardioprotection (34–36, 38).

NOBLE GASES: THE "NEW WORLD" OF CARDIOCEREBROVASCULAR PROTECTION

Helium

Helium is the second most abundant element in the universe after H_2; however, He is only sixth element in the composition of dry air (0.00052%) (40). It is the lightest noble gas with an atomic weight of 4 g/mol and has the lowest melting (−458°F, −272.2°C) and boiling (−452.1°F, −268.9°C) points of all the elements (36, 40). Due to the lower density and viscosity, heliox-21 (21% oxygen and 79% helium), which weight is one-third compared with air, can reduce work of breathing; therefore, heliox has been reported to be effective in a variety of respiratory conditions, including asthma exacerbation, post-extubation stridor, croup, upper airway obstruction, bronchiolitis, acute respiratory distress syndrome (ARDS), chronic obstructive pulmonary disease (COPD), and pulmonary function testing (36, 40, 41). He has the lower solubility than nitrogen; the mixture of helium and oxygen rather than nitrogen and oxygen decreases the formation of nitrogen bubbles and, therefore, alleviating decompression illness in deep-sea divers (41). Moreover, He is safe for abdominal insufflation and may be the insufflating agent of choice in patients with significant cardiopulmonary disease and laparoscopic renal surgery (42–44). He inhalation enhanced vasodilator effect of inhaled NO on pulmonary vessels in hypoxic dogs; this enhanced vasodilatory effect of NO on He might be associated with facilitated diffusion of NO diluted in the gas mixture with He (45). In the past decade, a series of studies showed that He has essential cytoprotective effects on endothelial cells (ECs) (46–48), heart (49–60), brain (59, 61–67), liver (68), and intestine (69).

Helium in Endothelial Protection

Caveolin-1 (Cav-1) was secreted after He exposure *in vitro*, altered the cytoskeleton, and increased the adherent junction protein vascular endothelial-cadherin (VE-cadherin) and gap junction protein connexin 43 (Cx43) expression thus, resulting in decreased permeability in ECs (47). These indicated that He protected endothelium by maintaining barrier function and preventing leakage and tissue edema and ultimately preserving endothelial function (47). Furthermore, the plasma of healthy volunteers breathing He protected ECs against hypoxic cell damage by increasing Cav-1 expression and Cav-1 knockdown in ECs abolished this effect (48); the interesting question is what contents from the plasma contribute to these effects. However, another study showed that pretreating with He increased ECs damage *in vitro* under the stimulation of tumor necrosis factor-α (TNF-α) or hydrogen peroxide (H_2O_2) (70).

Helium can induce preconditioning in human endothelium *in vivo*: inhalation of 3 cycles of heliox21 for 5 min, followed by 5 min of normal air breathing either directly before forearm ischemia (20 min) or 24 h before forearm ischemia (20 min), attenuated ischemia-reperfusion (I/R)-induced endothelial dysfunction independent of endothelial NO synthase (eNOS), as that the protection of He was not abolished after blockade of eNOS (46). However, *Eliana Lucchinetti* et al. (71) showed that heliox-50 (50% helium and 50% oxygen), breathing from 15 min before ischemia until 5 min after the onset of reperfusion, provided modest anti-inflammatory effects, but did not restore endothelial dysfunction of the forearm in humans *in vivo*. A case report indicated that accidental inhalation of He under high pressure can cause symptomatic cerebral and coronary artery gas embolism (72). Therefore, the concentration, time, and mode (continuously or intermittently) of supplying He, the different pathological stimuli, and *in vivo* and *in vitro* might be responsible for the above controversies.

Helium in Cardioprotection

Helium preconditioning (HePC) can considerably reduce infarct size in myocardial I/R injury model of rabbits, young rats but not aged rats, Zucker lean rat but not Zucker obese rats (49–51, 73) (**Table 1**). These He-induced cardioprotection are related to activating phosphoinositide 3-kinase (PI3K), p44/42 mitogen-activated protein kinase (MAPK) (ERK1/2), p70S6 kinase (p70s6K), cyclic AMP (cAMP)-dependent protein kinase (PKA), cyclooxygenase-2 (COX-2), opioid receptors, mitochondrial Ca^{2+}-sensitive potassium channel, and mitochondrial ATP-regulated potassium (KATP) channels (possibly producing small quantities of ROS); inhibiting mitochondrial permeability transition pore (mPTP) opening and NO production by eNOS (49, 50, 53, 73–76, 78). Moreover, suppression of glycogen synthase kinase-3 (GSK-3) or p53 lowered the threshold of He-induced preconditioning *via* the mPTP-dependent mechanism *in vivo* (77). He also induced post-conditioning in the myocardial I/R injury model of Zucker lean rats or male Wistar rats, these protective effects on Wistar rats are related to increasing genes involved in autophagy, inhibiting genes involved in apoptosis, increasing protein levels of Cav-1/3, and activating ERK1/2 and Akt (51, 56, 57) (**Table 1**). However, inhaled 30 or 60 min of 70% He during reperfusion dose does not induce cardioprotection in male adult Wistar rats (55). This process was not accompanied by reducing the hyperacute burst of inflammatory cytokines, but the prolonged He inhalation might contribute to the proinflammatory response, such as increasing cytokine-induced neutrophil chemoattractant 3 (CINC-3) and interleukin-1β (IL-1β) in myocardium from area at risk, but not from area not at risk (55). Moreover, one clinical investigation indicated that HePC (3 × 5 min of 70% He and 30% oxygen was applied before aortic cross-clamping), helium post-conditioning (15 min of He was applied before release of the aortic cross-clamp and was continued for 5 min after begin of reperfusion) or the combination had no effects on the activation of p38 MAPK, ERK1/2, or on the levels of protein kinase C-epsilon (PKC-ε)

TABLE 1 | Noble gases alleviate myocardial ischemia/reperfusion (I/R) injury in animal models.

Noble gases	Animals	Doses and Time	Key Results	References
Helium	Male New Zealand white rabbits (2.5–3.0 kg)	Rabbits received 1, 3 or 5 cycles of 70% He-30% O_2 for 5 min interspersed with 5 min of 70% N_2-30% O_2 or an air-oxygen mixture before ischemia	Reduced infarct size	(49–51, 53, 54, 56, 57, 73–78)
	Young male Hannover Wistar rats (352 ± 15 g)	Rats received 70% He-30% O_2 for three 5-min periods, interspersed with two 5-min washout periods 10 min before ischemia		
	Male Wistar rats (~328 g)	Rats received 70% He-30% O_2, 50% He-30% O_2-20% N_2, or 30% He-30% O_2-40% N_2 for 15 min 24 h before ischemia, or received 30% He-30% O_2-40% N_2 for 15 min on 3, 2, or 1 day(s), interspersed by 24 h, respectively		
	Zucker lean rat (238–262 g)	Rats received 70% He-30% O_2 for three 5-min periods, interspersed with two 5-min washout periods 10 min before ischemia, or inhaled 70% He-30% O_2 for 15 min at the onset of reperfusion		
	Male Wistar rats (354–426 g)	Rats were subjected to 25 min ischemia and 15 min reperfusion, and 70% He-30% O_2 post-conditioning (PostC) encompassed the entire reperfusion phase		
	Male Wistar Kyoto rats (WKR) and spontaneous hypertensive rats (SHR) (12–14 weeks)	PostC, Late preconditioning (LPC) + PostC, or Early preconditioning (EPC) + LPC + PostC was performed in WKR. EPC + LPC + PostC was performed in SHR. EPC comprised 3 short cycles of 70% He-30% O_2 (5 min each, with wash outs of 5 min in between and a final washout episode of 10 min before ischemia). LPC was induced by 15 min of 70% He-30% O_2 administration 24 h before ischemia. PostC was induced by 15 min of 70% He-30% O_2 administration since the beginning of reperfusion		
Neon	Male New Zealand white rabbits (2.5–3.0 kg)	Rabbits received 3 cycles of 70% Ne-30% O_2 for 5 min interspersed with 5 min of 70% N_2-30% O_2 before ischemia	Reduced infarct size	(73)
Argon	Male New Zealand white rabbits (2.5–3.0 kg)	Rabbits received 3 cycles of 70% Ar-30% O_2 for 5 min interspersed with 5 min of 70% N_2-30% O_2 before ischemia	Reduced infarct size	(73, 79)
	Male Wistar rats (240–380 g)	Inhalation of 80% Ar-20% O_2 for 20 min starting 5 min before reperfusion	Preserved left ventricular function at 1 and 3 weeks after surgery	
Krypton	No report yet	No report yet	No report yet	None
Xenon	New Zealand white rabbits (2.7–3.4 kg)	Inhalation of 70% Xe-30% O_2 during first 15 min of reperfusion	Reduced infarct size	(80–87)
	Male Wistar rats (275–350 g)	Administration of 20% Xe-80% O_2 was commenced 3 min prior to, and discontinued 30 min after, the onset of reperfusion. Moreover, active cooling was commenced 5 min prior to, and hypothermia maintained for 1 h after, the onset of reperfusion		
	Male Wistar rats (200–250 or 300–450 g)	Rats received 70% Xe-25% O_2-5% N_2 for three 5-min periods, interspersed with two 5 min and one final 10-min washout periods before ischemia		
	Male Wistar rats (280–340 g)	Rats received 3 cycles of 70% Xe-30% O_2 administered for 5- min periods interspersed with 5 -min intervals 70% N_2-30% O_2 following by a final 15-min interval of 70% N_2-30% O_2 before ischemia		
	Male Wistar rats (200–250 g)	24 h before ischemia, rats received 70% Xe-30% O_2 for 15 min		
Radon	No report yet	No report yet	No report yet	None

and heat-shock protein 27 (HSP27) in patient hearts undergoing coronary artery bypass graft surgery; HePC and helium post-conditioning did not affect postoperative troponin release in these patients (58). In contrast to the healthy Wistar Kyoto rats (WKRs), only a triple intervention of He conditioning can reduce cell damage after myocardial I/R in spontaneous hypertensive rats (SHR), suggesting the presence of a threshold in the hypertensive heart (54) (**Table 1**). An *in-vitro* study indicated that He conditioning contributed to cardioprotection by increasing fibroblast migration, but not by releasing protective medium extracellular vesicles or soluble factors from the cardiac fibroblasts (88). Our recent study indicated that intraperitoneal injection of 99.999% He gas improved lipopolysaccharide (LPS)-induced left ventricular dysfunction and cavity enlargement in a dose-dependent manner, it is better at the dose of 1.0 ml/100 g (89). Mechanistically, He inhibited Toll-like receptor 4 (TLR4) expression, reduced the phosphorylation of nuclear factor-kappa B (NF-κB), and subsequently alleviated interleukin-18 (IL-18) and TNF-α expression in heart (89). The dose effect of He gas has also been confirmed in intestine; the HePC profile consisting of three cycles of 10 or 15 min He breathing interspersed with three 5-min washout periods by breathing room air reduced I/R-induced intestinal injury, inflammatory response, and cell apoptosis; however, the 2- or 5-min He breathing dose does not confer any protective effects (69).

Helium in Neuroprotection

Helium displayed neuroprotective effects on a traumatic brain injury model *in vitro* (61) and in a decompression-induced neurological deficits model *in vivo* (90). Breathing 70% He during a middle cerebral artery occlusion (MCAO) for 2 h and early reperfusion (1 h) reduced infarct volume and improved neurological deficits 24 h after MCAO in rats (91). Seventy-five percentage He treatment from 1 h after reperfusion to 4 h after reperfusion also provided neuroprotection by producing hypothermia in rats (62). In a rat resuscitation model, HePC and He post-conditioning (received 70% He and 30% oxygen for 5 min before cardiac arrest and for 30 min after restoration of spontaneous circulation) reduced apoptosis in brain, but had no influence on viable neuron count and no beneficial effects were seen on neurofunctional outcome (59). He-PC-induced NO production and subsequent NO-mediated up-regulation of antioxidases (e.g, nuclear factor E2-related factor 2), angiogenesis, and inhibition of inflammation and apoptosis, all contributed to the neuroprotective effect of helium in a neonatal cerebral hypoxia/ischemia model (63, 65, 66). However, in a clinical perspective for the treatment of acute ischemic stroke, He should not be administered before or together with tissue plasminogen activator therapy due to the risk of inhibiting the benefit of tissue plasminogen activator-induced thrombolysis; He therapy could be an efficient neuroprotective agent, if given after tissue plasminogen activator-induced reperfusion (64).

Helium in Hepatic Protection

Fukuda et al. have confirmed that inhalation of H_2 gas (1–4% at 10 min before reperfusion until the end of reperfusion) suppressed hepatic I/R (90/180 min) injury through reducing oxidative stress in male C57 BL/6N mice (4–5 weeks old, 15–18 g); however, 4% He gas showed no protective effect (92). Similarly, HePC (three cycles of ventilation with inhalation of mixture of 70% He and 30% oxygen for 5 min, each followed by 5-min washout with inhalation of mixture of 30% oxygen and 70% nitrogen) did not attenuate hepatic I/R (45/240 min) injury in male Wistar rats (300 ± 30 g), although there was evidence for a modulation of the inflammatory response (93). In contrast, Zhang et al. have revealed that HePC (70% He-30% oxygen mixture inhalation for three 5-min periods interspersed with three 5-min washout periods using room air) alleviated 90 min ischemia-induced liver injury at 1, 3, and 6 h after reperfusion in male BALB/c mice (25–30 g); mechanistically, activation of hepatic adenosine A_{2A} receptor-PI3K-Akt axis, alleviation of necrosis and apoptosis, reduction of IκBα phosphorylation, and TNF-α, interleukin-6 (IL-6), monocyte chemotactic protein-1 (MCP-1) and chemokine (C-X-C motif) ligand 10 (CXCL10, IP-10) expression, and inhibition of inflammatory cell infiltration in liver all contributed to this protective effects of HePC (68). The difference of animal strains, the time of I/R, and even the gas mixture used in washout periods might be responsible for these controversy. Furthermore, Zhang et al. have confirmed that HePC-induced protection in hepatic I/R injury and Akt activation were dependent on the interaction between He inhalation and air gaps, but not any of the two factors alone (68). As the protection of the intermittent pattern of He inhalation, drinking hydrogen-rich water, or intermittent hydrogen gas exposure, but not lactulose or continuous hydrogen gas exposure, prevented 6-hydroxydopamine-induced Parkinson's disease in rats (94). Therefore, the continuous heliox inhalation, rather than intermittent pattern, might be responsible for the none alteration of myocardial infarct size or the extent of no reflow in rabbits with continuous heliox breathing during 30 min of ischemia and 180 min of reperfusion (95).

Argon

Argon in Neuroprotection

When 7-day-old postnatal Sprague-Dawley rats subjected to hypoxic-ischemia (moderate) injury, 2 h after hypoxic insult, exposure of He, Ar, and Xe (70% noble gas balanced with oxygen) for 90 min improved cell survival, brain structural integrity, and neurologic function on postnatal day 40 compared with nitrogen, whereas only Ar and Xe reduced infarct volume after more severe hypoxic-ischemic injury (96). The *in-vivo* and *in-vitro* studies indicated that Ar acted as a protector for cerebral ischemia injury, brain trauma, and cardiac arrest-induced neurological damage (97–110). The neuroprotective effects of Ar were involved in inhibiting microglia/macrophage activation and enhancing M2 microglia/macrophage polarization (107, 109, 110), reducing stress-activated protein kinase/c-Jun N-terminal kinase (SAPK/JNK) activation and high mobility group protein B1 (HMGB1) expression (106), inhibiting TLR2/4-mediated activation of signal transducer and activator of transcription 3 (STAT3) and NF-κB, and subsequently decreasing IL-8 expression (111).

Argon in Cardioprotection

Argon displayed cardioprotective effects both *in vitro* and *in vivo* (73, 79, 106, 112, 113). Pre-treatment with 30 or 50% Ar for 90 min before oxygen-glucose deprivation protected human cardiac myocyte-like progenitor cells against apoptosis *via* activation of ERK, Akt, and biphasic regulation of JNK (113). Preconditioning with three cycles of 50% Ar (50% Ar, 21% oxygen, and 29% nitrogen) for 5 min, interspersed with 5 min of 79% nitrogen-21% oxygen *in vivo*, enhanced post-ischemic cardiac functional recovery following cardioplegic arrest and global cold ischemia *in vitro*; this protective effect of Ar was related to improving cardiac energy metabolism, inhibiting JNK phosphorylation, and HMGB1 expression (106). The cardioprotection of Ar on ischemia was also confirmed in rabbit *in vivo* (73) (**Table 1**). Lemoine et al. have further revealed the therapeutic effect of Ar on left ventricular dysfunction in myocardial I/R injury *in vivo*, in which Ar activated PI3K/Akt mitogen-activated protein kinase kinase (MEK)-ERK1/2 signaling, inhibited the opening of mitochondrial permeability transition pore (79) (**Table 1**).

Argon in Hepatic Protection

Argon is the key modulator of IL-6 expression in different liver injury models. Under the physiological conditions, IL-6 is essential for proper hepatic tissue homeostasis, liver regeneration, infection defense, and fine-tuning of metabolic functions, while persistent activation of IL-6 seems to be detrimental, impairs liver regeneration and can even lead to the development of liver cancer (114, 115). Inhalation of 50% Ar inhibited liver regeneration after hepatic I/R or after partial hepatectomy in rats, the former may be related to upregulation of IL-1β and IL-6 in liver, and the latter may be related to the downregulation of hepatocyte growth factor (HGF) and IL-6 (116, 117). Breathing 70% Ar in a rabbit model of abdominal aorta occlusion for 30 min and reperfusion for 300 min also reduced the plasma concentrations of IL-6 and HMGB1, improved hepatic and renal injuries (118). The detail mechanisms of Ar-mediated IL-6 expression are not clear.

Xenon

Xenon in Neuroprotection

As that of Ar, Xe also has essential neuroprotective effects and it has been extensively investigated in the animal models of ischemia- and/or hypoxia-induced nervous system damage, such as, stroke, brain trauma, and hypoxic-ischemic injury in rat hippocampus (61, 96, 119–135). Glutamate mediates most excitatory neurotransmission in the mammalian central nervous system; normal activation of glutamate receptors mediates, in large measure, physiological excitatory synaptic transmission in the brain and is, therefore, crucial for the normal functioning of nervous system (136, 137). However, among three classical glutamate-gated ion channels, excessive activation of N-methyl-D-aspartate receptor (NMDA-R) leads to increasing intracellular calcium concentrations and the consequent production of damaging free radicals and activation of proteolytic processes that contribute to cell injury or death (136, 138). Xe has been identified to competitively inhibit the glycine site of NMDA-R, thus contributing to neuroprotective effects (128, 133, 139, 140) and it has carried out several clinical trials on brain–heart injury after cardiac arrest and achieved the positive results (141–143).

Xenon in Cardioprotection

Xenon is a new type of gaseous anesthetic with minimal hemodynamic side effects, thus, it is an ideal anesthetic for patients with heart damage (80, 144), while it has been suggested that Xe should be used with caution in patients with known intracranial hypertension (145–148). Global administration of 50 or 70% Xe only significantly reduced left ventricular systolic pressure and the maximum rate of pressure increase (dP/dtmax), the regional myocardial function and coronary blood flow in left anterior descending coronary artery- and left circumflex coronary artery-dependent myocardium were not changed; regional administration of 50 or 70% Xe only to the left anterior descending-perfused myocardium had no influence in global hemodynamics, regional myocardial function, and coronary blood flow in the circumflex coronary artery-dependent myocardium, while 70% xenon, rather than 50% xenon, reduced systolic wall thickening by 7.2 ± 4.0% and mean velocity of systolic wall thickening by 8.2 ± 4.0% in the left anterior descending coronary artery-perfused area, resulting in a small but consistent negative inotropic effect on beagle dog heart *in vivo* (149). Forty or 80% Xe did not significantly alter NO-dependent flow response, the electrical, mechanical, or metabolic effects in isolated guinea pig hearts, possibly due to no alteration of major cation currents in cardiomyocytes by Xe (150). Moreover, breathing 70% Xe had only minimal negative inotropic effects on rabbits with left ventricular dysfunction after coronary artery ligation (151). Schroth et al. also showed that 65% Xe did not alter myocardial contractility and the response to inotropic stimuli such as calcium, isoproterenol, or increase in pacing frequency in isolated guinea pig ventricular muscle bundles (144). The biological mechanisms of cardiovascular stability and unchanged muscle sympathetic activity during Xe anesthesia have been revealed by the *Peter Kienbaum* group; they found that the increased concentrations of norepinephrine at the synaptic cleft and in plasma by Xe in an NMDA-R-dependent mechanism contributed to the hemodynamic stability of patients during Xe anesthesia (152).

However, Xe (0, 20, 50, and 65%), in addition to basic intravenous anesthesia, has been shown to elicit downregulation of heart rate and cardiac output with no change in mean arterial pressure, decrease portal venous blood flow with no change in hepatic arterial blood flow, and reduce total hepatic oxygen delivery and venous hepatic oxygen saturation, but did not impair intestinal oxygenation in pigs (153, 154). 73–78% Xe with additional supplementation of pentobarbital and buprenorphine increased oxygen contents of hepatic venous blood in pigs (155). These indicate that the basic intravenous anesthesia might influence the effects of Xe on cardiovascular activities and hepatic oxygen contents.

Under pathological conditions, 70% Xe inhalation in the early stage of reperfusion can reduce infarct size after myocardial ischemia in rabbits (81); combined application of 20% Xe and 34°C hypothermia in early reperfusion can also reduce

myocardial infarction size in rats (82) (**Table 1**). The mechanisms of Xe in cardioprotection have been relatively clear. Xe first activates mitochondrial KATP channel and phosphatidylinositol-dependent kinase-1 (PDK-1); these two activates PKC-ε, PKC-ε activates p38 MAPK, subsequently, two downstream targets of p38 MAPK, MAPK-activated protein kinase-2 (MAPKAPK-2/MK-2) and HSP27, are phosphorylated, and then, induces the translocation of HSP27 to particulate fraction and increases F-actin polymerization (80, 83, 84). Besides p38 MAPK, ERK1/2, and COX-2 are essential mediators of Xe preconditioning (85, 86); Xe can also induce the phosphorylation of Akt and GSK-3β, inhibit Ca^{2+}-induced opening of mPTP, and preserve mitochondrial function (87). Similar to Ar, Xe also acts as an inhibitor of NF-κB activation and prevents adhesion molecule expression in TNF-α-treated ECs *in vitro* (156). The saturation point of Xe in water without a cage vehicle for encapsulation of xenon was 0.22 mM; when the cage molecule 2-hydroxypropyl-β-cyclodextrin (HPCD) was added, Xe solubility increased from 0.22 to 0.67 mM; supplement of this Xe-enriched solutions by gavage improved hypertension and left ventricular hypertrophy and dysfunction in aged apolipoprotein E (ApoE)-knockout mice fed high-fat diet (HFD) for 6 weeks (157).

Xenon in Renoprotection

Both the Ar and Xe have been shown as renoprotectants in kidney transplantation (158, 159). In addition, 70% Xe has been reported to improve kidney function and renal histology and decrease neutrophil chemoattractants expression in kidney, thereby attenuating the glomerular neutrophil infiltration in an accelerated and severe lupus nephritis model in female NZB/W F1 mice (160). This protective effects of Xe on kidney was mediated by enhancing renal hypoxia inducible factor 1-α expression; decreasing serum levels of antidouble-stranded DNA autoantibody; and inhibiting ROS production, glomerular deposition of IgG and C3 and apoptosis, nucleotide-binding oligomerization domain (NOD)-like receptor family protein 3 (NLRP3) inflammasome and NF-κB activation, and intercellular cell adhesion molecule-1 (CD54 or ICAM-1) expression in kidney (160). The role of Xe and other noble gases on the activation or inhibition of other forms of inflammasomes still need further investigation.

Neon and Kr

The biological effects of Ne and Kr have been relatively few investigated in the past. Similar to He and Ar, Ne has also been shown to reduce the infarct area in rabbit model of myocardial I/R injury (73) (**Table 1**). Kr gas can promote the survival rate of Japanese quails embryos under acute hypoxia, Kr partial pressure of 5–5.5 kg/cm^2 produces the narcotic effect on adult Japanese quails (161). However, in hypoxia/glucose deficiency injury model and in focal mechanical injury model of mouse hippocampal slices, only Ar and Xe showed the neuroprotective effects, while He, Ne, and Kr did not show neuroprotective effects (128, 133). Thus, the biological effects and mechanisms of Ne and Kr are worthy of further exploration.

Radioactive Rn

Radon is an imperceptible natural occurring radioactive noble gas that exists in soil, water, and outdoor and indoor air; exposure to Rn accounts for more than 50% of the annual effective dose of natural radioactivity, it contributes as the largest single fraction to radiation exposure from natural sources (162, 163). Rn is a recognized pathogenic factor of human lung cancer, it is the second leading cause of lung cancer death after tobacco smoke (162). However, a certain dose of Rn has been reported for treating chronic musculoskeletal diseases, e.g., ankylosing spondylitis, osteoarthritis, or rheumatoid arthritis, these effects may be related to the regulation of oxidative stress and inflammation (163).

PERSPECTIVE

The noble gases are chemically inert because their outer electron orbitals are completely filled; however, they have been found to be very biologically active (159, 164). The noble gas family has emerged as the essential cellular or organic protectants such as in ECs, heart, brain, liver, kidney, and intestine; therefore, it protects against CCVDs (**Figure 1**).

Helium, Ar, and Xe displayed the neuroprotective effects on acute brain I/R injury models *in vivo* or *in vitro*. He, Ne, Ar, and Xe can reduce infarct size; Ar can improve the impaired left ventricular function in myocardial I/R injury animal models; however, the roles of other noble gases on left ventricular function under I/R or other pathological conditions still need further investigation (**Table 1**). It has been reported that oral administration of 6 weeks of Xe-enriched solution can be a promising nutraceutical strategy for cardiovascular protection (157). However, the effects of noble gases on chronic CCVDs and the side effects of long-time supplement of noble gases still need further investigation.

Besides competitively inhibiting NMDA-R by Xe in nervous system, modulation of cell death (mainly apoptosis), inflammatory or immune signals, oxidative damage, and gases interaction are the essential mechanisms of noble gases (**Figure 1**). The detail roles of noble gases on redox signaling, necrosis, autophagy, pyroptosis, and ferroptosis, which all play essential roles in CCVDs (165–167), and on other novel cell death types, such as alkaliptosis (168) and oxeiptosis (169), still need further investigation. The modulation of TLR4 signaling by He (89), NLRP3 inflammasome by Xe (160), and TLR2/4-mediated signaling by Ar (111) indicated that noble gases might act as essential modulators of innate immune signaling. Innate immune signaling is a complex cascade that quickly recognizes pathogen-associated molecular patterns (PAMPs) or damage-associated molecular patterns (DAMPs) through multiple germline-encoded cell surface or cytoplasmic pattern recognition receptors (PRRs), then, transmits signals through adaptors, kinases, and transcription factors, resulting in the production of cytokines (170–174). The mammalian host innate defense system utilizes more than 50 PRRs, which can be divided into two classes: the membrane-bound PRRs [including TLRs, C-type lectin receptors (CLRs), and receptors for advanced glycation end-products (RAGE)] and the cytosolic

PRRs [including RIG-I-like receptors (RLRs), NOD-like receptors (NLRs), absent in melanoma 2 (AIM2)-like receptors (ALRs), and other nucleic acid-sensing receptors] (173, 174). Gasoimmunology, which investigates the effects of medical gases (such as NO, CO, H_2S, SO_2, H_2, CH_4, and noble gases) on innate immune signaling or on immune cells under both the homeostatic and perturbed conditions, will help us to open a novel door for medical gases investigation. Moreover, NO, CO, H_2S, SO_2, H_2, and CH_4 are essential endogenous gas molecules in modulating cardiocerebrovascular homeostasis (19–32). The cardioprotection of He is partially mediated by inducing NO production through eNOS in rabbits (78). It is not clear whether other noble gases can influence the levels and/or activities of these endogenous gases, if they can, what will happen to cardiocerebrovascular homeostasis and CCVDs?

It is not known the action forms of noble gases *in vivo*, by gases directly (in the alveolus where a gas phase exists) or dissolved non-electrolytes at very low concentration and with extremely weak interactions with other atoms/molecules. Therefore, as that of the small molecule signaling agents NO, CO, H_2S, and their derived species, the physical or chemical interactions between noble elements and biological targets will be an important factor in their roles as signaling agents; thus, a fundamental understanding of the physics, chemistry, and biochemistry of noble gas atoms will be essential to understand their biological, physiological, or pathophysiological utility (175).

AUTHOR CONTRIBUTIONS

YZ: conceptualization. JZ and YZ: writing-original draft preparation. YZ, HY, WL, and JX: writing-review and editing. MB and YZ: visualization. YZ and HY: supervision. All authors have read and agreed to the published version of the manuscript.

FUNDING

This study was funded by the National Natural Science Foundation of China (Grant nos. 81900376 and 81673772), the Natural Science Foundation of Guangdong Province (Grant nos. 2017A030313738 and 2018A030313657), Project of administration of Traditional Chinese Medicine of Guangdong province (20221116), the key discipline construction project for traditional Chinese Medicine in Guangdong province, and the construction project of inheritance studio of national famous and old traditional Chinese Medicine experts in 2021.

ACKNOWLEDGMENTS

We apologize to all of the authors whose invaluable work we could not discuss or cite in this review due to space constraints.

REFERENCES

1. Crea F, Camici PG, Bairey Merz CN. Coronary microvascular dysfunction: an update. *Eur Heart J.* (2014) 35:1101–11. doi: 10.1093/eurheartj/eht513
2. Khera AV, Kathiresan S. Genetics of coronary artery disease: discovery, biology and clinical translation. *Nat Rev Genet.* (2017) 18:331–44. doi: 10.1038/nrg.2016.160
3. Levy BI, Heusch G, Camici PG. The many faces of myocardial ischaemia and angina. *Cardiovasc Res.* (2019) 115:1460–70. doi: 10.1093/cvr/cvz160
4. Swarup S, Patibandla S, Grossman SA. *Coronary Artery Vasospasm.* Treasure Island, FL: StatPearls
5. Hill JA, Olson EN. Cardiac plasticity. *N Engl J Med.* (2008) 358:1370–80. doi: 10.1056/NEJMra072139
6. Nordon IM, Hinchliffe RJ, Loftus IM, Thompson MM. Pathophysiology and epidemiology of abdominal aortic aneurysms. *Nat Rev Cardiol.* (2011) 8:92–102. doi: 10.1038/nrcardio.2010.180
7. Simonneau G, Gatzoulis MA, Adatia I, Celermajer D, Denton C, Ghofrani A, et al. Updated clinical classification of pulmonary hypertension. *J Am Coll Cardiol.* (2013) 62:D34–41. doi: 10.1016/j.jacc.2013.10.029
8. Bastami M, Choupani J, Saadatian Z, Zununi Vahed S, Mansoori Y, Daraei A, et al. miRNA polymorphisms and risk of cardio-cerebrovascular diseases: a systematic review and meta-analysis. *Int J Mol Sci.* (2019) 20:293. doi: 10.3390/ijms20020293
9. Ritchie RH, Abel ED. Basic mechanisms of diabetic heart disease. *Circ Res.* (2020) 126:1501–25. doi: 10.1161/CIRCRESAHA.120.315913
10. Schiffrin EL. How structure, mechanics, and function of the vasculature contribute to blood pressure elevation in hypertension. *Can J Cardiol.* (2020) 36:648–58. doi: 10.1016/j.cjca.2020.02.003
11. Coffey S, Roberts-Thomson R, Brown A, Carapetis J, Chen M, Enriquez-Sarano M, et al. Global epidemiology of valvular heart disease. *Nat Rev Cardiol.* (2021) 18:853–64. doi: 10.1038/s41569-021-00570-z
12. Tschope C, Ammirati E, Bozkurt B, Caforio ALP, Cooper LT, Felix SB, et al. Myocarditis and inflammatory cardiomyopathy: current evidence and future directions. *Nat Rev Cardiol.* (2021) 18:169–93. doi: 10.1038/s41569-020-00435-x
13. Virani SS, Alonso A, Aparicio HJ, Benjamin EJ, Bittencourt MS, Callaway CW, et al. Heart disease and stroke statistics-2021 update: a report from the american heart association. *Circulation.* (2021) 143:e254–743. doi: 10.1161/CIR.0000000000000950
14. Jeong YW. Blood pressure awareness and knowledge of cardio-cerebrovascular diseases in south korean women with hypertension. *Healthcare.* (2021) 9:360. doi: 10.3390/healthcare9030360
15. World Health Organization. *Cardiovascular Disease (CVDs).* WHO (2020). Available online at: https://www.who.int/health-topics/cardiovascular-diseases#tab=tab_1 (accessed December 21, 2020).
16. Furchgott RF, Zawadzki JV. The obligatory role of endothelial cells in the relaxation of arterial smooth muscle by acetylcholine. *Nature.* (1980) 288:373–6. doi: 10.1038/288373a0
17. Furchgott RF. Endothelium-derived relaxing factor: discovery, early studies, and identification as nitric oxide. *Biosci Rep.* (1999) 19:235–51. doi: 10.1023/A:1020537506008
18. Farah C, Michel LYM, Balligand JL. Nitric oxide signalling in cardiovascular health and disease. *Nat Rev Cardiol.* (2018) 15:292–316. doi: 10.1038/nrcardio.2017.224
19. Otterbein LE, Zuckerbraun BS, Haga M, Liu F, Song R, Usheva A, et al. Carbon monoxide suppresses arteriosclerotic lesions associated with chronic graft rejection and with balloon injury. *Nat Med.* (2003) 9:183–90. doi: 10.1038/nm817
20. Ohsawa I, Ishikawa M, Takahashi K, Watanabe M, Nishimaki K, Yamagata K, et al. Hydrogen acts as a therapeutic antioxidant by selectively reducing cytotoxic oxygen radicals. *Nat Med.* (2007) 13:688–94. doi: 10.1038/nm1577
21. True AL, Olive M, Boehm M, San H, Westrick RJ, Raghavachari N, et al. Heme oxygenase-1 deficiency accelerates formation of arterial thrombosis through oxidative damage to the endothelium, which is rescued by inhaled carbon monoxide. *Circ Res.* (2007) 101:893–901. doi: 10.1161/CIRCRESAHA.107.158998

22. Du SX, Jin HF, Bu DF, Zhao X, Geng B, Tang CS, et al. Endogenously generated sulfur dioxide and its vasorelaxant effect in rats. *Acta Pharmacol Sin.* (2008) 29:923–30. doi: 10.1111/j.1745-7254.2008.00845.x
23. Ghyczy M, Torday C, Kaszaki J, Szabo A, Czobel M, Boros M. Hypoxia-induced generation of methane in mitochondria and eukaryotic cells: an alternative approach to methanogenesis. *Cell Physiol Biochem.* (2008) 21:251–8. doi: 10.1159/000113766
24. Yang G, Wu L, Jiang B, Yang W, Qi J, Cao K, et al. H2S as a physiologic vasorelaxant: hypertension in mice with deletion of cystathionine gamma-lyase. *Science.* (2008) 322:587–90. doi: 10.1126/science.1162667
25. Liu W, Wang D, Tao H, Sun X. Is methane a new therapeutic gas? *Med Gas Res.* (2012) 2:25. doi: 10.1186/2045-9912-2-25
26. Hine C, Harputlugil E, Zhang Y, Ruckenstuhl C, Lee BC, Brace L, et al. Endogenous hydrogen sulfide production is essential for dietary restriction benefits. *Cell.* (2015) 160:132–44. doi: 10.1016/j.cell.2014.11.048
27. Yetik-Anacak G, Sorrentino R, Linder AE, Murat N. Gas what: NO is not the only answer to sexual function. *Br J Pharmacol.* (2015) 172:1434–54. doi: 10.1111/bph.12700
28. Huang Y, Tang C, Du J, Jin H. Endogenous sulfur dioxide: a new member of gasotransmitter family in the cardiovascular system. *Oxid Med Cell Longev.* (2016) 2016:8961951. doi: 10.1155/2016/8961951
29. Otterbein LE, Foresti R, Motterlini R. Heme oxygenase-1 and carbon monoxide in the heart: the balancing act between danger signaling and pro-survival. *Circ Res.* (2016) 118:1940–59. doi: 10.1161/CIRCRESAHA.116.306588
30. Jia Y, Li Z, Liu C, Zhang J. Methane medicine: a rising star gas with powerful anti-inflammation, antioxidant, antiapoptosis properties. *Oxid Med Cell Longev.* (2018) 2018:1912746. doi: 10.1155/2018/1912746
31. Zhang Y, Tan S, Xu J, Wang T. Hydrogen therapy in cardiovascular and metabolic diseases: from bench to bedside. *Cell Physiol Biochem.* (2018) 47:1–10. doi: 10.1159/000489737
32. Zhang Y, Liu H, Xu J, Zheng S, Zhou L. Hydrogen gas: a novel type of antioxidant in modulating sexual organs homeostasis. *Oxid Med Cell Longev.* (2021) 2021:8844346. doi: 10.1155/2021/8844346
33. Hollig A, Schug A, Fahlenkamp AV, Rossaint R, Coburn M, Argon Organo-Protective N. Argon: systematic review on neuro- and organoprotective properties of an "inert" gas. *Int J Mol Sci.* (2014) 15:18175–96. doi: 10.3390/ijms151018175
34. Smit KF, Weber NC, Hollmann MW, Preckel B. Noble gases as cardioprotectants - translatability and mechanism. *Br J Pharmacol.* (2015) 172:2062–73. doi: 10.1111/bph.12994
35. Weber NC, Smit KF, Hollmann MW, Preckel B. Targets involved in cardioprotection by the non-anesthetic noble gas helium. *Curr Drug Targets.* (2015) 16:786–92. doi: 10.2174/1389450116666150120104459
36. Weber NC, Preckel B. Gaseous mediators: an updated review on the effects of helium beyond blowing up balloons. *Intensive Care Med Exp.* (2019) 7:73. doi: 10.1186/s40635-019-0288-4
37. Maze M, Laitio T. Neuroprotective properties of xenon. *Mol Neurobiol.* (2020) 57:118–24. doi: 10.1007/s12035-019-01761-z
38. Hollig A, Coburn M. Noble gases and neuroprotection: summary of current evidence. *Curr Opin Anaesthesiol.* (2021) 34:603–6. doi: 10.1097/ACO.0000000000001033
39. Cullen SC, Gross EG. The anesthetic properties of xenon in animals and human beings, with additional observations on krypton. *Science.* (1951) 113:580–2. doi: 10.1126/science.113.2942.580
40. Harris PD, Barnes R. The uses of helium and xenon in current clinical practice. *Anaesthesia.* (2008) 63:284–93. doi: 10.1111/j.1365-2044.2007.05253.x
41. Berganza CJ, Zhang JH. The role of helium gas in medicine. *Med Gas Res.* (2013) 3:18. doi: 10.1186/2045-9912-3-18
42. Fleming RY, Dougherty TB, Feig BW. The safety of helium for abdominal insufflation. *Surg Endosc.* (1997) 11:230–4. doi: 10.1007/s004649900332
43. Makarov DV, Kainth D, Link RE, Kavoussi LR. Physiologic changes during helium insufflation in high-risk patients during laparoscopic renal procedures. *Urology.* (2007) 70:35–7. doi: 10.1016/j.urology.2007.03.010
44. Carmona M, Lopes RI, Borba M, Omokawa M, Naufal R, Miyaji K, et al. Comparison of the effects of carbon dioxide and helium pneumoperitoneum on renal function. *J Endourol.* (2008) 22:1077–82. doi: 10.1089/end.2007.0369
45. Nie M, Kobayashi H, Sugawara M, Tomita T, Ohara K, Yoshimura H. Helium inhalation enhances vasodilator effect of inhaled nitric oxide on pulmonary vessels in hypoxic dogs. *Am J Physiol Heart Circ Physiol.* (2001) 280:H1875–81. doi: 10.1152/ajpheart.2001.280.4.H1875
46. Smit KF, Oei GT, Brevoord D, Stroes ES, Nieuwland R, Schlack WS, et al. Helium induces preconditioning in human endothelium *in vivo*. *Anesthesiology.* (2013) 118:95–104. doi: 10.1097/ALN.0b013e3182751300
47. Smit KF, Konkel M, Kerindongo R, Landau MA, Zuurbier CJ, Hollmann MW, et al. Helium alters the cytoskeleton and decreases permeability in endothelial cells cultured *in vitro* through a pathway involving caveolin-1. *Sci Rep.* (2018) 8:4768. doi: 10.1038/s41598-018-23030-0
48. Smit KF, Oei G, Konkel M, Augustijn QJJ, Hollmann MW, Preckel B, et al. Plasma from volunteers breathing helium reduces hypoxia-induced cell damage in human endothelial cells-mechanisms of remote protection against hypoxia by helium. *Cardiovasc Drugs Ther.* (2019) 33:297–306. doi: 10.1007/s10557-019-06880-2
49. Heinen A, Huhn R, Smeele KM, Zuurbier CJ, Schlack W, Preckel B, et al. Helium-induced preconditioning in young and old rat heart: impact of mitochondrial Ca(2+) -sensitive potassium channel activation. *Anesthesiology.* (2008) 109:830–6. doi: 10.1097/ALN.0b013e3181895aa0
50. Huhn R, Heinen A, Weber NC, Hieber S, Hollmann MW, Schlack W, et al. Helium-induced late preconditioning in the rat heart *in vivo*. *Br J Anaesth.* (2009) 102:614–9. doi: 10.1093/bja/aep042
51. Huhn R, Heinen A, Weber NC, Kerindongo RP, Oei GT, Hollmann MW, et al. Helium-induced early preconditioning and postconditioning are abolished in obese zucker rats *in vivo*. *J Pharmacol Exp Ther.* (2009) 329:600–7. doi: 10.1124/jpet.108.149971
52. Oei GT, Weber NC, Hollmann MW, Preckel B. Cellular effects of helium in different organs. *Anesthesiology.* (2010) 112:1503–10. doi: 10.1097/ALN.0b013e3181d9cb5e
53. Huhn R, Weber NC, Preckel B, Schlack W, Bauer I, Hollmann MW, et al. Age-related loss of cardiac preconditioning: impact of protein kinase A. *Exp Gerontol.* (2012) 47:116–21. doi: 10.1016/j.exger.2011.11.003
54. Oei GT, Huhn R, Heinen A, Hollmann MW, Schlack WS, Preckel B, et al. Helium-induced cardioprotection of healthy and hypertensive rat myocardium *in vivo*. *Eur J Pharmacol.* (2012) 684:125–31. doi: 10.1016/j.ejphar.2012.03.045
55. Oei GT, Aslami H, Kerindongo RP, Steenstra RJ, Beurskens CJ, Tuip-de Boer AM, et al. Prolonged helium postconditioning protocols during early reperfusion do not induce cardioprotection in the rat heart *in vivo*: role of inflammatory cytokines. *J Immunol Res.* (2015) 2015:216798. doi: 10.1155/2015/216798
56. Oei GT, Heger M, van Golen RF, Alles LK, Flick M, van der Wal AC, et al. Reduction of cardiac cell death after helium postconditioning in rats: transcriptional analysis of cell death and survival pathways. *Mol Med.* (2015) 20:516–26. doi: 10.2119/molmed.2014.00057
57. Flick M, Albrecht M, Oei G, Steenstra R, Kerindongo RP, Zuurbier CJ, et al. Helium postconditioning regulates expression of caveolin-1 and−3 and induces RISK pathway activation after ischaemia/reperfusion in cardiac tissue of rats. *Eur J Pharmacol.* (2016) 791:718–25. doi: 10.1016/j.ejphar.2016.10.012
58. Smit KF, Brevoord D, De Hert S, de Mol BA, Kerindongo RP, van Dieren S, et al. Effect of helium pre- or postconditioning on signal transduction kinases in patients undergoing coronary artery bypass graft surgery. *J Transl Med.* (2016) 14:294. doi: 10.1186/s12967-016-1045-z
59. Aehling C, Weber NC, Zuurbier CJ, Preckel B, Galmbacher R, Stefan K, et al. Effects of combined helium pre/post-conditioning on the brain and heart in a rat resuscitation model. *Acta Anaesthesiol Scand.* (2018) 62:63–74. doi: 10.1111/aas.13041
60. Weber NC, Schilling JM, Warmbrunn MV, Dhanani M, Kerindongo R, Siamwala J, et al. Helium-Induced changes in circulating caveolin in mice suggest a novel mechanism of cardiac protection. *Int J Mol Sci.* (2019) 20:2640. doi: 10.3390/ijms20112640
61. Coburn M, Maze M, Franks NP. The neuroprotective effects of xenon and helium in an *in vitro* model of traumatic brain injury. *Crit Care Med.* (2008) 36:588–95. doi: 10.1097/01.CCM.0B013E3181611F8A6

62. David HN, Haelewyn B, Chazalviel L, Lecocq M, Degoulet M, Risso JJ, et al. Post-ischemic helium provides neuroprotection in rats subjected to middle cerebral artery occlusion-induced ischemia by producing hypothermia. *J Cereb Blood Flow Metab.* (2009) 29:1159–65. doi: 10.1038/jcbfm.2009.40
63. Liu Y, Xue F, Liu G, Shi X, Liu Y, Liu W, et al. Helium preconditioning attenuates hypoxia/ischemia-induced injury in the developing brain. *Brain Res.* (2011) 1376:122–9. doi: 10.1016/j.brainres.2010.12.068
64. Haelewyn B, David HN, Blatteau JE, Vallee N, Meckler C, Risso JJ, et al. Modulation by the noble gas helium of tissue plasminogen activator: effects in a rat model of thromboembolic stroke. *Crit Care Med.* (2016) 44:e383–9. doi: 10.1097/CCM.0000000000001424
65. Li Y, Liu K, Kang ZM, Sun XJ, Liu WW, Mao YF. Helium preconditioning protects against neonatal hypoxia-ischemia via nitric oxide mediated up-regulation of antioxidases in a rat model. *Behav Brain Res.* (2016) 300:31–7. doi: 10.1016/j.bbr.2015.12.001
66. Li Y, Zhang P, Liu Y, Liu W, Yin N. Helium preconditioning protects the brain against hypoxia/ischemia injury via improving the neurovascular niche in a neonatal rat model. *Behav Brain Res.* (2016) 314:165–72. doi: 10.1016/j.bbr.2016.08.015
67. Deng RM, Li HY, Li X, Shen HT, Wu DG, Wang Z, et al. Neuroprotective effect of helium after neonatal hypoxic ischemia: a narrative review. *Med Gas Res.* (2021) 11:121–3. doi: 10.4103/2045-9912.314332
68. Zhang R, Zhang L, Manaenko A, Ye Z, Liu W, Sun X. Helium preconditioning protects mouse liver against ischemia and reperfusion injury through the PI3K/Akt pathway. *J Hepatol.* (2014) 61:1048–55. doi: 10.1016/j.jhep.2014.06.020
69. Du L, Zhang R, Luo T, Nie M, Bi J. Effects of helium preconditioning on intestinal ischemia and reperfusion injury in rats. *Shock.* (2015) 44:365–70. doi: 10.1097/SHK.0000000000000418
70. Smit KF, Kerindongo RP, Böing A, Nieuwland R, Hollmann MW, Preckel B, et al. Effects of helium on inflammatory and oxidative stress-induced endothelial cell damage. *Exp Cell Res.* (2015) 337:37–43. doi: 10.1016/j.yexcr.2015.06.004
71. Lucchinetti E, Wacker J, Maurer C, Keel M, Harter L, Zaugg K, et al. Helium breathing provides modest antiinflammatory, but no endothelial protection against ischemia-reperfusion injury in humans *in vivo*. *Anesth Analg.* (2009) 109:101–8. doi: 10.1213/ane.0b013e3181a27e4b
72. Tretjak M, Gorjup V, Mozina H, Horvat M, Noc M. Cerebral and coronary gas embolism from the inhalation of pressurized helium. *Crit Care Med.* (2002) 30:1156–7. doi: 10.1097/00003246-200205000-00034
73. Pagel PS, Krolikowski JG, Shim YH, Venkatapuram S, Kersten JR, Weihrauch D, et al. Noble gases without anesthetic properties protect myocardium against infarction by activating prosurvival signaling kinases and inhibiting mitochondrial permeability transition *in vivo*. *Anesth Analg.* (2007) 105:562–9. doi: 10.1213/01.ane.0000278083.31991.36
74. Pagel PS, Krolikowski JG, Pratt PF Jr, Shim YH, Amour J, Warltier DC, et al. Reactive oxygen species and mitochondrial adenosine triphosphate-regulated potassium channels mediate helium-induced preconditioning against myocardial infarction *in vivo*. *J Cardiothorac Vasc Anesth.* (2008) 22:554–9. doi: 10.1053/j.jvca.2008.04.005
75. Pagel PS, Krolikowski JG. Transient metabolic alkalosis during early reperfusion abolishes helium preconditioning against myocardial infarction: restoration of cardioprotection by cyclosporin A in rabbits. *Anesth Analg.* (2009) 108:1076–82. doi: 10.1213/ane.0b013e318193e934
76. Pagel PS, Krolikowski JG, Amour J, Warltier DC, Weihrauch D. Morphine reduces the threshold of helium preconditioning against myocardial infarction: the role of opioid receptors in rabbits. *J Cardiothorac Vasc Anesth.* (2009) 23:619–24. doi: 10.1053/j.jvca.2008.12.020
77. Pagel PS, Krolikowski JG, Pratt, P. F. Jr., Shim YH, Amour J, et al. Inhibition of glycogen synthase kinase or the apoptotic protein p53 lowers the threshold of helium cardioprotection *in vivo*: the role of mitochondrial permeability transition. *Anesth Analg.* (2008) 107:769–75. doi: 10.1213/ane.0b013e3181815b84
78. Pagel PS, Krolikowski JG, Pratt PF Jr, Shim YH, Amour J, Warltier DC, et al. The mechanism of helium-induced preconditioning: a direct role for nitric oxide in rabbits. *Anesth Analg.* (2008) 107:762–8. doi: 10.1213/ane.0b013e3181815995
79. Lemoine S, Blanchart K, Souplis M, Lemaitre A, Legallois D, Coulbault L, et al. Argon exposure induces postconditioning in myocardial ischemia-reperfusion. *J Cardiovasc Pharmacol Ther.* (2017) 22:564–73. doi: 10.1177/1074248417702891
80. Weber NC, Toma O, Wolter JI, Obal D, Mullenheim J, Preckel B, et al. The noble gas xenon induces pharmacological preconditioning in the rat heart *in vivo* via induction of PKC-epsilon and p38 MAPK. *Br J Pharmacol.* (2005) 144:123–32. doi: 10.1038/sj.bjp.0706063
81. Preckel B, Müllenheim J, Moloschavij A, Thämer V, Schlack W. Xenon administration during early reperfusion reduces infarct size after regional ischemia in the rabbit heart *in vivo*. *Anesth Analg.* (2000) 91:1327–32. doi: 10.1097/00000539-200012000-00003
82. Schwiebert C, Huhn R, Heinen A, Weber NC, Hollmann MW, Schlack W, et al. Postconditioning by xenon and hypothermia in the rat heart *in vivo*. *Eur J Anaesthesiol.* (2010) 27:734–9. doi: 10.1097/EJA.0b013e328335fc4c
83. Weber NC, Toma O, Wolter JI, Wirthle NM, Schlack W, Preckel B. Mechanisms of xenon- and isoflurane-induced preconditioning - a potential link to the cytoskeleton via the MAPKAPK-2/HSP27 pathway. *Br J Pharmacol.* (2005) 146:445–55. doi: 10.1038/sj.bjp.0706324
84. Weber NC, Toma O, Damla H, Wolter JI, Schlack W, Preckel B. Upstream signaling of protein kinase C-epsilon in xenon-induced pharmacological preconditioning. Implication of mitochondrial adenosine triphosphate dependent potassium channels and phosphatidylinositol-dependent kinase-1. *Eur J Pharmacol.* (2006) 539:1–9. doi: 10.1016/j.ejphar.2006.03.054
85. Weber NC, Stursberg J, Wirthle NM, Toma O, Schlack W, Preckel B. Xenon preconditioning differently regulates p44/42 MAPK (ERK 1/2) and p46/54 MAPK (JNK 1/2 and 3) *in vivo*. *Br J Anaesth.* (2006) 97:298–306. doi: 10.1093/bja/ael153
86. Weber NC, Frassdorf J, Ratajczak C, Grueber Y, Schlack W, Hollmann MW, et al. Xenon induces late cardiac preconditioning *in vivo*: a role for cyclooxygenase 2? *Anesth Analg.* (2008) 107:1807–13. doi: 10.1213/ane.Ob013e31818874bf
87. Mio Y, Shim YH, Richards E, Bosnjak ZJ, Pagel PS, Bienengraeber M. Xenon preconditioning: the role of prosurvival signaling, mitochondrial permeability transition and bioenergetics in rats. *Anesth Analg.* (2009) 108:858–66. doi: 10.1213/ane.0b013e318192a520
88. Jelemensky M, Kovacshazi C, Ferenczyova K, Hofbauerova M, Kiss B, Pallinger E, et al. Helium conditioning increases cardiac fibroblast migration which effect is not propagated via soluble factors or extracellular vesicles. *Int J Mol Sci.* (2021) 22:10504. doi: 10.3390/ijms221910504
89. Zhang Y, Zhang J, Xu K, Chen Z, Xu X, Xu J, et al. Helium protects against lipopolysaccharide-induced cardiac dysfunction in mice via suppressing toll-like receptor 4-nuclear factor kappaB-Tumor necrosis factor-alpha/ interleukin-18 signaling. *Chin J Physiol.* (2020) 63:276–85. doi: 10.4103/CJP.CJP_66_20
90. Zhang R, Yu Y, Manaenko A, Bi H, Zhang N, Zhang L, et al. Effect of helium preconditioning on neurological decompression sickness in rats. *J Appl Physiol.* (2019) 126:934–40. doi: 10.1152/japplphysiol.00275.2018
91. Pan Y, Zhang H, VanDeripe DR, Cruz-Flores S, Panneton WM. Heliox and oxygen reduce infarct volume in a rat model of focal ischemia. *Exp Neurol.* (2007) 205:587–90. doi: 10.1016/j.expneurol.2007.03.023
92. Fukuda K, Asoh S, Ishikawa M, Yamamoto Y, Ohsawa I, Ohta S. Inhalation of hydrogen gas suppresses hepatic injury caused by ischemia/reperfusion through reducing oxidative stress. *Biochem Biophys Res Commun.* (2007) 361:670–4. doi: 10.1016/j.bbrc.2007.07.088
93. Braun S, Plitzko G, Bicknell L, van Caster P, Schulz J, Barthuber C, et al. Pretreatment with helium does not attenuate liver injury after warm ischemia-reperfusion. *Shock.* (2014) 41:413–9. doi: 10.1097/SHK.0000000000000125
94. Ito M, Hirayama M, Yamai K, Goto S, Ito M, Ichihara M, et al. Drinking hydrogen water and intermittent hydrogen gas exposure, but not lactulose or continuous hydrogen gas exposure, prevent 6-hydorxydopamine-induced Parkinson's disease in rats. *Med Gas Res.* (2012) 2:15. doi: 10.1186/2045-9912-2-15
95. Hale SL, Vanderipe DR, Kloner RA. Continuous heliox breathing and the extent of anatomic zone of noreflow and necrosis following ischemia/reperfusion in the rabbit heart. *Open Cardiovasc Med J.* (2013) 8:1–5. doi: 10.2174/1874192401408010001

96. Zhuang L, Yang T, Zhao H, Fidalgo AR, Vizcaychipi MP, Sanders RD, et al. The protective profile of argon, helium, and xenon in a model of neonatal asphyxia in rats. *Crit Care Med.* (2012) 40:1724–30. doi: 10.1097/CCM.0b013e3182452164
97. Loetscher PD, Rossaint J, Rossaint R, Weis J, Fries M, Fahlenkamp A, et al. Argon: neuroprotection in *in vitro* models of cerebral ischemia and traumatic brain injury. *Crit Care.* (2009) 13:R206. doi: 10.1186/cc8214
98. Ryang YM, Fahlenkamp AV, Rossaint R, Wesp D, Loetscher PD, Beyer C, et al. Neuroprotective effects of argon in an *in vivo* model of transient middle cerebral artery occlusion in rats. *Crit Care Med.* (2011) 39:1448–53. doi: 10.1097/CCM.0b013e31821209be
99. David HN, Haelewyn B, Degoulet M, Colomb, D. G. Jr., Risso JJ, et al. *Ex vivo* and *in vivo* neuroprotection induced by argon when given after an excitotoxic or ischemic insult. *PLoS ONE.* (2012) 7:e30934. doi: 10.1371/journal.pone.0030934
100. Brucken A, Cizen A, Fera C, Meinhardt A, Weis J, Nolte K, et al. Argon reduces neurohistopathological damage and preserves functional recovery after cardiac arrest in rats. *Br J Anaesth.* (2013) 110 (Suppl. 1):i106–112. doi: 10.1093/bja/aes509
101. Brucken A, Kurnaz P, Bleilevens C, Derwall M, Weis J, Nolte K, et al. Dose dependent neuroprotection of the noble gas argon after cardiac arrest in rats is not mediated by K(ATP)-channel opening. *Resuscitation.* (2014) 85:826–32. doi: 10.1016/j.resuscitation.2014.02.014
102. Ristagno G, Fumagalli F, Russo I, Tantillo S, Zani DD, Locatelli V, et al. Postresuscitation treatment with argon improves early neurological recovery in a porcine model of cardiac arrest. *Shock.* (2014) 41:72–8. doi: 10.1097/SHK.0000000000000049
103. Brucken A, Kurnaz P, Bleilevens C, Derwall M, Weis J, Nolte K, et al. Delayed argon administration provides robust protection against cardiac arrest-induced neurological damage. *Neurocrit Care.* (2015) 22:112–20. doi: 10.1007/s12028-014-0029-1
104. Brucken A, Bleilevens C, Fohr P, Nolte K, Rossaint R, Marx G, et al. Influence of argon on temperature modulation and neurological outcome in hypothermia treated rats following cardiac arrest. *Resuscitation.* (2017) 117:32–9. doi: 10.1016/j.resuscitation.2017.05.029
105. Grusser L, Blaumeiser-Debarry R, Krings M, Kremer B, Hollig A, Rossaint R, et al. Argon attenuates the emergence of secondary injury after traumatic brain injury within a 2-hour incubation period compared to desflurane: an *in vitro* study. *Med Gas Res.* (2017) 7:93–100. doi: 10.4103/2045-9912.208512
106. Kiss A, Shu H, Hamza O, Santer D, Tretter EV, Yao S, et al. Argon preconditioning enhances postischaemic cardiac functional recovery following cardioplegic arrest and global cold ischaemia. *Eur J Cardiothorac Surg.* (2018) 54:539–46. doi: 10.1093/ejcts/ezy104
107. Liu J, Nolte K, Brook G, Liebenstund L, Weinandy A, Hollig A, et al. Post-stroke treatment with argon attenuated brain injury, reduced brain inflammation and enhanced M2 microglia/macrophage polarization: a randomized controlled animal study. *Crit Care.* (2019) 23:198. doi: 10.1186/s13054-019-2493-7
108. Ma S, Chu D, Li L, Creed JA, Ryang YM, Sheng H, et al. Argon inhalation for 24 hours after onset of permanent focal cerebral ischemia in rats provides neuroprotection and improves neurologic outcome. *Crit Care Med.* (2019) 47:e693–9. doi: 10.1097/CCM.0000000000003809
109. Fumagalli F, Olivari D, Boccardo A, De Giorgio D, Affatato R, Ceriani S, et al. Ventilation with argon improves survival with good neurological recovery after prolonged untreated cardiac arrest in pigs. *J Am Heart Assoc.* (2020) 9:e016494. doi: 10.1161/JAHA.120.016494
110. Moro F, Fossi F, Magliocca A, Pascente R, Sammali E, Baldini F, et al. Efficacy of acute administration of inhaled argon on traumatic brain injury in mice. *Br J Anaesth.* (2021) 126:256–64. doi: 10.1016/j.bja.2020.08.027
111. Ulbrich F, Lerach T, Biermann J, Kaufmann KB, Lagreze WA, Buerkle H, et al. Argon mediates protection by interleukin-8 suppression via a TLR2/TLR4/STAT3/NF-kappaB pathway in a model of apoptosis in neuroblastoma cells *in vitro* and following ischemia-reperfusion injury in rat retina *in vivo*. *J Neurochem.* (2016) 138:859–73. doi: 10.1111/jnc.13662
112. Mayer B, Soppert J, Kraemer S, Schemmel S, Beckers C, Bleilevens C, et al. Argon induces protective effects in cardiomyocytes during the second window of preconditioning. *Int J Mol Sci.* (2016) 17:1159. doi: 10.3390/ijms17071159
113. Qi H, Soto-Gonzalez L, Krychtiuk KA, Ruhittel S, Kaun C, Speidl WS, et al. Pretreatment with argon protects human cardiac myocyte-like progenitor cells from oxygen glucose deprivation-induced cell death by activation of akt and differential regulation of mapkinases. *Shock.* (2018) 49:556–63. doi: 10.1097/SHK.0000000000000998
114. Wustefeld T, Rakemann T, Kubicka S, Manns MP, Trautwein C. Hyperstimulation with interleukin 6 inhibits cell cycle progression after hepatectomy in mice. *Hepatology.* (2000) 32:514–22. doi: 10.1053/jhep.2000.16604
115. Schmidt-Arras D, Rose-John S. IL-6 pathway in the liver: from physiopathology to therapy. *J Hepatol.* (2016) 64:1403–15. doi: 10.1016/j.jhep.2016.02.004
116. Ulmer TF, Fragoulis A, Dohmeier H, Kroh A, Andert A, Stoppe C, et al. Argon delays initiation of liver regeneration after partial hepatectomy in rats. *Eur Surg Res.* (2017) 58:204–15. doi: 10.1159/000466690
117. Schmitz SM, Dohmeier H, Stoppe C, Alizai PH, Schipper S, Neumann UP, et al. Inhaled argon impedes hepatic regeneration after ischemia/reperfusion injury in rats. *Int J Mol Sci.* (2020) 21:5457. doi: 10.3390/ijms21155457
118. de Roux Q, Lidouren F, Kudela A, Slassi L, Kohlhauer M, Boissady E, et al. Argon attenuates multiorgan failure in relation with HMGB1 inhibition. *Int J Mol Sci.* (2021) 22:3257. doi: 10.3390/ijms22063257
119. Homi HM, Yokoo N, Ma D, Warner DS, Franks NP, Maze M, et al. The neuroprotective effect of xenon administration during transient middle cerebral artery occlusion in mice. *Anesthesiology.* (2003) 99:876–81. doi: 10.1097/00000542-200310000-00020
120. Schmidt M, Marx T, Gloggl E, Reinelt H, Schirmer U. Xenon attenuates cerebral damage after ischemia in pigs. *Anesthesiology.* (2005) 102:929–36. doi: 10.1097/00000542-200505000-00011
121. Martin JL, Ma D, Hossain M, Xu J, Sanders RD, Franks NP, et al. Asynchronous administration of xenon and hypothermia significantly reduces brain infarction in the neonatal rat. *Br J Anaesth.* (2007) 98:236–40. doi: 10.1093/bja/ael340
122. Derwall M, Timper A, Kottmann K, Rossaint R, Fries M. Neuroprotective effects of the inhalational anesthetics isoflurane and xenon after cardiac arrest in pigs. *Crit Care Med.* (2008) 36:S492–5. doi: 10.1097/CCM.0b013e31818a904a
123. Fries M, Nolte KW, Coburn M, Rex S, Timper A, Kottmann K, et al. Xenon reduces neurohistopathological damage and improves the early neurological deficit after cardiac arrest in pigs. *Crit Care Med.* (2008) 36:2420–6. doi: 10.1097/CCM.0b013e3181802874
124. Hobbs C, Thoresen M, Tucker A, Aquilina K, Chakkarapani E, Dingley J. Xenon and hypothermia combine additively, offering long-term functional and histopathologic neuroprotection after neonatal hypoxia/ischemia. *Stroke.* (2008) 39:1307–13. doi: 10.1161/STROKEAHA.107.499822
125. Limatola V, Ward P, Cattano D, Gu J, Giunta F, Maze M, et al. Xenon preconditioning confers neuroprotection regardless of gender in a mouse model of transient middle cerebral artery occlusion. *Neuroscience.* (2010) 165:874–81. doi: 10.1016/j.neuroscience.2009.10.063
126. Fries M, Brucken A, Cizen A, Westerkamp M, Lower C, Deike-Glindemann J, et al. Combining xenon and mild therapeutic hypothermia preserves neurological function after prolonged cardiac arrest in pigs. *Crit Care Med.* (2012) 40:1297–303. doi: 10.1097/CCM.0b013e31823c8ce7
127. Sheng SP, Lei B, James ML, Lascola CD, Venkatraman TN, Jung JY, et al. Xenon neuroprotection in experimental stroke: interactions with hypothermia and intracerebral hemorrhage. *Anesthesiology.* (2012) 117:1262–75. doi: 10.1097/ALN.0b013e3182746b81
128. Harris K, Armstrong SP, Campos-Pires R, Kiru L, Franks NP, Dickinson R. Neuroprotection against traumatic brain injury by xenon, but not argon, is mediated by inhibition at the N-methyl-D-aspartate receptor glycine site. *Anesthesiology.* (2013) 119:1137–48. doi: 10.1097/ALN.0b013e3182a2a265
129. Campos-Pires R, Armstrong SP, Sebastiani A, Luh C, Gruss M, Radyushkin K, et al. Xenon improves neurologic outcome and reduces secondary injury following trauma in an *in vivo* model of traumatic brain injury. *Crit Care Med.* (2015) 43:149–58. doi: 10.1097/CCM.0000000000000624
130. Campos-Pires R, Koziakova M, Yonis A, Pau A, Macdonald W, Harris K, et al. Xenon protects against blast-induced traumatic brain injury in an *in vitro* model. *J Neurotrauma.* (2018) 35:1037–44. doi: 10.1089/neu.2017.5360

131. Zhao CS, Li H, Wang Z, Chen G. Potential application value of xenon in stroke treatment. *Med Gas Res.* (2018) 8:116–20. doi: 10.4103/2045-9912.241077
132. Campos-Pires R, Hirnet T, Valeo F, Ong BE, Radyushkin K, Aldhoun J, et al. Xenon improves long-term cognitive function, reduces neuronal loss and chronic neuroinflammation, and improves survival after traumatic brain injury in mice. *Br J Anaesth.* (2019) 123:60–73. doi: 10.1016/j.bja.2019.02.032
133. Koziakova M, Harris K, Edge CJ, Franks NP, White IL, Dickinson R. Noble gas neuroprotection: xenon and argon protect against hypoxic-ischaemic injury in rat hippocampus *in vitro* via distinct mechanisms. *Br J Anaesth.* (2019) 123:601–9. doi: 10.1016/j.bja.2019.07.010
134. Terrando N, Warner DS. Xenon for traumatic brain injury: a noble step forward and a wet blanket. *Br J Anaesth.* (2019) 123:9–11. doi: 10.1016/j.bja.2019.04.004
135. Campos-Pires R, Onggradito H, Ujvari E, Karimi S, Valeo F, Aldhoun J, et al. Xenon treatment after severe traumatic brain injury improves locomotor outcome, reduces acute neuronal loss and enhances early beneficial neuroinflammation: a randomized, blinded, controlled animal study. *Crit Care.* (2020) 24:667. doi: 10.1186/s13054-020-03373-9
136. Lipton SA. Paradigm shift in neuroprotection by NMDA receptor blockade: memantine and beyond. *Nat Rev Drug Discov.* (2006) 5:160–70. doi: 10.1038/nrd1958
137. Hansen KB, Wollmuth LP, Bowie D, Furukawa H, Menniti FS, Sobolevsky AI, et al. Structure, function, and pharmacology of glutamate receptor ion channels. *Pharmacol Rev.* (2021) 73:298–487. doi: 10.1124/pharmrev.120.000131
138. Lau A, Tymianski M. Glutamate receptors, neurotoxicity and neurodegeneration. *Pflugers Arch.* (2010) 460:525–42. doi: 10.1007/s00424-010-0809-1
139. Dickinson R, Peterson BK, Banks P, Simillis C, Martin JC, Valenzuela CA, et al. Competitive inhibition at the glycine site of the N-methyl-D-aspartate receptor by the anesthetics xenon and isoflurane: evidence from molecular modeling and electrophysiology. *Anesthesiology.* (2007) 107:756–67. doi: 10.1097/01.anes.0000287061.77674.71
140. Banks P, Franks NP, Dickinson R. Competitive inhibition at the glycine site of the N-methyl-D-aspartate receptor mediates xenon neuroprotection against hypoxia-ischemia. *Anesthesiology.* (2010) 112:614–22. doi: 10.1097/ALN.0b013e3181cea398
141. Arola OJ, Laitio RM, Roine RO, Gronlund J, Saraste A, Pietila M, et al. Feasibility and cardiac safety of inhaled xenon in combination with therapeutic hypothermia following out-of-hospital cardiac arrest. *Crit Care Med.* (2013) 41:2116–24. doi: 10.1097/CCM.0b013e31828a4337
142. Laitio R, Hynninen M, Arola O, Virtanen S, Parkkola R, Saunavaara J, et al. Effect of inhaled xenon on cerebral white matter damage in comatose survivors of out-of-hospital cardiac arrest: a randomized clinical trial. *JAMA.* (2016) 315:1120–8. doi: 10.1001/jama.2016.1933
143. Arola O, Saraste A, Laitio R, Airaksinen J, Hynninen M, Backlund M, et al. Inhaled xenon attenuates myocardial damage in comatose survivors of out-of-hospital cardiac arrest: the xe-hypotheca trial. *J Am Coll Cardiol.* (2017) 70:2652–60. doi: 10.1016/j.jacc.2017.09.1088
144. Schroth SC, Schotten U, Alkanoglu O, Reyle-Hahn MS, Hanrath P, Rossaint R. Xenon does not impair the responsiveness of cardiac muscle bundles to positive inotropic and chronotropic stimulation. *Anesthesiology.* (2002) 96:422–7. doi: 10.1097/00000542-200202000-00030
145. Schmidt M, Marx T, Kotzerke J, Luderwald S, Armbruster S, Topalidis P, et al. Cerebral and regional organ perfusion in pigs during xenon anaesthesia. *Anaesthesia.* (2001) 56:1154–9. doi: 10.1046/j.1365-2044.2001.02322.x
146. Rylova AV, Lubnin A. [Intracranial pressure changes during xenon anesthesia in neurosurgical patients without intracranial hypertention]. *Anesteziol Reanimatol.* (2011) 13–17.
147. Rylova AV, Beliaev A, Lubnin A. [Effects of xenon anesthesia on cerebral blood flow in neurosurgical patients without intracranial hypertension]. *Anesteziol Reanimatol.* (2013) 4–9.
148. Rylova AV, Gavrilov AG, Lubnin A, Potapov AA. [Intracranial and cerebral perfusion pressure in neurosurgical patients during anaesthesia with xenon]. *Anesteziol Reanimatol.* (2014) 59:19–25.
149. Preckel B, Ebel D, Müllenheim J, Frässdorf J, Thämer V, Schlack W. The direct myocardial effects of xenon in the dog heart *in vivo*. *Anesth Analg.* (2002) 94:545–51. doi: 10.1097/00000539-200203000-00012
150. Stowe DF, Rehmert GC, Kwok WM, Weigt HU, Georgieff M, Bosnjak ZJ. Xenon does not alter cardiac function or major cation currents in isolated guinea pig hearts or myocytes. *Anesthesiology.* (2000) 92:516–22. doi: 10.1097/00000542-200002000-00035
151. Preckel B, Schlack W, Heibel T, Rütten H. Xenon produces minimal haemodynamic effects in rabbits with chronically compromised left ventricular function. *Br J Anaesth.* (2002) 88:264–9. doi: 10.1093/bja/88.2.264
152. Neukirchen M, Hipp J, Schaefer MS, Brandenburger T, Bauer I, Winterhalter M, et al. Cardiovascular stability and unchanged muscle sympathetic activity during xenon anaesthesia: role of norepinephrine uptake inhibition. *Br J Anaesth.* (2012) 109:887–96. doi: 10.1093/bja/aes303
153. Vagts DA, Hecker K, Iber T, Roesner JP, Spee A, Otto B, et al. Effects of xenon anaesthesia on intestinal oxygenation in acutely instrumented pigs. *Br J Anaesth.* (2004) 93:833–41. doi: 10.1093/bja/aeh271
154. Iber T, Hecker K, Vagts DA, Roesner JP, Otto B, Steinicke A, et al. Xenon anesthesia impairs hepatic oxygenation and perfusion in healthy pigs. *Minerva Anestesiol.* (2008) 74:511–9.
155. Reinelt H, Marx T, Kotzerke J, Topalidis P, Luederwald S, Armbruster S, et al. Hepatic function during xenon anesthesia in pigs. *Acta Anaesthesiol Scand.* (2002) 46:713–6. doi: 10.1034/j.1399-6576.2002.460614.x
156. Weber NC, Kandler J, Schlack W, Grueber Y, Fradorf J, Preckel B. Intermitted pharmacologic pretreatment by xenon, isoflurane, nitrous oxide, and the opioid morphine prevents tumor necrosis factor alpha-induced adhesion molecule expression in human umbilical vein endothelial cells. *Anesthesiology.* (2008) 108:199–207. doi: 10.1097/01.anes.0000299441.32091.ed
157. Yin X, Moody MR, Hebert V, Klegerman ME, Geng YJ, Dugas TR, et al. Oral delivery of xenon for cardiovascular protection. *Sci Rep.* (2019) 9:14035. doi: 10.1038/s41598-019-50515-3
158. Faure A, Bruzzese L, Steinberg JG, Jammes Y, Torrents J, Berdah SV, et al. Effectiveness of pure argon for renal transplant preservation in a preclinical pig model of heterotopic autotransplantation. *J Transl Med.* (2016) 14:40. doi: 10.1186/s12967-016-0795-y
159. Zhao H, Rossaint R, Coburn M, Ma D, Argon Organo-Protective N. The renoprotective properties of xenon and argon in kidney transplantation. *Eur J Anaesthesiol.* (2017) 34:637–40. doi: 10.1097/EJA.0000000000000632
160. Yang SR, Hua KF, Chu LJ, Hwu YK, Yang SM, Wu CY, et al. Xenon blunts NF-kappaB/NLRP3 inflammasome activation and improves acute onset of accelerated and severe lupus nephritis in mice. *Kidney Int.* (2020) 98:378–90. doi: 10.1016/j.kint.2020.02.033
161. Kussmaul AR, Gur'eva TS, Dadasheva OA, Pavlov NB, Pavlov BN. [Effect of krypton-containing gas mixture on Japanese quail embryo development]. *Aviakosm Ekolog Med.* (2008) 42:41–4.
162. Al-Zoughool M, Krewski D. Health effects of radon: a review of the literature. *Int J Radiat Biol.* (2009) 85:57–69. doi: 10.1080/09553000802635054
163. Maier A, Wiedemann J, Rapp F, Papenfuss F, Rodel F, Hehlgans S, et al. Radon exposure-therapeutic effect and cancer risk. *Int J Mol Sci.* (2020) 22:316. doi: 10.3390/ijms22010316
164. Sanders RD, Ma D, Maze M. Xenon: elemental anaesthesia in clinical practice. *Br Med Bull.* (2004) 71:115–35. doi: 10.1093/bmb/ldh034
165. Burchfield JS, Xie M, Hill JA. Pathological ventricular remodeling: mechanisms: part 1 of 2. *Circulation.* (2013) 128:388–400. doi: 10.1161/CIRCULATIONAHA.113.001878
166. Wang J, Deng B, Liu Q, Huang Y, Chen W, Li J, et al. Pyroptosis and ferroptosis induced by mixed lineage kinase 3 (MLK3) signaling in cardiomyocytes are essential for myocardial fibrosis in response to pressure overload. *Cell Death Dis.* (2020) 11:574. doi: 10.1038/s41419-020-02777-3
167. Shi H, Gao Y, Dong Z, Yang J, Gao R, Li X, et al. GSDMD-Mediated cardiomyocyte pyroptosis promotes myocardial I/R injury. *Circ Res.* (2021) 129:383–96. doi: 10.1161/CIRCRESAHA.120.318629
168. Song X, Zhu S, Xie Y, Liu J, Sun L, Zeng D, et al. JTC801 induces ph-dependent death specifically in cancer cells and slows growth of tumors in mice. *Gastroenterology.* (2018) 154:1480–93. doi: 10.1053/j.gastro.2017.12.004

169. Holze C, Michaudel C, Mackowiak C, Haas DA, Benda C, Hubel P, et al. Oxeiptosis, a ROS-induced caspase-independent apoptosis-like cell-death pathway. *Nat Immunol.* (2018) 19:130–40. doi: 10.1038/s41590-017-0013-y
170. Zhang Y, Huang Z, Li H. Insights into innate immune signalling in controlling cardiac remodelling. *Cardiovasc Res.* (2017) 113:1538–50. doi: 10.1093/cvr/cvx130
171. Zhang Y, Li H. Reprogramming interferon regulatory factor signaling in cardiometabolic diseases. *Physiology.* (2017) 32:210–23. doi: 10.1152/physiol.00038.2016
172. Zhang Y, Zhang XJ, Wang PX, Zhang P, Li H. Reprogramming innate immune signaling in cardiometabolic disease. *Hypertension.* (2017) 69:747–60. doi: 10.1161/HYPERTENSIONAHA.116.08192
173. Cai J, Xu M, Zhang X, Li H. Innate immune signaling in nonalcoholic fatty liver disease and cardiovascular diseases. *Annu Rev Pathol.* (2019) 14:153–84. doi: 10.1146/annurev-pathmechdis-012418-013003
174. Xu M, Liu PP, Li H. Innate immune signaling and its role in metabolic and cardiovascular diseases. *Physiol Rev.* (2019) 99:893–948. doi: 10.1152/physrev.00065.2017
175. Fukuto JM, Carrington SJ, Tantillo DJ, Harrison JG, Ignarro LJ, Freeman BA, et al. Small molecule signaling agents: the integrated chemistry and biochemistry of nitrogen oxides, oxides of carbon, dioxygen, hydrogen sulfide, and their derived species. *Chem Res Toxicol.* (2012) 25:769–93. doi: 10.1021/tx2005234

Conflict of Interest: The authors declare that the research was conducted in the absence of any commercial or financial relationships that could be construed as a potential conflict of interest.

Publisher's Note: All claims expressed in this article are solely those of the authors and do not necessarily represent those of their affiliated organizations, or those of the publisher, the editors and the reviewers. Any product that may be evaluated in this article, or claim that may be made by its manufacturer, is not guaranteed or endorsed by the publisher.

Copyright © 2022 Zhang, Liu, Bi, Xu, Yang and Zhang. This is an open-access article distributed under the terms of the Creative Commons Attribution License (CC BY). The use, distribution or reproduction in other forums is permitted, provided the original author(s) and the copyright owner(s) are credited and that the original publication in this journal is cited, in accordance with accepted academic practice. No use, distribution or reproduction is permitted which does not comply with these terms.

frontiers in Cardiovascular Medicine

MINI REVIEW
published: 22 March 2022
doi: 10.3389/fcvm.2022.778773

Formation and Maintenance of the Natural Bypass Vessels of the Brain

Tijana Perovic[1,2]*, *Christoph Harms*[2,3,4] *and Holger Gerhardt*[1,2]*

[1] *Integrative Vascular Biology, Max-Delbrück-Center for Molecular Medicine in the Helmholtz Association, Berlin, Germany,* [2] *DZHK (German Center for Cardiovascular Research), Partner Site Berlin, Berlin, Germany,* [3] *Center for Stroke Research Berlin with Department of Experimental Neurology, Charité Universitaetsmedizin Berlin, Berlin, Germany,* [4] *Einstein Center for Neurosciences Berlin, Charité-Universitaetsmedizin Berlin, Berlin, Germany*

Ischemic diseases are the leading cause of death and disability worldwide. The main compensatory mechanism by which our body responds to reduced or blocked blood flow caused by ischemia is mediated by collateral vessels. Collaterals are present in many healthy tissues (including brain and heart) and serve as natural bypass vessels, by bridging adjacent arterial trees. This review focuses on: the definition and significance of pial collateral vessels, the described mechanism of pial collateral formation, an overview of molecular players and pathways involved in pial collateral biology and emerging approaches to prevent or mitigate risk factor-associated loss of pial collaterals. Despite their high clinical relevance and recent scientific efforts toward understanding collaterals, much of the fundamental biology of collaterals remains obscure.

Keywords: collateral, cerebrovasculature, development, maintenance, ischemic disease

OPEN ACCESS

Edited by:
Yacine Boulaftali, Institut National de la Santé et de la Recherche Médicale (INSERM), France

Reviewed by:
Masanori Nakayama, Max Planck Society, Germany
James E. Faber, University of North Carolina at Chapel Hill, United States

***Correspondence:**
Tijana Perovic
tijana.perovic@mdc-berlin.de
Holger Gerhardt
holger.gerhardt@mdc-berlin.de

Specialty section:
This article was submitted to Atherosclerosis and Vascular Medicine, a section of the journal Frontiers in Cardiovascular Medicine

Received: *17 September 2021*
Accepted: *28 February 2022*
Published: *22 March 2022*

Citation:
Perovic T, Harms C and Gerhardt H (2022) Formation and Maintenance of the Natural Bypass Vessels of the Brain. Front. Cardiovasc. Med. 9:778773. doi: 10.3389/fcvm.2022.778773

INTRODUCTION

Collateral vessels are anatomically defined as inter-tree anastomoses cross-connecting adjacent arterial trees (1, 2).

Functionally, they represent a specialized network of endogenous bypass vessels, which serve to partially attenuate hypoperfusion or ischemic injury following blockage of an artery. Collateral retrograde perfusion from adjacent territories may provide transient or permanent endogenous protection against ischemic injury in various organs (caused by ischemic stroke, coronary atherosclerosis, myocardial infarction, peripheral artery disease, etc.). However, the extent to which collaterals endow individuals with protection against occlusive disease varies greatly and directly impacts clinical outcome (3, 4). Naturally occurring differences in the number and diameter of collateral vessels as well as their ability to rapidly increase their diameter upon arterial vessel occlusion limit the protective capacity of collaterals (5). In humans, angiography of patients suffering from acute middle cerebral artery (MCA) occlusion show that retrograde perfusion of the ischemic MCA territory downstream from the occlusion *via* pial collaterals exhibits significant variation among individuals. Good collateral flow correlates with improved likelihood of major reperfusion, reduced infarct expansion and other favorable outcomes: infarct volume and modified Rankin scale scores at discharge are significantly lower for patients with better pial collaterals (angiographically assessed), while the National Institutes of Health Stroke Scale (NIHSS) score and collateral flow scores show an inverse relationship. Nowadays, MRI diffusion and perfusion imaging together with angiographic collateral scoring during acute cerebral ischemia show that patients with good collaterals have larger areas with only mild hypoperfusion and reduced infarct growth within the penumbra (6).

In an effort to standardize the terminology around collateral vessels, Faber and colleagues (1) define collaterals as *naturally occurring artery-to-artery or arteriole-to-arteriole anastomoses present in healthy tissues that increase their anatomic diameter, i.e., outwardly remodel, in obstructive disease*. Furthermore, they describe two distinct types of collateral vessels:

- Collateral arteries, which are, in fact, artery-to-artery anastomoses and occur in anatomically similar locations among humans and other mammals. Due to their common anatomical location, they often have a defined name (e.g., superior ulnar collateral artery, anterior and posterior communicating arteries/collaterals of the circle of Willis). Mature healthy collateral arteries exhibit minimal or no tortuosity, have a considerably smaller capacity to increase their lumen in obstructive disease and form differently from microvascular collaterals.
- Microvascular collaterals are arteriole-to-arteriole anastomoses that cross-connect a small fraction of distal-end arterioles in the crowns of adjacent arterial trees. These vessels in healthy humans and animals average <100 microns in diameter. Interestingly, they are completely absent in the mouse retinal circulation. Examples are: pial (leptomeningeal) collaterals of the brain and spinal cord, coronary collaterals, collaterals of the skeletal muscle and skin. They are characterized by significant tortuosity in healthy young adults and their inherent capacity to enlarge their lumen 5–10-fold upon occlusive disease. Between different inbred mouse strains, there exists a large genetic background variability in collateral number, diameter and remodeling capacity. Considering that collateral arteries have distinct names, usually the term *collateral* implies the microvascular collaterals of a given tissue/organ.

MECHANISMS OF FORMATION—BRAIN VS. HEART

In mice, pial collaterals have been reported to begin forming between embryonic day 13.5 (E13.5) and 15.5 (E15.5), with the peak collateral formation at E18.5 (7, 8). The pial vasculature matures between E18.5 and approximately postnatal day 21 (P21), involving the pruning of a variable proportion of nascent collaterals. The remaining collaterals undergo wall maturation, increase their diameter and length and acquire their characteristic tortuosity. The process of collateral formation during embryonic and postnatal development to yield the collateral extent present in the healthy adult tissue is termed collaterogenesis (1). To date, many details on the mechanism of collateral formation remain unclear: collaterals present in the adult may arise either by 1) retention or transformation of a capillary vessel(s) present early in embryonic/early postnatal development (pre-existing arteriolar connections) or by 2) sprouting from established arterioles to form novel inter-arteriolar connections. One current hypothesis suggests that pial collaterals form *via* arteriolar sprouting during late gestation (8). This is based on the exclusion of intussusception as a forming mechanism, as no intussusceptive pillars could be observed *via* confocal or scanning electron microscopy. Additionally, the authors identified a vessel which appears to be sprouting from a pial arteriole.

One angiographic study (9) shows that in human embryonic hearts (between 19 and 39 weeks, from the mid-second trimester until the end of the third trimester), collateral coronary arteries are already present, ranging between 3 and 50 micrometers in diameter. It has, in fact, been confirmed that human hearts have inherent collateral vessels in individuals with no previous occlusion (individuals with *normal coronary arteries*) (10). A more recent report investigated the presence of pre-existing collaterals in the mouse heart using various techniques, namely: angiographic casting, casting with low-viscosity Microfil or with high pressure, casting after minimizing resistance, perfusion with Evans-blue PBS, staining with Isolectin and ephrin-B2$^{Lacz/+}$ on two different backgrounds (B6 and BALB/c) (11). This study alongside others indicates that in the mouse heart, collateral coronary arteries form only upon vascular occlusion (also termed neo-collateral formation, *de novo* collateral formation in adults), and once again, determine the clinical outcome of infarction. Patients with significant collateral coronary arteries can survive having one or two completely occluded native coronary arteries and exhibit normal heart function. Most studies of embryonic microvascular collaterogenesis in the past two decades have focused on microvascular collaterals of the brain and hindlimb. A genetic lineage tracing study by He et al. (12) identified that upon myocardial infarction in adult mice, new coronary collateral vessels are formed from existing arteries. Briefly, the genetic lineage tracing method uses a cell-type specific Cre driver mouse line, which in this case is the capillary-specific Apln-CreER. Cre is expressed as a fusion protein to the mutated estrogen receptor (ER) to mediate activation in a conditional fashion by treatment with Tamoxifen. Such a mouse line is then crossed with a Cre-dependent reporter mouse line, which can be pharmacologically activated by Tamoxifen as it harbors a stop cassette flanked by loxP sites that are Cre-responsive (13). This allows for the reporting of certain cell types and their permanent lineage tracing over time, as expression of the reporter is irreversible once activated, and passed on to daughter cells when they divide. By genetic tracing of capillary-specific Apln-CreER cells, the authors showed that a mid-embryogenesis Tamoxifen induction with Apln-CreER will label both coronary arteries and capillaries at P7. However, if Apln-CreER was induced only after birth, at P1 or in the adult mouse, only the coronary microvasculature is labeled. This implies that the embryonic coronary capillaries significantly contribute to the formation of coronary arteries. When myocardial infarction was induced in adult-induced Apln-labeled hearts, no contribution of capillaries was found to the newly formed collaterals. Kristy Red-horse and colleagues (14) looked specifically into the mechanisms of formation of collateral coronary arteries and found that upon permanent ligation of the left coronary artery (LCA) at P2 neonates, arterial endothelial cells migrate from existing arteries, along capillaries and reassemble into collateral arteries, which the authors termed *artery reassembly*. Moreover, this process was largely dependent on the chemokine CXCL12—CXCR4 receptor signaling axis. In adult mice, the *artery reassembly*

after myocardial infarction could be triggered by administering a single dose of CXCL12.

PIAL COLLATERALS—PATHWAYS THAT PLAY A ROLE IN THEIR DEVELOPMENT AND MAINTENANCE

Although the question of whether collaterals possess a truly unique transcriptional and proteomic profile remains open, several molecular factors have been shown to affect collateral formation, maturation, maintenance and response to ischemia.

Formation

Embryonic collateral formation is dependent on VEGF signaling. In two mouse strains which exhibit large differences in collateral density, namely C57BL/6 and BALB/c, *Vegfa* expression was higher in the C57Bl/6 (the strain with higher collateral density) than in BALB-c mice (7). Functionally, hypomorphic $Vegf^{lo/+}$ embryos developed almost no collaterals. Inducible, global knockdown of either *Vegfa* or *Flk1* (VEGFR2 gene) impairs embryonic collateral formation. However, endothelial specific inducible *Vegfa* deletion had no effect on collateral formation, suggesting that paracrine VEGF signaling is relevant in collateral formation (8). Notch signaling works in conjunction with VEGF signaling in the process of endothelial tip cell selection and sprout formation. Membrane-bound Notch becomes active only upon two cleavage steps (ADAM sheddases participate in the 1st step, gamma secretase in the 2nd step), which allow for its translocation to the nucleus and target gene activation (15). Both endothelial-specific *Adam10* knockdown and pharmacological inhibition of gamma-secretase lead to an increase in embryonic collateral formation (8). The authors suggested that paracrine VEGF through the endothelial VEGFR2-ADAM10-Notch signaling pathway is crucial for embryonic development of pial collaterals, and when altered, permanently changes collateral density in the adult.

Intercellular communication to Notch is transmitted *via* Delta-like 4 (Dll4). Dll4-Notch signaling is a pathway implicated in the regulation of arterial identity and angiogenic sprouting (15–17). Dll4 is a transmembrane ligand of Notch receptors, selectively expressed in arterial and angiogenic tip cells during development. Similarly, Dll4-Notch signaling restricts pial collateral artery formation by modulating arterial branching morphogenesis during embryogenesis (18). DLL4 heterozygous mice show an increased number of pial collaterals compared to littermates, whereas the infarct volume upon MCA occlusion remains unchanged. Furthermore, functional recovery and ischemic outcome in stroke and hindlimb ischemia models were not improved in $Dll4^{+/-}$ mice, despite the clear increase in collateral vessel number. The authors speculate that this discrepancy is due to the adverse effects Dll4-Notch loss has on vessel formation and remodeling during development. Together, these results indicate that the protection pial collateral networks provide in ischemic stroke is not only determined by collateral numbers, but also by collateral functionality.

Mouse strains with different genetic backgrounds exhibit wide variation in collateral density, ∼80% of which is assigned to a polymorphic region on chromosome 7, *Dce1*. A single gene, *Rabep2*, was identified as responsible for most of the differences in native collateral density. Collateral formation is impaired in $Rabep2^{-/-}$ embryos (5). Rabep2 is ubiquitously expressed and associated with vesicular trafficking, particularly in the internalization of cell surface receptors into vesicles which fuse into early endosomes in a Rab4- and Rab5-dependent matter. The embryonic pial plexus of $Rabep2^{-/-}$ mice exhibits increased vessel diameter and reduced branching. Moreover, early endosomes are enlarged in E14.5 $Rabep2^{-/-}$ mice. *In vitro*, Rabep2-deficiency leads to increased Rab7 co-localization of VEGFR2, indicating that in absence of Rabep2, a higher proportion of internalized VEGFR2 is targeted for degradation (19).

Maturation

Chloride intracellular channel-4 (CLIC4) is a member of a 7-membrane-spanning family of proteins (CLICs). Knockdown of CLIC4 impairs EC proliferation, as well as formation of EC cords and tubular plexus. Clic4(–/–) mice have reduced native collateral density, which results in more severe infarctions (20). In a follow-up study, the authors have shown that Clic deficiency has no effect on embryonic collaterogenesis, yet leads to reduced mural cell recruitment and excessive pruning of pial collaterals. VEGF-A overexpression in CLIC4-deficient mice partially rescues deficits in perinatal collateral mural cell investment, and fully rescues aberrant perinatal collateral pruning and enlarged infarct volume after stroke in adults (21). Whereas Vegfr2 signaling is involved in both formation and maturation of pial collaterals, other pathways are more confined: Notch signaling seems crucial in collateral formation and CLIC4 in collateral maturation.

Ephrin (Eph) receptors are known to control cell migration, proliferation and mediate responses to guidance/repulsive cues. They have well-identified roles in neuronal development (axon guidance, neural crest migration, etc.) (22). EphrinB2 and EphB4 null mice show defects in arterio-venous patterning. Ephrin-B2, an Eph family transmembrane ligand, marks arterial but not venous endothelial cells from the onset of angiogenesis whereas Eph-B4, a receptor for ephrin-B2, marks veins but not arteries. Interestingly, endothelial-specific EphA4 deletion leads to an early postnatal increase in collateral number, but not diameter (23). By P21, this number lowers to wild-type values. Further work suggests that EphA4 acts as a major suppressor of pial collateral remodeling, as well as cerebral blood flow (CBF) and functional recovery after permanent middle cerebral artery occlusion, by acting as a negative regulator of Tie2 receptor signaling (24).

Signaling in the Collaterals of the Heart

Molecular effectors and pathways responsible for collateral formation in the mouse heart have only started to be studied. In 2015, Zhang and Faber showed the dependency of neo-collateral formation on MCP1—CCR2 signaling. MCP1 is released from cardiomyocytes, endothelial, smooth muscle cells and a variety of hematopoietic cells types and binds

CCR2 receptors which are present on monocytes, CD4 T-cells, endothelial cells and others. Mice lacking either MCP1 or CCR2 exhibited reduced neo-collateral formation and increased infarct volume (11). Interestingly, a recent cohort study showed that low matrix metalloproteinase-9 (MMP-9) and high MCP1 levels are associated with good pretreatment collateral status in patients suffering from acute ischemic stroke with large vessel occlusion (25).

The chemokine CXCL12, also known as SDF1, has chemotactic and mitogenic activity on many cell types (26). CXCL12 signaling has an important role in vasculogenesis, including endothelial cell migration, arterial-nerve alignment and mediation of plexus connections to systemic arteries. CXCL12 primarily acts through the G protein coupled receptor CXCR4; global mouse knockouts of Cxcl12 or of Cxcr4 die shortly before birth with vascular deficiencies in the gut, kidney, and skin, and with a number of additional hematopoietic and neural defects (27). Cxcl12 is important for guiding coronary EC migration during embryonic development. One study identified the CXCR4—CXCL12 axis as necessary for early postnatal collateral formation in response to myocardial infarction. Moreover, coronary collateral development was inhibited upon endothelial Cxcl12 or arterial Cxcr4 deletion. One dose of CXCL12 at the time of adult myocardial infarction stimulated collateral growth. The authors suggest that in this mechanism of *arterial reassembly*, arterial endothelial cells are attracted by a capillary CXCL12 gradient, in order to migrate, expand and establish a novel collateral artery network (14).

PIAL COLLATERALS—EMERGING CONCEPTS IN ISCHEMIA: PREVENTIVE CONDITIONING OF COLLATERALS (ROLE OF EXERCISE, HYPOXIA, eNOS SIGNALING)

The field of pial collateral biology has gained a lot of momentum in the past two decades, yet there are still many unknowns. Important questions are yet to be answered: 1) What prevention measures can be taken to halt or revert the progressive loss (rarefaction) of collaterals in aging individuals? 2) What acute intervention steps can be taken to stimulate the inherent *bypassing* capacity of collaterals upon stroke? 3) What acute intervention steps might stimulate neo-collateral growth in the adult?

A report from Rzechorzek et al. studied the effect of voluntary wheel running, a proxy for aerobic exercise in mice, on the outcome of permanent MCA occlusion in aging mice (26-month-old mice). In this study, the authors compared 3-month-old sedentary mice to 26-month-old sedentary and running mice. Their results indicate that regular aerobic exercise prevents age-induced rarefaction of pial collaterals and associated increase in infarct volume (28). Another interesting report from Zhang et al., examined the impact of hypoxia on adult mice neo-collateral formation. After gradually acclimating mice to lower concentrations of inspired oxygen and maintaining them for 2–8 weeks at 12, 10, 8.5, or 7% inspired oxygen concentrations, the authors observed a correlation between neo-collateral formation and hypoxemia, as well as remodeling of native collaterals and decreased infarct volume after permanent MCA occlusion and hypoxemia. Hypoxia led to an increased expression of *Hif2α, Vegfa, Rabep2, Angpt2, Tie2,* and *Cxcr4*. Moreover, neo-collateral formation was abolished in mice lacking Rabep2, and inhibited by conditional knockout of *Vegfa*, *Flk1,* and *Cxcr4* (29). These results suggest mechanistic links between embryonic collateral formation and neo-collateral formation in adult mice. Whether an increased need for oxygen is enough of a stimulus for adult physiological neo-collateral formation in humans as well is not known.

Additionally, a recent publication indicated that pial collateral cells are endowed with primary cilia more frequently than their neighboring vessels, distal-most arterioles. Moreover, collateral vessels showed an increased expression of *Pycard, Ki67, Pdgfb, Angpt2, Dll4,* and *Ephrinb2* when compared to their neighboring distal-end arterioles. Collaterals were enriched in both eNOS and phospho-eNOS compared to distal-most arterioles (30).

Interestingly, global eNOS KO mice have fewer pial collaterals and worse perfusion capacity upon femoral artery ligation (31). One recent report (32) proposed the cell cycle gene networks as the pathways responsible for the role of eNOS in collateral health and disease. It remains to be seen which of the effects of eNOS loss are specific for the endothelium and what is the role of paracrine signaling in pial collateral response to injury. In rodents, aging correlates with collateral rarefaction (33). According to Wang et al. (31), in a hind-limb ischemia model, aging decreases collateral responsiveness to angiogenic stimuli and increases endothelial and smooth muscle cell susceptibility to apoptosis *via* lack of functional eNOS signaling.

CONCLUDING REMARKS AND OUTLOOK

Collateral vessels are a rare gem in vascular biology. They undergo massive remodeling in a matter of days upon an ischemic event, all while maintaining vessel integrity and function. In the brain, an organ of high complexity and metabolic demand and low regenerative capacity, this ability of pial collateral vessels to quickly expand directly determines the volume of the damaged neuronal tissue. Therefore, it is of utmost importance for vascular biologists to understand the fundamentals of collateral formation, maintenance and remodeling in order to harness this knowledge and translate it into generation of more targeted therapeutics. If we understood exactly how pial collaterals form on the levels of brain morphogenesis, individual cell behavior and molecular drivers, we would know more about how to reactivate collateral formation or opening in patients suffering from ischemia with particularly poor prognosis due to collateral rarefaction or low collateral blood flow. In this review, we aimed to highlight the most important findings in collateral biology, in terms of endothelial cellular behavior in developing collaterals as well as in

terms of molecular effectors driving collateral formation and maturation. Despite their anatomical and biomechanical uniqueness, we still do not know whether native collaterals are somehow molecularly equipped to adapt to new blood flow requirements so rapidly. Only in recent years have scientists started to understand ways of preserving or increasing the abundance of collaterals in tissues by means of exercise and hypoxic treatment.

Pre-clinical models and animal research is currently highlighting commonalities and differences in heart and brain collaterals, and point toward signaling mechanisms of general importance in vascular formation and remodeling, such as hypoxia and VEGF, as well as blood flow, shear forces and chemokine signaling. Future research will need to identify whether specific endothelial cell types are uniquely endowed with the capacity to form neo-collaterals upon injury, what genetic and epigenetic mechanisms confer the risk to progressively lose collaterals in aging, and how we can devise both preventative and therapeutic measures to maintain and functionalize collaterals to mitigate the most devastating consequences of ischemic disease.

AUTHOR CONTRIBUTIONS

TP and HG contributed to conception and design of the mini review. TP performed the literature research and wrote the initial draft of the manuscript. CH and HG provided valuable feedback to the multiple versions of the manuscript and helped edit it. All authors read and approved the submitted version.

FUNDING

This work was supported in parts by the Leducq Foundation (Leducq ATTRACT 17 CVD 03), by Deutsche Forschungsgemeinschaft (DFG, German Research Foundation: HA5741/5-1, Project-ID 417284923, and Project-ID 424778381 –TRR 295), and German Federal Ministry of Education and Research (BMBF CSB 01EO1301).

ACKNOWLEDGMENTS

We are grateful to all the members of the Integrative Vascular Biology Laboratory for helpful discussions.

REFERENCES

1. Faber JE, Chilian WM, Deindl E, van Royen N, Simons M. A brief etymology of the collateral circulation. *Arterioscler Thromb Vasc Biol.* (2014) 34:1854–9. doi: 10.1161/ATVBAHA.114.303929
2. Heubner O. D*ie luetischen Erkrankungen der Hirnarterien*. Leipzig: FC Vogel (1874). p. 170–214.
3. Seyman E, Shaim H, Shenhar-Tsarfaty S, Jonash-Kimchi T, Bornstein NM, Hallevi H. The collateral circulation determines cortical infarct volume in anterior circulation ischemic stroke. *BMC Neurol.* (2016) 16:206. doi: 10.1186/s12883-016-0722-0
4. Seiler C. The human coronary collateral circulation. *Eur J Clin Invest*. (2010) 40:465–76. doi: 10.1111/j.1365-2362.2010.02282.x
5. Lucitti JL, Sealock R, Buckley BK, Zhang H, Xiao L, Dudley AC, et al. Variants of Rab GTPase–effector binding protein-2 cause variation in the collateral circulation and severity of stroke. *Stroke*. (2016) 47:3022–31. doi: 10.1161/STROKEAHA.116.014160
6. Winship IR. Cerebral collaterals and collateral therapeutics for acute ischemic stroke. *Microcirculation.* (2015) 22:228–36. doi: 10.1111/micc.12177
7. Chalothorn D, Faber JE. Formation and maturation of the native cerebral collateral circulation. *J Mol Cell Cardiol.* (2010) 49:251–9. doi: 10.1016/j.yjmcc.2010.03.014
8. Lucitti JL, Mackey JK, Morrison JC, Haigh JJ, Adams RH, Faber JE. Formation of the collateral circulation is regulated by vascular endothelial growth factor-A and A disintegrin and metalloprotease family members 10 and 17. *Circ Res.* (2012) 111:1539–50. doi: 10.1161/CIRCRESAHA.112.279109
9. Cortis BS, Serratto M. The collateral coronary circulation in the human fetus: angiographic findings. *Cardiologia.* (1998) 43:77–81.
10. Wustmann K, Zbinden S, Windecker S, Meier B, Seiler C. Is there functional collateral flow during vascular occlusion in angiographically normal coronary arteries? *Circulation.* (2003) 107:2213–20. doi: 10.1161/01.CIR.0000066321.03474.DA
11. Zhang H, Faber JE. *De-novo* collateral formation following acute myocardial infarction: Dependence on CCR2+ bone marrow cells. *J Mol Cell Cardiol.* (2015) 87:4–16. doi: 10.1016/j.yjmcc.2015.07.020
12. He L, Liu Q, Hu T, Huang X, Zhang H, Tian X, et al. Genetic lineage tracing discloses arteriogenesis as the main mechanism for collateral growth in the mouse heart. *Cardiovasc Res.* (2016) 109:419–30. doi: 10.1093/cvr/cvw005
13. Nagy A. Cre recombinase: The universal reagent for genome tailoring. *Genesis* (2000) 26:99–109.
14. Das S, Goldstone AB, Wang H, Farry J, D'Amato G, Paulsen MJ, et al. A unique collateral artery development program promotes neonatal heart regeneration. *Cell.* (2019) 176:1128–42.e18. doi: 10.1016/j.cell.2018.12.023
15. Hofmann JJ, Iruela-Arispe ML. Notch signaling in blood vessels. *Circ Res.* (2007) 100:1556–68. doi: 10.1161/01.RES.0000266408.42939.e4
16. Phng LK, Gerhardt H. Angiogenesis: a team effort coordinated by notch. *Dev Cell.* (2009) 16:196–208. doi: 10.1016/j.devcel.2009.01.015
17. Swift MR, Weinstein BM. Arterial-venous specification during development. *Circ Res.* (2009) 104:576–88. doi: 10.1161/CIRCRESAHA.108.188805
18. Cristofaro B, Shi Y, Faria M, Suchting S, Leroyer AS, Trindade A, et al. Dll4-Notch signaling determines the formation of native arterial collateral networks and arterial function in mouse ischemia models. *Development.* (2013) 140:1720–9. doi: 10.1242/dev.092304
19. Kofler N, Corti F, Rivera-Molina F, Deng Y, Toomre D, Simons M. The Rab-effector protein RABEP2 regulates endosomal trafficking to mediate vascular endothelial growth factor receptor-2 (VEGFR2)-dependent signaling. *J Biol Chem.* (2018) 293:4805–17. doi: 10.1074/jbc.M117.812172
20. Chalothorn D, Zhang H, Smith JE, Edwards JC, Faber JE. Chloride intracellular channel-4 is a determinant of native collateral formation in skeletal muscle and brain. *Circ Res.* (2009) 105:89–98. doi: 10.1161/CIRCRESAHA.109.197145
21. Lucitti JL, Tarte NJ, Faber JE. Chloride intracellular channel 4 is required for maturation of the cerebral collateral circulation. *Am J Physiol Heart Circ Physiol.* (2015) 309:H1141–50. doi: 10.1152/ajpheart.00451.2015
22. Adams RH. Vascular patterning by Eph receptor tyrosine kinases and ephrins. *Semin Cell Dev Biol.* (2002) 13:55–60. doi: 10.1006/scdb.2001.0289
23. Okyere B, Giridhar K, Hazy A, Chen M, Keimig D, Bielitz RC, et al. Endothelial-specific EphA4 negatively regulates native pial collateral formation and re-perfusion following hindlimb ischemia. *PLoS ONE.* (2016) 11:e0159930. doi: 10.1371/journal.pone.0159930
24. Okyere B, Mills WA, Wang X, Chen M, Chen J, Hazy A, et al. EphA4/Tie2 crosstalk regulates leptomeningeal collateral remodeling following ischemic stroke. *J Clin Investig.* (2020) 130:1024–35. doi: 10.1172/JCI131493
25. Mechtouff L, Mechtouff L, Bochaton T, Bochaton T, Paccalet A, Crola Da Silva C, et al. matrix metalloproteinase-9 and monocyte chemoattractant protein-1

are associated with collateral status in acute ischemic stroke with large vessel occlusion. *Stroke.* (2020) 51:2232–5. doi: 10.1161/STROKEAHA.120.029395
26. Ivins S, Chappell J, Vernay B, Suntharalingham J, Martineau A, Mohun TJ, et al. The CXCL12/CXCR4 axis plays a critical role in coronary artery development. *Dev Cell.* (2015) 33:455–68. doi: 10.1016/j.devcel.2015.03.026
27. Cavallero S, Shen H, Yi C, Lien CL, Kumar SR, Sucov HM. CXCL12 signaling is essential for maturation of the ventricular coronary endothelial plexus and establishment of functional coronary circulation. *Dev Cell.* (2015) 33:469–77. doi: 10.1016/j.devcel.2015.03.018
28. Rzechorzek W, Zhang H, Buckley BK, Hua K, Pomp D, Faber JE. Aerobic exercise prevents rarefaction of pial collaterals and increased stroke severity that occur with aging. *J Cereb Blood Flow Metab.* (2017) 37:3544–55. doi: 10.1177/0271678X17718966
29. Zhang H, Rzechorzek W, Aghajanian A, Faber JE. Hypoxia induces de novo formation of cerebral collaterals and lessens the severity of ischemic stroke. *J Cereb Blood Flow Metab.* (2020) 40:1806–22. doi: 10.1177/0271678X20924107
30. Zhang H, Chalothorn D, Faber JE. Collateral vessels have unique endothelial and smooth muscle cell phenotypes. *Int J Mol Sci.* (2019) 20:3608. doi: 10.3390/ijms20153608
31. Wang J, Peng X, Lassance-Soares RM, Najafi AH, Alderman LO, Sood S, et al. Aging-induced collateral dysfunction: Impaired responsiveness of collaterals and susceptibility to apoptosis *via* dysfunctional eNOS signaling. *J Cardiovasc Transl Res.* (2011) 4:779–89. doi: 10.1007/s12265-011-9280-4
32. Dai X, Faber JE. Endothelial nitric oxide synthase deficiency causes collateral vessel rarefaction and impairs activation of a cell cycle gene network during arteriogenesis. *Circ Res.* (2010) 106:1870. doi: 10.1161/CIRCRESAHA.109.212746
33. Ma J, Ma Y, Shuaib A, Winship IR. Impaired collateral flow in pial arterioles of aged rats during ischemic stroke. *Transl Stroke Res.* (2020) 11:243–53. doi: 10.1007/s12975-019-00710-1

Conflict of Interest: The authors declare that the research was conducted in the absence of any commercial or financial relationships that could be construed as a potential conflict of interest.

Publisher's Note: All claims expressed in this article are solely those of the authors and do not necessarily represent those of their affiliated organizations, or those of the publisher, the editors and the reviewers. Any product that may be evaluated in this article, or claim that may be made by its manufacturer, is not guaranteed or endorsed by the publisher.

Copyright © 2022 Perovic, Harms and Gerhardt. This is an open-access article distributed under the terms of the Creative Commons Attribution License (CC BY). The use, distribution or reproduction in other forums is permitted, provided the original author(s) and the copyright owner(s) are credited and that the original publication in this journal is cited, in accordance with accepted academic practice. No use, distribution or reproduction is permitted which does not comply with these terms.

frontiers | Frontiers in Cardiovascular Medicine

ORIGINAL RESEARCH
published: 04 April 2022
doi: 10.3389/fcvm.2022.853583

Novel Insight Into Long-Term Risk of Major Adverse Cardiovascular and Cerebrovascular Events Following Lower Extremity Arteriosclerosis Obliterans

Ji Sun[1†], Qiang Deng[1†], Jun Wang[1†], Shoupeng Duan[1], Huaqiang Chen[1], Huixin Zhou[1], Zhen Zhou[1], Fu Yu[1], Fuding Guo[1], Chengzhe Liu[1], Saiting Xu[1], Lingpeng Song[1], Yijun Wang[1], Hui Feng[2] and Lilei Yu[1]**

[1] Department of Cardiology, Renmin Hospital of Wuhan University, Cardiac Autonomic Nervous System Research Centre of Wuhan University, Cardiovascular Research Institute, Wuhan University, Hubei Key Laboratory of Cardiology, Wuhan, China, [2] Information Center, Renmin Hospital of Wuhan University, Wuhan, China

Background: Patients with lower extremity arteriosclerosis obliterans (LEASO) are more likely to appear to be associated with adverse cardiovascular outcomes. Currently, few studies have reported the sex-specific characteristics and risk of major cardiovascular and cerebrovascular adverse events (MACCEs) in LEASO. Our study was conducted to determine the characteristics and contributions of LEASO to MACCEs in males and females.

Methods: We conducted a single-center retrospective study of consecutively enrolled patients with first-diagnosed LEASO at Renmin Hospital of Wuhan University from November 2017 to November 2019. The ratio of patients between the LEASO and control groups was 1 to 1 and based on age, sex, comorbid diabetes mellitus and hypertension, current smoking and medications. The occurrence of MACCEs was used as the primary endpoint of this observational study.

Results: A LEASO group (n = 430) and control group (n = 430) were enrolled in this study. A total of 183 patients experienced MACCEs during an average of 38.83 ± 14.28 months of follow-up. Multivariate Cox regression analysis indicated that LEASO was an independent predictor of the occurrence of MACCEs in all patients (HR: 2.448, 95% CI: 1.730–3.464, $P < 0.001$). Subgroup analysis by sex subgroup was conducted for sex, and LEASO was also an independent predictor of the occurrence of MACCEs in both male cases (HR: 2.919, 95% CI: 1.776–4.797, $P < 0.001$) and female cases (HR: 1.788, 95% CI: 1.110–2.880, $P = 0.017$). Moreover, Kaplan–Meier analysis indicated no significant difference in event-free survival between patients of different sexes with LEASO ($\chi^2 = 0.742$, $P = 0.389$).

Conclusion: LEASO tended to a useful risk stratified indicator for MACCEs in both male and female patients in our study. Notably, attention should be

OPEN ACCESS

Edited by:
Jinwei Tian,
The Second Affiliated Hospital of Harbin Medical University, China

Reviewed by:
Jinn-Rung Kuo,
Chi Mei Medical Center, Taiwan
Li Chen,
Chinese Academy of Medical Sciences and Peking Union Medical College, China
Junnan Tang,
First Affiliated Hospital of Zhengzhou University, China
Chunli Shao,
Peking University Third Hospital, China

***Correspondence:**
Hui Feng
Fenghui7@whu.edu.cn
Lilei Yu
lileiyu@whu.edu.cn

[†] These authors have contributed equally to this work

Specialty section:
This article was submitted to General Cardiovascular Medicine, a section of the journal Frontiers in Cardiovascular Medicine

Received: 12 January 2022
Accepted: 23 February 2022
Published: 04 April 2022

Citation:
Sun J, Deng Q, Wang J, Duan S, Chen H, Zhou H, Zhou Z, Yu F, Guo F, Liu C, Xu S, Song L, Wang Y, Feng H and Yu L (2022) Novel Insight Into Long-Term Risk of Major Adverse Cardiovascular and Cerebrovascular Events Following Lower Extremity Arteriosclerosis Obliterans. Front. Cardiovasc. Med. 9:853583. doi: 10.3389/fcvm.2022.853583

given to patients with LEASO who should undergo comprehensive cardiovascular evaluation and intervention, even if there is a lack of traditional cardiovascular risk factors.

Keywords: lower extremity arteriosclerosis obliterans, major cardiovascular and cerebrovascular adverse events, gender, panvascular disease, coronary artery disease

INTRODUCTION

Lower extremity arteriosclerosis obliterans (LEASO), the main and most common type of lower extremity peripheral arterial disease (PAD), tends to increase with age (1, 2). Notably, accumulating evidence suggests that people suffering from PAD are at higher risk of other health risks, including cardiovascular death, stroke, heart failure, and myocardial infarction (MI) (3, 4). Furthermore, patients with lower extremity PAD maintained higher cardiovascular (CV) mortality than MI patients due to less intensive treatment, which is closely associated with heart failure hospitalization, ischemic stroke and CV death (5, 6). Notably, LEASO shares cardiovascular risk factors in common with coronary heart disease (CHD) and may also have a similar pathophysiologic basis. Therefore, it is significant for patients with LEASO to carry out comprehensive cardiovascular follow-up examinations and medical prevention.

It is well known that sex is a substantial unchangeable cardiovascular risk factor, and men and women differ in terms of characteristics and management of coronary artery disease (CAD) (7, 8). A previous study showed that females with acute ischemic stroke who received parallel in-hospital care had more vascular risk factors and were more likely to be discharged with disability (9). In addition, female patients with CAD carry a higher risk of heart failure, ischemic stroke and all-cause mortality than male patients with CAD (10). Nevertheless, men with AF reported better overall health-related quality of life (11). Moreover, males and females also differ with regard to key features of other cardiovascular diseases (12–14). Although lower extremity PAD is a component of systemic atherosclerosis and carries a dramatically heightened risk of cardiovascular morbidity and mortality, sex differences were not included in further analyses (3, 15). Moreover, existing data are limited to correcting for a possible confounder, including routine laboratory results and drug treatments. Therefore, in this study, we aimed to evaluate whether LEASO could serve as an independent predictor of major cardiovascular and cerebrovascular adverse events (MACCEs) and determine whether these quantitative assessments provide parallel prognostic intelligence in males and females.

MATERIALS AND METHODS

Study Population

A single-center retrospective cohort study was launched at the Renmin Hospital of Wuhan University. In total, 430 consecutive patients with a first diagnosis of LEASO and without a history of LEASO or CAD who received optimal clinical intervention from November 2017 to November 2019 were enrolled in our retrospective study. Patients suffering from a history of LEASO, prior CAD, malignancy, severe renal insufficiency (eGFR $<$ 30 ml/min), severe liver disease, stroke, and severe lung disease were not recruited for the study. Individuals without LEASO who underwent coronary angiogram to rule out CAD in the same period were included in the control group (n = 430), which was matched with the LEASO group at a 1-to-1 ratio, according to age, sex, diabetes, hypertension, current smoking status, and medications.

Data Collection

Venous blood taken from all patients on the day of admission was sent to the Department of Clinical Laboratory of Renmin Hospital of Wuhan University to measure the parameters of routine blood examination and biochemistry, such as white blood cell count (WBC), lymphocyte cell count, neutrophil cell count, platelet count, neutrophil-to-lymphocyte ratio (NLR), platelet-to-lymphocyte ratio (PLR), uric acid (UA), glucose, total cholesterol (TC), total triglycerides (TG), high-density lipoprotein cholesterol (HDL-c), low-density lipoprotein cholesterol (LDL-C), apolipoprotein A1 (Apo A1), apolipoprotein B (Apo B), lipoprotein a, hypersensitive C-reactive protein (hs-CRP), total bilirubin (TBil), direct bilirubin (DBil), fibrinogen, and D-dimers.

Follow-Up and End-Point

After discharge, all the patients were followed-up by telephone or outpatient visits, and the mean follow-up time was approximately 38.83 months. The observed outcome of this study was identified as the occurrence of MACCEs together with (a) all-cause mortality, (b) cardiac mortality, (c) acute coronary syndromes, (d) stroke, (e) admission to the hospital necessitated by heart failure, (f) admission to the hospital necessitated by atrial fibrillation, and (g) revascularization.

Propensity Score Matching

Potential confounding factors were controlled by matching the covariates of the LEASO groups and controls group as many as possible based on the propensity scores calculated, implementing logistic multiple regression analysis after applying propensity scores matching (PSM), as recommended in the literature (16). Final covariates were age, sex, diabetes, hypertension, current smoking status, and medications according to the results of the pre-survey. Propensity score analysis with 1-to-1 ratio matching and the nearest neighbor matching method was applied to ensure well-balanced features between the LEASO groups and controls group. The propensity score with a standard caliper width of 0.2.

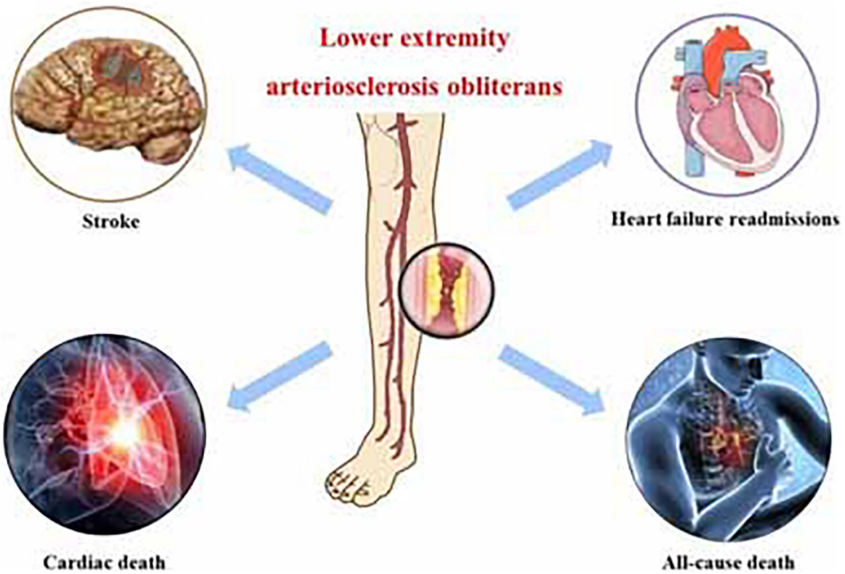

GRAPHICAL ABSTRACT | Central illustration: lower extremity arteriosclerosis obliterans as a prognostic factor for the occurrence of major cardiovascular and cerebrovascular adverse events.

Statistical Methods

The mean and standard deviation (SD) or median and interquartile range (IQR) were applied to our results to represent continuous variables, whereas percentage was used to represent categorical variables. For data processing methods, *t* tests were used for continuous variables, and chi-square ($\chi 2$) tests were used for categorical variables. The Kaplan–Meier survival method was applied to identify prognostic factors for the occurrence of MACCEs. The Kaplan–Meier survival curves were compared using the logrank test. Univariate analysis was performed first, and the significant variables were included in a subsequent multivariate Cox analysis. Comparisons were performed to analyze whether adding LEASO to the traditional cardiovascular risk factors, including gender, age, hypertension, diabetes, current smoking, current drinking, for MACCEs could improve the predictive ability of the models. The addition of LEASO to the existing models 1 with the traditional cardiovascular risk was evaluated with the predicted probabilities of MACCEs, using increase in the area under the receiver operating characteristic curve (AUC), sensitivity, specificity and C-index and Youden index. A statistically significant difference was denoted when the *P* value was < 0.05. SPSS 23.0 (SPSS, Inc., Chicago, IL, United States) was applied for all analyses.

RESULTS

Patient Characteristics of the Lower Extremity Arteriosclerosis Obliterans Group and Control Group

A total of 860 patients were identified, of whom 430 were diagnosed with LEASO. Four-hundred thirty patients composed a control group, and their clinical characteristics are shown in **Table 1**. The data showed that white blood cell count ($P < 0.001$), neutrophil cell count ($P < 0.001$), NLR ($P < 0.001$), PLR ($P = 0.002$), glucose ($P < 0.001$), TG ($P = 0.001$), TC ($P < 0.001$), LDL-C ($P = 0.002$), Apo B ($P = 0.27$), Lp (a) ($P = 0.017$), fibrinogen ($P < 0.001$), D-dimer ($P < 0.001$), and DBil ($P < 0.001$) tended to be higher in LEASO patients than in the control patients. In addition, patients with LEASO remained more likely to have lower lymphocyte counts ($P < 0.001$), HDL-C levels ($P = 0.001$), and Apo A1 levels ($P < 0.001$) than did the control group patients.

Predictors of Patients' Clinical Outcomes

In our study, patients were followed-up for 38.83 ± 14.28 months. The clinical outcomes of all patients are presented in **Table 2**, and a total of 183 patients suffered from MACCEs during the follow-up period. Our study showed that, compared to the control group patients, patients subjected to LEASO tended to have a higher incidence of MACCEs ($P < 0.001$), all-cause death ($P < 0.001$), cardiac death ($P < 0.001$), stroke ($P = 0.002$) and admission to the hospital necessitated by heart failure ($P < 0.001$). According to Kaplan–Meier analysis, an obvious difference could be found in the incidence of MACCEs between the LEASO patients and controls ($\chi^2 = 47.128$, $p < 0.001$), and the incidence of MACCEs in the LEASO group was higher than that in the control group, as shown in **Figure 1**.

According to univariate Cox analysis, hypertension, diabetes, LEASO, WBC, neutrophil, lymphocyte, NLR, PLR, UA, Apo A1, fibrinogen, D-dimers, and the application of aspirin and β-blockers were predictors of MACCEs, as shown in **Table 3**. Multivariate Cox analysis was then applied to identify independent influencing factors that predict MACCEs in

TABLE 1 | Characteristics of LEASO group and control group.

	Control (n = 430)	LEASO (n = 430)	$t/Z/\chi$ 2	p
Gender (male)	205 (47.7)	223 (51.9)	1.507	0.220
Age (years)	65.75 ± 7.98	66.55 ± 11.54	1.182	0.237
Hypertension (%)	203 (47.2)	216 (50.2)	0.787	0.375
Duration of Hypertension (years)	10.00 (5.00, 15.00)	10.00 (6.00, 15.00)	1.179	0.238
Diabetes (%)	66 (15.3)	87 (20.2)	3.506	0.061
Duration of Diabetes (years)	9.00 (3.00, 10.25)	10.00 (5.00, 12.00)	1.765	0.078
Current Smoking (%)	87 (20.2)	106 (24.7)	2.412	0.120
Duration of smoking (years)	30.00 (20.00, 35.00)	30.00 (20.00, 40.00)	0.255	0.799
Current smoking cigarettes (per day)	20.00 (10.00, 20.00)	20.00 (10.00, 20.00)	0.956	0.339
Current Drinking (%)	44 (10.2)	56 (13.0)	1.629	0.202
WBC ($\times 10^9$/L)	6.09 ± 1.72	7.74 ± 3.72	8.375	<0.001
Neutrophil ($\times 10^9$/L)	3.82 ± 1.63	5.34 ± 3.47	8.218	<0.001
Lymphocyte ($\times 10^9$/L)	1.72 ± 0.56	1.54 ± 0.59	4.653	<0.001
NLR	2.04 (1.51, 2.83)	2.82 (1.88, 4.84)	8.348	<0.001
PLT ($\times 10^9$/L)	212.60 ± 58.21	214.32 ± 84.65	0.346	0.729
PLR	124.81 (101.30, 156.37)	136.92 (98.58, 188.62)	3.060	0.002
Creatinine (μmol/L)	73.14 ± 29.43	71.40 ± 12.19	1.131	0.259
UA (μmol/L)	354.17 ± 99.39	368.37 ± 116.86	1.920	0.055
Glucose (mmol/L)	5.61 ± 1.70	6.21 ± 2.57	3.993	<0.001
TG (mmol/L)	1.13 (0.87, 1.38)	1.20 (0.90, 1.67)	3.433	0.001
TC (mmol/L)	3.74 ± 0.59	4.03 ± 1.04	4.990	<0.001
HDL-C (mmol/L)	1.15 ± 0.31	1.08 ± 0.31	3.454	0.001
LDL-C (mmol/L)	2.12 ± 0.56	2.27 ± 0.87	3.047	0.002
Apo A1 (g/L)	1.36 ± 0.22	1.27 ± 0.22	6.307	<0.001
Apo B (g/L)	0.73 ± 0.17	0.76 ± 0.23	2.217	0.027
Lp (a) (g/L)	145.50 (68.00, 305.38)	189.00 (80.75, 401.50)	2.379	0.017
hs-CRP (mg/L)	1.89 (0.32, 8.98)	1.52 (0.58, 5.98)	1.359	0.174
Fibrinogen (g/L)	2.90 ± 0.74	3.62 ± 1.36	9.551	<0.001
D-dimer (ug/ml)	0.24 (0.17, 0.41)	0.73 (0.38, 1.56)	14.976	<0.001
TBil (μmol/L)	11.63 (9.18, 15.60)	12.00 (8.88, 15.70)	0.429	0.668
DBil (μmol/L)	3.40 (2.70, 4.40)	4.00 (3.08, 5.80)	5.577	<0.001
Medications				
Aspirin (%)	284 (66.0)	262 (60.9)	2.428	0.119
Statins (%)	291 (67.7)	277 (64.4)	1.016	0.313
β-blocker (%)	113 (26.3)	106 (24.7)	0.300	0.584
ACEI/ARB (%)	48 (11.2)	45 (10.5)	0.109	0.742
CCB (%)	109 (25.3)	86 (20.0)	3.508	0.061

WBC, white blood cell count; NLR, neutrophil-to-lymphocyte ratio; PLT, platelet count; PLR, platelet-to-lymphocyte ratio; UA, uric acid; TG, triglycerides; TC, total cholesterol; HDL-C, high-density lipoprotein cholesterol; LDL-C, low-density lipoprotein cholesterol; Apo A1, Apolipoprotein A1; Apo B, Apolipoprotein B; Lp (a), lipoprotein a; hs-CRP, hypersensitive C-reactive protein; TBil, total bilirubin; DBil, direct bilirubin; ACEI, angiotensin converting enzyme inhibitor; ARB, angiotensin receptor blockers; CCB, calcium ion channel blockers; LEASO, lower extremity arteriosclerosis obliterans.

TABLE 2 | Incidence of MACCEs of LEASO group and control group.

	Control (n = 430)	LEASO (n = 430)	χ2	p
MACCEs	52 (12.1)	131 (30.5)	43.322	<0.001
All-cause death	1 (0.2)	75 (17.4)	79.037	<0.001
Cardiac death	1 (0.2)	39 (9.1)	37.861	<0.001
Revascularization	4 (0.9)	10 (2.3)	2.614	0.106
Stroke	17 (4.0)	40 (9.3)	9.939	0.002
Acute coronary syndromes	37 (8.6)	31 (7.2)	0.575	0.448
Admission to the hospital necessitated by Atrial fibrillation	13 (3.0)	10 (2.3)	0.402	0.526
Admission to the hospital necessitated by Heart failure	5 (1.2)	37 (8.6)	25.633	<0.001

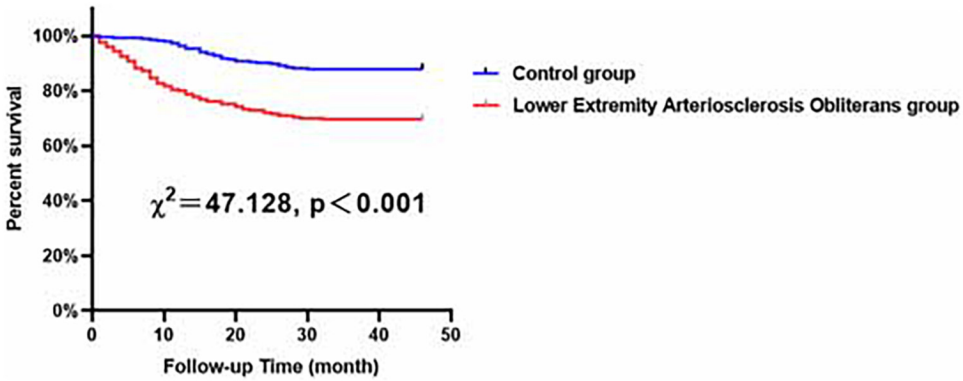

FIGURE 1 | Major adverse cardiovascular and cerebrovascular events (MACCEs)-free survival rates for patients with LEASO group and control group during the follow-up period.

patients. The results showed that hypertension (HR: 1.795, 95% CI: 1.320–2.440, $P < 0.001$), NLR (HR: 1.109, 95% CI: 1.057–1.163, $P < 0.001$), and LEASO (HR: 2.448, 95% CI: 1.730–3.464, $P < 0.001$) were independent risk factors for MACCEs, as presented in **Table 3** (Central illustration). Moreover, the application of aspirin (HR: 0.608, 95% CI: 0.450–0.821, $P = 0.001$) or β-blockers (HR: 0.423, 95% CI: 0.280–0.638, $P < 0.001$) remained a protective factor for MACCEs, as shown in **Table 3**.

In the multivariable analysis model, when added to clinical risk factors, LEASO increased the discriminatory indices (**Figure 2**). Distribution of predicted risks for MACCEs from model 1 based on age, sex, hypertension, diabetes, current smoking, and current drinking (AUC: 0.614; C-index: 0.632; Youden index: 0.176; sensitivity: 84.2%; specificity: 33.4%; $P < 0.001$). For the predictability of MACCEs, the positive Youden index of the combined LEASO increased in model 2 (AUC: 0.690; C-index: 0.700; Youden index: 0.318; sensitivity: 66.1%; specificity: 65.7%; $P < 0.001$). This suggested that incorporating LEASO enhanced the ability to predict accurately the MACCEs compared with Model 1, which included traditional cardiovascular risk factors only (AUC: 0.690 versus 0.614; C-index: 0.700 versus 0.632).

Predictors of Clinical Outcomes in Male Patients

According to Kaplan–Meier analysis, in all of the evaluated male patients, compared with the control patients, the patients with LEASO seemed to maintain lower MACCE-free survival rates ($\chi^2 = 22.818$, $P < 0.001$, **Figure 3**).

According to univariable Cox analysis, diabetes, current smoking, LEASO, NLR, and HDL-C (all $P < 0.05$) were predictors of MACCEs in all of the evaluated male patients (**Table 4**). Moreover, multivariate Cox analysis indicated that diabetes (HR: 1.725, 95% CI: 1.068–2.787, $P = 0.026$), current smoking (HR: 1.734, 95% CI: 1.133–2.652, $P = 0.011$), LEASO (HR: 2.919, 95% CI: 1.776–4.797, $P < 0.001$), and HDL-C (HR: 0.269, 95% CI: 0.117–0.620, $P = 0.002$) were independent influencing factors for MACCEs in all of the evaluated male patients (**Table 4**).

Predictors of Clinical Outcomes in Female Patients

Compared with the female control patients, the female LEASO patients tended to be at a higher risk for the incidence of MACCEs during the follow-up period ($\chi^2 = 24.979$, $P < 0.001$, **Figure 4**).

Univariable Cox analysis demonstrated that hypertension, LEASO, WBC, neutrophils, lymphocytes, NLR, PLR, UA, glucose, Apo A1, fibrinogen, DBil, and the application of aspirin and β-blockers (all $P < 0.05$) were independent factors for MACCEs in all evaluated female patients in this study, as shown in **Table 5**. According to multivariate Cox analysis, independent influencing factors for the incidence of MACCEs in female patients included hypertension (HR: 2.010, 95% CI: 1.293–3.124, $P = 0.002$), LEASO (HR: 1.788, 95% CI: 1.110–2.880, $P = 0.017$), NLR (HR: 1.113, 95% CI: 1.041–1.190, $P = 0.002$), UA (HR: 1.002, 95% CI: 1.000–1.004, $P = 0.049$), and application of aspirin (HR: 0.472, 95% CI: 0.311–0.715, $P < 0.001$) or β-blockers (HR: 0.321, 95% CI: 0.176–0.586, $P < 0.001$) (**Table 5**).

Sex Differences in the Characteristics and Prognosis of Lower Extremity Arteriosclerosis Obliterans Patients

Our results demonstrated that, compared with male patients with LEASO, female patients with LEASO remained more likely to suffer from hypertension and had higher levels of HDL-C and Apo B and lower levels of UA (**Table 6**). In addition, Kaplan–Meier analysis indicated no significant difference in event-free survival rate between male and female LEASO patients ($\chi^2 = 0.742$, $P = 0.389$, **Figure 5**).

TABLE 3 | Predictors of the occurrence of MACCEs in LEASO patients: results of univariate and multivariate Cox-regression analyses.

Indicators	Univariate			Multivariate		
	HR	95%CI	*p*	HR	95%CI	*p*
Gender (female)	1.134	0.848–1.515	0.397			
Age (years)	0.999	0.984–1.014	0.891			
Hypertension (%)	1.759	1.307–2.368	<0.001	1.795	1.320–2.440	<0.001
Diabetes (%)	1.478	1.051–2.081	0.025	1.242	0.872–1.771	0.230
Current Smoking (%)	1.282	0.922–1.781	0.140			
Current Drinking (%)	0.921	0.579–1.466	0.730			
LEASO (%)	2.914	2.113–4.019	<0.001	2.448	1.730–3.464	<0.001
WBC ($\times 10^9$/L)	1.086	1.049–1.124	<0.001	0.971	0.918–1.028	0.308
Neutrophil ($\times 10^9$/L)	1.106	1.067–1.146	<0.001			
Lymphocyte ($\times 10^9$/L)	0.643	0.491–0.841	0.001			
NLR	1.104	1.075–1.134	<0.001	1.109	1.057–1.163	<0.001
PLT ($\times$109/L)	0.998	0.996–1.000	0.098			
PLR	1.002	1.001–1.004	0.006	0.998	0.996–1.001	0.198
Creatinine (μmol/L)	1.002	0.996–1.008	0.464			
UA (μmol/L)	1.001	1.000–1.003	0.046	1.000	0.999–1.002	0.449
Glucose (mmol/L)	1.043	0.983–1.108	0.165			
TG (mmol/L)	0.992	0.812–1.212	0.940			
TC (mmol/L)	1.042	0.880–1.233	0.635			
HDL-C (mmol/L)	0.654	0.400–1.071	0.091			
LDL-C (mmol/L)	0.997	0.817–1.217	0.976			
Apo A1 (g/L)	0.493	0.259–0.939	0.032	0.882	0.450–1.731	0.716
Apo B (g/L)	1.109	0.532–2.310	0.782			
Lp (a) (g/L)	1.001	0.999–1.001	0.983			
hs-CRP (mg/L)	1.001	0.994–1.007	0.800			
Fibrinogen (g/L)	1.231	1.112–1.362	<0.001	1.057	0.923–1.210	0.424
D-dimer (ug/ml)	1.038	1.009–1.069	0.010	0.982	0.931–1.035	0.502
TBil (μmol/L)	1.005	0.987–1.023	0.590			
DBil (μmol/L)	1.023	0.995–1.052	0.109			
Medications						
Aspirin (%)	0.677	0.506–0.906	0.009	0.608	0.450–0.821	0.001
Statins (%)	0.928	0.685–1.258	0.630			
β-blocker (%)	0.472	0.314–0.711	<0.001	0.423	0.280–0.638	<0.001
ACEI/ARB (%)	1.236	0.798–1.913	0.342			
CCB (%)	1.236	0.889–1.718	0.207			

HR, hazard ratio; CI, confidence interval.

DISCUSSION

We have confirmed that LEASO can serve as a potential and powerful predictor for MACCEs. Moreover, subgroup analysis based on sex showed that LEASO also remained an independent predictor for the occurrence of MACCEs. These important observations show that our results support that LEASO is a robust predictor of the occurrence of MACCEs, irrespective of sex.

Cardiovascular disease is a complication of LEASO, which is explained by the theory of "panvascular disease," which considers the vascular system as a whole (17). LEASO and cardiovascular diseases share a common atherosclerosis pathology, and both present the same risk factors (17). In other words, LEASO may be considered a poor prognostic predictor for the incidence of MACCEs. A retrospective cohort study including 1442 ACS patients showed that patients with PAD of the lower extremities carried a higher risk for cardiovascular disease (18). Another retrospective cohort study showed that lower extremity PAD patients with simultaneous CAD had a completely increased risk of all-cause mortality and MACCEs, which is in good agreement with our clinical result (19). Although there have been many similar studies regarding the potential association between LEASO and CAD in recent years, few studies have considered quantifying the potential impact and comparing important demographic characteristics, including risk factor exposure history and blood biochemical test data. Our study indicated that LEASO is an important prognostic factor for MACCEs, regardless of whether

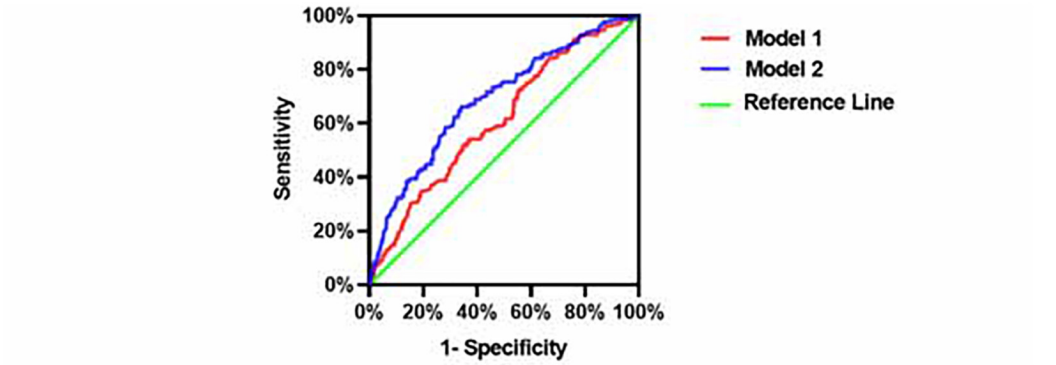

Model	AUC	SE	P	95%CI	Sensitivity	Specificity	Youden index	C-index
Model1	0.614	0.023	<0.001	0.569-0.659	84.2	33.4	0.176	0.632
Model2	0.690	0.022	<0.001	0.646-0.733	66.1	65.7	0.318	0.700

FIGURE 2 | Receiver operating character analysis for the predictive efficacy of variables for MACCEs (Model 1, Gender + Age + Hypertension + Diabetes + current smoking + current drinking; Model 2, Model 1 + LEASO).

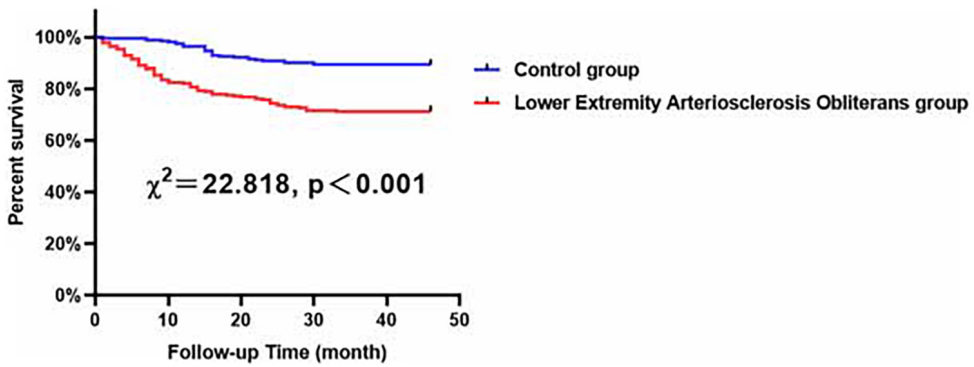

FIGURE 3 | Major adverse cardiovascular and cerebrovascular events-free survival rates for male patients with LEASO group and control group during the follow-up period.

the influence of lipid profiles, inflammatory markers and other potentially prognostic confounders is considered. Therefore, our study provides more detailed data support for the concept of panvascular disease and demonstrates the importance of establishing an interdisciplinary center for panvascular disease management. In particular, whether the LEASO differs between females and males and whether these assessments provide parallel prognostic intelligence remain uncertain.

Inflammatory cytokines follow various stages of atherosclerosis, emphasizing the vital function of inflammation in the pathogenesis of atherosclerosis (20, 21). Recently, the popularity of atherosclerotic inflammation theory has mainly focused on emerging indicators such as NLR and PLR (22–25). The NLR, a novel meaningful and easily obtained inflammatory biomarker, serves not only as an independent predictor of carotid plaque vulnerability but also as a key predictor of future CV events and all-cause mortality (26, 27). Moreover, previous studies reported a close association between PLR and adverse outcomes (28, 29). Therefore, NLR, PLR and other inflammatory indicators, including white blood cells and hs-CRP, were included to further explore the relationship between inflammation and LEASO in our study. Our results showed that LEASO patients were more likely to have higher NLR, PLR, WBC, and neutrophil counts than the control group was, which implied that they remained in a higher inflammatory state. In light of this, inflammation is thought to play a vital role in the underlying mechanism between LEASO and poor outcome. However, whether inflammation acts as a bridge or only shares a common trigger with LEASO remains to be identified.

At the same time, we examined other measures of routine clinical test indicators, such as lipid profiles and coagulation function. Our results also found that patients with LEASO were inclined to have higher levels of TGs, TC, LDL-C, Apo B, and lipoprotein a and lower levels of HDL-C and Apo A1. The results of our study are consistent with previous results concerning atherosclerotic diseases, such

TABLE 4 | Predictors of the occurrence of MACCEs in male patients: results of univariate and multivariate Cox-regression analyses.

Indicators	Univariate			Multivariate		
	HR	95%CI	*p*	HR	95%CI	*p*
Age (years)	1.006	0.984–1.028	0.606			
Hypertension (%)	1.397	0.914–2.136	0.123			
Diabetes (%)	1.918	1.190–3.092	0.008	1.725	1.068–2.787	0.026
Current Smoking (%)	1.670	1.093–2.551	0.018	1.734	1.133–2.652	0.011
Current Drinking (%)	0.989	0.600–1.631	0.966			
LEASO (%)	3.058	1.884–4.966	<0.001	2.919	1.776–4.797	<0.001
WBC ($\times 10^9$/L)	1.050	0.992–1.112	0.094			
Neutrophil ($\times 10^9$/L)	1.054	0.991–1.120	0.095			
Lymphocyte ($\times 10^9$/L)	0.829	0.562–1.222	0.343			
NLR	1.069	1.016–1.126	0.011	1.044	0.985–1.106	0.148
PLT ($\times 10^9$/L)	0.998	0.995–1.001	0.260			
PLR	1.001	0.998–1.004	0.471			
Creatinine (mmol/L)	1.006	0.998–1.014	0.162			
UA (mmol/L)	1.001	0.999–1.002	0.671			
Glucose (mmol/L)	0.939	0.845–1.044	0.242			
TG (mmol/L)	1.106	0.826–1.482	0.498			
TC (mmol/L)	1.097	0.853–1.411	0.471			
LDL-C (mmol/L)	0.920	0.684–1.239	0.585			
HDL-C (mmol/L)	0.242	0.101–0.584	0.002	0.269	0.117–0.620	0.002
Apo A1 (g/L)	0.933	0.341–2.548	0.892			
Apo B (g/L)	0.569	0.170–1.897	0.358			
Lp (a) (g/L)	1.001	0.999–1.001	0.390			
hs-CRP (mg/L)	0.999	0.988–1.009	0.803			
Fibrinogen (g/L)	1.124	0.968–1.304	0.124			
D-dimer (ug/ml)	1.035	0.999–1.072	0.051			
TBil (μmol/L)	0.998	0.973–1.025	0.904			
DBil (μmol/L)	1.007	0.964–1.051	0.766			
Medications						
Aspirin (%)	0.778	0.505–1.199	0.256			
Statins (%)	1.112	0.705–1.753	0.648			
β-blocker (%)	0.567	0.320–1.004	0.052			
ACEI/ARB (%)	1.146	0.593–2.216	0.685			
CCB (%)	1.028	0.611–1.728	0.918			

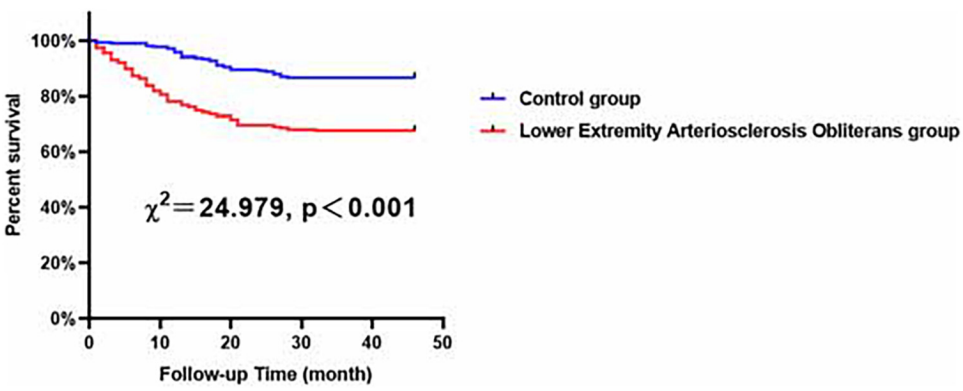

FIGURE 4 | Major adverse cardiovascular and cerebrovascular events-free survival rates for female patients with LEASO group and control group during the follow-up period.

TABLE 5 | Predictors of the occurrence of MACCEs in female patients: results of univariate and multivariate Cox-regression analyses.

Indicators	Univariate			Multivariate		
	HR	95%CI	*p*	HR	95%CI	*p*
Age (years)	0.993	0.973–1.013	0.493			
Hypertension (%)	2.178	1.426–3.326	<0.001	2.010	1.293–3.124	0.002
Diabetes (%)	1.150	0.703–1.880	0.578			
LEASO (%)	2.845	1.849–4.377	<0.001	1.788	1.110–2.880	0.017
WBC ($\times 10^9$/L)	1.117	1.070–1.166	<0.001	0.960	0.887–1.040	0.318
Neutrophil ($\times 10^9$/L)	1.163	1.112–1.217	<0.001			
Lymphocyte ($\times 10^9$/L)	0.541	0.375–0.779	<0.001			
NLR	1.121	1.088–1.155	<0.001	1.113	1.041–1.190	0.002
PLT ($\times 10^9$/L)	0.998	0.995–1.001	0.212			
PLR	1.004	1.002–1.007	<0.001	0.998	0.995–1.002	0.424
Creatinine (μmol/L)	0.998	0.990–1.007	0.732			
UA (μmol/L)	1.002	1.001–1.004	0.005	1.002	1.000–1.004	0.049
Glucose (mmol/L)	1.147	1.071–1.230	<0.001	1.076	0.988–1.171	0.093
TG (mmol/L)	0.913	0.693–1.203	0.517			
TC (mmol/L)	0.991	0.788–1.248	0.942			
HDL-C (mmol/L)	1.042	0.568–1.910	0.894			
LDL-C (mmol/L)	1.060	0.812–1.384	0.668			
Apo A1 (g/L)	0.287	0.123–0.668	0.004	0.624	0.241–1.617	0.332
Apo B (g/L)	1.611	0.656–3.956	0.298			
Lp (a) (g/L)	0.999	0.999–1.000	0.439			
hs-CRP (mg/L)	1.002	0.994–1.010	0.594			
Fibrinogen (g/L)	1.384	1.201–1.595	<0.001	1.168	0.970–1.406	0.100
D-dimer (ug/ml)	1.061	0.992–1.136	0.086			
TBil (μmol/L)	1.014	0.988–1.041	0.290			
DBil (μmol/L)	1.058	1.014–1.103	0.009	1.026	0.961–1.096	0.441
Medications						
Aspirin (%)	0.607	0.407–0.903	0.014	0.472	0.311–0.715	<0.001
Statins (%)	0.793	0.527–1.195	0.268			
β-blocker (%)	0.397	0.221–0.712	0.002	0.321	0.176–0.586	<0.001
ACEI/ARB (%)	1.315	0.733–2.359	0.358			
CCB (%)	1.404	0.913–2.160	0.122			

as acute coronary syndromes and acute ischemic stroke (30, 31). Moreover, a previous study found that steady outpatients with PAD and higher levels of plasma fibrinogen had increased rates of equivalent ischemic events, which is consistent with findings in our study (32). Thus, our data also indicate that clinicians should attach importance to the routine examination results of LEASO patients, and timely intervention should be given to improve the prognosis of these patients.

Cardiovascular risk factors integrating sex-specific research have shown that although males and females share similar risk factors for CAD, certain risk factors are more potent in women (33). In particular, men remain more likely to suffer from ischemic heart disease, and women with coronary artery disease rarely present syndromes (34). Furthermore, compared to men, women more often experience less atherosclerotic plaque, manifested by chest pain and a lower risk of subsequent myocardial infarction (35). Our available data demonstrated that LEASO is an effective predictor in women as men, with a LEASO relative to a twofold increase in the risk of MACCEs. However, given sex-specific cardiovascular risk factor characterization, we found that female patients with LEASO tend to be more susceptible to hypertension, whereas male patients with LEASO are more at risk for higher Apo B and UA and lower HDL-C. Our studies were in the agreement with the previous studies indicated that the prevalence of hypertension is higher among post-menopausal women than among both premenopausal women and men (36–38). Additionally, our findings, together with previous observations that men have higher levels of UA (39) and hyperlipidemia (40), relative to women, which may be because of a high frequency of smoking, higher body mass index and other cardiovascular risk factors in men (40, 41). Thus, we should be cognizant of sex-specific cardiovascular risk factors in patients with LEASO. Further planning of effective preventive interventions for multiple cooccurring drivers may indicate poor clinical outcomes and provide patients with optimal clinical treatment decisions.

TABLE 6 | Characteristics of male and female patients with LEASO.

	Male (*n* = 223)	Female (*n* = 207)	$t/Z/\chi^2$	*p*
Age (years)	66.88 ± 11.56	66.19 ± 11.54	0.619	0.536
Hypertension (%)	100 (44.8)	116 (56.0)	5.382	0.020
Duration of Hypertension (years)	10.00 (6.25, 13.75)	10.00 (5.25, 15.00)	0.161	0.872
Diabetes (%)	43 (19.3)	44 (21.3)	0.259	0.611
Duration of Diabetes (years)	10.00 (6.00, 14.00)	10.00 (5.00, 14.50)	0.672	0.502
WBC ($\times 10^9$/L)	7.89 ± 3.45	7.58 ± 3.99	0.723	0.470
Neutrophil ($\times 10^9$/L)	5.45 ± 3.32	5.21 ± 3.62	0.727	0.468
Lymphocyte ($\times 10^9$/L)	1.52 ± 0.54	1.55 ± 0.63	0.476	0.634
NLR	3.05 (1.94, 5.04)	2.63 (1.81, 4.47)	1.593	0.111
PLT ($\times 10^9$/L)	219.01 ± 88.10	209.27 ± 80.67	1.193	0.234
PLR	139.07 (96.27, 191.71)	133.09 (102.38, 188.41)	0.454	0.650
Creatinine (μmol/L)	71.04 ± 12.12	71.79 ± 12.28	0.631	0.529
UA (μmol/L)	382.32 ± 120.26	353.34 ± 111.42	2.587	0.010
Glucose (mmol/L)	6.19 ± 2.69	6.23 ± 2.45	0.151	0.880
TG (mmol/L)	1.15 (0.87, 1.63)	1.23 (0.94, 1.75)	1.526	0.127
TC (mmol/L)	3.94 ± 1.01	4.12 ± 1.07	1.731	0.084
HDL-C (mmol/L)	1.04 ± 0.30	1.13 ± 0.32	2.879	0.004
LDL-C (mmol/L)	2.25 ± 0.85	2.30 ± 0.90	0.620	0.536
Apo A1 (g/L)	1.26 ± 0.23	1.28 ± 0.22	0.710	0.478
Apo B (g/L)	0.74 ± 0.22	0.79 ± 0.24	2.088	0.037
Lp (a) (g/L)	178.00 (73.00, 375.00)	205.00 (87.60, 461.00)	1.299	0.194
hs-CRP (mg/L)	1.42 (0.57, 5.37)	1.62 (0.59, 7.02)	1.043	0.297
Fibrinogen (g/L)	3.69 ± 1.41	3.54 ± 1.30	1.173	0.242
D-dimer (ug/ml)	0.65 (0.38, 1.37)	0.78 (0.39, 1.76)	1.123	0.261
TBil (μmol/L)	11.50 (8.80, 15.30)	12.50 (8.90, 16.50)	1.005	0.315
DBil (μmol/L)	4.00 (3.10, 5.60)	4.00 (3.00, 6.20)	0.145	0.885
Medications				
Aspirin (%)	141 (63.2)	121 (58.5)	1.028	0.311
Statins (%)	141 (63.2)	136 (65.7)	0.286	0.593
β-blocker (%)	50 (22.4)	56 (27.1)	1.240	0.266
ACEI/ARB (%)	20 (9.0)	25 (12.1)	1.107	0.293
CCB (%)	38 (17.0)	48 (23.2)	2.536	0.111

STUDY LIMITATIONS

There are several limitations of our study. First, our diagnosis was based on the clinical record system, which means that our inclusion in the study was influenced by the experience of the clinician. Second, this study is retrospective; thus, our results may be subject to much bias (such as recall bias). Third, we eliminated many known confounding factors, but there is no guarantee about other unknown confounding factors. Fourth, we did not quantitatively assess atherosclerotic plaques in the lower extremities.

CONCLUSION

This study indicates that LEASO tends to be a useful risk-stratified indicator for MACCEs in both male and female patients, regardless of sex. Where applicable, we highlight that attention should be given to patients with LEASO regardless of other risk factors and who should undergo comprehensive cardiovascular evaluation and intervention. Moreover, appropriate prevention programs should be tailored to different sex LEASO groups as well as different risk factors.

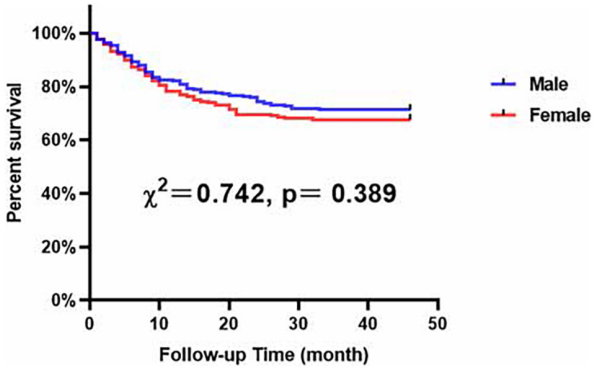

FIGURE 5 | Major adverse cardiovascular and cerebrovascular events-free survival rates for male and female patients with LEASO during the follow-up period.

DATA AVAILABILITY STATEMENT

The datasets used and/or analyzed during this study are available from the corresponding author on reasonable request. Requests to access these datasets should be directed to LY, lileiyu@whu.edu.cn.

ETHICS STATEMENT

Ethical approval was not provided for this study on human participants because this was a retrospective observational study, the Renmin Hospital of Wuhan University Ethics Committee granted an exemption from requiring ethics approval from eligible patients was waived. Written informed consent was not provided because this was a retrospective observational study, the Renmin Hospital of Wuhan University Ethics Committee granted an exemption from requiring informed consent from eligible patients was waived.

AUTHOR CONTRIBUTIONS

LY and HF made substantial contributions to conception and design, data acquisition, or data analysis and interpretation. JS, QD, JW, SD, HC, HZ, ZZ, FY, FG, CL, SX, LS, and YW drafted the manuscript or critically revised it for important intellectual content. LY gave final approval of the version to be published and agreed to be accountable for all aspects of the work in ensuring that questions related to the accuracy or integrity of the work were appropriately investigated and resolved. All authors contributed to the article and approved the submitted version.

FUNDING

This work was supported by the National Natural Science Foundation of China (81871486).

REFERENCES

1. Takahara M. Diabetes mellitus and lower extremity peripheral artery disease. *JMA J.* (2021) 4:225–31. doi: 10.31662/jmaj.2021-0042
2. Frank U, Nikol S, Belch J, Boc V, Brodmann M, Carpentier PH, et al. ESVM guideline on peripheral arterial disease. *Vasa.* (2019) 48(Suppl. 102):1–79. doi: 10.1024/0301-1526/a000834
3. Gerhard-Herman MD, Gornik HL, Barrett C, Barshes NR, Corriere MA, Drachman DE, et al. 2016 AHA/ACC guideline on the management of patients with lower extremity peripheral artery disease: a report of the American college of cardiology/American heart association task force on clinical practice guidelines. *Circulation.* (2017) 135:e726–79.
4. Vitalis A, Shantsila A, Proietti M, Vohra RK, Kay M, Olshansky B, et al. Peripheral arterial disease in patients with atrial fibrillation: the AFFIRM study. *Am J Med.* (2021) 134:514–8. doi: 10.1016/j.amjmed.2020.08.026
5. Sigvant B, Hasvold P, Thuresson M, Jernberg T, Janzon M, Nordanstig J. Myocardial infarction and peripheral arterial disease: treatment patterns and long-term outcome in men and women results from a Swedish nationwide study. *Eur J Prev Cardiol.* (2021) 28:1426–34. doi: 10.1177/2047487319893046
6. Lin Y-S, Tung T-H, Wang J, Chen Y-F, Chen T-H, Lin M-S, et al. Peripheral arterial disease and atrial fibrillation and risk of stroke, heart failure hospitalization and cardiovascular death: a nationwide cohort study. *Int J Cardiol.* (2016) 203:204–11. doi: 10.1016/j.ijcard.2015.10.091
7. Gasbarrino K, Di Iorio D, Daskalopoulou SS. Importance of sex and gender in ischaemic stroke and carotid atherosclerotic disease. *Eur Heart J.* (2022) 43:460–73. doi: 10.1093/eurheartj/ehab756
8. Bairey Merz CN, Shaw LJ, Reis SE, Bittner V, Kelsey SF, Olson M, et al. Insights from the NHLBI-sponsored women's ischemia syndrome evaluation (WISE) study: part II: gender differences in presentation, diagnosis, and outcome with regard to gender-based pathophysiology of atherosclerosis and macrovascular and microvascular coronary disease. *J Am Coll Cardiol.* (2006) 47(3 Suppl.):S21–9. doi: 10.1016/j.jacc.2004.12.084
9. Gu H-Q, Wang C-J, Yang X, Liu C, Wang X, Zhao X-Q, et al. Sex differences in vascular risk factors, in-hospital management, and outcomes of patients with acute ischemic stroke in China. *Eur J Neurol.* (2022) 29:188–98. doi: 10.1111/ene.15124
10. Akyea RK, Kontopantelis E, Kai J, Weng SF, Patel RS, Asselbergs FW, et al. Sex disparity in subsequent outcomes in survivors of coronary heart disease. *Heart.* (2022) 108:37–45. doi: 10.1136/heartjnl-2021-319566
11. Silva RL, Guhl EN, Althouse AD, Herbert B, Sharbaugh M, Essien UR, et al. Sex differences in atrial fibrillation: patient-reported outcomes and the persistent toll on women. *Am J Prev Cardiol.* (2021) 8:100252. doi: 10.1016/j.ajpc.2021.100252
12. Todorov A, Kaufmann F, Arslani K, Haider A, Bengs S, Goliasch G, et al. Gender differences in the provision of intensive care: a Bayesian approach. *Intensive Care Med.* (2021) 47:577–87. doi: 10.1007/s00134-021-06393-3
13. Wiegers HMG, van Es J, Pap ÁF, Lensing AWA, Middeldorp S, Scheres LJJ. Sex-specific differences in clot resolution 3 weeks after acute pulmonary embolism managed with anticoagulants-A substudy of the EINSTEIN-PE study. *J Thromb Haemost.* (2021) 19:1759–63. doi: 10.1111/jth.15326
14. Kotini-Shah P, Del Rios M, Khosla S, Pugach O, Vellano K, McNally B, et al. Sex differences in outcomes for out-of-hospital cardiac arrest in the United States. *Resuscitation.* (2021) 163:6–13. doi: 10.1016/j.resuscitation.2021.03.020
15. Hassan A, Abugroun A, Daoud H, Mahmoud S, Awadalla S, Volgman A, et al. Impact of gender differences on outcomes of peripheral artery disease intervention (from a nationwide sample). *Am J Cardiol.* (2021) 141:127–32. doi: 10.1016/j.amjcard.2020.11.003
16. Lonjon G, Porcher R, Ergina P, Fouet M, Boutron I. Potential pitfalls of reporting and bias in observational studies with propensity score analysis assessing a surgical procedure: a methodological systematic review. *Ann Surg.* (2017) 265:901–9. doi: 10.1097/SLA.0000000000001797
17. Chan AW. Expanding roles of the cardiovascular specialists in panvascular disease prevention and treatment. *Can J Cardiol.* (2004) 20:535–44.
18. Gresele P, Guglielmini G, Del Pinto M, Calabrò P, Pignatelli P, Patti G, et al. Peripheral arterial disease has a strong impact on cardiovascular outcome in patients with acute coronary syndromes: from the START antiplatelet registry. *Int J Cardiol.* (2021) 327:176–82. doi: 10.1016/j.ijcard.2020.10.079
19. Chen DC, Singh GD, Armstrong EJ, Waldo SW, Laird JR, Amsterdam EA. Long-term comparative outcomes of patients with peripheral artery disease with and without concomitant coronary artery disease. *Am J Cardiol.* (2017) 119:1146–52. doi: 10.1016/j.amjcard.2016.12.023
20. Boland J, Long C. Update on the inflammatory hypothesis of coronary artery disease. *Curr Cardiol Rep.* (2021) 23:6. doi: 10.1007/s11886-020-01439-2
21. Ajala ON, Everett BM. Targeting inflammation to reduce residual cardiovascular risk. *Curr Atheroscler Rep.* (2020) 22:66. doi: 10.1007/s11883-020-00883-3
22. Mannarino MR, Bianconi V, Gigante B, Strawbridge RJ, Savonen K, Kurl S, et al. Neutrophil to lymphocyte ratio is not related to carotid atherosclerosis progression and cardiovascular events in the primary prevention of cardiovascular disease: results from the IMPROVE study. *Biofactors.* (2022) 48:100–10. doi: 10.1002/biof.1801
23. Louloudis G, Ambrosini S, Paneni F, Camici GG, Benke D, Klohs J. Adeno-associated virus-mediated gain-of-function mPCSK9 expression in the mouse induces hypercholesterolemia, monocytosis, neutrophilia, and a hypercoagulative state. *Front Cardiovasc Med.* (2021) 8:718741. doi: 10.3389/fcvm.2021.718741

24. Selvaggio S, Abate A, Brugaletta G, Musso C, Di Guardo M, Di Guardo C, et al. Platelet-to-lymphocyte ratio, neutrophil-to-lymphocyte ratio and monocyte-to-HDL cholesterol ratio as markers of peripheral artery disease in elderly patients. *Int J Mol Med.* (2020) 46:1210–6. doi: 10.3892/ijmm.2020.4644
25. Candemir M, Kiziltunç E, Nurkoç S, Şahinarslan A. Relationship between systemic immune-inflammation index (SII) and the severity of stable coronary artery disease. *Angiology.* (2021) 72:575–81. doi: 10.1177/0003319720987743
26. Li X, Li J, Wu G. Relationship of neutrophil-to-lymphocyte ratio with carotid plaque vulnerability and occurrence of vulnerable carotid plaque in patients with acute ischemic stroke. *Biomed Res Int.* (2021) 2021:6894623. doi: 10.1155/2021/6894623
27. Adamstein NH, MacFadyen JG, Rose LM, Glynn RJ, Dey AK, Libby P, et al. The neutrophil-lymphocyte ratio and incident atherosclerotic events: analyses from five contemporary randomized trials. *Eur Heart J.* (2021) 42:896–903. doi: 10.1093/eurheartj/ehaa1034
28. Yang Y, Xie D, Zhang Y. Increased platelet-to-lymphocyte ratio is an independent predictor of hemorrhagic transformation and in-hospital mortality among acute ischemic stroke with large-artery atherosclerosis patients. *Int J Gen Med.* (2021) 14:7545–55. doi: 10.2147/IJGM.S329398
29. Oylumlu M, Oylumlu M, Arslan B, Polat N, Özbek M, Demir M, et al. Platelet-to-lymphocyte ratio is a predictor of long-term mortality in patients with acute coronary syndrome. *Postepy Kardiol Interwencyjnej.* (2020) 16:170–6. doi: 10.5114/aic.2020.95859
30. Ning D-S, Ma J, Peng Y-M, Li Y, Chen Y-T, Li S-X, et al. Apolipoprotein A-I mimetic peptide inhibits atherosclerosis by increasing tetrahydrobiopterin via regulation of GTP-cyclohydrolase 1 and reducing uncoupled endothelial nitric oxide synthase activity. *Atherosclerosis.* (2021) 328:83–91. doi: 10.1016/j.atherosclerosis.2021.05.019
31. Attie AD. Recruiting a transcription factor in the liver to prevent atherosclerosis. *J Clin Invest.* (2021) 131:e154677. doi: 10.1172/JCI154677
32. Altes P, Perez P, Esteban C, Sánchez Muñoz-Torrero JF, Aguilar E, García-Díaz AM, et al. Raised fibrinogen levels and outcome in outpatients with peripheral artery disease. *Angiology.* (2018) 69:507–12. doi: 10.1177/0003319717739720
33. Mehta NK, Strickling J, Mark E, Swinehart S, Puthumana J, Lavie CJ, et al. Beyond cardioversion, ablation and pharmacotherapies: risk factors, lifestyle change and behavioral counseling strategies in the prevention and treatment of atrial fibrillation. *Prog Cardiovasc Dis.* (2021) 66:2–9. doi: 10.1016/j.pcad.2021.05.002
34. Lau ES, Paniagua SM, Guseh JS, Bhambhani V, Zanni MV, Courchesne P, et al. Sex differences in circulating biomarkers of cardiovascular disease. *J Am Coll Cardiol.* (2019) 74:1543–53. doi: 10.1016/j.jacc.2019.06.077
35. Williams MC, Kwiecinski J, Doris M, McElhinney P, D'Souza MS, Cadet S, et al. Sex-specific computed tomography coronary plaque characterization and risk of myocardial infarction. *JACC Cardiovasc Imaging.* (2021) 14:1804–14. doi: 10.1016/j.jcmg.2021.03.004
36. Chobanian AV, Bakris GL, Black HR, Cushman WC, Green LA, Izzo JL, et al. The seventh report of the joint national committee on prevention, detection, evaluation, and treatment of high blood pressure: the JNC 7 report. *JAMA.* (2003) 289:2560–72. doi: 10.1001/jama.289.19.2560
37. Zhang W, Li N. Prevalence, risk factors, and management of prehypertension. *Int J Hypertens.* (2011) 2011:605359. doi: 10.4061/2011/605359
38. Jones DW, Hall JE. Seventh report of the joint national committee on prevention, detection, evaluation, and treatment of high blood pressure and evidence from new hypertension trials. *Hypertension.* (2004) 43):1–3. doi: 10.1161/01.HYP.0000110061.06674.ca
39. Gao X, O'Reilly ÉJ, Schwarzschild MA, Ascherio A. Prospective study of plasma urate and risk of Parkinson disease in men and women. *Neurology.* (2016) 86:520–6. doi: 10.1212/WNL.0000000000002351
40. Goto T, Baba T, Ito A, Maekawa K, Koshiji T. Gender differences in stroke risk among the elderly after coronary artery surgery. *Anesth Analg.* (2007) 104:1016–22. doi: 10.1213/01.ane.0000263279.07361.1f
41. Shankar A, Wang JJ, Rochtchina E, Mitchell P. Positive association between plasma fibrinogen level and incident hypertension among men: population-based cohort study. *Hypertension.* (2006) 48:1043–9. doi: 10.1161/01.HYP.0000245700.13817.3c

Conflict of Interest: The authors declare that the research was conducted in the absence of any commercial or financial relationships that could be construed as a potential conflict of interest.

Publisher's Note: All claims expressed in this article are solely those of the authors and do not necessarily represent those of their affiliated organizations, or those of the publisher, the editors and the reviewers. Any product that may be evaluated in this article, or claim that may be made by its manufacturer, is not guaranteed or endorsed by the publisher.

Copyright © 2022 Sun, Deng, Wang, Duan, Chen, Zhou, Zhou, Yu, Guo, Liu, Xu, Song, Wang, Feng and Yu. This is an open-access article distributed under the terms of the Creative Commons Attribution License (CC BY). The use, distribution or reproduction in other forums is permitted, provided the original author(s) and the copyright owner(s) are credited and that the original publication in this journal is cited, in accordance with accepted academic practice. No use, distribution or reproduction is permitted which does not comply with these terms.

frontiers | Frontiers in Cardiovascular Medicine

ORIGINAL RESEARCH
published: 10 May 2022
doi: 10.3389/fcvm.2022.825890

Alcohol Abuse Associated With Increased Risk of Angiographic Vasospasm and Delayed Cerebral Ischemia in Patients With Aneurysmal Subarachnoid Hemorrhage Requiring Mechanical Ventilation

Lei Zhao[1], Chao Cheng[1], Liwei Peng[1], Wei Zuo[1], Dong Xiong[1], Lei Zhang[1], Zilong Mao[1], Jin'an Zhang[1], Xia Wu[2], Xue Jiang[1], Peng Wang[1] and Weixin Li[1]**

[1] Department of Neurosurgery, Tangdu Hospital, The Fourth Military Medical University, Xi'an, China, [2] Department of Public Health, School of Health Sciences and Practice, New York Medical College, Valhalla, NY, United States

OPEN ACCESS

Edited by:
Anne-Clémence Vion,
INSERM U1087 Institut du Thorax, France

Reviewed by:
Nicolas K. Khattar,
University of Louisville, United States
Jing Xu,
Johns Hopkins University, United States

***Correspondence:**
Weixin Li
neuropub@163.com
Lei Zhao
conrad03037@163.com

Specialty section:
This article was submitted to Atherosclerosis and Vascular Medicine, a section of the journal Frontiers in Cardiovascular Medicine

Received: 30 November 2021
Accepted: 21 March 2022
Published: 10 May 2022

Citation:
Zhao L, Cheng C, Peng L, Zuo W, Xiong D, Zhang L, Mao Z, Zhang J, Wu X, Jiang X, Wang P and Li W (2022) Alcohol Abuse Associated With Increased Risk of Angiographic Vasospasm and Delayed Cerebral Ischemia in Patients With Aneurysmal Subarachnoid Hemorrhage Requiring Mechanical Ventilation. Front. Cardiovasc. Med. 9:825890. doi: 10.3389/fcvm.2022.825890

Objective: Although alcohol abuse has been indicated to cause cerebral aneurysm development and rupture, there is limited data on the impact of alcohol abuse on outcomes after an aneurysmal subarachnoid hemorrhage (aSAH). This study aims to investigate whether alcohol abuse increases the risk of angiographic vasospasm and delayed cerebral ischemia (DCI) in critically ill patients with aSAH.

Methods: We conducted a secondary analysis based on a retrospective study in a French university hospital intensive care unit (ICU). Patients with aSAH requiring mechanical ventilation hospitalized between 2010 and 2015 were included. Patients were segregated according to alcohol abuse (yes or no). Multivariable logistic regression analysis was used to identify the independent risk factors associated with angiographic vasospasm and DCI.

Results: The patient proportion of alcohol abuse was dramatically greater in males than that in females ($p < 0.001$). The Simplified Acute Physiology Score II (SAPSII) score on admission did not show a statistical difference. Neither did the World Federation of Neurosurgical Societies (WFNS) and Fisher scores. Patients with alcohol abuse were more likely to develop angiographic vasospasm (OR 3.65, 95% CI 1.17–11.39; $p = 0.0260$) and DCI (OR 3.53, 95% CI 1.13–10.97; $p = 0.0294$) as evidenced by multivariable logistic regression analysis.

Conclusions: In this study, patients with alcohol abuse are at higher odds of angiographic vasospasm and DCI, which are related to poor prognosis following aSAH. These findings are important for the prevention and clinical management of aSAH.

Keywords: aneurysmal subarachnoid hemorrhage, alcohol abuse, retrospective study, clinical outcomes, angiographic vasospasm, delayed cerebral ischemia

INTRODUCTION

Alcohol abuse is associated with an increased risk of death and cardiovascular disease (CVD). Excessive alcohol intake is one of the top three leading causes of premature deaths in the US (the other two are smoking and obesity) (1, 2). Also, the prevalence of alcohol use is still rising (3). Alcohol abuse is a chronic disease characterized by uncontrolled drinking and preoccupation with alcohol. The patients generally exhibit an inability to control drinking due to both a physical and emotional dependence on alcohol. Notably, it has been indicated that alcohol abuse may cause cerebral aneurysm development and rupture, leading to aneurysmal subarachnoid hemorrhage (aSAH) (4–7). Also, reduced alcohol intake may substantially decrease subarachnoid hemorrhage (SAH) risk (4).

The clinical outcomes following aSAH are associated with multiple factors, including the patient's severity on admission, angiographic vasospasm, and delayed cerebral ischemia (DCI) (8–11). Angiographic vasospasm is the arterial narrowing of large cerebral vessels observed on a radiological test such as CT angiography (CTA), magnetic resonance angiography (MRA), or digital subtraction angiography (DSA) (12). Additionally, angiographic vasospasm is considered a critical factor leading to DCI, which causes poor outcomes or death in up to 30% of patients with SAH (11, 13). While alcohol abuse is a potential risk factor for aSAH, the impact of alcohol abuse on outcomes after aSAH has not been fully evaluated. Herein, we investigated the effect of alcohol abuse on angiographic vasospasm and DCI in a cohort of patients with aSAH requiring mechanical ventilation.

METHODS

Data Source

We obtained data from the "DATADRYAD" database (https://datadryad.org/search). This website permitted users to freely download the raw dataset. According to Dryad Terms of Service, we cited the Dryad data package in this study [Dryad data package: Chalard et al. (14), Long-term outcome in patients with aSAH requiring mechanical ventilation, Dryad, Dataset, https://doi.org/10.5061/dryad.47d7wm3b4].

Study Cohort

Chalard et al. completed the entire dataset in the previous study (14). The details were described in the original article. Between January 2010 and December 2015, adult patients with aSAH hospitalized in the neuro-ICU were recruited. Only patients with mechanical ventilation were included in the current study. CTA was performed in all patients at admission to confirm SAH was caused by an aneurysm rupture.

Patients Characteristics and Clinical Outcomes Collection

The following variables were collected: age, sex, tobacco use, alcohol abuse, diabetes, CVD, Simplified Acute Physiology Score II (SAPSII), World Federation of Neurosurgical Societies (WFNS) score, Fisher score, aneurysm location, and presence of intracerebral hemorrhage (ICH). Type of aneurysm treatment procedure and presence of angiographic vasospasm and DCI were also recorded.

Statistical Analysis

Continuous variables were expressed as mean ± SD (normal distribution) and categorical variables were expressed in frequency (percentage). The Student's *t*-test (normal distribution) and chi-square test (categorical variables) were used to determine statistical differences between the means and proportions of the groups. Univariate logistic regression analysis was initially performed to identify factors of potential risk, then a multivariable logistic regression model was used to identify independently associated risk factors for the outcomes. The variables included in the multivariable logistic regression analysis were selected on the basis of their associations with the outcomes of interest or a change in effect estimate of more than 10%. All of the analyses were performed using the statistical software packages R (http://www.R-project.org, The R Foundation) and EmpowerStats (http://www.empowerstats.com, X&Y Solutions, Inc., Boston, MA). A p-value < 0.05 (two-sided) were considered statistically significant.

RESULTS

Patient Demographics and Outcomes

There were 236 patients in this cohort, including 20 patients with alcohol abuse and 216 patients without alcohol abuse. As shown in **Table 1**, the mean age of non-alcohol abuse patients was 54.87 (SD = 13.32). The mean age of patients with alcohol abuse was 56.25 (SD = 9.94). The comparison of age in the two groups of patients indicated no statistical significance ($p = 0.651$). There were 17 male patients included in the group of alcohol abuse, which was of statistical significance compared with the proportion of alcohol abuse in the female patients ($p < 0.001$). There were 16 patients with tobacco use in alcohol abuse patients with a percentage of 80.00%, which was markedly greater than that in non-alcohol abuse patients ($p < 0.001$). There were 8 patients with diabetes in the non-alcohol abuse group with a percentage of 3.7%. In patients with alcohol abuse, no patients had diabetes. There were 37 patients with CVD in the non-alcohol abuse group (17.13%). In the alcohol abuse group, 3 patients had CVD (15.00%). No statistical significance was observed as to diabetes and CVD ($p = 0.381$, 0.808, respectively) in these two groups.

As for the location of the aneurysm, there were 180 patients with anterior circulation aneurysms in the non-alcohol abuse group (83.72%). In the alcohol abuse group, 17 patients had anterior circulation aneurysms (85.00%). No statistical significance was detected between the two groups ($p = 0.882$). The mean SAPS II of non-alcohol abuse patients was 42.22 (SD = 12.09). The mean SAPS II of alcohol abuse patients was 44.00 (SD = 11.79). The differences between SAPS II, WFNS score, and Fisher score were of no statistical significance ($p = 0.528$, 0.931, 0.807, respectively). There were 99 patients with ICH in the non-alcohol abuse group (45.83%). In the alcohol abuse group, 10 patients exhibited ICH (50.00%). No statistical

TABLE 1 | Patient demographics and outcomes.

Alcohol abuse	No	Yes	*p*-value
N	216	20	
Age	54.87 ± 13.32	56.25 ± 9.94	0.651
Sex			<0.001
Female	144 (66.67%)	3 (15.00%)	
Male	72 (33.33%)	17 (85.00%)	
Tobacco use			<0.001
No	156 (72.22%)	4 (20.00%)	
Yes	60 (27.78%)	16 (80.00%)	
Diabetes			0.381
No	208 (96.30%)	20 (100.00%)	
Yes	8 (3.70%)	0 (0.00%)	
CVD			0.808
No	179 (82.87%)	17 (85.00%)	
Yes	37 (17.13%)	3 (15.00%)	
Aneurysm location			0.882
Ant circ	180 (83.72%)	17 (85.00%)	
Post circ	35 (16.28%)	3 (15.00%)	
SAPSII	42.22 ± 12.09	44.00 ± 11.79	0.528
WFNS score			0.931
III	22 (10.19%)	2 (10.00%)	
IV	88 (40.74%)	9 (45.00%)	
V	106 (49.07%)	9 (45.00%)	
Fisher score			0.807
I	1 (0.46%)	0 (0.00%)	
II	4 (1.85%)	1 (5.00%)	
III	42 (19.44%)	4 (20.00%)	
IV	169 (78.24%)	15 (75.00%)	
ICH			0.721
No	117 (54.17%)	10 (50.00%)	
Yes	99 (45.83%)	10 (50.00%)	
Treatment			0.475
Coil	138 (70.05%)	12 (63.16%)	
Clipping	56 (28.43%)	6 (31.58%)	
Combined	3 (1.52%)	1 (5.26%)	
Angiographic vasospasm			0.058
No	143 (66.20%)	9 (45.00%)	
Yes	73 (33.80%)	11 (55.00%)	
DCI			0.060
No	161 (74.54%)	11 (55.00%)	
Yes	55 (25.46%)	9 (45.00%)	

CVD, cardiovascular disease; Ant circ, anterior circulation; Post circ, posterior circulation; SAPSII, Simplified Acute Physiology Score II; WFNS, World Federation of Neurosurgical Societies; ICH, intracerebral hemorrhage; DCI, delayed cerebral ischemia.

significance was detected in the comparison of ICH between the two groups ($p = 0.721$).

A total of 138 patients were treated with a coil and 56 patients were treated with clipping in the non-alcohol abuse group. No statistical significance was observed in the comparison of treatment between the two groups ($p = 0.475$). A total of 73 patients (33.80%) presented with angiographic vasospasm in the non-alcohol abuse group, and 11 patients (55.00%) presented with angiographic vasospasm in the alcohol abuse group, with the *p*-value approaching significance ($p = 0.058$). There were 55 patients (25.46%), who presented with DCI in the non-alcohol abuse group, vs. 9 patients (45.00%) with DCI in the non-alcohol abuse group, a difference that also nearly reached statistical significance ($p = 0.060$).

Univariate Analysis of Risk Factors for Angiographic Vasospasm and DCI

The risk factors for angiographic vasospasm and DCI were then identified using univariate logistic regression analysis. Alcohol abuse [odds ratio (OR) 2.39, 95% confidence interval (CI) 0.95–6.04; $p = 0.0643$] was likely associated with an increased risk of angiographic vasospasm, with the *p*-value approaching significance. Clipping treatment was associated with a reduced likelihood of angiographic vasospasm (OR 0.26, 95% CI 0.13–0.54; $p = 0.0003$). The results of the univariate analysis of risk factors for angiographic vasospasm are presented in **Table 2**.

Alcohol abuse (OR 2.40, 95% CI 0.94–6.09; $p = 0.0664$) was likely associated with increased risk of DCI, with the *p*-value nearly reaching statistical significance. ICH (OR 0.42, 95% CI.23–0.78; $p = 0.0056$) and clipping treatment were associated with a reduced likelihood of DCI (OR 0.19, 95% CI 0.07–0.46; $p = 0.0003$). The results of the univariate analysis of risk factors for DCI are presented in **Table 3**.

Multivariable Analysis of Independent Risk Factors for Angiographic Vasospasm and DCI

The multivariable logistic regression analysis used non-adjusted (crude) and adjusted models to examine the independent risk factors. As shown in **Table 4**, in model I (adjusted for age and sex), the OR is 2.75, 95% CI 1.03–7.36 ($p = 0.0440$). In model II (adjusted for age, sex, Fisher score, and treatment), the OR is 3.61, 95% CI 1.17–11.17 ($p = 0.0259$). In model III (adjusted for age, sex, Fisher score, treatment, CVD, and SAPS II), the OR is 3.65, 95% CI 1.17–11.39 ($p = 0.0260$). The results of multivariable logistic regression analysis indicated that alcohol abuse was independently associated with increased odds of angiographic vasospasm after adjusting for age, sex, Fisher score, treatment, CVD, and SAPS II.

Similarly, the ORs of alcohol abuse for DCI were calculated in different adjusted models (**Table 5**). The results suggested that alcohol abuse was independently associated with increased odds of DCI (OR 3.53, 95% CI 1.13–10.97; $p = 0.0294$, model III).

DISCUSSION

Angiographic vasospasm and DCI are strongly associated with the outcomes following aSAH (11, 13). This study aims to have a better understanding of the risk factors involved that may lead to angiographic vasospasm and DCI. Alcohol abuse has about 2.5-fold higher odds of angiographic vasospasm and DCI *via* multivariable logistic regression analysis when adjusting

TABLE 2 | Univariate logistic regression analysis of risk factors for angiographic vasospasm.

Variable	OR (95% CI)	*P*-value
Age	0.98 (0.96, 1.00)	0.0613
Sex		
Female	Ref	
Male	0.95 (0.55, 1.64)	0.8492
Tobacco use		
No	Ref	
Yes	1.28 (0.73, 2.25)	0.3913
Alcohol abuse		
No	Ref	
Yes	2.39 (0.95, 6.04)	0.0643
Diabetes		
No	Ref	
Yes	1.09 (0.25, 4.67)	0.9088
CVD		
No	Ref	
Yes	0.47 (0.21, 1.04)	0.0618
Aneurysm location		
Ant circ	Ref	
Post circ	0.69 (0.32, 1.48)	0.3414
SAPSII	0.98 (0.96, 1.00)	0.0460
WFNS score		
III	Ref	
IV	1.02 (0.41, 2.54)	0.9574
V	0.56 (0.23, 1.39)	0.2148
Fisher score		
I	Ref	
II	0.00 (0.00, Inf)	0.9899
III	0.00 (0.00, Inf)	0.9944
IV	0.00 (0.00, Inf)	0.9943
ICH		
No	Ref	
Yes	0.75 (0.44, 1.29)	0.3010
Treatment		
Coil	Ref	
Clipping	0.26 (0.13, 0.54)	0.0003
Combined	3.62 (0.37, 35.58)	0.2702

CVD, cardiovascular disease; Ant circ, anterior circulation; Post circ, posterior circulation; SAPSII, Simplified Acute Physiology Score II; WFNS, World Federation of Neurosurgical Societies; ICH, intracerebral hemorrhage; ref, reference (OR = 1.0).

TABLE 3 | Univariate logistic regression analysis of risk factors for DCI.

Variable	OR (95% CI)	*p*-value
Age	0.99 (0.96, 1.01)	0.2141
Sex		
Female	Ref	
Male	1.08 (0.60, 1.95)	0.7940
Tobacco use		
No	Ref	
Yes	0.94 (0.51, 1.75)	0.8484
Alcohol abuse		
No	Ref	
Yes	2.40 (0.94, 6.09)	0.0664
Diabetes		
No	Ref	
Yes	0.37 (0.05, 3.10)	0.3623
CVD		
No	Ref	
Yes	0.42 (0.17, 1.05)	0.0646
Aneurysm location		
Ant circ	Ref	
Post circ	0.55 (0.23, 1.33)	0.1872
SAPSII	0.98 (0.96, 1.00)	0.1136
WFNS score		
III	Ref	
IV	1.03 (0.40, 2.66)	0.9492
V	0.50 (0.19, 1.31)	0.1587
Fisher score		
I	Ref	
II	0.00 (0.00, Inf)	0.9899
III	0.00 (0.00, Inf)	0.9944
IV	0.00 (0.00, Inf)	0.9941
ICH		
No	Ref	
Yes	0.42 (0.23, 0.78)	0.0056
Treatment		
Coil	Ref	
Clipping	0.19 (0.07, 0.46)	0.0003
Combined	0.58 (0.06, 5.67)	0.6362

CVD, cardiovascular disease; Ant circ, anterior circulation; Post circ, posterior circulation; SAPSII, Simplified Acute Physiology Score II; WFNS, World Federation of Neurosurgical Societies; ICH, intracerebral hemorrhage; ref, reference (OR = 1.0).

for other potential confounding variables. Our findings provide important evidence for the prevention and clinical management of aSAH.

Although previous studies have suggested that alcohol abuse increases the risk of aSAH (4), the role of alcohol abuse in the development of angiographic vasospasm and DCI has not been fully investigated yet. Because alcohol abuse is present in a large proportion of patients with aSAH, especially in men, identification of alcohol abuse as an independent risk factor of angiographic vasospasm and DCI is of great clinical significance in determining how closely the patients should be monitored for these two events.

Alcohol has been suggested to induce vessel constriction *via* various mechanisms. Alcohol can increase the activity of the sympathetic nervous system and the release of catecholamines, leading to the constriction of blood vessels (15, 16). Besides, alcohol has been indicated to decrease the levels of electrically charged (i.e., ionized) magnesium in plasma (17). A delicate balance between magnesium and calcium ions is needed to maintain vascular tone at a normal level. Magnesium triggers vessel relaxation and

TABLE 4 | Relationship between alcohol abuse and angiographic vasospasm in different models by multivariable logistic regression analysis.

Exposure	Crude	Adjust I (OR, 95% CI, *p*)	Adjust II (OR, 95% CI, *p*)	Adjust III (OR, 95% CI, *p*)
Alcohol abuse				
No	1.0	-	-	-
Yes	2.39 (0.95, 6.04) 0.0643	2.75 (1.03, 7.36) 0.0440	3.61 (1.17, 11.17) 0.0259	3.65 (1.17, 11.39) 0.0260

Crude model: we did not adjust other variables.
Adjust I: we adjusted age and sex.
Adjust II: we adjusted age, sex, Fisher score, and treatment.
Adjust III: we adjusted age, sex, Fisher score, treatment, CVD, and SAPS II.
CVD, cardiovascular disease; SAPSII, Simplified Acute Physiology Score II.

TABLE 5 | Relationship between alcohol abuse and DCI in different models by multivariable logistic regression analysis.

Exposure	Crude	Adjust I (OR, 95% CI, *p*)	Adjust II (OR, 95% CI, *p*)	Adjust III (OR, 95% CI, *p*)
Alcohol abuse				
No	1.0	-	-	-
Yes	2.40 (0.94, 6.09) 0.0664	2.54 (0.94, 6.87) 0.0656	3.52 (1.14, 10.85) 0.0285	3.53 (1.13, 10.97) 0.0294

Crude model: we did not adjust other variables.
Adjust I: we adjusted age and sex.
Adjust II: we adjusted age, sex, Fisher score, and treatment.
Adjust III: we adjusted age, sex, Fisher score, treatment, CVD, and SAPS II.
DCI, delayed cerebral ischemia; CVD, cardiovascular disease; SAPSII, Simplified Acute Physiology Score II.

calcium, on the contrary, causes vessel constriction. When the level of magnesium ions is reduced by alcohol, the calcium ions will predominate, resulting in vessel constriction. These mechanisms help to explain alcohol abuse as an independent risk factor for angiographic vasospasm after aSAH in this study.

Apart from the effect on vascular tone, alcohol may lead to endothelial dysfunction. A high dose of alcohol consumption leads to an increased endothelin level, which is also involved in vessel constriction (18, 19). Alcohol abuse also leads to oxidative stress. For example, a high dose of alcohol leads to the overproduction of reactive oxygen species, leading to the peroxidation of lipids, proteins, and DNA and ultimately to necrosis and apoptosis (20). The increased level of endothelin induced by alcohol abuse is also associated with oxidative stress (18). The blockade of oxidative stress may prevent endothelial dysfunctions induced by alcohol. A study by Sacanella et al. indicated that alcohol abuse increases the expression of intercellular adhesion molecule (ICAM-1) and E-selectin, which participates in the adhesion and migration of inflammatory cells. As for inflammation, a high dose of alcohol consumption may cause an increase in tumor necrosis factor-alpha (TNF-alpha) and interleukin-6 (IL-6) (21), contributing to the aggregation of inflammatory cells and vessel constriction or spasm.

Alcohol also acts on coagulation and fibrinolysis. It has been demonstrated that heavy alcohol intake is associated with lower fibrinolytic capacity and a more procoagulant state, with an elevation in the plasma levels of factor VII, fibrinogen, and viscosity (22). Fibrinolysis is mainly regulated by two proteins in the blood: tissue plasminogen activator (tPA) and plasminogen activator inhibitor 1 (PAI-1). TPA promotes fibrinolysis, whereas PAI-1 inhibits fibrinolytic activity. Heavy alcohol consumption has been indicated to stimulate PAI-1 production and thereby suppress fibrinolysis (23). Fibrinolysis suppression may lead to subsequent thrombosis and vessel spasms.

Angiographic vasospasm has been indicated to be present in up to 70% of patients following SAH (9), and it has been regarded as an important factor causing DCI for a long time. However, recent findings have suggested that angiographic vasospasm alone is not sufficient to trigger DCI (9). DCI is only found in about 30% of patients and does not always fall within the vascular distribution of the angiographic vasospasm (24). DCI, therefore, may occur in an area that does not involve angiographic vasospasm. In our study, DCI was found in 27% of patients, which is nearly 30%. For the non-alcohol abuse group, 73 patients presented with angiographic vasospasm and 55 with DCI. For the alcohol abuse group, 11 with angiographic vasospasm, and 9 with DCI. Notably, the patients with DCI all presented with the presence of angiographic vasospasm, which verified the critical role of angiographic vasospasm in the development of DCI following aSAH. However, further research is still needed to find out other causes of DCI.

Limitations

There are some limitations to our study. First, this is a single-center study based on a French patients cohort, and only patients with mechanical ventilation were analyzed. Therefore, the generalizability of the results to other geographical areas and the patient groups may be limited. Second, this is a retrospective study, so we can only conclude that alcohol abuse was associated with angiographic vasospasm and DCI, but causation cannot be proved. Therefore, only an OR could be

calculated, not the relative risk. Third, due to raw data limitations, the dose of alcohol consumption was not recorded, which would otherwise provide more details regarding the effect of alcohol on angiographic vasospasm and DCI.

CONCLUSIONS

In this study, we have demonstrated that patients with alcohol abuse havehas about 2.5-fold higher odds of angiographic vasospasm and DCI compared to non-alcohol abuse patients after aSAH, independent of age, sex, Fisher score, treatment, CVD, and SAPS II. Our findings may be helpful in monitoring patients with known risk factors for the development of angiographic vasospasm and DCI following aSAH.

DATA AVAILABILITY STATEMENT

The dataset is available on Dryad at DOI: 10.5061/dryad.47d7wm3b4.

ETHICS STATEMENT

The studies involving human participants were reviewed and approved by Comite de Protection des Personnes Sud-Mediterannee IV, Montpellier, France; ID: Q-2015-09-07. Written informed consent for participation was not required for this study in accordance with the national legislation and the institutional requirements.

AUTHOR CONTRIBUTIONS

LZhao wrote the first draft of the manuscript. All authors contributed to the conception and design of the study, statistical analysis, manuscript revision, read, and approved the submitted version.

ACKNOWLEDGMENTS

We are very grateful to the data providers of the study.

REFERENCES

1. O'Keefe EL, DiNicolantonio JJ, O'Keefe JH, Lavie CJ. Alcohol and CV health: Jekyll and Hyde J-curves. *Prog Cardiovasc Dis.* (2018) 61:68–75. doi: 10.1016/j.pcad.2018.02.001
2. Mokdad AH, Marks JS, Stroup DF, Gerberding JL. Actual causes of death in the United States, 2000. *JAMA.* (2004) 291:1238–45. doi: 10.1001/jama.291.10.1238
3. Grant BF, Chou SP, Saha TD, Pickering RP, Kerridge BT, Ruan WJ, et al. Prevalence of 12-month alcohol use, high-risk drinking, and DSM-IV alcohol use disorder in the United States, 2001-2002 to 2012-2013: results from the national epidemiologic survey on alcohol and related conditions. *JAMA Psychiatry.* (2017) 74:911–23. doi: 10.1001/jamapsychiatry.2017.2161
4. Kissela BM, Sauerbeck L, Woo D, Khoury J, Carrozzella J, Pancioli A, et al. Subarachnoid hemorrhage: a preventable disease with a heritable component. *Stroke.* (2002) 33:1321–6. doi: 10.1161/01.STR.0000014773.57733.3E
5. Juvela S, Hillbom M, Numminen H, Koskinen P. Cigarette smoking and alcohol consumption as risk factors for aneurysmal subarachnoid hemorrhage. *Stroke.* (1993) 24:639–46. doi: 10.1161/01.STR.24.5.639
6. King JT, Jr. Epidemiology of aneurysmal subarachnoid hemorrhage Neuroimaging. *Clin N Am.* (1997) 7:659–68.
7. Feigin VL, Rinkel GJ, Lawes CM, Algra A, Bennett DA, van Gijn J, et al. Risk factors for subarachnoid hemorrhage: an updated systematic review of epidemiological studies. *Stroke.* (2005) 36:2773–80. doi: 10.1161/01.STR.0000190838.02954.e8
8. Galea JP, Dulhanty L, Patel HC, UK and Ireland Subarachnoid Hemorrhage Database Collaborators. Predictors of outcome in aneurysmal subarachnoid hemorrhage patients: observations from a multicenter data set. *Stroke.* (2017) 48:2958–63. doi: 10.1161/STROKEAHA.117.017777
9. Crowley RW, Medel R, Dumont AS, Ilodigwe D, Kassell NF, Mayer SA, et al. Angiographic vasospasm is strongly correlated with cerebral infarction after subarachnoid hemorrhage. *Stroke.* (2011) 42:919–23. doi: 10.1161/STROKEAHA.110.597005
10. Rumalla K, Lin M, Ding L, Gaddis M, Giannotta SL, Attenello FJ, et al. Risk factors for cerebral vasospasm in aneurysmal subarachnoid hemorrhage: a population-based study of 8346 patients. *World Neurosurg.* (2021) 145:e233–e41. doi: 10.1016/j.wneu.2020.10.008
11. Macdonald RL. Delayed neurological deterioration after subarachnoid haemorrhage. *Nat Rev Neurol.* (2014) 10:44–58. doi: 10.1038/nrneurol.2013.246
12. Vergouwen MD, Vermeulen M, van Gijn J, Rinkel GJ, Wijdicks EF, Muizelaar JP, et al. Definition of delayed cerebral ischemia after aneurysmal subarachnoid hemorrhage as an outcome event in clinical trials and observational studies: proposal of a multidisciplinary research group. *Stroke.* (2010) 41:2391–5. doi: 10.1161/STROKEAHA.110.589275
13. Suarez JI, Tarr RW, Selman WR. Aneurysmal subarachnoid hemorrhage. *N Engl J Med.* (2006) 354:387–96. doi: 10.1056/NEJMra052732
14. Chalard K, Szabo V, Pavillard F, Djanikian F, Dargazanli C, Molinari N, et al. Long-term outcome in patients with aneurysmal subarachnoid hemorrhage requiring mechanical ventilation. *PLoS ONE.* (2021) 16:e0247942. doi: 10.1371/journal.pone.0247942
15. Russ R, Abdel-Rahman AR, Wooles WR. Role of the sympathetic nervous system in ethanol-induced hypertension in rats. *Alcohol.* (1991) 8:301–7. doi: 10.1016/0741-8329(91)90433-W
16. O'Connor AD, Rusyniak DE, Bruno A. Cerebrovascular and cardiovascular complications of alcohol and sympathomimetic drug abuse. *Med Clin North Am.* (2005) 89:1343–58. doi: 10.1016/j.mcna.2005.06.010
17. Altura BM, Altura BT. Role of magnesium and calcium in alcohol-induced hypertension and strokes as probed by *in vivo* television microscopy, digital image microscopy, optical spectroscopy, 31P-NMR, spectroscopy and a unique magnesium ion-selective electrode. *Alcohol Clin Exp Res.* (1994) 18:1057–68. doi: 10.1111/j.1530-0277.1994.tb00082.x
18. Soardo G, Donnini D, Varutti R, Moretti M, Milocco C, Basan L, et al. Alcohol-induced endothelial changes are associated with oxidative stress and are rapidly reversed after withdrawal. *Alcohol Clin Exp Res.* (2005) 29:1889–98. doi: 10.1097/01.alc.0000183004.28587.23
19. Zilkens RR, Burke V, Hodgson JM, Barden A, Beilin LJ, Puddey IB. Red wine and beer elevate blood pressure in normotensive men. *Hypertension.* (2005) 45:874–9. doi: 10.1161/01.HYP.0000164639.83623.76
20. Pacher P, Beckman JS, Liaudet L. Nitric oxide and peroxynitrite in health and disease. *Physiol Rev.* (2007) 87:315–424. doi: 10.1152/physrev.00029.2006
21. Luedemann C, Bord E, Qin G, Zhu Y, Goukassian D, Losordo DW, et al. Ethanol modulation of TNF-alpha biosynthesis and signaling in endothelial cells: synergistic augmentation of TNF-alpha mediated endothelial cell dysfunctions by chronic ethanol. *Alcohol Clin Exp Res.* (2005) 29:930–8. doi: 10.1097/01.ALC.0000171037.90100.6B

22. Lee KW, Lip GY. Effects of lifestyle on hemostasis, fibrinolysis, and platelet reactivity: a systematic review. *Arch Intern Med*. (2003) 163:2368–92. doi: 10.1001/archinte.163.19.2368
23. Ballard HS. The hematological complications of alcoholism. *Alcohol Health Res World*. (1997) 21:42–52.
24. Hijdra A, Van Gijn J, Stefanko S, Van Dongen KJ, Vermeulen M, Van Crevel H. Delayed cerebral ischemia after aneurysmal subarachnoid hemorrhage: clinicoanatomic correlations. *Neurology*. (1986) 36:329–33. doi: 10.1212/WNL.36.3.329

Conflict of Interest: The authors declare that the research was conducted in the absence of any commercial or financial relationships that could be construed as a potential conflict of interest.

Publisher's Note: All claims expressed in this article are solely those of the authors and do not necessarily represent those of their affiliated organizations, or those of the publisher, the editors and the reviewers. Any product that may be evaluated in this article, or claim that may be made by its manufacturer, is not guaranteed or endorsed by the publisher.

Copyright © 2022 Zhao, Cheng, Peng, Zuo, Xiong, Zhang, Mao, Zhang, Wu, Jiang, Wang and Li. This is an open-access article distributed under the terms of the Creative Commons Attribution License (CC BY). The use, distribution or reproduction in other forums is permitted, provided the original author(s) and the copyright owner(s) are credited and that the original publication in this journal is cited, in accordance with accepted academic practice. No use, distribution or reproduction is permitted which does not comply with these terms.

frontiers | Frontiers in Cardiovascular Medicine

TYPE Original Research
PUBLISHED 14 September 2022
DOI 10.3389/fcvm.2022.885426

Check for updates

OPEN ACCESS

EDITED BY
Anne-Clémence Vion,
INSERM U1087 Institut du Thorax, France

REVIEWED BY
Hong Jin,
Karolinska Institutet (KI), Sweden
Frrédéric Clarençon,
Hôpitaux Universitaires Pitié Salpêtrière, France

*CORRESPONDENCE
Omer F. Eker
omer.eker@chu-lyon.fr

SPECIALTY SECTION
This article was submitted to Atherosclerosis and Vascular Medicine, a section of the journal Frontiers in Cardiovascular Medicine

RECEIVED 28 February 2022
ACCEPTED 27 July 2022
PUBLISHED 14 September 2022

CITATION
Eker OF, Lubicz B, Cortese M, Delporte C, Berhouma M, Chopard B, Costalat V, Bonafé A, Alix-Panabières C, Van Anwterpen P and Zouaoui Boudjeltia K (2022) Effects of the flow diversion technique on nucleotide levels in intra-cranial aneurysms: A feasibility study providing new research perspectives. *Front. Cardiovasc. Med.* 9:885426. doi: 10.3389/fcvm.2022.885426

COPYRIGHT
© 2022 Eker, Lubicz, Cortese, Delporte, Berhouma, Chopard, Costalat, Bonafé, Alix-Panabières, Van Anwterpen and Zouaoui Boudjeltia. This is an open-access article distributed under the terms of the Creative Commons Attribution License (CC BY). The use, distribution or reproduction in other forums is permitted, provided the original author(s) and the copyright owner(s) are credited and that the original publication in this journal is cited, in accordance with accepted academic practice. No use, distribution or reproduction is permitted which does not comply with these terms.

Effects of the flow diversion technique on nucleotide levels in intra-cranial aneurysms: A feasibility study providing new research perspectives

Omer F. Eker[1,2]*, Boris Lubicz[3], Melissa Cortese[4], Cedric Delporte[4], Moncef Berhouma[5], Bastien Chopard[6], Vincent Costalat[7], Alain Bonafé[7], Catherine Alix-Panabières[8,9], Pierre Van Anwterpen[4] and Karim Zouaoui Boudjeltia[10]

[1]Department of Neuroradiology, Hôpital Pierre Wertheimer, Hospices Civils de Lyon, Lyon, France, [2]CREATIS Laboratory, UMR 5220, U1206, Université Lyon, INSA-Lyon, Université Claude Bernard Lyon 1, UJM-Saint Etienne, CNRS, Inserm, Lyon, France, [3]Department of Interventional Neuroradiology, Erasme Hospital, Université Libre de Bruxelles, Brussels, Belgium, [4]RD3–Pharmacognosy, Bioanalysis, and Drug Discovery and Analytical Platform, Faculty of Pharmacy, Université Libre de Bruxelles, Brussels, Belgium, [5]Department of Vascular Neurosurgery, Hôpital Pierre Wertheimer, Hospices Civils de Lyon, Lyon, France, [6]Scientific and Parallel Computing Group, CUI, University of Geneva, Geneva, Switzerland, [7]Department of Neuroradiology, Hôpital Gui de Chauliac, Montpellier, France, [8]Laboratory of Rare Human Circulating Cells, University Medical Center of Montpellier, University of Montpellier, Montpellier, France, [9]CREEC, MIVEGEC, University of Montpellier, CNRS, IRD, Montpellier, France, [10]Laboratory of Experimental Medicine (ULB 222), Medicine Faculty, Université Libre de Bruxelles, CHU de Charleroi, Charleroi, Belgium

Introduction: The flow diverter stent (FDS) has become a first-line treatment for numerous intra-cranial aneurysms (IAs) by promoting aneurysm thrombosis. However, the biological phenomena underlying its efficacy remain unknown. We proposed a method to collect *in situ* blood samples to explore the flow diversion effect within the aneurysm sac. In this feasibility study, we assessed the plasma levels of nucleotides within the aneurysm sac before and after flow diversion treatment.

Materials and methods: In total, 14 patients with unruptured IAs who were selected for FDS implantation were prospectively recruited from February 2015 to November 2015. Two catheters dedicated to (1) FDS deployment and (2) the aneurysm sac were used to collect blood samples within the parent artery (P1) and the aneurysm sac before (P2) and after (P3) flow diversion treatment. The plasma levels of adenosine monophosphate (AMP), adenosine diphosphate (ADP), and adenosine triphosphate (ATP) at each collection point were quantified with liquid chromatography and tandem mass spectrometry.

Results: The aneurysms were extradural in nine (64.3%) patients and intradural in five (35.7%) patients. They presented an average diameter of 15.5 ± 7.1 mm, height of 15.8 ± 4.6 mm, and volume of 2,549 ± 2,794 ml. In all patients (100%), 16 FDS implantations and 42 *in situ* blood collections

were performed successfully without any complications associated with the procedure. The ATP, ADP, and AMP concentrations within the aneurysm sac were decreased after flow diversion (p = 0.005, p = 0.03, and p = 0.12, respectively). Only the ATP levels within the aneurysm sac after flow diversion were significantly correlated with aneurysm volume (adjusted R^2 = 0.43; p = 0.01).

Conclusion: *In situ* blood collection within unruptured IAs during a flow diversion procedure is feasible and safe. Our results suggest that the flow diversion technique is associated with changes in the nucleotide plasma levels within the aneurysm sac.

KEYWORDS

intra-cranial aneurysm, flow diversion, nucleotides, *in situ* blood collection, thrombosis – etiology

Introduction

The flow diversion technique is recognized as a safe and efficacious first-line therapy for selected intra-cranial aneurysms (IAs). Although initially dedicated to the treatment of large or giant complex IAs in proximal intra-cranial arteries (i.e., the internal carotid or vertebral arteries), this technique has been expanded to various types of aneurysms and locations, such as ruptured aneurysms (1). Unlike surgical clipping and endovascular coiling, which target the aneurysm itself, the flow diversion technique relies on the primary endoluminal reconstruction of the parent vessel through the deployment of a flow diverter stent (FDS), thus leading to the secondary occlusion of the aneurysm (1, 2). The aneurysm cure results from intra-saccular thrombosis are favored by this technique and therefore are not immediate but progressive. Indeed, a recent meta-analysis has reported complete occlusion rates of 68% (65–72%) and 90% (88–92%) with this technique in follow-up before 6 months and at 6–12 months, respectively (3, 4).

Despite the increasing use of FDSs in recent years and the introduction of newer-generation surface-modified FDSs, the mechanism of flow diversion and its therapeutic effects remain unclear. Two mechanisms are commonly understood to be involved in FDS action: (1) the hemodynamic alteration in the aneurysm sac induced by the flow redirection within the parent vessel and (2) the promotion of endothelialization at the aneurysm neck favored by the implant acting as a "scaffold" that increases endothelial cell migration and colonization (2, 5, 6). These two mechanisms, dependently or independently, have been proposed to explain the intra-saccular thrombosis resulting from the treatment and leading to IA cure. Numerous studies exploring these two mechanisms have improved the understanding of this technique (2, 7–9). However, they have not provided a comprehensive picture of the flow diversion effect that may explain why as many as 10% of IAs treated with FDSs remain patent at 1-year follow-up (4).

Little is known regarding the biological phenomena induced by the flow diversion technique within the IA. Notably, the effect of intra-saccular blood stasis on platelet aggregation remains unknown. Nucleotides (intra- and/or extracellular) play diverse physiological roles but are pathological under certain conditions (10). The role of adenosine diphosphate (ADP) in platelet aggregation through the P2Y12 receptors is well known, and many antiplatelet therapies target its action (11). Adenosine triphosphate (ATP) is released from erythrocytes and platelets under certain pathophysiological conditions, such as hypoxia or venous stasis (12). ATP is also known to induce platelet aggregation in whole blood *via* conversion to ADP by ecto-ATPases on leukocytes (11).

In this article, we propose an original investigative technique to collect blood samples from the aneurysm sac during endovascular treatment (EVT) of unruptured IAs with the flow diversion technique. We demonstrated its feasibility in patients treated with FDSs for unruptured IAs. The collected blood samples were analyzed to assess the levels of intra-saccular nucleotides before and after flow diversion treatment.

Materials and methods

Population

In total, 14 patients with unruptured IAs who were selected for FDS implantation were prospectively recruited from February 2015 to November 2015 in two INR centers. The indications for FDS implantation were assessed after a multidisciplinary meeting at the relevant institution for all patients. Local ethics committee guidelines were followed for this study (DGRI CCTIRS MG/CP 2012.528; Comité d'Ethique du CHU de Lyon;

Lyon/France). Informed consent was obtained from all patients. This work was funded partly by the THROMBUS VPH Project (7th Framework Programme/Seventh Framework Programme of European Commission/Virtual Physiological Human ICT-2009.5.3/Project reference: 269966; http://www.thrombus-vph.eu).

Aneurysm treatment

All patients were treated under general anesthesia with a biplane angiographic system (Phillips Allura, Philips, Best, Netherlands) after preparation according to the institutional protocol common to both centers (loading dose of 300 mg of clopidogrel administered 1 day before EVT; systemic heparinization administered during the endovascular procedure and stopped at the end of the treatment; per-procedural loading dose of 300 mg of acetylsalicylic acid after FDS deployment; and double antiplatelet therapy initiated for 6 months starting on day 1 after treatment, with 75 mg of acetylsalicylic acid and 75 mg of clopidogrel per day). The aneurysm and parent vessel underwent 3D rotational angiography before the EVT, thus allowing for 3D reconstruction and treatment planning. One or more FDSs were deployed in one session according to the aneurysm neck size (Pipeline^{TM} Embolization Device, PED^{TM}, ev3-Covidien, Irvine, CA, United States; Flow Redirection Endoluminal Device, FRED^{TM}, Microvention Terumo, Aliso Viejo, CA, United States; and p64 Flow Modulation Device, Phenox, Germany). If deemed necessary by the interventional neuroradiologist, additional coiling was performed (Target Coils, Stryker Neurovascular, Fremont, CA, United States).

Aneurysm assessment

The 3D aneurysms and parent vessel geometries were segmented and reconstructed from the 3D angiographic acquisition before the EVT (spatial resolution 0.48 mm × 0.48 mm), according to a new active contour method dedicated to the near real-time segmentation of 3D objects with the level-set method (13). This method allowed for the calculation of the two maximal diameters (mm), the depth (mm), the neck size (mm), and the volume (i.e., the volume of the patent intra-saccular lumen; mm^3) of all aneurysms in dedicated software (ITK-SNAP, Penn Image Computed and Science Laboratory, University of Pennsylvania, United States).

In vivo intra-aneurysmal blood collection

The principle of the technique relies on using the catheter normally dedicated to the FDS deployment and to coiling for the blood collection. During the EVT, a 0.027-inch Marksman Microcatheter (ev3 Neurovascular, Irvine, CA, United States) dedicated to FDS deployment was positioned within the parent artery and allowed for blood collection at the P1 position (i.e., parent artery catheter, PAC). The catheter was positioned upstream of the target IA for blood collection. The PAC was then positioned in the parent artery downstream of the IA for FDS deployment. Before FDS deployment, a 0.021-inch Headway Microcatheter (Microvention Terumo, Aliso Viejo, CA, United States) normally dedicated to coiling was positioned within the aneurysm sac and allowed for blood collection at this position (i.e., intra-IA catheter, IIAC). The deployment of the FDS while the IIAC was within the aneurysm lumen enabled the aneurysm neck to be covered and the IIAC to be jailed. The intra-aneurysmal blood samples were collected *via* the IIAC within the aneurysm sac before and after FDS deployment (blood collection P2 and P3, respectively). All microcatheter navigations were performed with 0.014-inch Synchro Guidewires, which were withdrawn before blood collection (Stryker Neurovascular, Fremont, CA, United States). From each catheter at each location (i.e., P1, P2, and P3), before each blood sampling, the catheter (i.e., either PAC or IIAC) was purged with a 1-cc Luer lock syringe (Becton Dickinson, Belgium). The purged volume corresponded approximately to their dead volume space of 0.87 and 0.55 ml for the 0.087-inch and the 0.021-inch catheters, respectively. At the end of the purging, when the blood appeared at the tip of the syringe, a new 1-cc Luer lock syringe was used to collect at least 700 µl of blood. The catheter purging and the blood collection were performed slowly during approximately 30 s of aspiration to minimize the red blood cell (RBC) hemolysis. Thus, three samples per patient were yielded, in the following order, to minimize the intra-luminal device manipulation:

- Within the parent artery upstream of the aneurysm and before the flow diversion (P1);
- Within the aneurysm sac before the flow diversion (P2); and
- Within the aneurysm sac after 10 min of flow diversion (P3).

After collection, the blood samples were collected in 1.5 ml tubes containing citrate and stored at +4°C for less than 2 h. Second, the samples were centrifuged at 3,500 *g* for 10 min, thus allowing for separation and extraction of the serum, which was stored at −80°C until further analyses.

Biological analyses

In each blood sample, the plasma levels of adenosine monophosphate (AMP), ADP, and ATP were quantified through a liquid chromatography and tandem mass spectrometry

TABLE 1 Population and aneurysm characteristics, procedural features, and follow-up.

Case	Age	Sex	Symptoms	Aneurysm characteristics							Procedural characteristics				Occlusion (time)
				Localization*	Height (mm)	Diameter 1 (mm)	Diameter 2 (mm)	Volume (mm^3)	Mural thrombus	n of FDSs	Type of FDS	Coiling	Complications	Contrast media stagnation	
1	30	M	Cavernous sinus syndrome	R ICA C4	12.00	14.00	15.00	1319	No	2	PED™	No	No	Yes	Complete (12 months)
2	55	F	Cavernous sinus syndrome	R ICA C4	24.50	33.50	22.50	9669	No	1	PED™	Yes	No	Yes	Complete (48 months)
3	43	M	Headaches	L ICA C5	20.00	16.00	20.00	3351	No	1	PED™	No	No	Yes	Complete (48 months)
4	79	F	Incidental discovery	L ICA C2	12.00	8.00	9.00	452	No	1	PED™	No	No	Yes	Complete (12 months)
5	50	M	Incidental discovery	L Pericallosal a.	9.00	5.60	7.70	203	Yes	1	PED™	No	No	Yes	Complete (6 months)
6	78	F	Cavernous sinus syndrome	R ICA C4	13.50	12.00	11.50	975	No	1	PED™	No	No	Yes	Complete (12 months)
7	71	F	Cavernous sinus syndrome	R ICA C4	21.00	26.00	23.00	6575	No	1	PED™	No	No	Yes	Complete (48 months)
8	63	F	Cavernous sinus syndrome	L ICA C4	10.00	13.00	18.00	1225	No	1	FRED™	No	No	Yes	Complete (6 months)
9	61	F	Headaches	L ICA C1–C2	18.00	9.50	9.50	851	No	1	PED™	Yes	No	No	Complete (12 months)
10	53	M	Incidental discovery	R ICA C2	18.50	7.80	8.00	604	No	1	PED™	Yes	No	Yes	Complete (12 months)
11	51	F	Incidental discovery	R ICA C3	13.00	19.00	20.00	2587	No	2	P64	No	No	Yes	Complete (6 months)
12	61	F	Headaches	R ICA C2	14.00	7.00	8.00	411	No	1	PED™	Yes	No	No	Complete (12 months)
13	39	M	Cavernous sinus syndrome	R ICA C4	20.00	15.50	14.00	2272	Yes	1	PED™	No	No	Yes	Complete (12 months)
14	58	F	Cavernous sinus syndrome	R ICA C3–C4	16.00	20.00	31.00	5194	Yes	1	PED™	No	No	Yes	Complete (12 months)

F, female; FDS, flow diverter stent; FRED™, flow redirection endoluminal device; ICA, internal carotid artery; L, left; M, male; P64, P64 flow modulation device; PED™, Pipeline™ embolization device; R, right;
*ICA localizations according to Fisher's classification: C1, communicating segment; C2, ophthalmic segment; C3, clinoidal segment; C4, cavernous segment; C5, intra-petrous.

10.3389/fcvm.2022.885426

method that was previously developed, validated, and fully described by our team (10). This technique provides the advantages of a lower limit of quantification than other methods and the ability to simultaneously quantify all nucleotides within a single injection within less than 10 min on the same blood sample (10).

Statistical analyses

Categorical variables are expressed as counts and percentages. Continual variables are expressed as mean ± standard deviation (SD). The nucleotide levels at the three blood collection points (P1, P2, and P3) were compared with Student's *t*-test, the Mann–Whitney rank sum test, the one-way analysis of variance (ANOVA), or the Kruskal–Wallis rank test, according to the results of the Shapiro–Wilk normality test and the Levene test of homogeneity. Linear regression analyses were performed to evaluate any correlation between the nucleotide levels and the aneurysm volume at each blood collection point. A two-sided *p*-value of <0.05 was considered statistically significant. Statistical analyses were performed in R version 3.2 (R Foundation for Statistical Computing, Vienna, Austria) (14).

Results

Table 1 summarizes the demographic characteristics of the population, the aneurysm characteristics, the procedural features, and the aneurysm occlusion status at follow-up. **Figure 1** shows the blood collection workflow during EVT.

Table 2 summarizes the nucleotide plasma concentrations at each blood collection point.

Figure 2 illustrates the sampling process in one case (in patient 2).

Figures 3–5 report the nucleotide levels at each blood collection point.

Figure 6 reports the distribution of ATP levels according to the aneurysm volume.

Study population

In total, 9 (60.0%) patients were women. The median patient age was of 57 ± 15 years (range 30–79 years). Seven (50%) patients had a cavernous sinus syndrome associated with headaches, ipsilateral ptosis, and ophthalmoplegia, due to III, IV, or VI nerve palsy, without any decrease in visual acuity or pupillary abnormalities. Three (21.4%) patients had headaches whose symptoms had no confirmed relationship with their aneurysms. Four (28.6%) patients were asymptomatic, and their aneurysms were incidentally discovered (**Table 1**). The patients' medical histories included high blood pressure in three (21.4%) patients, cigarette smoking in six (42.9%) patients, and diabetes mellitus in one (7.1%) patient. No patients presented any vascular steno-occlusive lesions of the supra-aortic trunks or intra-cranial arteries or any hypoxic conditions.

Aneurysm characteristics

One (7.1%) partially thrombosed aneurysm was located on the left pericallosal artery, and all other aneurysms were located on the right (n = 9, 64.3%) and the left (n = 4, 28.6%) intra-cranial carotid arteries (**Table 1**), from their intra-petrous segment to termination. Nine (64.3%) aneurysms were in extradural locations, and five (35.7%) were in intra-dural locations. The maximal aneurysm diameters were 1 and 2, heights and volumes were 14.8 ± 7.8 mm (range 5.6–33.5 mm), 15.5 ± 7.1 mm (range 7.7–31.0 mm), 15.8 ± 4.6 mm (range 9–24.5 mm), and 2,549 ± 2,794 ml (range 203–9,669 ml), respectively. Three (21.4%) aneurysms presented a mural thrombus (**Table 1**).

Procedure safety and aneurysm occlusion

In all patients, the intra-arterial and intra-aneurysmal navigations with the IIAC and the PAC were performed successfully. The aneurysms were treated with PED^{TM} in 12 (85.7%), FRED^{TM} in 1 (7.1%), and P64 in 1 (7.1%) cases, respectively. In two (14.3%) patients, two FDSs were deployed in a telescopic fashion to treat the aneurysm. All stents were successfully deployed. Intra-aneurysmal contrast media stagnation after flow direction was observed in 12 (85.7%) patients. In three (21.4%) cases, the aneurysm coil embolization was deemed necessary by the physician and was performed in addition to the flow diversion technique through the jailed IIAC after P3 blood collection (**Table 1**). Apart from a groin hematoma in one (7.1%) patient, no postoperative complications were observed in all procedures. In all patients (100%), the blood collection through the PAC and IIAC did not affect the EVT and its duration. The aneurysm occlusion was obtained between 6 and 48 months of follow-up in all patients. The occlusion status did not change during the follow-up between 2015 and 2021. No patients presented any clinical consequences of the intra-cranial blood sampling. All patients who initially presented with cavernous sinus syndrome showed clinical improvement or complete regression of their symptoms at the 1-year follow-up. The other patients remained clinically unchanged.

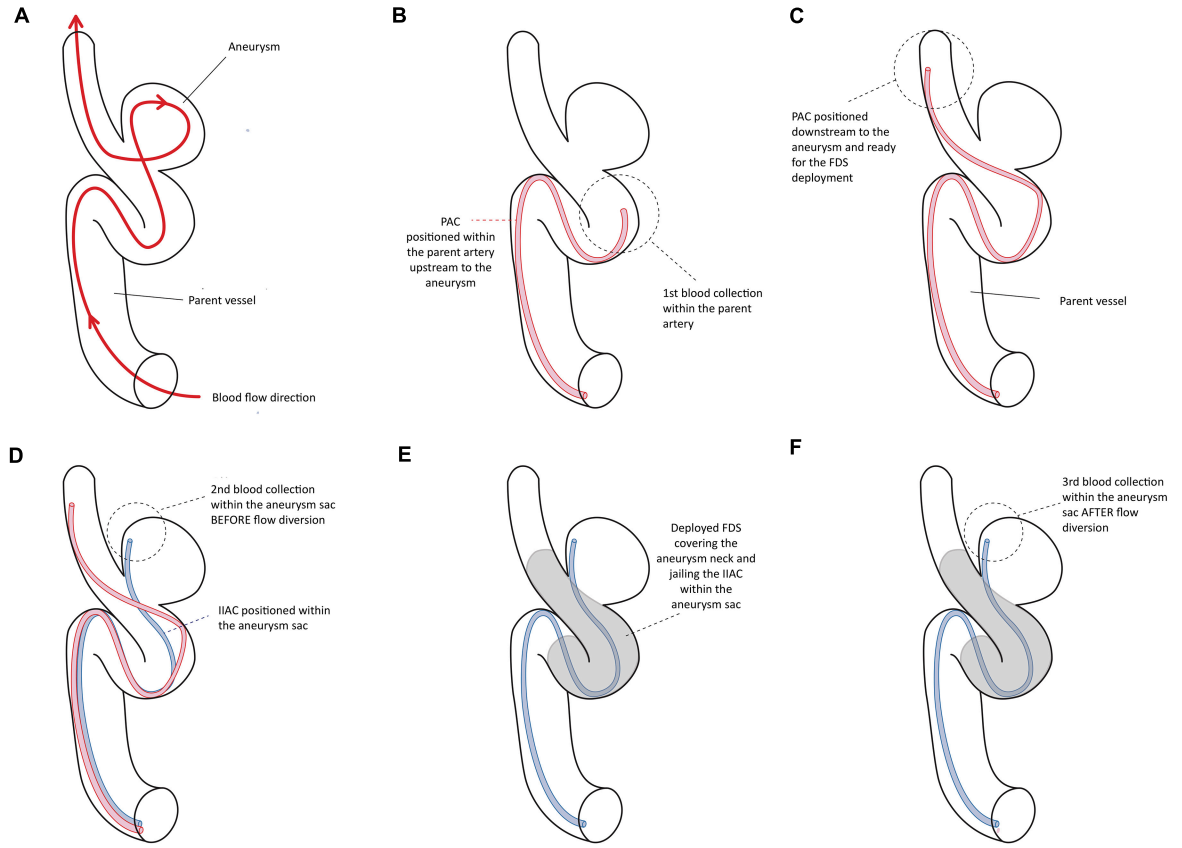

FIGURE 1
Illustrates the different steps of the blood collection within the parent vessel and the aneurysm sac during the endovascular treatment with the flow diverter stent.

TABLE 2 Nucleotide plasma concentrations at each blood collection point.

	Blood collection points			*p*-Value
	P1	P2	P3	
AMP (μM)	911 ± 520	624 ± 385	600 ± 393	0.12*
ADP (μM)	1,163 ± 286	1,009 ± 283	903 ± 467	0.03*
ATP (μM)	2,566 ± 453	2,158 ± 193	2,049 ± 179	0.005**

P1, parent vessel; P2, intra-aneurysmal before flow diversion stent implantation; P3, intra-aneurysmal after flow diversion stent implantation; ADP, adenosine diphosphate; AMP, adenosine monophosphate; ATP, adenosine triphosphate.
For each measured metabolite, a one-way analysis of variance (ANOVA; *) or the Kruskal–Wallis test (**) was used to compare the mean values among the three blood collection points, according to the results of the Shapiro–Wilk normality test and the Levene test for homogeneity of variance.

Biological results

In total, 42 blood collections were successfully performed in 14 patients without any difficulties or per-procedural complications. We observed significantly lower ATP, ADP, and AMP concentrations within the aneurysm sac after flow diversion than within the parent artery and the aneurysm sac before flow diversion (p = 0.005, p = 0.03, and p = 0.01, respectively; Table 2 and Figures 3–5). No differences were observed in the nucleotide levels between smoker (n = 6) and non-smoker (n = 8) patients. The ATP level within the aneurysm sac after flow diversion was significantly correlated with the aneurysm volume (adjusted R^2 = 0.44, p = 0.01; Figure 6 and Supplementary material). No significant correlations were observed between aneurysm volume and ATP levels within the aneurysm sac before flow diversion or within the parent vessel, or AMP and ADP levels at each blood collection point (Supplementary material).

Discussion

In this work, we used an approach to collect blood samples within the parent artery and the aneurysm sac during EVT for IAs with the flow diversion technique. In this feasibility study, the collected blood was analyzed, and the nucleotide levels were measured. The blood collection had no consequences on the EVT, and there were no complications observed in any

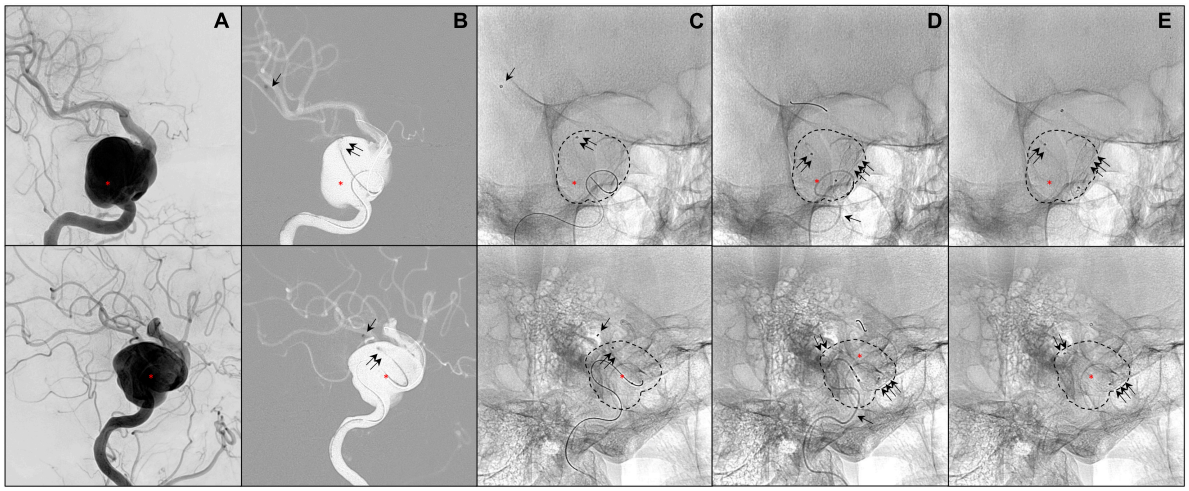

FIGURE 2
Illustrates a patient presenting a giant aneurysm of the right internal carotid artery (segment C4; red asterisk; **A–E**). The 0.027-inch catheter for the first blood collectio (P1) is visible in panels **(B–E)** (single black arrow). The 0.021-inch catheter within the aneurysm sac is visible in panels **(B–E)** (double black arrows). The flow diverter stent is deployed in panels **(C–E)** (triple black arrows).

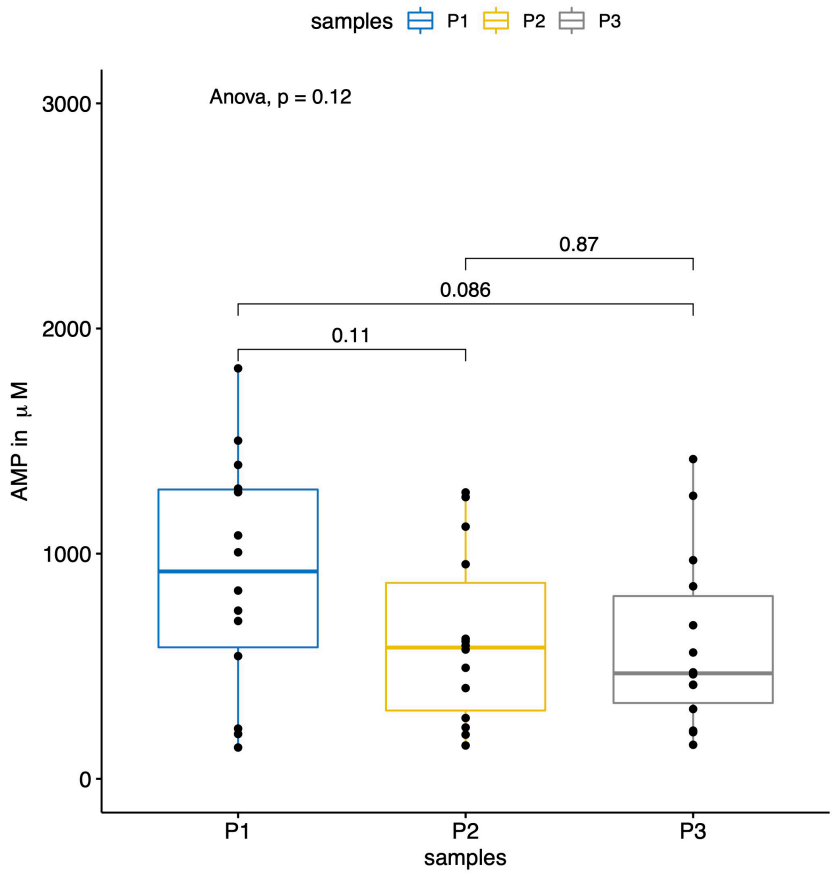

FIGURE 3
The boxplot shows the results of the measured AMP levels (in μM) within the parent vessels (P1) and the aneurysm sacs before (P2) and after (P3) flow diversion. No significant differences were observed for the AMP levels between the three sampling locations.

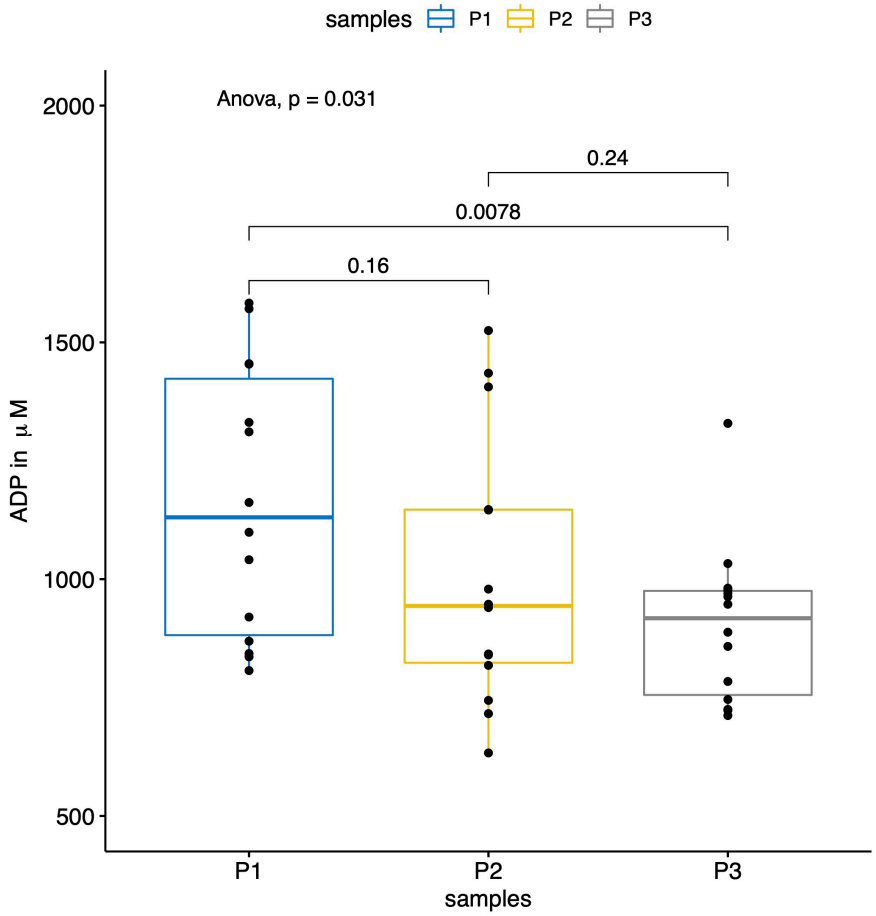

FIGURE 4
The boxplot shows the results of the measured ADP levels (in μM) within the parent vessel (P1) and the aneurysm sac before (P2) and after (P3) flow diversion. The ADP levels were significantly lower within the aneurysm sacs after flow diversion (P3) compared to the ones in the parent vessels (P1) (p = 0.008).

patients. First, we observed significant decreases in the ATP and ADP levels within the aneurysm sac after flow diversion. Second, our results showed a significant correlation between the intra-aneurysmal ATP decrease after flow diversion and the aneurysm volume.

The flow diversion technique has revolutionized the treatment of large and complex IAs that were difficult (or even impossible) to treat with previous techniques. Compared with conventional techniques (i.e., coiling, stent-assisted coiling, parent vessel occlusion, or surgical clipping), FDSs showed higher rates of occlusion and lower rates of recurrence without increasing the rate of complications in the treatment of specific aneurysms, such as giant or complex aneurysms (3, 4, 15). Their efficacy relies on the ability to redirect the blood flow out of the aneurysmal sac, thus decreasing the intra-aneurysmal blood flow and the endothelization of the aneurysm neck, hence promoting thrombosis of the aneurysm and its regression (2). Despite the improvements in IA treatment with this technique, its mechanism of action is not fully understood. Previous studies on flow diversion have focused on hemodynamic alterations within the aneurysm sac and/or the endothelization processes within the parent artery that promote IA thrombosis (2, 5, 6). Those studies have not provided information on the intra-saccular biological phenomena occurring after flow diversion. We believe that these phenomena may play a key role in the curative effect of this technique. Better knowledge of the blood modification within the IA induced by flow diversion should aid in understanding its efficacy (or lack thereof) and eventually enable the identification of patients who will not benefit from this technique.

However, any exploration of the blood biology within the IA lumen requires *in situ* real-time blood samples that are not available or accessible in normal conditions or after IA treatment through conventional techniques. A method to obtain sufficient usable blood to explore these mechanisms is lacking. The ideal technique to obtain *in situ* blood samples should

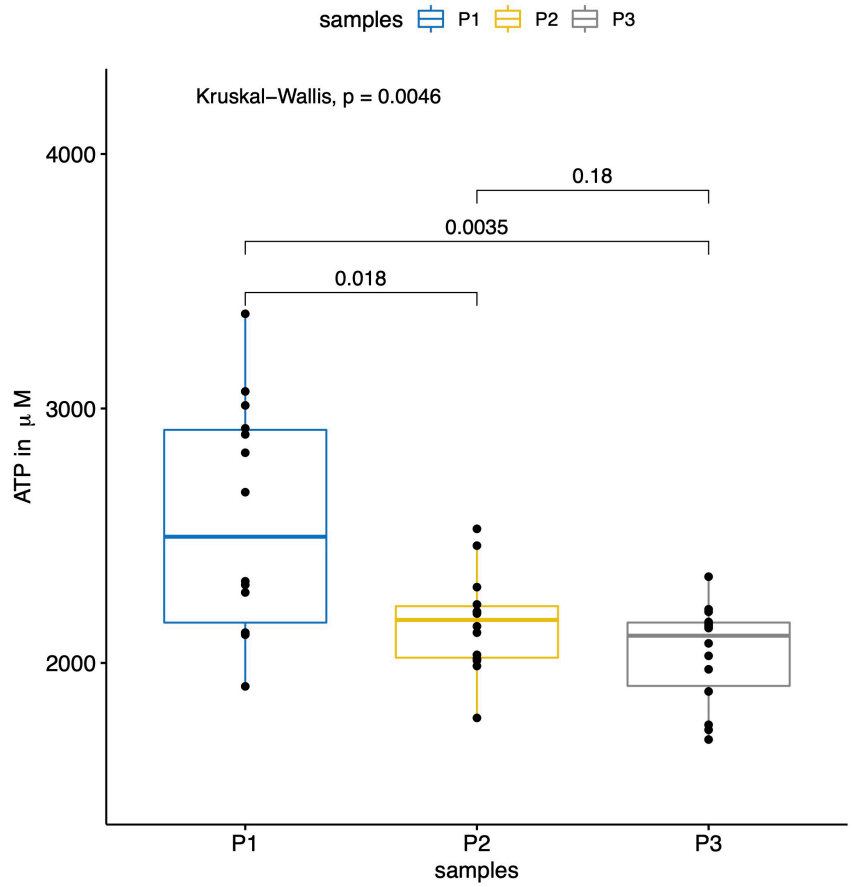

FIGURE 5
The boxplot shows the results of the measured ATP levels (in μM) within the parent vessel (P1) and the aneurysm sac before (P2) and after (P3) flow diversion. The AMP levels were significantly lower within the aneurysm sacs before (P2) and after (P3) flow diversion compared to the ones in the parent vessels (P1) (p = 0.018 between P1 and P2, and p = 0.003 between P1 and P3).

meet several criteria. First, it must be safe, posing minimal complication risk to patients. Second, it must be as rapid as possible to prevent or minimize any potential modification of the assessed biological environment by the collection devices or techniques. Third, it must be standardized and reproducible to allow the comparison of blood samples in the same patient or among patients. Fourth, it must be as easy as possible to perform, to enable the dissemination of the technique, and to promote research in this field. For these purposes, we propose a minimally invasive method to achieve this goal while meeting all these criteria. Our approach exploits the flow diversion EVT itself and the materials used during the procedure, i.e., the catheters dedicated to the intra-cranial navigation, the FDS deployment, and additional coiling of the aneurysm if necessary. The catheters are positioned sequentially within the parent artery and the aneurysm sac. The blood collection at each targeted location lasts approximately 30 s through the catheters, a duration compatible with that of EVT. The last collection (i.e., within the aneurysm sac after flow diversion) is performed 10 min after flow diversion, on the basis of previous reports of the changes in nucleotide levels in venous blood after 4 min of stasis (10), to maximize the chances of detecting any changes in nucleotide levels after flow diversion.

The nucleotides in the blood play complex and various roles that are closely associated with local conditions. Indeed, in addition to functioning as an intra-cellular energy source, ATP and ADP are important extracellular signaling molecules (16). Extracellular circulating ATP is rapidly degraded into ADP, AMP, and adenosine by ectonucleotidases (17). ATP and ADP activate P2 receptors on various cells, particularly blood cells, such as platelets and endothelial cells (18, 19), thus regulating several physiological responses. These responses include platelet aggregation, vascular tone (20), and the release of endothelial factors. At least 15 nucleotide-activated cell surface receptors have been found in humans (P2X and P2Y receptors) and show remarkably varied physiological responses.

Platelet aggregation is mediated by ADP through the P2Y12 receptors (21, 22), in a process involving leukocytes,

10.3389/fcvm.2022.885426

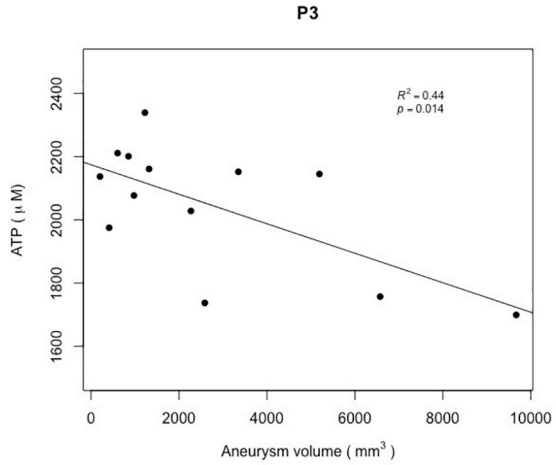

FIGURE 6
The scatter plot reports the ATP levels (in μM) within the aneurysm sacs after flow diversion (P3) according to the aneurysm volumes (in mm3). A significant correlation was observed between the ATP levels within the aneurysm sacs after flow diversion (P3) and the aneurysm volumes (R^2 = 0.44; p = 0.014).

which present cell surface enzymes that degrade ATP into ADP and then AMP, such as the ectonucleoside triphosphate diphosphohydrolase-1 (also known as cluster of differentiation 39, CD39) (23). ATP itself is not considered a platelet-aggregating agent. However, it can induce platelet aggregation when it is added to whole blood (24). In addition, RBCs play a role in platelet aggregation by capturing adenosine (23). These mechanisms may be involved in the progressive intra-aneurysmal thrombosis observed after flow diversion treatment.

Our work showed that ATP and ADP significantly decrease within the aneurysm sac after flow diversion and that aneurysmal volume may influence these phenomena (or at least the ATP decrease). However, given the limited sample size and analyses performed (i.e., measurement of only nucleotide levels), our results cannot explain this observation or indicate a clear conclusion. At most, among the potentially unknown mechanisms triggered by flow diversion, the decreases in ATP and ADP might suggest that flow diversion induces intra-aneurysmal local hypoxia. Indeed, RBCs are known to function as O_2 sensors, which contribute to the regulation of blood flow and O_2 delivery. They perform this role by releasing ATP depending on the oxygenation state of hemoglobin and the pH (20, 25–33). In this physiologically important signaling system, when O_2 decreases, ATP is rapidly degraded to ADP in circulation by ectonucleotidases. The ADP in turn acts on $P2Y_{13}$ receptors on RBCs in a negative feedback pathway for the inhibition of ATP release (34). The increase in ADP levels is also known as a primary mediator of platelet aggregation, thus leading to a sustained response *via* activation of the P2Y12 receptors (21, 22). The rapid degradation of ATP into ADP within the stagnating blood "trapped" outside the FDS might explain the decrease in ATP. After its initial transient increase secondary to the previously described mechanism, the consumption of ADP by the P2Y13 receptors on RBCs and the P2Y12 receptors on platelets might explain the decrease in ADP.

Limitations

Our work is hypothesis generating but does not provide further answers because of several limitations. First, this was a preliminary feasibility study. Hence, we included only a limited number of patients, and we assessed only the nucleotide levels. The patients had large intra-cranial, mostly internal carotid artery, aneurysms. This design aspect was aimed at minimizing the risk of complications to the patients while maximizing the possibility of successfully collecting blood samples within the aneurysmal sac. Indeed, the internal carotid artery aneurysms are proximal and less prone to accessibility issues than distally located aneurysms. The large aneurysm size also minimized the risk of complications during the intra-aneurysmal catheter manipulation (particularly the risk of aneurysm perforation). Second, we did not evaluate the effects of platelet activation or many other factors with roles in thrombosis, such as the von Willebrand factor, thrombin, thromboxane A2, coagulation activators (such as thrombin-antithrombin complex), and components of the glycocalyx at the endothelial cell surface. Third, we did not consider the dual platelet inhibition required with flow diversion treatment in the analyses of the nucleotide levels. The antiplatelet regimen is commonly based on a combination of acetylsalicylic acid and a P2Y12 inhibitor (i.e., clopidogrel, prasugrel, or ticagrelor) that targets the P2Y12 receptor and therefore may theoretically affect nucleotide levels. For instance, ticagrelor has been reported to induce ATP release from human RBCs (35). Fourth, the intra-aneurysmal flow conditions after flow diversion were also not considered in the analyses of the nucleotide levels. The intra-aneurysmal hemodynamic alterations due to flow diversion markedly vary from no effects (i.e., almost normal patency of the aneurysm) to abrupt stasis. In the first scenario, few or no changes in nucleotide levels within the aneurysm when compared with the parent vessel can reasonably be expected, whereas maximal changes should be expected in stagnating blood. In our work, the intra-aneurysmal contrast media stagnation (indicating blood stagnation) was unevenly distributed and was observed in 85.7% of patients, thus preventing us from drawing any conclusion. Finally, we collected blood within the aneurysm sac after flow diversion at only one time point (i.e., 10 min after the FDS deployment). Sequential and consecutive blood collection might be considered to analyze the kinetics of the intra-aneurysmal biological cascades after flow diversion.

Conclusion

Blood collection within unruptured IAs during a flow diversion procedure is feasible and appeared safe in our case series. Our preliminary work suggests that flow diversion treatment is associated with changes in plasma nucleotide levels within the aneurysm sac after flow diversion. Further studies in larger populations are needed to better understand the mechanisms involved in thrombus formation after flow diversion.

Data availability statement

The raw data supporting the conclusions of this article will be made available by the authors, without undue reservation.

Ethics statement

The studies involving human participants were reviewed and approved by the Comité d'Ethique du CHU de Lyon; Lyon/France. The patients/participants provided their written informed consent to participate in this study.

Author contributions

OE and KZ contributed equally to the conception and design of the study. OE collected the clinical, biological, and imaging data, performed the imaging post-processing and statistical analysis, and wrote the first draft of the manuscript and the iterative versions. CA-P provided the facilities and means to condition the blood samples after the sampling. All authors contributed substantially to the work described by critically revising the manuscript for important intellectual content.

Funding

This work was partly funded by the THROMBUS VPH Project (7th Framework Programme/Seventh Framework Programme of European Commission/Virtual Physiological Human ICT-2009.5.3/Project reference: 269966; http://www.thrombus-vph.eu) and by grants from the CHU Charleroi (Fonds de la Chirurgie Cardiaque; Fonds de la Recherche Medicale en Hainaut).

Acknowledgments

We thank the members of the clinical research teams of the Neuroradiology Department of Hôpital Gui de Chauliac (Montpellier, France) and of the Interventional Neuroradiology Department of Erasme Hospital (Brussels, Belgium), as well as the teams of the Laboratory of Experimental Medicine of CHU de Charleroi (Charleroi, Belgium).

Conflict of interest

The authors declare that the research was conducted in the absence of any commercial or financial relationships that could be construed as a potential conflict of interest.

Publisher's note

All claims expressed in this article are solely those of the authors and do not necessarily represent those of their affiliated organizations, or those of the publisher, the editors and the reviewers. Any product that may be evaluated in this article, or claim that may be made by its manufacturer, is not guaranteed or endorsed by the publisher.

Supplementary material

The Supplementary Material for this article can be found online at: https://www.frontiersin.org/articles/10.3389/fcvm.2022.885426/full#supplementary-material

SUPPLEMENTARY FIGURE 1
The scatter plots report the nucleotide levels (in ţM) at each location and timepoints (i.e., P1, P2, and P3) according to the aneurysm volume (in mm3). A significant correlation was observed only between the ATP levels within the aneurysm sacs after flow diversion (P3) and the aneurysm volumes (R2 = 0.44; p = 0.014).

References

1. Chancellor B, Raz E, Shapiro M, Tanweer O, Nossek E, Riina HA, et al. Flow diversion for intracranial aneurysm treatment: trials involving flow diverters and long-term outcomes. *Neurosurgery*. (2020) 86:S36–45. doi: 10.1093/neuros/nyz345

2. Chua MMJ, Silveira L, Moore J, Pereira VM, Thomas AJ, Dmytriw AA. Flow diversion for treatment of intracranial aneurysms: mechanism and implications. *Ann Neurol*. (2019) 85:793–800. doi: 10.1002/ana.25484

3. Brinjikji W, Murad MH, Lanzino G, Cloft HJ, Kallmes DF. Endovascular treatment of intracranial aneurysms with flow diverters: a meta-analysis. *Stroke.* (2013) 44:442–7. doi: 10.1161/STROKEAHA.112.678151

4. Wang Y, Yuan C, Shen S, Xu L, Duan H. Whether intracranial aneurysm could be well treated by flow diversion: a comprehensive meta-analysis of large-sample studies including anterior and posterior circulation. *Biomed Res Int.* (2021) 2021:6637780. doi: 10.1155/2021/6637780

5. Briganti F, Leone G, Marseglia M, Mariniello G, Caranci F, Brunetti A, et al. Endovascular treatment of cerebral aneurysms using flow-diverter devices: a systematic review. *Neuroradiol J.* (2015) 28:365–75. doi: 10.1177/1971400915602803

6. Bouillot P, Brina O, Ouared R, Lovblad K-O, Farhat M, Pereira VM. Particle imaging velocimetry evaluation of intracranial stents in sidewall aneurysm: hemodynamic transition related to the stent design. *PLoS One.* (2014) 9:e113762. doi: 10.1371/journal.pone.0113762

7. Kadirvel R, Ding Y-H, Dai D, Rezek I, Lewis DA, Kallmes DF. Cellular mechanisms of aneurysm occlusion after treatment with a flow diverter. *Radiology.* (2014) 270:394–9. doi: 10.1148/radiol.13130796

8. Ou C, Huang W, Yuen MM-F. A computational model based on fibrin accumulation for the prediction of stasis thrombosis following flow-diverting treatment in cerebral aneurysms. *Med Biol Eng Comput.* (2017) 55:89–99. doi: 10.1007/s11517-016-1501-1

9. Marosfoi M, Langan ET, Strittmatter L, van der Marel K, Vedantham S, Arends J, et al. In situ tissue engineering: endothelial growth patterns as a function of flow diverter design. *J Neurointerv Surg.* (2017) 9:994–8. doi: 10.1136/neurintsurg-2016-012669

10. Cortese M, Delporte C, Dufour D, Noyon C, Chaumont M, De Becker B, et al. Validation of a LC/MSMS method for simultaneous quantification of 9 nucleotides in biological matrices. *Talanta.* (2019) 193:206–14. doi: 10.1016/j.talanta.2018.10.003

11. Lecka J, Bloch-Boguslawska E, Molski S, Komoszynski M. Extracellular purine metabolism in blood vessels (Part II): activity of ecto-enzymes in blood vessels of patients with abdominal aortic aneurysm. *Clin Appl Thromb Hemost.* (2010) 16:650–7. doi: 10.1177/1076029609354329

12. Holmsen H. Platelet metabolism and activation. *Semin Hematol.* (1985) 22:219–40.

13. Eker OF, Boudjeltia KZ, Jerez RAC, Le Bars E, Sanchez M, Bonafe A, et al. MR derived volumetric flow rate waveforms of internal carotid artery in patients treated for unruptured intracranial aneurysms by flow diversion technique. *J Cereb Blood Flow Metab.* (2015) 35:2070–9. doi: 10.1038/jcbfm.2015.176

14. R Core Team. *R: A Language and Environment for Statistical Computing [Internet]*. Vienna: R Foundation for Statistical Computing (2020).

15. Xin W-Q, Xin Q-Q, Yuan Y, Chen S, Gao X-L, Zhao Y, et al. Comparison of flow diversion and coiling for the treatment of unruptured intracranial aneurysms. *World Neurosurg.* (2019) 128:464–72. doi: 10.1016/j.wneu.2019.05.149

16. Burnstock G, Verkhratsky A. *Receptors for Purines and Pyrimidines. Purinergic Signalling and the Nervous System*. Berlin: Springer (2012). p. 119–244. doi: 10.1007/978-3-642-28863-0_5

17. Gordon JL. Extracellular ATP: effects, sources and fate. *Biochem J.* (1986) 233:309. doi: 10.1042/bj2330309

18. Wang L, Östberg O, Wihlborg A-K, Brogren H, Jern S, Erlinge D. Quantification of ADP and ATP receptor expression in human platelets. *J Thromb Haemost.* (2003) 1:330–6. doi: 10.1046/j.1538-7836.2003.00070.x

19. Di Virgilio F, Chiozzi P, Ferrari D, Falzoni S, Sanz JM, Morelli A, et al. Nucleotide receptors: an emerging family of regulatory molecules in blood cells. *Blood.* (2001) 97:587–600. doi: 10.1182/blood.V97.3.587

20. González-Alonso J, Olsen DB, Saltin B. Erythrocyte and the regulation of human skeletal muscle blood flow and oxygen delivery: role of circulating ATP. *Circ Res.* (2002) 91:1046–55. doi: 10.1161/01.RES.0000044939.73286.E2

21. Jin J, Daniel JL, Kunapuli SP. Molecular basis for ADP-induced platelet activation: II. The P2Y1 receptor mediates ADP-induced intracellular calcium mobilization and shape change in platelets. *J Biol Chem.* (1998) 273:2030–4. doi: 10.1074/jbc.273.4.2030

22. Gachet C. ADP receptors of platelets and their inhibition. *Thromb Haemost.* (2001) 86:222–32. doi: 10.1055/s-0037-1616220

23. Glenn JR, White AE, Johnson A, Fox SC, Behan MWH, Dolan G, et al. Leukocyte count and leukocyte ecto-nucleotidase are major determinants of the effects of adenosine triphosphate and adenosine diphosphate on platelet aggregation in human blood. *Platelets.* (2005) 16:159–70. doi: 10.1080/09537100500063889

24. Stafford NP, Pink AE, White AE, Glenn JR, Heptinstall S. Mechanisms involved in adenosine triphosphate–induced platelet aggregation in whole blood. *Arterioscler Thromb Vasc Biol.* (2003) 23:1928–33. doi: 10.1161/01.ATV.0000089330.88461.D6

25. Cosby K, Partovi KS, Crawford JH, Patel RP, Reiter CD, Martyr S, et al. Nitrite reduction to nitric oxide by deoxyhemoglobin vasodilates the human circulation. *Nat Med.* (2003) 9:1498–505. doi: 10.1038/nm954

26. Ellsworth ML, Forrester T, Ellis CG, Dietrich HH. The erythrocyte as a regulator of vascular tone. *Am J Physiol Heart Circ Physiol.* (1995) 269:H2155–61. doi: 10.1152/ajpheart.1995.269.6.H2155

27. McMahon TJ, Moon RE, Luschinger BP, Carraway MS, Stone AE, Stolp BW, et al. Nitric oxide in the human respiratory cycle. *Nat Med.* (2002) 8:711–7. doi: 10.1038/nm718

28. Bergfeld GR, Forrester T. Release of ATP from human erythrocytes in response to a brief period of hypoxia and hypercapnia. *Cardiovasc Res.* (1992) 26:40–7. doi: 10.1093/cvr/26.1.40

29. Sprague RS, Ellsworth ML, Stephenson AH, Lonigro AJ. Participation of cAMP in a signal-transduction pathway relating erythrocyte deformation to ATP release. *Am J Physiol Cell Physiol.* (2001) 281:C1158–64. doi: 10.1152/ajpcell.2001.281.4.C1158

30. Sprague RS, Stephenson AH, Ellsworth ML, Keller C, Lonigro AJ. Impaired release of ATP from red blood cells of humans with primary pulmonary hypertension. *Exp Biol Med.* (2001) 226:434–9. doi: 10.1177/153537020122600507

31. Dietrich HH, Ellsworth ML, Sprague RS, Dacey J RG. Red blood cell regulation of microvascular tone through adenosine triphosphate. *Am J Physiol Heart Circ Physiol.* (2000) 278:H1294–8. doi: 10.1152/ajpheart.2000.278.4.H1294

32. Malmsjö M, Edvinsson L, Erlinge D. P2U-receptor mediated endothelium-dependent but nitric oxide-independent vascular relaxation. *Br J Pharmacol.* (1998) 123:719–29. doi: 10.1038/sj.bjp.0701660

33. Malmsjö M, Erlinge D, Högestätt ED, Zygmunt PM. Endothelial P2Y receptors induce hyperpolarisation of vascular smooth muscle by release of endothelium-derived hyperpolarising factor. *Eur J Pharmacol.* (1999) 364:169–73. doi: 10.1016/S0014-2999(98)00848-6

34. Wang L, Olivecrona G, Götberg M, Olsson ML, Winzell MS, Erlinge D. ADP acting on P2Y13 receptors is a negative feedback pathway for ATP release from human red blood cells. *Circ Res.* (2005) 96:189–96. doi: 10.1161/01.RES.0000153670.07559.E4

35. Öhman J, Kudira R, Albinsson S, Olde B, Erlinge D. Ticagrelor induces adenosine triphosphate release from human red blood cells. *Biochem Biophys Res Commun.* (2012) 418:754–8. doi: 10.1016/j.bbrc.2012.01.093

Advantages of publishing in Frontiers

OPEN ACCESS
Articles are free to read for greatest visibility and readership

FAST PUBLICATION
Around 90 days from submission to decision

HIGH QUALITY PEER-REVIEW
Rigorous, collaborative, and constructive peer-review

TRANSPARENT PEER-REVIEW
Editors and reviewers acknowledged by name on published articles

Frontiers
Avenue du Tribunal-Fédéral 34
1005 Lausanne | Switzerland

Visit us: www.frontiersin.org
Contact us: frontiersin.org/about/contact

REPRODUCIBILITY OF RESEARCH
Support open data and methods to enhance research reproducibility

DIGITAL PUBLISHING
Articles designed for optimal readership across devices

FOLLOW US
@frontiersin

IMPACT METRICS
Advanced article metrics track visibility across digital media

EXTENSIVE PROMOTION
Marketing and promotion of impactful research

LOOP RESEARCH NETWORK
Our network increases your article's readership